THE TETRASPANIN CD81 DYNAMICS: INVESTIGATING THE ROLE IN HEPATITIS C VIRUS ENTRY

BY

AMY HEATHER BARNES

A THESIS SUBMITTED TO THE UNIVERSITY OF BIRMINGHAM FOR THE DEGREE OF DOCTOR OF PHILOSOPHY

SCHOOL OF IMMUNITY AND INFECTION

COLLEGE OF MEDICAL AND DENTAL SCIENCES

UNIVERSITY OF BIRMINGHAM

MAY 2015

UNIVERSITYOF
BIRMINGHAM

University of Birmingham Research Archive

e-theses repository

ABSTRACT

Hepatitis C Virus (HCV) infects hepatocytes, a liver cell type with complex polarity. Virus entry is a multi-step process that is dependent on a number of host proteins including CD81, scavenger receptor BI, and the tight junction proteins claudin-1 and occludin. CD81 is an attachment receptor for the virus, however, internalization is dependent upon CD81 association with claudin-1 to form a coreceptor complex.

 The presentation and diffusion kinetics of CD81 shows variable conformation between diverse cell types. Using live imaging I show that CD81 diffusion is regulated by cellular localisation and polarity. Whilst the addition of growth factors and cytokines can modulate infection these effects are not consistently reflected by changes in CD81 diffusion, suggesting that CD81 diffusion kinetics alone does not define HCV entry. I demonstrate that the diffusion of the claudin-1 co-receptor also plays a role in defining infection. In addition, I demonstrate a complex interplay between the coreceptors and EGFR signalling that may involve the rearrangement of membrane domains to promote virus entry.

DEDICATION

I am immensely grateful to my parents, John and Wendy, to Jamie McIntosh and to my sister

Jo for their constant, unquestioning support. The same is true of the friends, old and new,

that I have been so lucky to have over the last 4 years.

Thank you.

"Don't *wish*, Miss Tick had said. *Do* things."

Sir Terry Pratchett, Wee Free Men

ACKNOWLEDGEMENTS

FREQUENTLY USED ABBREVIATIONS

AcGFP	Aequorea coerulescens Green Fluorescent Protein
BC	Bile Canaliculus
CD81	Cluster of Differentiation 81
CLDN-1	Claudin-1
CMFDA	5-chloromethylfluorescein diacetate
EGF	Epidermal Growth Factor
EGFR	Epidermal Growth Factor Receptor
ERM	Ezrin, radixin, moesin
EWI	Glu-Trp-Ile motif
FRAP	Fluorescence Recovery After Photobleaching
FRET	Förster Resonance Energy Transfer
Grb2	Growth factor receptor-bound protein 2
HCV	Hepatitis C Virus
HCVpp	Hepatitis C Virus pseudoparticle
IFN	Interferon
ITGβ1	Integrin β1
LDL	Low Density Lipoprotein
LEL	Large Extracellular Loop
MAPK	Mitogen-Activated Protein Kinase
MFI	Median Fluorescence Intensity
MRP2	Multidrug Resistance-associated Protein 2
PHH	Primary Human Hepatocytes
PM	Plasma Membrane
RFC	Relative Fold Change
RLU	Relative Light Units
RTK	Receptor Tyrosine Kinase

SEL	Small Extracellular Loop
SH2	Src Homology 2
Shc1	(Src homology 2 domain containing) transforming protein 1
SR-B1	Scavenger Receptor class B member 1
SPT	Single Particle Tracking
SPR	Surface Plasmon Resonance
TEM	Tetraspanin Enriched Microdomains
TJ	Tight Junction
TM	Transmembrane
TNF-α	Tumour Necrosis Factor alpha
WT	Wild Type

TABLE OF CONTENTS

TABLE OF FIGURES

TABLE OF TABLES

1. INTRODUCTION

1.1 BRIEF HISTORY OF NON-A, NON-B POST TRANSFUSION HEPATITIS

The Second World War holds a significant place in history. It heralded the beginning of a new era with the rise of the USA and USSR as new superpowers, and the falling of the Iron Curtain between the East and West. In the aftermath, whilst the world recovered, the field of medicine was consolidating the huge advances it had made during the conflict. These included the industrialisation of penicillin production and pioneering skin graft technologies.

A field which saw considerable improvement in the 6 years between 1939 and 1945 was that of blood transfusions. Before the war, the organisation of this had been primitive, but by its conclusion ran like a well-oiled machine, and as a result the National Blood Transfusion Service was formed in 1946.

There is no doubt that blood transfusions saved countless lives during the most deadly conflict in history. However, it also served medical advancement as due to the sheer number of blood transfusions performed, the potential dangers of the practice were noticed far more quickly than may otherwise have been possible. One of these was post transfusion hepatitis (PTH).

During the war, numerous transmission and epidemiology studies led to the identification of two distinct possible viral causes of PTH. These were named hepatitis A and hepatitis B and were distinguished by their routes of transmission: hepatitis A was transmitted via the faecal-oral route, whereas hepatitis B was transmitted via blood and blood products (Havens 1944, MacCallum 1944, Neefe, Stokes et al. 1944, MacCallum 1972, Krugman 1976, Reuben

2002). Due to the faecal/oral route of transmission, hepatitis A was thought unlikely to be the cause of PTH.

In 1965 an investigation into the immune reactivity of plasma proteins identified a unique protein in the serum of Australian aborigines – the 'Australia antigen' (Blumberg, Alter et al. 1965). This was shown to have a strong association with acute hepatitis, and was later identified as the surface antigen of the hepatitis B virus (HBsAg) (HBV). (Prince 1968, London, Sutnick et al. 1969, Dane, Cameron et al. 1970). With the detection of HBV possible (Bayer, Blumberg et al. 1968, Feinstone, Kapikian et al. 1973), compulsory screening of blood transfusions was introduced in US federal regulation in 1972 (Alter, Holland et al. 1972), and PTH rates subsequently fell by 97%.

Despite this, 10% of transfusion patients continued to develop hepatitis despite being given blood that had tested negative for HBsAg during screening. Furthermore, the symptoms observed in these patients indicated a shorter incubation period than observed with HBV suggesting that this form of PTH was caused by a different agent. This hypothesis was further supported by the observation that these patients could be subject to recurrent hepatitis episodes post-transfusion, an occurrence not seen in either hepatitis A or B (Alter, Holland et al. 1975, Alter, Holland et al. 1975, Feinstone, Kapikian et al. 1975). Therefore, it became known as non-A non-B hepatitis (NANBH) (Feinstone, Kapikian et al. 1975).

Despite significant research, the agent responsible for NANBH was not identified due to the lack of available cell culture or animal models. In 1978 the NANBH agent was successfully transmitted into chimpanzees (Tabor, Gerety et al. 1978). In subsequent work, Houghton and colleagues at Chiron and Daniel Bradley at the Centre for Disease Control carried out a

non-biased genetic screen and successfully identified the agent responsible (Choo, Kaya et al. 1989).

The team extracted and reverse transcribed nucleic acid from the plasma of chimps that had been infected with NANBH agent. They used the resulting cDNA fragments to design a recombinant expression library in *E.Coli* and screened the expressed proteins against the serum of a chronically infected NANBH patient. The resulting clone was isolated and sequenced to give a single immunoreactive clone (Choo, Kuo et al. 1989, Choo, Weiner et al. 1990).

Further analysis showed that the nucleotide sequence of the NANBH agent comprised a 9,600 nucleotide positive-strand RNA genome and it was designated the hepatitis C Virus (HCV). It was classified within a separate *Hepacivirus* genus of the *Flaviviridae* family alongside arthropod-borne human pathogens including yellow fever virus (YFV), West Nile virus (WNV) and Dengue virus (DNV) (Kuo, Choo et al. 1989, Houghton 2009). Today, the *Hepacivirus* genus includes not only HCV, but also GB virus B (GBV-B) and a number of non-primate, rodent and bat hepaciviruses (Kapoor, Simmonds et al. 2011, Drexler, Corman et al. 2013, Kapoor, Simmonds et al. 2013, Quan, Firth et al. 2013).

Following the discovery of HCV, diagnostic assays were developed that could detect HCV in blood, and due to the introduction of screening in the 1990s the risk of transmission via blood products is now low. Whereas the primary routes of transmission of HCV had previously been blood transfusion or organ transplantation (Balogun, Ramsay et al. 2002), today the predominant route of transmission is sharing contaminated hypodermic needles.

However, vertical and sexual transmission do contribute moderately to the global prevalence of HCV (Busch 2001, Shepard, Finelli et al. 2005).

1.1.1 Epidemiology of HCV

Current studies estimate that there are around 115 million post-viraemic HCV infections worldwide, with up to 4 million people newly infected every year (Gower, Estes et al. 2014). This number accounts for 1.6% of the global population, and in the vast majority of cases (104 million) refers to adults (Westbrook and Dusheiko 2014). The most recent World Health Organisation (WHO) epidemiological record taken in 2009 reports that there are around 10 million cases in Africa, 6-12 million cases in Asia, 5-10 million cases in Europe, 3-5 million cases in India and 2-4 million cases in North America (WHO Epidemiological Record 2009).

To date seven genotypes of HCV have been identified, and these have about 30% divergence (Simmonds, Holmes et al. 1993, Simmonds, McOmish et al. 1993, Simmonds 2004). While these strains have a broadly similar mode of infection and progression, they show differences in geographical prevalence.

Genotype 1 is the most common genotype globally, as well as in Australasia, Europe, Latin America and North America, accounting for 62-71% of total cases in these countries. In contrast, genotype 3 accounts for 40% of infections in Asia. Genotype 4 is the most common genotype in North Africa and the Middle East, but when Egypt is excluded genotype 1 is the most common. Worldwide, genotype 3 represents 22% of cases, with genotypes 2 and 4 contributing to 13% of cases each (Gower, Estes et al. 2014). However, more than half the countries in the world do not have reports of the HCV infected population and so these estimates are likely to be an underrepresentation.

1.1.2 Outcome and treatment of HCV

It has been reported that more than 60% of HCV infections will progress to chronic liver disease, with 20% of infected patients developing cirrhosis of the liver and 5-7% developing end-stage liver disease (Seeff 2002, Chen and Morgan 2006, Seeff 2009). However, between 15-40% of those infected with HCV will spontaneously clear the virus. This is a process that is still poorly understood (Rustgi 2007, Grebely, Page et al. 2014).

Multiple lines of epidemiological evidence have shown that persistent infection with HCV is a major risk for the development of hepatocellular carcinoma (HCC), (de Oliveria Andrade, D'Oliveira et al. 2009) and the outcome of infection with HCV seems to be at least partly associated with the genotype of the virus. In general, individuals infected with genotype 1 appear to be more likely to develop a chronic infection and liver carcinoma (Mazzeo, Azzaroli et al. 2003, Resti, Jara et al. 2003). In contrast, individuals carrying a genotype 3 virus are more susceptible to steatosis, an abnormal retention of lipids (Farci, Shimoda et al. 2000).

Many HCV infections are asymptomatic, especially in the acute and early stages. This often results in a delay in detection and as such HCV infection may not be diagnosed until there is severe liver injury (Alter 1997, Shepard, Finelli et al. 2005). However, once detected chronic HCV can be treated and a 'cure' is deemed to be the achievement of a sustained virologic response (SVR), in which the level of viral RNA in the patient blood remains undetectable for 24 weeks following cessation of antiviral therapy.

At the time of writing, the standard of care (SOC) for chronic HCV infection in the UK is a combination treatment of pegylated interferon (PEG-IFN) and ribavirin (RBV). Whilst providing a relatively effective treatment in patients infected with genotype 2 or 3 viruses

(76%-86% SVR rates), the percentage of genotype 1 patients achieving SVR using this therapy is much lower (40%-64%) (Di Bisceglie and Hoofnagle 2002, Fried, Shiffman et al. 2002, Davis, Wong et al. 2003, McHutchison, Lawitz et al. 2009, Lawitz, Lalezari et al. 2013).

In recent years the landscape of HCV treatment has changed dramatically, and attention has moved towards drugs targeting multiple steps in the viral lifecycle (Gao, Nettles et al. 2010, Jacobson, McHutchison et al. 2011, Poordad, McCone et al. 2011). In 2011 the first generation of direct acting antivirals (DAAs) telaprevir and boceprevir were licensed for use (Lin, Kwong et al. 2006, Berman and Kwo 2009), and these raised genotype 1 patient SVR rates to 60.8% - 74.7% and 54.2% - 74.8% respectively. These drugs were developed to be particularly effective against the dominant NS3 protease in genotype 1, and have limited efficacy against other genotypes.

These numbers represent a significant improvement on the SVR rates obtained by use of IFN and RBV alone. However, levels of HCV RNA do not correlate directly with disease severity (Rustgi 2007), and the SVR for triple therapy with the first generation DAAs have remained relatively low due to a number of host, virus and treatment-related factors.

Host factors are numerous, and include age, male gender, cirrhosis, diabetes, alcohol consumption, coinfection with HIV or HBV, and the *IL28B* gene (Seeff 2002, Asselah, Estrabaud et al. 2010). Viral factors include genotype and high viral load, alongside the development of resistance: the HCV polymerase is highly error prone, leading to significant virus diversity and the potential for a rapid development of resistance. Indeed, both treatment-naive and treatment-experienced patients have been reported to carry HCV sequences that are predicted to be resistant to boceprevir and telaprevir (Kuntzen, Timm et

al. 2008, Lemm, O'Boyle et al. 2010, Susser, Vermehren et al. 2011, Palanisamy, Danielsson et al. 2013). Finally, treatment factors have provided significant obstacles to achieving SVR, particularly with regimens involving PEG-IFN. This regime can lead to anaemia, fatigue, headache and neutropenia, all of which can cause patients to discontinue their treatment (Manns, McHutchison et al. 2001, Torriani, Rodriguez-Torres et al. 2004). In addition to this, there can be compatibility issues between HCV drugs and other therapies, leading to a narrow range of possible treatments for some coninfected patients.

In late 2013 sofosbuvir and simeprevir were approved for use, and since have been used in combination with PEG-IFN and either with or without RBV. These have been demonstrated to be easier to use and result in higher efficiency rates and better tolerability alongside better patient reported outcomes (PRO) (Manns and Cornberg 2013, Younossi and Henry 2014).

Despite the significant advances made in HCV treatment in recent years, the long asymptomatic period of HCV infection means that chronic infection can still cause significant liver damage even if patients later achieve SVR.

1.2 VIROLOGY

1.2.1 The structure and genome of HCV

Despite significant breakthroughs in our understanding of HCV since its discovery, the structure of the virion is still poorly understood. Our current understanding is that it has a diameter of 50-80 nm, and is encompassed by a lipid bilayer in which the E1E2 glycoproteins are anchored (Gastaminza, Dryden et al. 2010, Catanese, Uryu et al. 2013). This bilayer

surrounds a nulceocapsid composed of the core protein which contains a positive sense single stranded RNA genome of 9600 base pairs (Gastaminza, Dryden et al. 2010, Bassendine, Sheridan et al. 2011) (Figure 1.1).

The HCV virion is known to associate with low density and very low density lipoproteins (LDL and vLDL) in the host (Andre, Komurian-Pradel et al. 2002, Merz, Long et al. 2011) and therefore has a lower buoyant density than many other viruses. Furthermore, due to this association with lipoproteins the virus is also able to associate with apolipoproteins such as apoE, apoB, apoA1, apoC1, C2 and C3 (Itzhaki, Irving et al. 2003, Chang, Jiang et al. 2007, Hishiki, Shimizu et al. 2010). This variation in associated proteins means that HCV virions have a range of buoyant densities (Lindenbach, Meuleman et al. 2006).
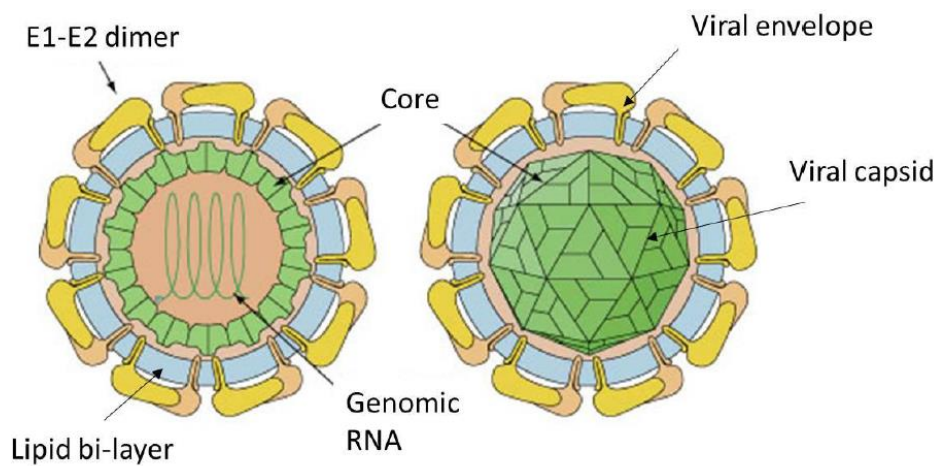
Figure 1.1: HCV viral particle. *The viral RNA genome is stabilised and surrounded by the capsid, which is icosahedral and composed of the viral core protein. The nucleocapsid is surrounded by a host cell-derived lipid envelope into which the viral glycoproteins E1 and E2 are inserted. These glycoproteins form a heterodimer which stabilises the viral particle and interacts with host receptors. Diagram from http://viralzone.expasy.org.*

1.2.2   Entry and uncoating

HCV entry is a complex, multistage process involving the interaction of HCV glycoproteins E1 and E2 with a number of cellular receptors. As with many viruses, entry is initiated by the formation of low affinity interactions between the virus and the host cell, and this facilitates subsequent high affinity interactions with a number of receptors. For HCV, the initial low affinity interactions occur with heparan sulphate proteoglycans, glycosaminoglycans (GAGs), lectins, and low density lipoprotein receptor (LDLR) 2 (Barth, Schnober et al. 2006, Koutsoudakis, Kaul et al. 2006).

HCV entry has been shown to be dependent on the expression of four entry receptors; scavenger receptor B1 (SR-B1) (Scarselli, Ansuini et al. 2002), the tetraspanin CD81 (Pileri, Uematsu et al. 1998), claudin-1 (Evans, von Hahn et al. 2007), and occludin (Ploss, Evans et al. 2009) (Figure 1.2).

In recent years, a number of further proteins with roles in HCV entry have been identified. Niemann-Pick C1-like 1 (NCP1L1) cholesterol absorption receptor appears to be involved at a very late stage of viral entry by interacting with virus-associated cholesterol (Ray 2012, Sainz, Barretto et al. 2012). Additionally, epidermal growth factor receptor (EGFR) and EphA2 have been identified as HCV entry cofactors which are able to boost levels of HCV entry both *in vitro* and *in vivo* (Lupberger, Zeisel et al. 2011, Diao, Pantua et al. 2012, Zona, Lupberger et al. 2013). Interestingly, CD63 has been shown to interact with E2 and to restrict HCV entry when knocked down, and it has been speculated that it may be involved in the entry process (Park, Park et al. 2013). Finally, it has been demonstrated that silencing transferrin receptor
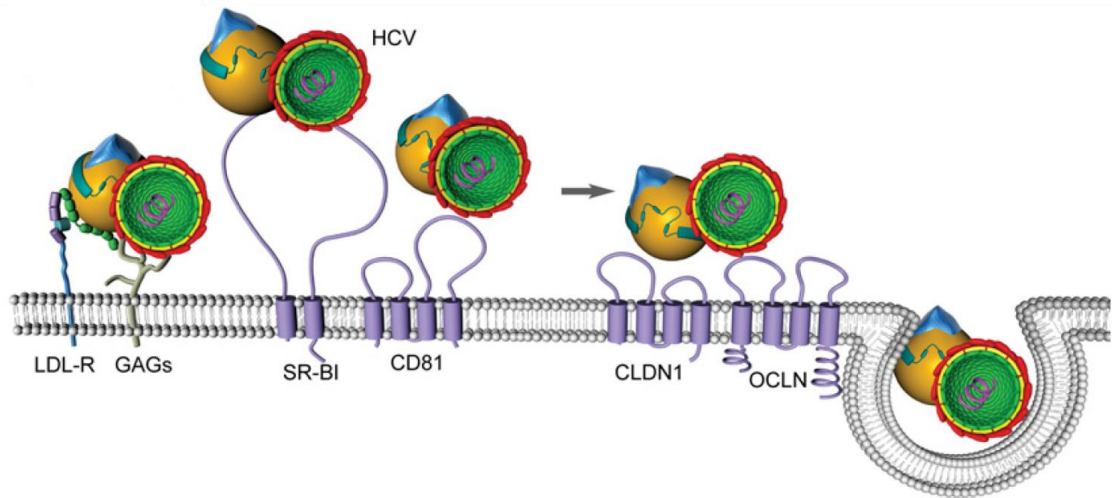
Figure 1.2: Host receptors in the HCV entry process. *Following initial binding steps involving LDL-R and GAGs, HCV entry has been demonstrated to be dependent upon in the expression of SR-B1, CD81, claudin-1, and occludin along with the endocytosis of the viral particle (Popescu and Dubuisson 2010).*

1 (TfR1) or adding antibodies to the protein either before or after viral inoculation inhibits HCV infection, suggesting that it acts at a post-binding step (Martin and Uprichard 2013).

The following section will discuss in detail the known roles and characteristics of the major HCV receptors.

1.2.2.1   SR-BI

SR-BI is a scavenger protein and is expressed mainly on steroidogenic tissues, macrophages, and in the liver (Krieger, Lohmann et al. 2001). It is involved in the selective uptake of cholesterol from ligands such as high density lipoproteins (HDLs) and their particle endocytosis or selective transfer to the membrane (reviewed in (Fidge 1999). In normal liver, it is predominantly expressed at the basolateral membrane of hepatocytes (Reynolds, Harris et al. 2008) (Figure 1.3).

SR-BI was identified as an HCV receptor by virtue of its specific interaction with HCV-E2 (Bartosch, Vitelli et al. 2003), likely facilitated by the hypervariable region 1 (HVR-1) domain of E2 (Scarselli, Ansuini et al. 2002, Bartosch, Dubuisson et al. 2003, Bartosch, Vitelli et al. 2003, Callens, Ciczora et al. 2005, Voisset, Op de Beeck et al. 2006). The importance of SR-B1 in HCV entry has since been verified using gene silencing and addition of anti – SRB1 antibodies (Lavillette, Tarr et al. 2005, von Hahn, Lindenbach et al. 2006, Grove, Huby et al. 2007, Dreux and Cosset 2009). Furthermore, HDLs have been shown to promote HCV infection in an SR-BI dependent manner (Bartosch, Verney et al. 2005, Meunier, Engle et al. 2005, Voisset, Callens et al. 2005).

Deleting the HVR1 domain has been shown to decrease the dependency of virus entry on SR-B1, but to increase the affinity of the E2-CD81 interaction (Bankwitz, Steinmann et al. 2010, McCaffrey, Gouklani et al. 2011, Prentoe, Serre et al. 2014). Therefore, HVR1 may interact directly or indirectly with SR-B1 to cause a conformational change in E2 exposing the CD81 binding site (Bankwitz, Steinmann et al. 2010).

1.2.2.2 CD81

CD81 was first described in 1990 (Oren, Takahashi et al. 1990), and was initially identified as an HCV receptor due to its interaction with HCV-E2 (Pileri, Uematsu et al. 1998). Its role was later confirmed by the discovery that its expression in a CD81-deficient cell line confers infectivity (Bartosch, Vitelli et al. 2003, Hsu, Zhang et al. 2003, Cormier, Tsamis et al. 2004, Zhang, Randall et al. 2004, Lavillette, Tarr et al. 2005, Lindenbach, Evans et al. 2005), and that the level of HCV infection is closely related to cellular CD81 expression levels (Akazawa, Date et al. 2007, Koutsoudakis, Herrmann et al. 2007, Rocha-Perugini, Lavie et al. 2009). In support of this, downregulating CD81 levels using siRNA in hepatoma cells has been shown to abolish infection (Zhang, Randall et al. 2004, Akazawa, Date et al. 2007, Koutsoudakis, Herrmann et al. 2007, Molina, Castet et al. 2008).

CD81 is expressed on all cells of the body with the exception of red blood cells, neutrophils and platelets, and in the liver is expressed on the sinusoidal epithelium and hepatocytes. In normal liver, CD81 is expressed predominantly at the basolateral surface of hepatocytes, with minimal expression at the apical membrane (Reynolds, Harris et al. 2008) (Figure 1.3).

Due to the direct nature of the interaction between CD81 and HCV-E2, there has been extensive research into therapeutically targeting CD81 to prevent HCV entry and this has

robustly demonstrated the essential role of CD81 in the process. Neutralising antibodies against the CD81-LEL have been shown to inhibit entry of HCV pseudoparticles (HCVpp) and HCV in cell culture (HCVcc) infection as well as serum-derived HCV (Scarselli, Ansuini et al. 2002, Bartosch, Vitelli et al. 2003, Hsu, Zhang et al. 2003, Cormier, Tsamis et al. 2004, Zhang, Randall et al. 2004, Lavillette, Tarr et al. 2005, Wakita, Pietschmann et al. 2005, Zhong, Gastaminza et al. 2005, Koutsoudakis, Kaul et al. 2006, Kapadia, Barth et al. 2007) along with protecting against HCV infection *in vivo* (Meuleman, Hesselgesser et al. 2008). Furthermore, antibodies specific to CD81 can neutralise infection post entry (Farquhar, Hu et al. 2012).

1.2.2.3   Claudin-1

In 2007, Evans et al., (Evans, von Hahn et al. 2007) created a complimentary DNA (cDNA) library from the permissive hepatocarcinoma cell line Huh-7.5 and used an iterative expression cloning approach to express the relevant proteins in the non-permissive 293T cell line. Infection of these cells led to claudin-1 subsequently being identified as a potential HCV receptor (Evans et al. 2007). Both claudin-6 and -9 are to compensate as receptors if claudin-1 is absent (Meertens, Bertaux et al. 2008), however these are expressed at a very low level in the liver (Zheng, Yuan et al. 2007) and cannot be used by all genotypes: genotype 2a and 2b viruses cannot use claudin-6 for infection, whereas viruses with broad viral tropism can use claudin-6 for escape from antibodies specific for claudin-1 (Haid, Grethe et al. 2013).

Claudin-1 is expressed at its highest concentrations in the liver, but is also present in many other tissues (Furuse, Fujita et al. 1998). In healthy liver tissue, it is expressed at both the canalicular and basolateral membranes of hepatocytes (Reynolds, Harris et al. 2008) (Figure 1.3). It is a 25 kDa integral transmembrane protein with a structure that is similar to that of

CD81, with four transmembrane domains, two extracellular loops and one intracellular region (Furuse, Hata et al. 2002). The residues in claudin-1 which are necessary for HCV infection are in the first extracellular loop in the highly conserved W_{30}-GLW_{51}-C_{54}-C_{64} domain (Cukierman, Meertens et al. 2009).

Claudin-1 plays a key role in the formation of tight junctions (Krause, Winkler et al. 2008), and members of the claudin-1 family are able to form dimers between proteins both on the same cell and on adjacent cells (Piontek, Winkler et al. 2008). The latter interaction has been implicated in HCV entry (Liu, Yang et al. 2009). Claudins are also able to form heterodimers with SR-B1, occludin and CD81, (Farquhar, Harris et al. 2008, Piontek, Winkler et al. 2008, Reynolds, Harris et al. 2008, Harris, Davis et al. 2010, Zona, Lupberger et al. 2013). The formation of the CD81- claudin-1 interaction is essential for HCV entry (Yang, Qiu et al. 2008; Cukierman et al. 2009; Harris et al. 2010; Krieger et al. 2010) and appears to be necessary for clathrin-mediated endocytosis of the receptor complex and for fusion with Rab5a endosomes (Farquhar, Hu et al. 2012). Recent evidence also suggests that claudin-1 may potentiate the interaction between CD81 and HCV-E2 (Krieger, Zeisel et al. 2010).

However, there is no evidence for a direct interaction between claudin-1 and infectious viral particles, although recent work has shown that E1E2 complexes can interact with claudin-1 (Douam, Dao Thi et al. 2014) and the authors suggest that the lack of binding is due to host-derived lipoproteins masking the viral envelope.

1.2.2.4   Occludin

cDNA screening identified the tight junction protein occludin as necessary to confer HCVpp entry into the non-permissive murine fibroblast cell line NIH3T3 expressing CD81, claudin-1

and SRB1 (Ploss, Evans et al. 2009). In the same year, occludin was independently identified as an HCV receptor by siRNA silencing of proteins known to associate with claudin-1 in Huh-7.5 cells (Liu, Yang et al. 2009). Whilst occludin has been reported to interact with the E2 glycoprotein, it is unknown whether this is direct or indirect via CD81- claudin-1 (Meredith, Wilson et al. 2012). Occludin is a tight junction protein, and internalises with claudin-1 in caveolae and clathrin-dependent processes (Stamatovic, Keep et al. 2009). In healthy liver, occludin is expressed solely at the apical surface of hepatocytes (Figure 1.3).

1.2.2.5   Other factors which affect HCV entry

There are a number of additional factors which have been demonstrated to affect HCV entry. For example, enrichment of ceramide at the plasma membrane induces the internalisation of CD81, and thus inhibits infection (Tribouillard-Tanvier, Beringue et al. 2008). Additionally, the depletion of cholesterol inhibits HCV infection, possibly as a result of interactions with CD81 (Charrin, Manie et al. 2003, Kapadia, Barth et al. 2007).

CD81 **SR-BI** **Claudin-1** **Occludin**
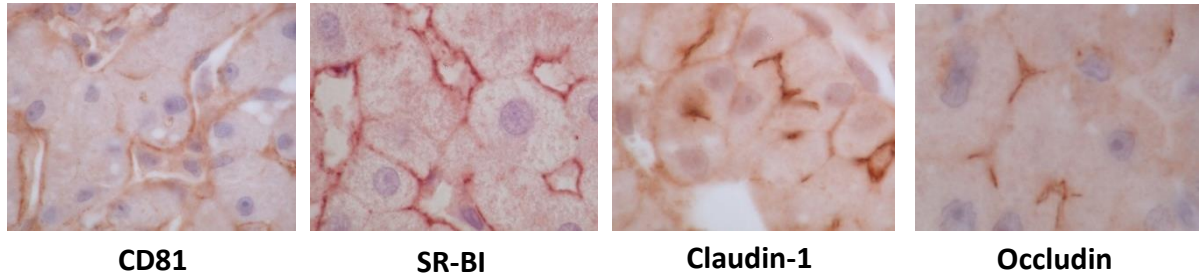
Figure 1.3: Localisation of HCV receptors in normal liver tissue. The expression of CD81, SR-B1, claudin-1 and occludin in hepatocytes in a healthy liver (Reynolds, Harris et al. 2008).

1.2.3 Internalisation of the virus

Internalisation of HCV has been shown to occur by dynamin-dependent clathrin-mediated endocytosis into Rab5 positive endosomes (Blanchard, Belouzard et al. 2006, Meertens, Bertaux et al. 2006, Coller, Berger et al. 2009) in a Rho dependent manner (Farquhar, Hu et al. 2012). Studies using both HCVpp (Hsu, Zhang et al. 2003) and HCVcc (Tscherne, Jones et al. 2006) have demonstrated that this occurs in a pH dependent manner. In other enveloped viruses, a drop in pH causes a conformational change in the envelope glycoproteins to expose fusion peptides. These are responsible for triggering a fusion with the endosomal membrane and their exposure therefore leads to the release of the viral genome into the cytosol (Thorley, McKeating et al. 2010).

Three classical fusion loop motifs have been reported in the HCV E1 and E2 glycoproteins, and their importance confirmed using site-directed mutagenesis (Lavillette, Pecheur et al. 2007), suggesting that the HCV genome is released by a similar fusion to process to that described above. However, in contrast to the initial structure of the E2 ectodomain (Krey, d'Alayer et al. 2010) the recently published crystal structures did not identify any classical fusion peptides, and this model does not demonstrate any significant changes in conformation when exposed to a low pH (Kong, Giang et al. 2013, Khan, Whidby et al. 2014). Therefore, the exact mechanism of HCV genome release is not understood. The diagram below illustrates the current model of the HCV lifecycle (Figure 1.4).
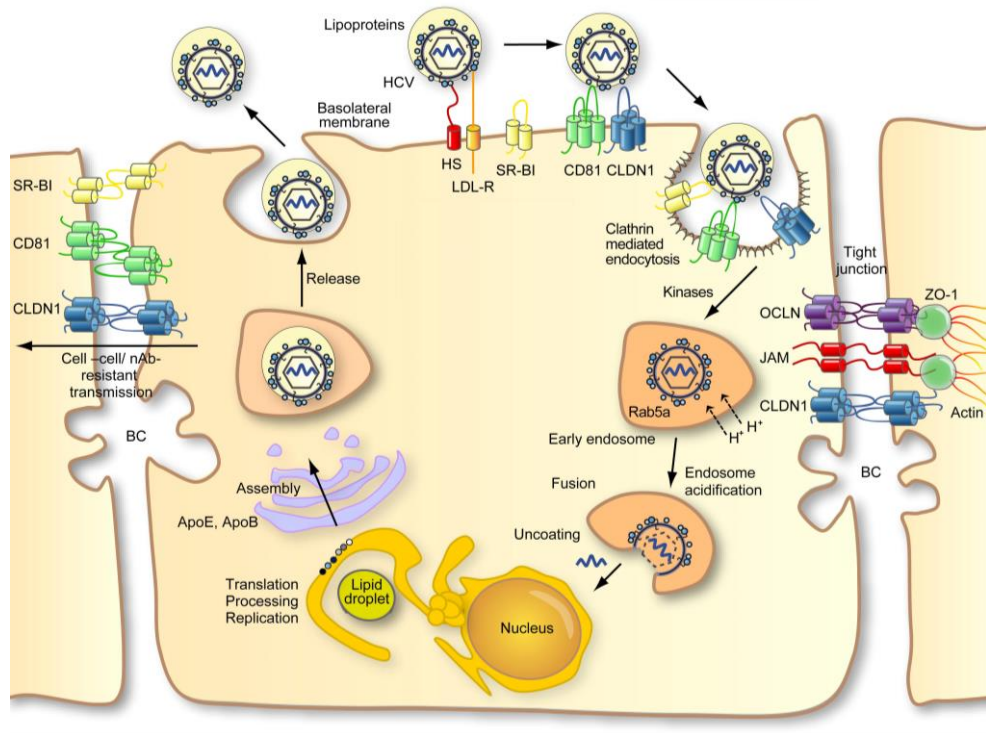
Figure 1.4: The HCV lifecycle. *Following initial interactions with LDLR and GAGs, the virion undergoes high affinity interactions with SR-B1, CD81 and claudin-1 in a coreceptor complex, and occludin. Following virus internalisation in a clathrin-dependent mechanism, the virus fuses with the endosome and the genome is released into the cytoplasm. Here, it associates with ER-derived membranous webs where the viral replication processes take place. The resulting assembly process is highly associated with the apolipoprotein synthesis. Diagram from (Zeisel, Fofana et al. 2011).*

1.3 THE HCV VIRAL GENOME

The HCV genome comprises a 9600 base uncapped positive sense single RNA strand, whose 5' and 3' untranslated regions act as control elements for translation and replication. The area between these regions is a single uninterrupted open reading frame (ORF), which when translated results in a single polyprotein of around 3011 amino acids (aa). This polyprotein is modified by host and viral proteases to give 3 structural proteins – core, E1 and E2 - and 7 non-structural proteins – p7, NS2, NS3, NS4A, NS4B, NS5A and NS5B (for review see (Lindenbach, Evans et al. 2005, Zeisel, Koutsoudakis et al. 2007, Ashfaq, Javed et al. 2011) (Figure 1.5). The host proteins involved in this process are signalase and signal peptide peptidase, and the viral proteases involved are NS2-NS3 and NS3-NS4A (Kuo, Choo et al. 1989).

Figure 1.5: Diagram of the HCV genome. Modified from (Moradpour, Penin et al. 2007).

21

1.3.1 Translation of the viral genome and polyprotein maturation

Following internalisation the viral capsid is uncoated, and translation of the HCV genome has been demonstrated to occur in the rough endoplasmic reticulum (ER). It is at this stage of the replication cycle that the majority of changes to the HCV glycoproteins E1 and E2 are made. The C terminal and transmembrane domains of the glycoproteins form hairpin structures which cross the ER membrane twice. When they are separated the C-terminal domains translocate to the cytoplasm, where the type 1 membrane topology of the mature glycoproteins is formed whilst the proteins remain facing the ER (Akazawa, Date et al. 2007). These proteins later undergo the final maturation steps of glycosylation and disulphide rearrangement in the Golgi apparatus.

At this point, NS2 and the highly hydrophobic NS3 are cleaved by zinc-dependent cysteine protease activity at the C-terminal of NS2 and the N –terminal of NS3 (Akazawa, Date et al. 2007, Moradpour, Penin et al. 2007, Lango Allen, Estrada et al. 2010). The remaining polyprotein is cleaved by the serine protease activity of the N terminal of NS3 in association with NS4.

In addition to its role as a serine protease, NS3 also has RNA helicase/NTPase activity. This is necessary for separating dsRNA replication intermediates, removing nucleic acid binding proteins from the genome and for eliminating RNA secondary structures. Therefore, it is thought that NS3 plays a role in RNA unwinding. NS4A also has RNA helicase/NTPase activity, and in addition to acting as the NS3 cofactor has a role in locating NS3 to the ER membrane (Dubuisson 2007; Moradpour, Penin et al. 2007; Suzuki, Ishii et al. 2007; Joyce and Tyrrell 2010; Kim and Chang). Alongside its role in the virus lifecycle, the HCV protease NS3 also

disrupts the IFN and TLR3 pathways which are activated in response to the recognition of pathogens by the host cell. Specifically, NS3 cleaves a number of host proteins including the caspase recruitment domain of MAVS (Li, Foy et al. 2005, Meylan, Curran et al. 2005) and TRIF (Li, Foy et al. 2005).

1.3.2   Viral replication

Following translation, the viral replicase protein NS4B in association with NS5A initiates a complex membrane remodelling process to form a membranous web composed of double and multi-membrane vesicles (DMV and MMV), and this is the site of replication of the HCV virus (Egger, Wolk et al. 2002, Moradpour, Penin et al. 2007, Romero-Brey, Merz et al. 2012). In addition to initiating the formation of these essential structures, NS4B may be necessary for recruiting the non-structural proteins to this site, including the RNA dependent RNA polymerase (RdRp) NS5B (Elazar, Liu et al. 2004).

NS5B is responsible for synthesising the complementary negative strand RNA from the original positive strand genome which is then used to make a positive genome for viral assembly (Gu and Rice 2013; Kim and Chang 2013; Moradpour 2007; Suzuki 2007). NS5B does this in a primer-dependent manner, with 3' UTR structures creating a cis-acting 'copy back' strand, and secondary structures priming the complimentary strand for replication. The phosphorylation state of NS5B regulates the balance between RNA replication and downstream processes (Neddermann, Quintavalle et al. 2004) and acts as an RdRp (Behrens, Tomei et al. 1996).

 NS5B exhibits a significant lack of proofreading and error correction mechanism and as a result, HCV replication is highly error prone and generates a high degree of genetic diversity

(Cruz-Rivera, Carpio-Pedroza et al. 2013) (Honegger, Kim et al. 2013). This means that HCV is able to rapidly adapt to pressures such as the immune response and antiviral therapy (von Hahn, Yoon et al. 2007, Ralston, Jacobson et al. 2011, Honegger, Kim et al. 2013).

NS5A has been demonstrated to interact with a number of host and viral partners including core (Masaki 2008), cyclophillin A (Lim and Hwang et al., 2011) and PI4KIIIα (Foster 2011). It also binds to positive and negative strands before replication (Huang 2005) in a manner dependent upon its phosphorylation status (Shulla and Randall 2012).

1.3.3 Assembly and release of HCV virions

Following replication, signal peptidase and signal peptide peptidase cleave the polyprotein to form a mature protein on the ER-derived membranous web. The protein then relocates to cytoplasmic lipid droplets (McLauchlan, Lemberg et al. 2002, Boulant, Montserret et al. 2006) in a process assisted by diacylglycerol diacyltransferase-1 (DGAT1) (Herker, Harris et al. 2010).

This stage of the HCV lifecycle is not completely understood. In the current model, newly synthesised RNA and structural proteins are assembled on ER-derived lipid droplets in association with the membranous web.

The core protein is concentrated on these lipid droplets, and there are surrounded by membranous structures containing the non-structural viral proteins (Miyanari 2007). NS5A associates with host apolipoproteins including ApoE, which are incorporated into the viral envelope (Benga 2010). The core protein also plays an essential role in this process, and if it is not present studies have shown a reduction in infectious particle release (Miyanari 2007).

During viral packing, NS2 is believed to interact with p7, and this stabilises the structure of NS2 alongside promoting the association of NS2 and NS3/4A (Lindenbach 2013; Lindenbach and Rice 2013; Stapleford and Lindenbach 2011). The latter interaction leads to the trafficking of core from the lipid droplets to the assembly site (Coller 2012). In addition to core, NS2 also recruits E1E2 to the assembly site (Stapleford and Lindenbach 2011), and the interaction between core and NS5A at this point on lipid droplets is thought to play a central role in genome packaging and the formation of the icosahedral capsid (Miyanari 2007).

The final assembly stages of the virus are thought to occur by budding into the ER, where the last stages of viral maturation is closely linked with the vLDL secretion pathway (Gastaminza 2008). A study using HCVcc has demonstrated that it is translocated to the Golgi, where the final maturation steps are thought to occur (Gastaminza 2008) and E2 is glycosylated by Golgi glycosidases and glycosyltransferases (Vieyres 2010). Following this, the virions are sorted into endosomal compartments and released at the PM (Coller 2012). The non-structural p7 protein plays an essential role at this point by forming ion channels in artificial bilayers, thus preventing acidification of endolysosomal compartments during the secretion (Wozniak 2010).

1.4 VIRAL TRANSMISSION

HCV can be transmitted between cells via two routes – by extracellular virus particles or cell-cell transmission (Marsh and Helenius 2006, Timpe, Stamataki et al. 2008). The cell-cell route was initially described following the identification of foci of positive cells in infected human livers (Chang, Williams et al. 2003, Wieland, Makowska et al. 2014), suggesting a preferential transference of infection between contacting cells. Whilst all four receptors play a role in

HCV entry (Grove, Huby et al. 2007, Grove, Nielsen et al. 2008, Brimacombe, Grove et al. 2011, Syder, Lee et al. 2011), cell-cell transmission is relatively more dependent on SR-B1 expression (Meredith, Harris et al. 2013).

It has been demonstrated recently that tetraspanin-rich exosomes from cells infected with HCV can infect naive human hepatoma cells even in the presence of neutralising antibodies (Ramakrishnaiah, Thumann et al. 2013, Bukong, Momen-Heravi et al. 2014), and are also able to transfer the HCV viral RNA to both uninfected human hepatoma cells and plasmacytoid dendritic cells (pDCs). In the latter, transference of viral RNA has been demonstrated to induce the production of type 1 interferon (IFN) in a TLR-7-dependent manner (Dreux, Garaigorta et al. 2012). These exosomes have been observed both in the serum of HCV-infected patients and in the supernatant of HCV-infected cells (Pietschmann, Lohmann et al. 2002, Masciopinto, Giovani et al. 2004, Gastaminza, Dryden et al. 2010, Bukong, Momen-Heravi et al. 2014). Exosomes have been reported to be involved in the mediation of infection by a number of agents including viruses and bacteria (Bhatnagar, Shinagawa et al. 2007, Silverman and Reiner 2011).

1.5   HEPATIC POLARITY AND HEPATOCYTES AS A TARGET

1.5.1   Liver physiology

The liver is a large and complex organ consisting of numerous specialised cell types which allow it to carry out a range of essential functions. Hepatocytes are the parenchymal cells of the liver and make up 80% of liver mass, with the other 20% comprising non-parenchymal cell types such as liver sinusoidal endothelial cells (LSECs) and liver myofibroblasts. The blood supply to the liver enters via the sinusoids, and leaves via the portal vein (Figure 1.6).

Structurally, the hepatocytes are separated from the sinusoidal blood vessels by the Space of Disse, and are arranged into plates giving a large area for nutrient absorption (Branch, Stump et al. 2005). One of the many functions of the liver is to produce bile, and this is secreted by the hepatocytes into the extensive network of bile canaliculi (BC), which merge to form ductules and eventually the common hepatic duct (Figure 1.6). Hepatocytes are also responsible for carrying out a range of metabolic and detoxification functions which are unique to the liver (Kim and Rajagopalan 2010), such as detoxification (Decaens, Durand et al. 2008).
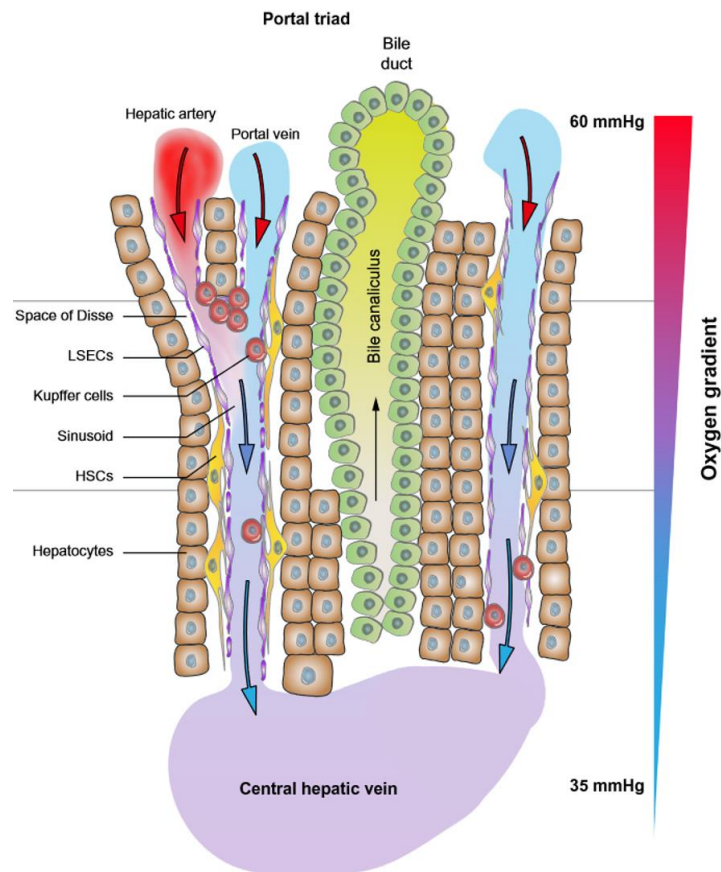
Figure 1.6: Schematic diagram of liver physiology. *Hepatic blood vessels are shown bounded by LSECs, Kupffer cells and hepatic stellate cells (HSC) and separated from the hepatocytes by the Space of Disse. The bile canaliculus is shown bounded by a single layer of hepatocytes and separated from the hepatic blood vessels by at least one layer of hepatocytes. Adapted from (Wilson, Tennant et al. 2014).*

1.5.2   Hepatic Polarity

Many tissues in the body contain polarised cells, and their polarity contributes not only to their function but also to the formation of a barrier, for example in the gut or airways. The majority of epithelial cells exhibit a simple, columnar polarity with only one apical and one basal surface (Cereijido, Valdes et al. 1998, Shin, Fogg et al. 2006). These surfaces appose each other, with the lateral surfaces in contact with neighbouring cells forming interactions such as tight junctions (TJ) and adherens junctions (AJ) (Figure 1.7a). These junctions contain characteristic sets of proteins, with claudin, occludin and junctional adhesion molecule (JAM) in tight junctions and cadherin and nectin in adherens junctions (Figure 1.7b).

In contrast to this, hepatocytes exhibit a more complex polarity, and instead are polygonal and multipolar, with several apical membranes bounded by tight junctions. The apical membranes of adjacent cells form the walls of BC lumen (Feldmann 1989, Selden, Khalil et al. 1999, Decaens, Durand et al. 2008, Mee, Harris et al. 2009, Perrault and Pecheur 2009), with at least two basolateral membranes facing the sinusoids (Figure 1.7c). Therefore, the polarised nature of the hepatocyte is essential to maintaining the separation between blood and bile (Figure 1.6).

The apical and basal poles of the cell contain specific proteins which allow the hepatocyte to carry out essential functions. The apical surface carries out secretory functions via the actions of proteins such as multidrug resistance protein 2 (MRP2) and bile salt export pump (BSEP) (Trauner and Boyer 2003, Decaens, Durand et al. 2008). In contrast, the hepatic basal membrane expresses characteristic proteins such as Na^+/Taurocholate cotransporting

(a) Polarised epithelial cell
apical (lumen)
TJ
AJ
basal (tissue)

(b) The junctional complex
Actin
ZO1
ZO2
CLDN
OCLN — TJ
JAM
Cadherin — AJ
Nectin

(c) Polarised hepatocyte
basal (sinusoid)
Apical
Bile Canalicula (BC)
basal (sinusoid)
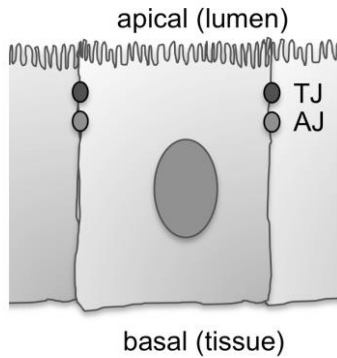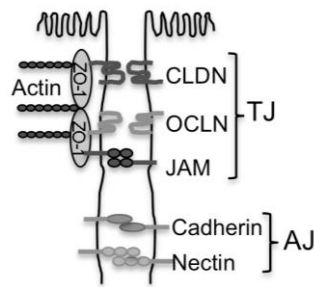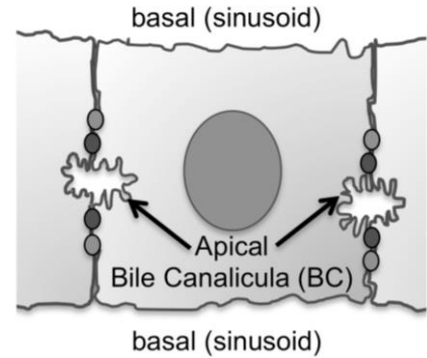
Figure 1.7: Organisation of epithelial polarity. *In polarised epithelial cells a single apical and basal membrane appose each other and are separated by tight junctions (TJ) and adherens junctions (AJ), with the apical surface facing the lumen and the basal surface facing the tissue (a). The junctional complex is shown in more detail, with typical proteins of the TJ and AJ annotated alongside their linkage to the cytoskeleton (b). Polarised hepatocytes have several apical membranes which form the walls of the bile canaliculus, and these are separated by TJs and AJs from the basal membranes which face the sinusoids (c).*

polypeptide (NTCP) and organic anion transporting polypeptide proteins which allow the uptake of biliary salts from the circulation. The tight junctions in hepatocytes are composed of transmembrane proteins with associated cytoplasmic proteins. Such proteins include members of the zona occludins (ZO) and claudin families. The HCV receptors also localise distinctly in a polarised cell, with CD81 at the apical and basolateral surfaces, claudin-1 at the apical surface with minimal basolateral expression, and SR-B1 at the basolateral surface (Reynolds, Harris et al. 2008) (Figure 1.3).

The establishment of hepatic polarity also necessitates the coordination of the cytoskeleton and the Golgi apparatus, along with the organisation of tight junctions and specialised membrane domains.

The major components of the cytoskeleton have both direct and indirect associations to the plasma membrane, especially at the tight junctions of polarised cells. In hepatocytes, the BC is surrounded by two circumferential belts of actin and actin binding proteins. The first belt contains myosin II, is in association with the adherens junctions, and is involved in the contractility of the BC. The second regulates transport near the plasma membrane (Tsukada and Phillips 1993). Microtubules are also very highly concentrated around the BC, and are central to the development of cellular polarity (Novikoff, Cammer et al. 1996). They are organised in a polar fashion with the minus ends facing the apical membrane allowing the trafficking of not only apical membrane proteins (Bacallao, Antony et al. 1989, Cohen, Brennwald et al. 2004), but also the arrangement of the Golgi between the nucleus and apical membrane (Musat, Sattler et al. 1993). Indeed, the Golgi apparatus exhibits changes in structure and function along this axis (Baumann and Walz 2001). Along with the high

concentration of microtubules around the BC, these structures are also stabilised by intermediate filaments.

1.6 VIRUS INFECTION OF POLARISED CELLS

The establishment of cellular polarity is refractory to the entry stages of a number of viruses, as many utilise junctional receptors in their entry pathways. A number of viruses have therefore evolved mechanisms to overcome these barrier sites and disseminate viral particles, and some of the most notable examples are discussed briefly below.

The rotavirus expresses two viral proteins which allow it to manipulate cellular polarity. The non-structural protein NSP4 and capsid spike protein VP4 have both been demonstrated to induce changes in the actin cytoskeleton (Gardet, Breton et al. 2006, Berkova, Crawford et al. 2007), and the expression of NSP4 alone causes epithelial leakage, tight junction disruption and membrane destabilisation (Tafazoli, Zeng et al. 2001). This has the effect of making the intracellular actin network more accessible for virus entry and trafficking.

Similarly, the adenovirus has established a complex mechanism to utilise receptors from the basolateral domains – Coxsackievirus adenovirus receptor (CAR) and $\alpha_v\beta_{3-5}$- to infect from the apical surface. Adenovirus-infected macrophages secrete IL-8, which cause CAR and $\alpha_v\beta_{3-5}$ to relocate to the apical membrane in a Src-dependent manner (Lutschg, Boucke et al. 2011). These receptors are then available for the virus to utilise in entry. In a similar manner, the coxsackie virus B (CVB) initially interacts with decay accelerating factor (DAF) at the apical surface (Bergelson, Modlin et al. 1997, Shieh and Bergelson 2002, Coyne and Bergelson 2006). Cross-linking of apically-located DAF can induce it to form larger lipid rafts containing other

proteins, and as a result Abl is activated. Abl is a tyrosine kinase, and its activation results in a Rac-dependent actin reorganisation which relocates the CVB-DAF dimer to the TJ in an actin-dependent process (Coyne and Bergelson 2006). This then allows the complex to interact with CAR, whose involvement is necessary for the initiation of CVB uncoating.

These examples demonstrate the ability of viruses to utilise the association of actin with the cell membrane, actin signalling and regulatory components and TJ proteins to facilitate viral entry despite the polarised nature of their target cells.

1.7 TOOLS TO STUDY HCV

Attempting to recreate complex hepatic polarity *in vitro* has proved problematic. Whilst it is possible to use primary human hepatocytes (PHH) for research into the viral lifecycle, over time in cell culture PHH and primary non-parenchymal cells dedifferentiate and undergo a number of physiological and metabolic changes. These include the dissolution of the nucleus (karyolysis) and cytoskeletal rearrangement, and this leads to a fibroblast-like appearance and cells ultimately detach and die (Berthiaume, Moghe et al. 1996, Wang and Boyer 2004). Additionally, PHH are generally hard to use and maintain and the methods of doing so vary considerably between labs. Specifically in terms of HCV, primary hepatocyte cultures support low levels of HCV infection, and preparations of hepatocytes from different donors exhibit heterogeneous viral populations (Bartenschlager and Lohmann 2001, Gondeau, Pichard-Garcia et al. 2009).

The expense and difficulty of obtaining and using model systems necessitates the use of cell culture systems across the field of biology. However, finding such a system which accurately

replicates the specialised and complex nature of the liver has been a major challenge in the progression of HCV research.

1.7.1   In vitro systems

In addition to being essential for the correct functioning of the liver, hepatic polarity has also been demonstrated restrict HCV entry (Mee, Grove et al. 2008, Mee, Harris et al. 2009, Harris, Clerte et al. 2013). As a result, identifying a cell type which polarizes and supports HCV replication has been a key area for research.

The HepG2 cell line is a perpetual cell line isolated from the well-differentiated hepatocellular carcinoma of a 15 year old Caucasian male (ATCC). It is able to polarise and to generate apical cysts equivalent to bile canaliculi (BCs) which can span several cells (Herrema, Czajkowska et al. 2006), are functional as BCs and are easily visible (Mee, Harris et al. 2009) (Figure 1.8). These cysts contain integral TJs, and cultures of HepG2s have been demonstrated to achieve up to 40% of cells polarised over time in culture (Theard, Steiner et al. 2007, Decaens, Durand et al. 2008, Mee, Harris et al. 2009). Whilst HepG2 cells also display the correct localisation of apical membrane markers, claudin (Zegers and Hoekstra 1997, Kubitz, Sutfels et al. 2004, Reynolds, Harris et al. 2008) and cytoskeletal components (Sormunen, Eskelinen et al. 1993), they do not naturally express CD81, and therefore this must be done exogenously. Additionally, they do not express miR-122, a liver-specific miRNA which is required for HCV replication (Jopling, Yi et al. 2005), and (Jopling, Yi et al. 2005), and therefore HepG2s only weakly support HCV replication and viral assembly, around 850-fold lower than Huh-7.5 (Lindenbach, Evans et al. 2005, Flint, von Hahn et al. 2006, Narbus, Israelow et al. 2011).

In terms of infectivity studies then, a different cell type is necessary and for this the Huh- 7 cell line and its derivatives are widely used (Lohmann, Korner et al. 1999). This immortal cell line was derived from the well-differentiated hepatocellular carcinoma of a 57 year old Japanese male. Although these polarise very poorly, they naturally express the four essential HCV receptors and are capable of supporting a robust level of infection (Lohmann, Korner et al. 1999). The latter characteristic is attributed to a defective retinoic acid inducible gene-I (RIG-I) pathway (Preiss, Thompson et al. 2008).
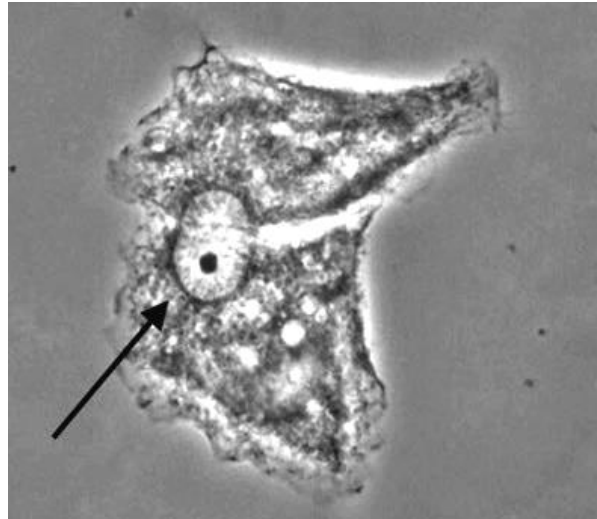
Figure 1.8: Phase contrast image of two polarised HepG2 cells forming a bile canaliculus
(black arrow). Thanks to Sven van Ijzendoorn.

1.7.2 Animal models

The use of chimpanzee animal models has been central to the breakthroughs in our understanding of HCV to date, and is the only animal model of HCV able to support infection by all HCV genotypes (Bukh 2012). Most notably, chimpanzees were used to isolate the virus itself (Choo, Kuo et al. 1989), but the similarity of their innate and adaptive immune responses to that of infected humans (Bukh 2004, Bukh, Meuleman et al. 2010) means that they have been essential to furthering our understanding of HCV disease processes since (Houghton 2009). In terms of understanding the host response to HCV infection, chimpanzee models have been used to investigate the immune response and intrahepatic response to primary and secondary infections (Bukh 2004, Bowen and Walker 2005, Rehermann 2009). They have also been heavily involved in the development of other model systems, as their use in demonstrating the infectivity of HCV clones (Kolykhalov, Agapov et al. 1997, Yanagi, Purcell et al. 1997, Yanagi, Purcell et al. 1999, Sakai, Takikawa et al. 2007, Gottwein, Scheel et al. 2010) led to the development of HCV culture systems (Lohmann, Korner et al. 1999, Wakita, Pietschmann et al. 2005, Lindenbach, Meuleman et al. 2006) and that of small, genetically humanized animal models that can be challenged with modified forms of HCV (Dorner, Horwitz et al. 2011, Bukh 2012). This is the only alternative *in vivo* model available, as mouse livers are otherwise unable to support HCV infection and no other primate model has yet been identified.

1.7.3 Virus models

1.7.3.1 Cell culture virus systems

Early attempts to study the virus-host interaction and entry stages of the viral lifecycle utilised the viral glycoproteins E1E2 expressed in isolation from other the viral proteins. However, expressing high levels of these proteins in a cellular background resulted in their misfolding and aggregation due their transmembrane domains containing sequences which promote ER retention and heterodimerisation (Cocquerel, Wychowski et al. 2000). Therefore, chimeric E1E2 proteins were developed which incorporated only sections of the TM regions of E1E2 known to be expressed at the plasma membrane, or were truncated proteins lacking TM domains entirely (Flint, Maidens et al. 1999, von Hahn and Rice 2008). This latter method resulted in a soluble form of E2 (sE2) (Michalak, Wychowski et al. 1997, Flint, Maidens et al. 1999). This approach laid the foundation for many studies identifying receptors, and was subsequently used to identify both SR-B1 and CD81 as receptors.

Retroviruses are able to incorporate glycoproteins into their membranes during budding, and this characteristic was used to develop the infectious HCV pseudoparticle system (HCVpp) (Hsu, Zhang et al. 2003) which is now widely used. HCVpp are generated using human embryonic kidney (293T) cells into which the *gag-pol* gene of murine leaukaemia virus (MLV) or HIV is transfected alongside the E1E2 glycoproteins and a GFP or luciferase reporter gene (Figure 1.9). Expression of gag-pol leads to the assembly of retroviral particles, and these contain the provirus genome encoding the reporter gene. During release, E1E2 is incorporated into the envelope resulting in an infectious particle whose entry is mediated solely by the expression of E1E2 glycoproteins. Following entry and the delivery of the

retroviral nucleocapsid protein into the cytoplasm, the viral genome is reverse transcribed and incorporated into the host cell genome, with the reporter gene expressed for a readout (Voisset, Op de Beeck et al. 2006, Regeard, Lepere et al. 2007, von Hahn and Rice 2008).

HCVpp infection can be blocked by neutralising antibodies to the viral glycoproteins E1 and E2, providing confirmation that they are essential for HCV entry (Lagging, Meyer et al. 1998, Bartosch, Dubuisson et al. 2003, Hsu, Zhang et al. 2003) and this system was central to the identification of occludin and claudin-1 as receptors. In the time since, glycoproteins from different genotypes have been isolated and used to create HCVpp for studying genotype specific events and characteristics (Bartosch, Dubuisson et al. 2003). However, this system only models the entry stages of the viral lifecycle, and does not allow the association of the virus with lipoproteins.

Until its development, the lack of HCV cell culture (HCVcc) system was a major obstacle to the study of the full HCV lifecycle. However, since 2005 it has been possible to study the full viral lifecycle of HCV with complete viral replication processes and infectious particle release, following the cloning of a genotype 2a virus from a patient carrying an acute HCV infection (Lindenbach, Evans et al. 2005, Wakita, Pietschmann et al. 2005, Zhong, Gastaminza et al. 2005). The clone is referred to as Japanese Fulminant Hepatitis 1 (JFH-1), and is infectious in chimpanzees and mice transplanted with human hepatocytes.

The development of the HCVcc systems has greatly improved our understanding of the complete lifecycle of HCV, confirming many findings made using HCVpp and enabling the development of chimeric HCVcc constructs covering diverse genotypes (Gottwein, Scheel et al. 2007, Scheel, Gottwein et al. 2008, Gottwein, Scheel et al. 2009).
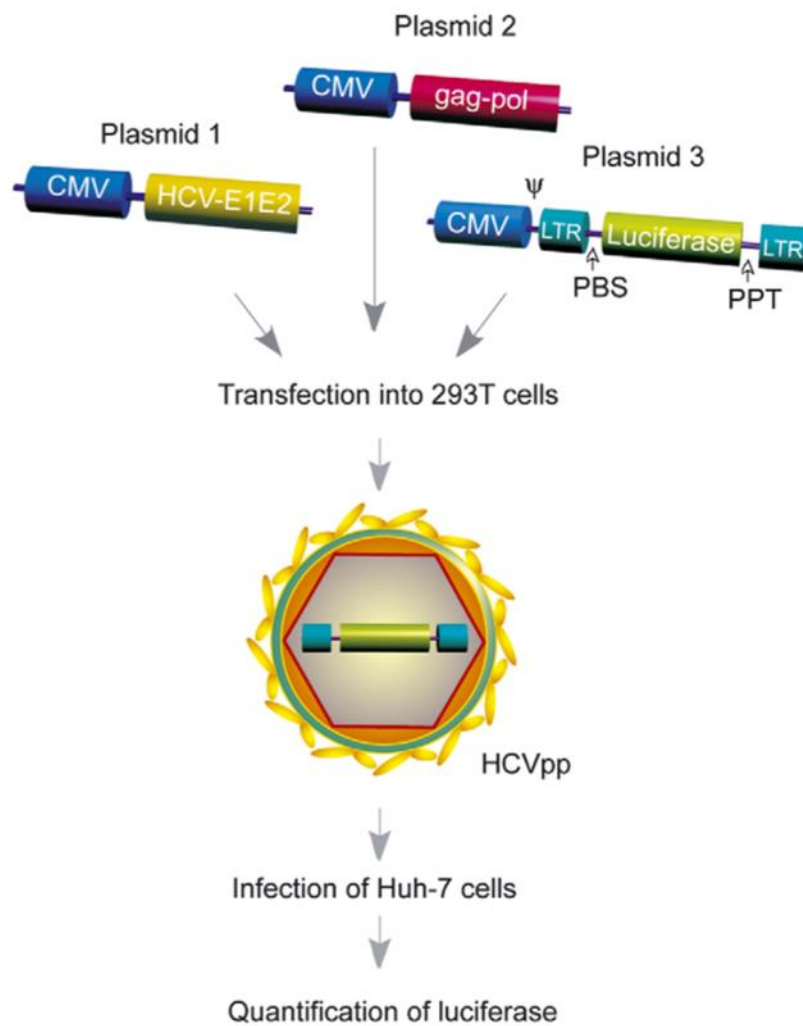
Figure 1.9: Cartoon depicting HCVpp generation (Voisset and Dubuisson 2004). Plasmids expressing the HCV glycoprotein dimer E1E2, gag-pol and luciferase under CMV promoters are transfected into 293T cell. These are assembled into HCV pseudoparticles which are then released, harvested and can be used to infect permissive cells. Level of infection is quantified by luciferase read-out. Modified from (Voisset and Dubuisson 2004).

1.8 TETRASPANINS

1.8.1 Tetraspanin interactions

The first members of the tetraspanin family of proteins were discovered when studies cloning membrane antigens identified tetraspanin 8 and a number of cluster of differentiation (CD) proteins CD63, CD53, CD37, CD81 and CD9 (Maecker, Todd et al. 1997, Boucheix and Rubinstein 2001, Yanez-Mo, Barreiro et al. 2009). Members of the tetraspanin family have since been identified in all metazoans, and related proteins have been found in plants. To date, 33 tetraspanins have been described in mammals, 37 in *Drosophila melanogaster*, and 20 in *C. Elegans* (Huang, Yuan et al. 2005). In humans, tetraspanins have been shown to be expressed at varying levels on all cells except for sperm cells (Boucheix and Rubinstein 2001).

CD81 is a 26kDa tetraspanin containing 236 amino acids, and has a structure typical of the tetraspanin family of proteins, described below. However, unlike most tetraspanins, CD81 is not glycosylated. CD81 is palmitoylated on 6 juxtamembranous cysteine residues (Charrin, Manie et al. 2002, Delandre, Penabaz et al. 2009) and this palmitolyation has been demonstrated to negatively affect HCV entry to a moderate degree by mediating the associations between CD81 heterodimers and partner proteins, and by cholesterol partitioning (Nakajima, Cocquerel et al. 2005).

Tetraspanins are type IV glycoproteins (Oren, Takahashi et al. 1990), and first appeared 600 million years ago. They are highly conserved (Huang, Tian et al. 2010), with the sub loop structure containing most of the sequence diversity within the family (Kitadokoro, Bordo et al. 2001). Tetraspanins are relatively small for transmembrane proteins, containing only 200-

350 residues (Kitadokoro, Bordo et al. 2001). They have a specific structure, with four

transmembrane domains linked by one small extracellular loop, one short intracellular

domain, and one large extracellular loop (LEL) which in the case of CD81 protrudes 3.5 nm

from the cell surface (Kitadokoro, Bordo et al. 2001). They contain 4-6 cysteine residues and

these form critical disulphide bonds with the second large extra cellular loop.

It is possible to study tetraspanin interactions by co-immunoprecipation, as specific

detergents can be used which preserve tetraspanin associations. Studies using this

technique have demonstrated that tetraspanins are able to form cell-type specific, direct

interactions with tetraspanin partners to form small complexes (Yauch, Berditchevski et al.

1998, Serru, Le Naour et al. 1999), which then form dynamic secondary interactions to form

a tetraspanin enriched microdomain (TEM). These structures are linked to form a cell type-

specific tetraspanin web (Boucheix and Rubinstein 2001, Hemler 2003). These domains are

highly dynamic in terms of the interactions formed within them, with many interactions

being transient (Barreiro, Zamai et al. 2008, Espenel, Margeat et al. 2008).

Tetraspanins are known as 'molecular organisers', and can form secondary interactions with

a diverse range of proteins alongside other tetraspanins. It has been demonstrated that

these interactions involve either the LEL or TM domains of the proteins (Hemler 2003,

Charrin, le Naour et al. 2009, Yanez-Mo, Barreiro et al. 2009), and typically consist of at least

three proteins (Claas, Stipp et al. 2001). Such protein partners include: integrins and other

adhesion receptors; immunoglobulin domain-containing factors; growth factor and cytokine

receptors; ectoenzyme receptors; MHC antigens; immunoglobulin family members; and

signalling molecules (reviewed in (Boucheix and Rubinstein 2001, Yanez-Mo, Barreiro et al.

2009). Tetraspanins are able to regulate the function of these binding partners and as a result, have roles in a wide variety of processes including cell proliferation, cell-cell adhesion, and tumourigenesis (Hemler 2005), alongside signal transduction, cell migration, and membrane remodelling (reviewed in (Boucheix and Rubinstein 2001). Therefore, it is possible that TEMs represent sites of activity, and studying agonist ligands of tetraspanins has shown that alongside the interaction between CD81 and HCV-E2, CD9 has been robustly shown to bind the pregnancy specific glycoprotein 17 (PSG17) (Waterhouse, Ha et al. 2002, Ellerman, Ha et al. 2003, Ha, Waterhouse et al. 2008, Sulkowski, Warren et al. 2011). The latter interaction may play a role in the release of anti-inflammatory cytokines (Ha, Waterhouse et al. 2005) .

The ability of CD151 and CD9 to link their partner proteins to other tetraspanins in primary and secondary complexes has been demonstrated (Berditchevski, Odintsova et al. 2002, Charrin, Manie et al. 2003, Takeda, Kazarov et al. 2007). The high affinity interactions formed by CD151 with integrins in TEMs provides them with varying partner and associated proteins. As a result, the responses to binding of laminin substrates can vary from integrin ligand binding, trafficking and signalling (Stipp 2010).

TEMs are highly regulated structures, and the interactions between tetraspanins and their partner proteins are regulated by lipids in TEMS and by cholesterol and gangliosides in the membrane (Berditchevski, Odintsova et al. 2002, Yang, Claas et al. 2002, Charrin, Manie et al. 2003, Odintsova, Butters et al. 2006). They can also be influenced by the physiological stage of the cell and palmitoylation (Berditchevski, Odintsova et al. 2002, Yang, Claas et al. 2002, Kovalenko, Yang et al. 2004).

1.9 TETRASPANINS IN DISEASE

Members of the tetraspanin family have been shown to be involved in the infection of numerous viruses, bacteria and protozoa (Monk and Partridge 2012). For example, CD151 is involved in the endocytosis of HPV (Scheffer, Gawlitza et al. 2013), and CD81 and TSPAN9 have been identified as cofactors in influenza virus and *alphavirus* infection (Karlas, Machuy et al. 2010, Konig, Stertz et al. 2010, Ooi, Stiles et al. 2013) where it has been suggested that CD81 regulates viral fusion in endosomes (He, Sun et al. 2013, Ooi, Stiles et al. 2013).

CD81 in particular plays a major role in infectious diseases alongside HCV, having been implicated in infection by *Plasmodium* (Charrin, Yalaoui et al. 2009), HIV (Deneka, Pelchen-Matthews et al. 2007, Krementsov, Weng et al. 2009, Fournier, Peyrou et al. 2010, Krementsov, Rassam et al. 2010, Monk and Partridge 2012), influenza (Karlas, Machuy et al. 2010, Konig, Stertz et al. 2010), HPV 16 (Spoden, Freitag et al. 2008), *Listeria monocytogenes* (Yauch and Hemler 2000, Tham, Gouin et al. 2010), and protozoal infections (Silvie, Rubinstein et al. 2003, Silvie, Greco et al. 2006, Yalaoui, Zougbede et al. 2008).

1.10 CD81 AND HCV

Very few pathogen-tetraspanin interactions have been reported and one of the best characterised is that of the CD81-LEL loop with HCV-E2, although there is also considerable literature surrounding the interaction between Uropathogenic Escherichia coli and the tetraspanin uroplakin 1B. In the context of HCV infection, the direct interaction of the HCV-E2 glycoprotein with CD81 makes a tempting target for therapeutic intervention, and there has been extensive research in this area which will be discussed in chapter 3.

HCV has a relatively narrow species tropism, infecting only humans and chimpanzees. It is possible that CD81 may play a significant role in this specificity, as sE2 cannot bind to mouse, rat or African green monkey CD81 (Flint, Maidens et al. 1999, Higginbottom, Quinn et al. 2000) However, it cannot be the sole determinant of HCV species tropism as mice expressing hCD81 are also not able to support infection (Masciopinto, Freer et al. 2002), and sE2 is capable of binding tamarin CD81 despite the observation that HCV does not infect this species (Allander, Forns et al. 2000, Meola, Sbardellati et al. 2000).

Aside from the formation of the essential CD81- claudin-1 coreceptor complex (Harris, Clerte et al. 2013), other interactions formed by CD81 have been shown to be central to HCV tropism. CD81 is associated with an Ig superfamily protein containing a Glu-Trp-Ile (EWI) motif, EWI-2, in a high stoichiometry in most cell lines, along with a cleaved product of EWI lacking the N terminus, EWI-2wint, in hepatocytes. The physical association of CD81 and EWI-2 has been shown to inhibit the binding of HVC-E2 to CD81 (Rocha-Perugini, Montpellier et al. 2008), but the association with EWI-2wint allows infection and it is possible that it is this interaction which causes the hepatic specificity of HCV.

1.11 CD81 STRUCTURE

The CD81-LEL contains five helices which are stabilised by two disulphide bridges to form a mushroom-shaped antiparallel dimer composed of two subdomains (Kitadokoro, Bordo et al. 2001, Kitadokoro, Galli et al. 2001, Olaby, Azzazy et al. 2013). The first subdomain is comprised of two antiparallel helices denoted A and E, along with a third helix B which together form the stem of a 'mushroom' (Figure 1.10). The second subdomain is situated above the first 'stem' subdomain and is composed of two shorter C and D helices stabilised by two disulphide bonds.

This region contains the E2 binding region (Kitadokoro, Bordo et al. 2001, Kong, Giang et al. 2013) and thus the stabilisation of this structure is central to the CD81-E2 interaction (Petracca, Falugi et al. 2000). A nuclear magnetic resonance (NMR) study has identified a dynamic motif linking helix C (subdomain 2) and helix E (subdomain 1) which may form the basis of the initial hydrophobic interaction with E2. The authors suggest that this interaction becomes more substantial following the formation of a helical domain in the D-helix region. Therefore, this dynamic region may be involved in a structural change in CD81 during E2 binding (Rajesh, Sridhar et al. 2012).
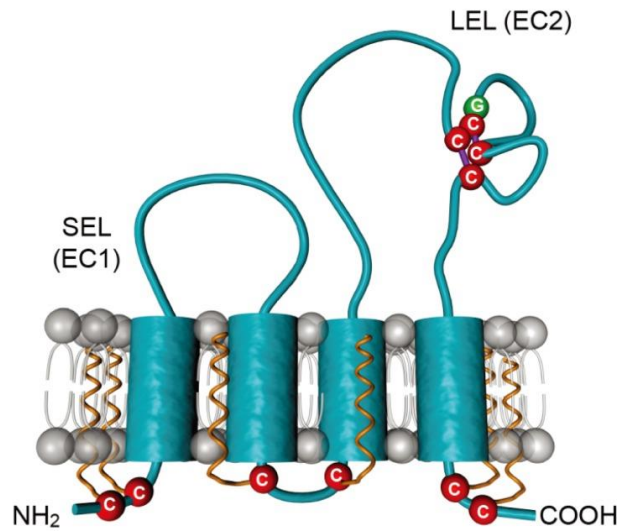
Figure 1.10: CD81 structure. *The structure of CD81 comprises four transmembrane domains, and two extracellular loop known as the small extracellular loop (SEL or EC1) and large extracellular loop (LEL or EC2), along with a small intracellular loop and intracellular N and C termini. The diagram shows the conserved cysteine residues (red) along with the conserved CCG motif in the LEL. This forms disulphide bridges (shown as purple lines) with additional cysteine residues. The orange structures in the intracellular and transmembrane domains represent palmitoylated cysteine residues. Diagram from (Feneant, Levy et al. 2014).*

1.12 VISUALISING THE VIRUS-HOST CELL INTERACTION

That the membrane of eukaryotic cells is best viewed as a 'mosaic' of diverse membrane microdomains is now well accepted (Maxfield 2002), and the lateral segregation of eukaryotic plasma membrane into compartments is essential for the function of most biological processes. The initial discovery of and subsequent research into microdomains used detergents for membrane solubilisation which maintained interactions in these regions. These interactions were then studied by fixed cell imaging by conventional fluorescence and electron microscopy. However, these approaches were not able to probe the dynamics of these structures.

Membrane microdomains have long been associated with virus infections (first reviewed in (Yanez-Mo, Barreiro et al. 2009), and this relationship was first identified following the observation that influenza A viral proteins colocalised with raft markers of apical lipid ordered domains in epithelial cells (Guess and Quaranta 2009, Stipp 2010). In addition, HIV also been demonstrated to associate with rafts (Boon, den Hollander et al. 2008, Charrin, le Naour et al. 2009). Investigating the dynamics of receptor and virus movement prior to entry can lead to insights into the early stages of the viral lifecycle, as viruses undergo a series of well-defined actions prior to entry. Binding is initiated by low affinity interactions with non-specific receptors such as LDL receptors, and is followed by high affinity binding to one or a number of receptors before trafficking to sites of entry. Live imaging can be used to study both receptor associations and locations alongside virus trafficking.

A notable example of the ability of live imaging to significantly increase in our understanding of viral processes is the observation by Walter Mothes (Sherer, Lehmann et al. 2007) that

particles containing an MLV GAG-CFP bind to and travel along the filopodia of the kidney cell line COS-2 from infected to non-infected cells (Sherer, Lehmann et al. 2007). Similarly, it has been demonstrated that HIV moves along T-cell nanotubes between infected and non-infected cells at the speed of actin flow (Jolly, Kashefi et al. 2004, Jolly, Mitar et al. 2007). As many T cells can be connected by these nanotubes, this is believed be an efficient method of viral spread.

Viruses have been observed to undergo three types of diffusion trajectories, and these are diffusion, directed drift, and confinement (Reviewed in (Burckhardt, Suomalainen et al. 2011). These trajectories are very highly conserved between viruses, (Burckhardt and Greber 2009) suggesting that the processes dictating these movements are inherent to plasma membranes rather than distinct to viruses.

There are currently two major techniques employed in the study of protein dynamics. The first, Fluorescence Recovery After Photobleaching (FRAP) involves the bleaching of one area of a cell membrane containing a fluorescently tagged protein with a high powered laser, and observing the change in fluorescence in that area over time. This will be discussed in more detail in the introduction to Chapter 4, but in brief allows the researcher to find the speed of diffusion and mobile fraction of a large population of a protein in a relatively short period of time (Yang, Xiao et al. 2011). This technique can provide data on the speed of movement (diffusion coefficient) and mobile fraction of the population of fluorescently tagged proteins within the membrane.

The second major technique is single particle tracking (SPT), which uses individual molecules tagged with fluorescent markers to follow the movement of individual proteins frame by

frame (Miyado, Yamada et al. 2000, Karamatic Crew, Burton et al. 2004). The major differentiation of this from FRAP is that this technique can be used to determine the trajectory of proteins in addition to the diffusion coefficient and mobile fraction.

SPT studies have identified three types of protein trajectories: Brownian, confined and mixed (Harris, Clerte et al. 2013, Potel, Rassam et al. 2013). Confined proteins tend to have a slow speed of diffusion and travel a very short distance or not at all, whereas diffusing proteins have a relatively quicker diffusion speed and cover a larger area. Proteins undergoing mixed diffusion display a proportion of both of these. Several studies have suggested that directional, diffusive receptor-defined movements allow viruses to scan large areas of the membrane quickly and to escape from non-productive confinements (Helmuth et al., 2007; Ewers et al., 2005; and Lehmann et al., 2005(Burckhardt, Suomalainen et al. 2011).

 A major difference between FRAP and SPT is that FRAP measures a population of proteins whereas SPT measures the movement of one protein at the time. As a result, whilst SPT is arguably a more informative technique, it is more expensive and time consuming. However, studies of viral and protein movements on host cell plasma membranes using SPT have identified a number of common traits which will be discussed below. Therefore once it has been understood how these changes in trajectory relate to changes in global protein diffusion, it is efficient to continue to use a combination of FRAP and SPT to drive forward our knowledge of protein dynamics.

1.13 PROJECT AIMS

The work presented here provides insights into the role of CD81 in HCV entry mechanisms. CD81 is an essential receptor for HCV and forms a direct and well-studied interaction with the virus, although the entry mechanism as a whole is complex and is still relatively poorly understood. However, it is essential and therefore an attractive target for therapeutic intervention and continued research.

CD81 is almost ubiquitously expressed, but its specific role in the entry cycle of HCV - a virus with a narrow organ and species tropism - is unclear. However, it is known to have a limiting effect on virus entry in terms of its diffusion and protein associations. This project aims to further interrogate the role of CD81 in HCV entry in terms of its expression, protein diffusion and impact on cell signalling. We intend to do this largely with the use of the live imaging technique, FRAP. Specifically, it will address the following issues:

1. There are currently no published data examining the availability of CD81 residues relevant to HCV infection between cell types expressing the protein. We aim to investigate whether antibodies to functionally and pathogenically-important residues in CD81 can be used to identify the protein between cell types.

2. The majority of infection studies rely on hepatocellular carcinoma-derived cell lines which do not exhibit complex hepatic polarity, despite published data demonstrating that hepatic polarity defines HCV infection. Therefore, we aim to characterise polarised HepG2s as an *in vitro* model for CD81 diffusion and to use this model to

further our knowledge of the factors governing protein diffusion across the cell membrane.

3. Recent work in a non-polarised cell line has demonstrated a link between EGFR signalling, HCV infection and the CD81-claudin-1 complex. We aim to further interrogate this association, looking specifically at the dependence of the EGFR signalling pathway and EGF-stimulated CD81 diffusion on the formation of the HCV coreceptor complex in a polarised cell type.

2   MATERIALS AND METHODS

2.1   CELL LINES, PRIMARY CELLS AND TISSUE CULTURE

All cells (Table 2.1) were incubated in 20% O_2 and 5% CO_2 at 37˚C. Hepatoma cells were maintained in Dulbecco's Modified Eagle Medium (DMEM) (Life Technologies, USA) supplemented with 10% foetal bovine serum (FBS), 1% L-glutamine, 1% non-essential amino acids and 50 units/mL penicillin/streptavidin (Life Technologies, USA). Jurkat and Raji cell lines were maintained in Roswell Park Memorial Institute medium (RPMI) 1640 (Sigma, USA) supplemented with 2mM Glutamine + 10% FBS and incubated in the same manner. In all cases, in order to enumerate cells they were washed thoroughly with PBS and incubated in trypsin (Life Technologies, USA) for 3-6 minutes at 37˚C. The resulting suspension was then mixed with an equal amount of DMEM or RPMI and cells counted with a haemocytometer.

Primary human hepatocytes were a kind gift from Dr Ragai Mitry (Kings College, London) and were obtained from unused donor liver tissue rejected for transplantation due to a long ischaemic period. Both isolation and preservation were performed in accordance with good laboratory practice guidelines using pharmaceutical grade reagents (Mitry 2009). Signed ethical consent forms were obtained prior to tissue processing. Hepatocytes were frozen and recovered from liquid nitrogen following lab standard procedures. Briefly, cells were stored by aliquoting 10^6 cells into 1 mL of freezing medium (95% FBS, 5%DMSO) and slowly cooling to -80°C in an insulated chiller box designed to cool the cells at ~1°C/ min ("Mr Frosty" chiller, Thermo Fisher), for longer term storage cells were transferred to liquid Nitrogen (-165°C). Cells were recovered by rapid thawing in a 37°C water bath followed by immediate transfer into 10 volumes on DMEM/10%FBS.

Mononuclear cells were isolated from human peripheral blood following established

methodology (Aspinall, Curbishley et al. 2010). CD4^{+} T cells were isolated from peripheral

blood mononuclear cells (PBMCs) using the CD4 Easysep enrichment kit (Stemcell

technologies) following the manufacturer's instructions. The resulting population were

shown to consist of 99% CD4+ T cells by flow cytometry. This procedure was carried out by

Dominik Niesen and Sudha Purswani.

Cell type	Tissue type	Growth media	Source
HepG2	Human Hepatoblastoma	DMEM	American Type Culture Collection
HepG2.CD81	Human Hepatoblastoma	DMEM	In House
Huh-7.5	Human Hepatoma	DMEM	C Rice, Rockefeller University, NY, USA
293T	Human Embryonic Kidney	DMEM	American Type Culture Collection
Jurkat	Human leukaemic T cell lymphoblast	RPMI	American Type Culture Collection
Raji	Human B cell lymphoblast	RPMI	American Type Culture Collection
Primary hepatocytes	Human Liver	Williams E	Ragai Mitry, Kings College London, UK
PBMCs	Peripheral blood mononucleocytes	Used immediately upon isolation	Zania Stamataki, University of Birmingham, UK

Table 2.1: Cell lines used, tissue type, growth media and source

2.2 ROUTINE TECHNIQUES

2.2.1 Flow cytometry

Flow cytometry was used to quantify the expression levels of proteins of interest using live cell staining, and also to isolate cells type of interest from heterogeneous primary cell populations.

For experiments looking at binding of CD81 mAbs across cell types, cell lines were grown in tissue culture flasks in DMEM or RPMI before being trypsinised for 3-6 minutes at 37˚C and resuspended in an equal amount of DMEM or RPMI for quantification. Primary cells were obtained as described above and were used immediately upon isolation (primary immune cells) or following thawing from storage (PHH).

Following quantification with a haemocytometer, cells were pelleted at 1500 rpm for 3 minutes before resuspension in a blocking solution (PBS/1% BSA/ 0.01% sodium azide) at a density of $2x10^6$ cells/mL. 100 µl of this solution was seeded per well of a 96 well plate (Sigma, UK) in triplicate for each condition tested. Following a 15 minute incubation in blocking solution at 37˚C, the cells were spun down and the solution replaced with fresh blocking solution containing anti-CD81 primary antibodies of interest or species matched IgGs at the required concentration (1 µg/mL)(Table 2.2 and 2.3). Binding of IgGs is shown throughout. Cells were incubated with primary antibody for 30 minutes at 37˚C before washing 3x in PBS. To detect primary cell-bound antibodies, anti-Ig AlexaFluor secondary antibodies were diluted 1:1000 in the antibody buffer and incubated with the cells for 30 minutes at 37˚C in the dark to prevent photobleaching. Cells were washed extensively with

PBS and fixed with 1% PFA for 20 minutes at 4˚C. The antibodies used, their sources, applications and concentrations can be found in tables 2.2 and 2.3.

For identification of PBMC cell types, live cell staining was carried out as above, with a third staining step added before fixing to identify components of the PBMC population. CD3+ T cells were identified using a CD3-APC conjugate antibody and B cells using a CD19-Tricolour conjugate antibody, both of which were added for 30 minutes at 37˚C in the dark to prevent bleaching (Table 2.2 and 2.3). This dual staining approach allowed cell types to be identified simultaneously with the quantification of the level of CD81 binding.

2.2.2   Analysis of and comparisons using CD81 flow cytometry data

Protein expression was measured using a FacsCalibur flow cytometer (Becton Dickinson, Europe), and the cell population data analysed using FlowJo software (Tree Star, OR, USA) following the identification of intact, live cells by size and density. Where a dual staining approach was used, intact live cells were selected and PBMCs isolated according to their relative size and density in the context of the populations of live cells within the sample. CD3+ and CD19+ cells were then identified by their relative levels of APC and tricolour staining. The levels of CD81 mAb binding could then be determined for each cell type. In all cases, CD81-mAb binding levels are expressed relative to the IgG control for each experiment in order to normalise results across multiple repetitions of experiments.

Where the binding capacity is compared to binding affinities to MBP-CD81-FL and MBP-CD81-LEL, these values were obtained by Michelle Farquhar (manuscript in preparation, see appendix table 2).

Primary Antibodies

Antibody	Antigen	Type	Specificity	Species	Source
Anti-MRP2	Human MRP-2	Purified	Monoclonal	Mouse	Abcam, UK
Anti-β-actin	Human β-actin	Purified IgG	Monoclonal	Mouse	Sigma Aldrich, USA
Anti-EGFR	Human EGFR	Purified IgG	Monoclonal	Rabbit	Cell Signalling Technology, USA
Anti-EGFR pY1068	Human EGFR pY1068	Purified IgG	Monoclonal	Rabbit	Cell Signalling Technology, USA
Anti-CD3-APC	Human CD3	Purified IgG	Monoclonal	Mouse	BD Biosciences, USA
Anti-CD56-PE	Human CD56	Purified IgG	Monoclonal	Mouse	BD Biosciences, USA
Anti-CD19-Tricolour	Human CD19	Purified IgG	Monoclonal	Mouse	Invitrogen, CA
Anti-CD81 (1s73)	Human CD81	Purified IgG	Monoclonal	Mouse	In House
Anti-CD81 (1s135)	Human CD81	Purified IgG	Monoclonal	Mouse	In House
Anti-CD81 (1s201)	Human CD81	Purified IgG	Monoclonal	Mouse	In House
Anti-CD81 (1s262)	Human CD81	Purified IgG	Monoclonal	Mouse	In House
Anti-CD81 (1s337)	Human CD81	Purified IgG	Monoclonal	Mouse	In House
Anti-CD81 (2s20)	Human CD81	Purified IgG	Monoclonal	Mouse	In House
Anti-CD81 (2s24)	Human CD81	Purified IgG	Monoclonal	Mouse	In House
Anti-CD81 (2s63)	Human CD81	Purified IgG	Monoclonal	Mouse	In House
Anti-CD81 (2s131)	Human CD81	Purified IgG	Monoclonal	Mouse	In House
Anti-CD81 (2s139)	Human CD81	Purified IgG	Monoclonal	Mouse	In House
Anti-CD81 (2s141)	Human CD81	Purified IgG	Monoclonal	Mouse	In House
Anti-CD81 (2s155)	Human CD81	Purified IgG	Monoclonal	Mouse	In House

Secondary Antibodies

Antibody	Antigen	Type	Specificity	Species	Source
Rabbit Alexa Fluor 633	Rabbit IgG	Purified IgG (H+L)	Polyclonal	Goat	Molecular Probes, Invitrogen, USA
Mouse Alexa Fluor 488	Mouse IgG	Purified IgG (H+L)	Polyclonal	Goat	Molecular Probes, Invitrogen, USA
Anti-Rabbit HRP	Rabbit IgG	Purified IgG	Polyclonal	Goat	Cell Signalling Technology, USA

Table 2.2: List of antibodies used

Primary Antibodies

Antibody	Application	Working concentration (μg/ml)
Anti-MRP2	IF	2
Anti-β-actin	WB	0.5
Anti-EGFR	WB, IF	1
Anti-EGFR pY1068	WB	1
Anti-CD3-APC	FC	1
Anti-CD56-PE	FC	1
Anti-CD19-Tricolour	FC	1
Anti–CD81 (1s73)	WB	1
Anti–CD81 (1s135)	WB	1
Anti–CD81 (1s201)	WB	1
Anti–CD81 (1s262)	WB	1
Anti–CD81 (1s337)	WB	1
Anti–CD81 (2s20)	WB	1
Anti–CD81 (2s24)	WB	1
Anti–CD81 (2s63)	WB	1
Anti–CD81 (2s131)	WB	1
Anti–CD81 (2s139)	WB	1
Anti–CD81 (2s141)	WB	1
Anti–CD81 (2s155)	WB	1

Secondary Antibodies

AlexaFluor anti-mouse488	IF	1:500
AlexaFluor anti-rabbit 633	IF	1:500
Anti-rabbit-HRP	WB, IF	1:2000

Table 2.3: List of antibodies concentrations used

2.2.3   Western Blotting

Western blotting was used to determine levels of total and phosphorylated EGFR in

HepG2.AcGFP-CD81 cells and HepG2 cells expressing AcGFP-tagged mutant CD81 proteins.

Cells were seeded at $3x10^4$/well and allowed to polarise for 5 days in DMEM. On the fifth

day, they were subjected to a serum starvation period of 30 minutes before the addition of

EGF at 1μg/mL or 30 μg/mL anti-CD81 mAb for defined periods of up to 60 minutes. As these

time course experiments were carried out in a 6 well plate, the procedure was carried out in

media supplemented with 4-(2-hydroxyethyl)-1-piperazineethanesulfonic acid (HEPES)

buffer on a heat block at 37˚C.

Once the treatment period was complete, cells were transferred to ice to prevent any

further stimulation of signalling. All subsequent steps were carried out on ice with ice-cold

reagents. Cells were washed with PBS, removed from the wells with a cell scraper and the

suspension transferred to Universal tubes for pelleting at 1500 rpm (1000 g) at 4˚C for 5

minutes. Cells were resuspended in lysis buffer (PBS, 1% Brij97, 20mM Tris [pH 7.5], 300 mM

$CaCl_2$, and 2mM $MgCl_2$) supplemented with protease and phosphate inhibitors (Roche, UK)

and incubated on ice for 30 minutes. The resulting lysate was centrifuged at 15000 rpm for

20 minutes at 4˚C to remove nuclei and cell membranes. The supernatant was aspirated

from the pellet and the protein present quantified with a BCA Protein Assay Kit (Thermo

Scientific, USA) following the manufacturer's instructions. Briefly, 100 μl of BSA standard or

of lysate were mixed with 200 μl of BCA working reagent, in a 96 well plate in triplicate. The

plates were incubated at 37˚C for 30 minutes and the absorbance read at a wavelength of

490nm in an ELISA plate reader. The concentration of protein in the samples was found by

comparing the average (blank corrected) 490nm measurement for each sample to that found for the BSA standards forming the standard curve.

2.2.4 Sodium Dodecyl Sulphate PolyAcrylamide Gel Electrophoresis (SDS-PAGE)

Samples were made up to a 25µl volume by mixing with 3x Laemmeli dye (30% v/v Glycerol, 6% w/v SDS, 0.02% v/v Bromophenol Blue and 0.2M Tris-HCl; pH 6.8) with or without 2-β-mercaptoethanol (to create non-reducing conditions). Samples were denatured at 95˚C for 5 minutes and allowed to cool before gel loading.

20 µl of samples were separated on 6% SDS gels by gel electrophoresis at a constant 200 volts for 20-30 minutes using the Mini Protean 3 System (Bio-Rad Laboratories, USA) according to the manufacturer's instructions.

Following completion of the run, proteins on the gel were transferred to a polyvinylidene membrane (Millipore, USA) using a Mini Trans-Blot Electrophoresis Transfer System (Bio-Rad). The membranes were treated with methanol for 2 minutes and washed with H_2O before incubation in transfer buffer (25mM Trizma Base, 0.2M Glycine, 200mL/L methanol and 10% SDS) for 5 minutes at room temperature. Gels were also equilibrated in the transfer buffer to prevent shrinking. Electrophoretic transfer was carried out at room temperature at 350mA for 90 minutes using the Mini Protean 3 System (Bio-Rad Laboratories, USA).

2.2.5 Immunoblotting and chemiluminescent detection of proteins

The following protocol was used for the staining and detection of total and phosphorylated EGFR and for β-actin, which was used as a control.

Following transfer membranes were placed in 50 mL falcon tubes and washed extensively with PBS. To prevent non-specific antibody binding membranes were incubated at room temperature in blocking buffer for 1 hour in (TBS-T[10mM Trizma base, 0.1M Sodium Chloride, 10% v/v Tween-20] with 5%w/v Marvel dry milk powder) before extensive washing with PBS. Primary antibody was added at the recommended dilution in antibody buffer (TBS-T with 5% bovine serum albumin) and incubated overnight at 4˚C before 4 washes for 5 minutes each with PBS. Membranes were incubated with HRP-conjugated secondary antibody at the recommended dilution in antibody buffer for 1 hour at room temperature followed again by extensive washing. The antibodies used, their sources, applications and concentrations can be found in tables 2.2 and 2.3.

Detection of the antibodies by chemiluminescence was carried out using an ECL Western Blotting Detection System (GE Healthcare, UK). This process involved incubating the membranes in detection reagent for 1 minute before detecting luminescence using the PXi Multi-application gel imaging system (Syngene, UK).

2.2.6 Analysis of Western Blotting experiments

Following detection of fluorescence using the PXi Multi-application gel imaging system (Syngene, UK), the densities of protein bands quantified using the Gel analysis function of ImageJ (NIH, USA). The data were then analysed to find the density of each band of total or phosphorylated EGFR in relation to the level of β-actin in each lane. Once these had been determined, the level of pEGFR in comparison to total EGFR could be found as a ratio.

2.3 TRANSFECTIONS AND VIRUS

2.3.1 Generation of cell lines expressing proteins of interest

HepG2 cells were transduced to express AcGFP.CD81, AcGFP.claudin-1 and the mutant AcGFP.CD81 plasmids using TRIP lentiviruses containing the relevant insert. A list of plasmids used and their sources can be found in table 2.4.

To make TRIP virus 6 well tissue culture plates were pre-coated with poly-L-lysine (Sigma) for 5 minutes. These were washed extensively with PBS and 293-T cells seeded at a density of $7x10^5$/well in DMEM/10%FBS. The following day cells were incubated in 1 mL of 3% antibiotic-free DMEM for 1 hour prior to transfection. For each well, a total of 1.6µg of DNA in the ratio 600ng:400ng:600ng of pGag-pol 8.2, VSV and the pTRIP plasmid of interest respectively was made up to 10µl with sterile distilled water. 6µl of Fugene (Roche) was added to 100µl of serum free media (Optimem) and incubated at room temperature for 5 minutes and then added to the DNA, mixed gently and incubated at room temperature for 20 minutes. The entire reaction mixture was then added to the 1mL of 3%, antibiotic-free media in each well and incubated at 37°C for 6 hours. After this time, the media was replaced with DMEM/10%FBS and the cells incubated for 72 hours, with harvests at 48 and 72 hours. The harvested virus containing supernatant was pooled and clarified at 1500 rpm for 5 minutes in a centrifuge.

For transduction, target HepG2 cells were seeded at $3.5x10^4$/well in 2mL of media. After 24 h the media containing virus was added at a 1:2 dilution with 3% DMEM with antibiotics for 24

hours before removal and replacement with normal media. Cells were checked at 48 hours post-transfection for a high level of expression before use. For studies using the cell lines expressing mutant CD81 proteins, cells were freshly transfected for each experiment.

Name	Source	Working concentration
Tumour necrosis factor alpha	R&D Systems, USA	10ng/mL
Epidermal growth factor	Peprotech, USA	1µg/ml
Cytochalasin D	Sigma, USA	2.5µM
Latrunculin B	Sigma, USA	1 µM
Erlotinib	LC Laboratories, USA	10 µM

Table 2.4: Cytokines, growth factors and drugs used

2.3.2 HCVpp Genesis and Infection

H77 HCV (HCVpp), vesicular stomatitis virus (VSVpp) and No Env (NEpp) pseudoparticles were produced as described (Fafi-Kremer, Fofana et al. 2010). Specifically, 6 well tissue culture plates were pre-treated with poly-L-Lysine as previously described and 293-T cells seeded at a density of $7x10^5$. The following day cells were incubated with 1 mL of 3% antibiotic free DMEM for 1 hour prior to the beginning of the process.

The cells were co-transfected with a plasmid encoding the Gag-pol gene of HIV, the luciferase reporter gene, (NL4.3R-E-Luc) and a plasmid encoding either the HCV strain H77 E1E2 envelope glycoprotein, an empty vector control (Env-pp) or Vesicular Stomatitis Virus G (VSV-G) protein.

6µl of Fugene was incubated with 100µl Optimem for each well of cells for 5 minutes at room temperature. This was then added to a 10µl solution containing 600 ng of NL4.3R-E-Luc, 600ng of HIV gag-pol and 600ng envelope protein expression plasmid. The mixture was

then incubated at room temperature for 20 minutes, added to the cells and incubated for 6 hours. The media was then replaced with fresh 3% FBS, antibiotic-free DMEM. At 48 and 72 hours post transfection the media was removed and stored at 4˚C and replaced with fresh 3%, antibiotic-free media. The virus containing supernatant was either used immediately or aliquoted for storage at -80˚C.

2.3.3   Virus infectivity assay

For experiments looking at the effect of polarisation on infection, HepG2 cells were seeded in a 96 well plate at 1.5×10^5/mL for 1, 3 and 5 days to polarise. To examine the effect of EGF stimulation on HCVpp infection, HepG2.AcGFP-CD81 cells and HepG2 cells, which had been seeded at 1.5×10^5/mL for 5 days, and Huh-7.5 cells, which had been seeded at 1.5×10^5/mL, were subjected to a serum starvation period of 30 minutes. They were than stimulated with EGF for 30 minutes at a concentration of 1 µg/mL prior to the addition of virus. The untreated cells in this experiment were also serum starved, but remained unstimulated. These experiments studying the effect of TNF-α on infection have now been published by Nicola Fletcher (Fletcher, Sutaria et al. 2014).

Cells were seeded in triplicate for each condition and pseudoparticle type tested. Virus pseudoparticles containing H77pp or NEpp were added at a 1:2 dilution whilst MLVpp was added at a 1:50 dilution in a 100µl total volume of 3% FBS media.

After a 72 hours of incubation at 37˚C with the virus, the media was replaced with 40µl cell lysis buffer (12.5 mL 1M TrisPO$_4$ solution pH7.8, 5mL CDTA, 50mL Glycerol, 5mL Triton-X-100, 1mL 1M DTT, made up to 500mL with dH$_2$O) and incubated at 4˚C for 1 hour. The infection levels of the sample lysates were assessed using a Luciferase Assay System Kit

(E1501, Promega, Madison, USA) by adding 40μl of lysate to a 35μl volume of Luciferase

Assay Substrate mixed with Luciferase Assay Buffer. Luciferase output was monitored with a

luminometer (Berthold Technologies, UK).

The level of infection was determined by subtracting the values obtained for a 'blank read'

of the infection plate with no lysate and the values for infection with a NEpp virus from

those obtained with H77pp or MLVpp.

2.4 SPECIFIC ASSAYS

2.4.1 Quantification of polarity

HepG2.CD81 cells were seeded at least one day prior to the experiment on glass coverslips.

These were fixed for 30 minutes in 3% EM-grade paraformaldehyde at room temperature

and stained with anti-MRP2 in 0.1% Triton-X100 (Sigma Aldrich) with 0.5% bovine serum

albumin (BSA) in phosphate buffered saline (PBS) for 1 hour. AlexaFluor 488-conjugated goat

anti-mouse was used as a secondary antibody and nuclei were visualised using 4', 6'-

diamidino-2-phenylindole (DAPI; Invitrogen, UK). The polarity index was determined by

counting the number of MRP2-positive apical structures per 100 nuclei using a Nikon Eclipse

TE2000-S fluorescence microscope (Figure 2.1a).

Where this technique was used to examine the effect of time in culture, cells were seeded at

3×10^4 and allowed to polarise for 1, 3 or 5 days before commencement of the experiment.

Where TNF-α was used, this was added to 5 day polarised cells at 100ng/mL for 1 hr prior to

beginning the experiment alongside a control at the appropriate dilution. Cytochalasin D and

latrunculin B were again added to 5 day polarised cells at concentrations of 1μM and 2.5 μM

respectively for 1 hour before imaging, again alongside an appropriately diluted control.

2.4.2 Tight junctional integrity

The trapping of fluorescent molecules within bile canaliculi (BC) is a well-established technique to identify these structures and can be used to quantify the amount of polarisation of a hepatocyte cell culture. HepG2.CD81 cells were seeded at least one day prior to beginning the experiment before washing three times with PBS at 37˚C. Cells were incubated with 5μM 5-chloromethylfluorescein diacetate (CMFDA, Invitrogen) at 37°C for 10 min. After washing extensively with PBS, the cells were incubated for 15 minutes at 37˚C and the capacity of BC lumens to retain CMFDA monitored using a fluorescence microscope. The percentage of cells retaining CMFDA at their BC was compared to the total number of BCs visible by phase microscopy (Figure 2.1 b, c). The protocols for using this technique to study the effect of time in culture and addition of TNF-α, cytochalasin D and Latrunculin B are detailed in the above section on quantification of polarity.

2.5 ADDITION OF DRUGS, CYTOKINES AND GROWTH FACTORS

2.5.1 Cytoskeletal disruption and phalloidin staining

Latrunculin B and cytochalasin D were purchased from Sigma and added to media at 1μM and 2.5 μM respectively for 1 hour before imaging. Phalloidin-633 (Alexa-Fluor) was used to label actin following the manufacturer's protocol described below. A list of the cytokines used in this study, their working concentrations and sources can be found in table 2.5. Glass-bottomed MatTek™ dishes containing cells expressing fluorescent CD81 were washed 3x with PBS and stained for actin with 633-phalloidin using a simultaneous fixation,

(a) MRP2   (b) CMFDA   (c) Phase contrast
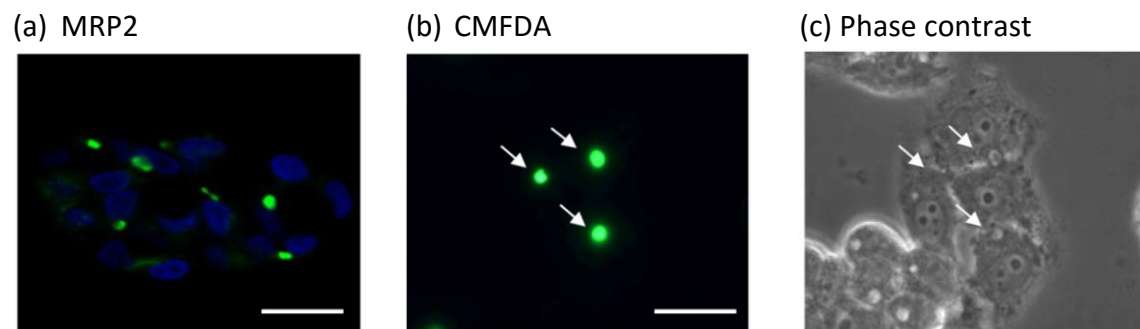
Figure 2.1: MRP-2 staining and CMFDA retention in polarised HepG2 cells.
Immunfluorescent staining of MRP-2 (green) with DAPI nuclear stain (blue) (a). Fluorescence images of CMFDA retention (green) in HepG2 bile canaliculi (arrows) (b). Phase contrast images of polarised HepG2 cells with bile canaliculi (arrows) (c). Scale bars represent 20μm.

permeabilisation and staining method recommended by the manufacturer (Life

Technologies, USA). Briefly, a solution of lysopalmitoylphosphatidylcholine, 3.7%

formaldehyde and fluorescent phalloidin was added to cells and incubated at 4˚C for 20

minutes. Cells were then washed 3x with PBS and mounted for imaging.

2.5.2 EGF addition and inhibition with Erlotinib

Erlotinib-HCl (LC Labs) was added at 10µM in SF media for 1 hour after a 30 min period of

serum starvation. Similarly, EGF (Peprotech, USA) was added at 10ug following a 30 min

period of serum starvation. In all cases, untreated samples were subjected to a 30 minute

serum starvation. A list of the cytokines used in this study, their working concentrations and

sources can be found in table 2.5.

2.5.3 Addition of TNFα

Following 5 days of polarisation, cells in which protein diffusion, infection and tight

junctional integrity and function had been tested were treated with TNF-α (10 ng/mL) or a

control in the normal culture medium for 1h before the beginning of the experiment, and

the cytokine left on for the remainder of the procedure.

2.6 LIVE IMAGING STUDIES

2.6.1 Fluorescence recovery after photobleaching (FRAP)

For all FRAP experiments, cells transduced to express fluorescent proteins were plated onto

MatTek™ glass-bottomed 35mm dishes at a density of $3x10^4$ cells/well and incubated for 5

days to allow polarisation. For studies of non-polarised cells, cells were seeded at $1x10^5$ the

day before imaging. Prior to imaging cells were washed thoroughly with PBS and the media replaced with phenol red-free DMEM supplemented with HEPES buffer along with any cytokines, growth factor and drugs (Table 2.5). The protocols for use of TNFα, cytochalasin D, latrunculin B, EGF and erlotinib are detailed in separate sub sections above. Where the effect of time in culture was studied, cells were seeded at $3x10^4$ and allowed to polarise for 1 (non-polarised) or 5 days (polarised) before beginning the experiment. all cases, cells were imaged at 37˚C using a 100x Plan Achromat 1.4 NA oil immersion objective on a Zeiss LSM 780 confocal microscope fitted with a GaAsP spectral detector. 16 bit images were obtained with optimal pixel resolution. Fluorescently tagged proteins were excited with an argon laser at <2% of full power to capture 4 initial iterative images before bleaching of selected circular regions on the base of the cell in contact with the glass for 10 iterations at 100% laser power. Following bleaching, recovery was recorded over 300 iterations which allowed the recovery curve to reach a plateau. Subsequent analysis of the fluorescence recovery was normalised to the natural bleach rate, and the curve fitted with the exponential decay formula Y=Span(1-exp (-K*X))+plateau. An unbleached background region of interest (ROI) and sampled ROIs were selected using the inbuilt Zeiss Zen software and statistical analysis carried out using GraphPad Prism software.

Regions were selected on polarised HepG2 cells expressing AcGFP-CD81 or AcGFP-claudin-1. In all regions, bleached spots were placed randomly, and the diameter of the regions chosen so as not to encompass any other membrane structures. The recovery curve was modelled in GraphPad Prism using an analysis where the program determined whether the curve best fitted a single (equation 1) or double exponential equation, in addition to finding the *k* value (equation 3) and mobile fraction.

Where the diffusion parameters of CD81 at different cellular locations was investigated, the PM was defined as the regions of the cell membrane in contact with the glass surface and ECM, the filopodia were identified as small, motile projections from the cell surface attached at only one end, thus distinguishing them from microtubules. The cell contact regions were defined as parts of the cell surface in physical contact with the plasma membrane of another, and where a BC-like structure was present. In these cases, one cell contact region was analysed per two cells.

Name	Source
TRIP AcGFP.CD81	In House
TRIP AcGFP.CLDN-1	In House
TRIP AcGFP.CD81 – K148A	In House
TRIP AcGFP.CD81 – T149A	In House
TRIP AcGFP.CD81 – K148A/T149A	In House
TRIP AcGFP.CD81 – E152A	In House
TRIP AcGFP.CD81 – T153A	In House
TRIP AcGFP.CD81 – E152A/T153A	In House
VSV-G	Aaron Diamond AIDS Research Centre
Luciferase Reporter	Aaron Diamond AIDS Research Centre
HIV Gag-pol 8.2	Aaron Diamond AIDS Research Centre

Table 2.5: Plasmids used

2.6.2 Analysis of FRAP data

To establish the necessary samples sizes for FRAP data, Montecarlo bootstrap analysis was carried out by repeated selection of the stated sample sizes with replacement from the population. The mean diffusion coefficient and mobile fraction of these compared to that of the population to find the coefficient of variation using GraphPad Prism 6.

In order to establish the diffusion mode of CD81, the fluorescence intensity of bleached regions were plotted against the time post-bleaching to form a recovery curve. The curve

was then analysed using GraphPad Prism 6 to confirm the equation of the curve – single or double exponential. Additionally, the mean $T_{1/2}$ was plotted against the size of the bleached region from which it was calculated to establish to direction of diffusion.

2.7 CONFOCAL MICROSCOPY

In all cases, cells were seeded in glass bottomed MatTek™ dishes or plates five days before the experiment. Cells were imaged using a 100x Plan Achromat 1.4 NA oil immersion objective on a Zeiss LSM 780 confocal microscope with a GaAsP spectral detector. 16 bit images were attained with optimal pixel resolution. Fluorescently tagged proteins were excited with 488 nm or 633 nm lasers which had been adjusted to prevent bleed-through.

2.7.1 Effect of CD81 mutant proteins on CD81 and EGF localisation

To examine the effect of the mutant CD81 proteins on CD81 and EGFR localisation, cells expressing AcGFP-tagged versions of the proteins were seeded at $3x10^4$ on the glass bottomed MatTek™ dishes and were allowed to polarise for 5 days. Cells were subjected to a serum starvation of 30 minutes prior to fixation for 15 minutes at room temperature with 3.6% formaldehyde diluted in the serum free medium. Cells were washed 3x with PBS and incubated with the blocking buffer (1X PBS / 5% normal serum / 0.3% Triton™ X-100) for 60 minutes at room temperature. The primary antibody (EGFR, Cell Signalling Technology, USA) was then added at a dilution of 1:50 in antibody dilution buffer (1X PBS / 1% BSA / 0.3% Triton X-100) at 4˚C overnight. Following a further thorough wash with PBS, dishes were incubated with anti-rabbit IgG-633 at 1:1000 for 1 hour at room temperature in the dark. Cells were again washed 3x with PBS and nuclei visualised with DAPI (Invitrogen, UK) prior to

a final wash and mounting with Prolong Gold Antifade reagent (Cell Signalling Technology, USA). The staining was then visualised as described above.

2.8 BACTERIAL WORK

2.8.1 Transformation

Competent cells (One Shot ®TOP10 Chemical Competent *E.coli*, Invitrogen) were thawed on ice. For each transformation, 20 µl of competent cells was added to 1 µl of plasmid and the mixture agitated carefully before incubating for 30 minutes on ice to allow uptake of the DNA. The reaction mixture was then subjected to a heatshock of 42˚C for 45 seconds in a water bath before a further 5 min incubation on ice. 100 µl of culture broth (S.O.C. medium, Invitrogen) was added to the reaction mixture and incubated for 30 minutes to allow recovery. The entire reaction mixture was then spread on plates containing 2% Luria Broth (LB, Invitrogen) + 1% agarose (Bioline) supplemented with ampicillin (100ng/mL) (Sigma-Aldrich). This was incubated at 37˚C overnight to allow colonies to grow.

2.8.2 Preparation and multiplication of plasmid DNA

Two colonies were picked from each transformation reaction. These were incubated in 5 mL of 2% LB broth with ampicillin (100ng/mL) at 300 rpm at 32˚C overnight. The suspension was centrifuged at 4000 rpm for 10 minutes and the resulting pellet used to isolate the plasmid using a Qiaprep Spin Miniprep Kit (Qiagen) according to the manufacturer's instructions. Briefly, pellets were resuspended in 250 µl Suspension Buffer P1 (containing LyseBlue pH indicator) followed by the addition of 250 µl ice cold Lysis Buffer P2. The tube containing this suspension was then inverted gently until the solution turned blue. This lysis product was

then mixed with Neutralising Buffer N3 and the tube inverted again until the blue colour had disappeared. The lysates were transferred to sterile 1.5mL eppendorf tubes and centrifuged at 13000 rpm for 10 minutes to remove the bacterial precipitate. The supernatant was transferred to a spin column and centrifuged for 30-60 seconds to capture the DNA. The column filter was washed by centrifugation with Buffer PB and then Buffer PE, and then by a further centrifugation to remove any remaining buffer. Finally, the dry filter was incubated with Buffer EB for 1 minute followed by a 1 minute centrifugation to elute the DNA. The concentration and purity of the resulting purified plasmid was measured by spectrometry and stored at -20°C. Typical yields were 10 – 25 μg of plasmid with purity of 1.8 – 1.85 (260/280nm ratio).

2.9 STATISTICAL ANALYSIS

All statistical tests and analyses were carried out using Prism 6.0 software (GraphPad, CA). In order to avoid testing the assumptions of a particular data distribution, all tests were performed using non-parametric methods. Statistics used in FRAP experiments were Mann-Whitney U tests for non-parametric distributions, and a probability value (P) <0.05 was considered statistically significant. All tests and significance values are quoted in the figure legends. Where necessary corrections for multiple comparisons were made (Bonferroni method).

3. A COMPARATIVE ANALYSIS OF CD81 PRESENTATION BETWEEN CELL TYPES

3.1 INTRODUCTION

The development of HCV model systems has enabled the entry stages of the viral lifecycle to be studied extensively, and early work showed the direct interaction of HCV-E2 with residues in the CD81 large extracellular loop (CD81-LEL) to be essential for HCV entry (Pileri, Uematsu et al. 1998, Flint, Maidens et al. 1999, Higginbottom, Quinn et al. 2000, Zhang, Randall et al. 2004, Flint, von Hahn et al. 2006). Numerous studies have since identified key amino acid residues in the CD81-LEL that define protein dimerization (K124, V146, F150, C157, T166, C190), claudin-1 association (K148, T149, E152, T153) and CD81 association with HCV-E2 (L162, I182, N184, F186) (Higginbottom, Quinn et al. 2000, Kitadokoro, Galli et al. 2001, Drummer, Wilson et al. 2002, Drummer, Wilson et al. 2005) (Figure 3.1). Regions in the small extracellular loop and the transmembrane (TM) domains TM3 and TM4 of CD81 have also been reported to contribute to HCV entry by mediating CD81 cell surface expression and its interaction with partner proteins (Masciopinto, Campagnoli et al. 2001, Montpellier, Tews et al. 2011).
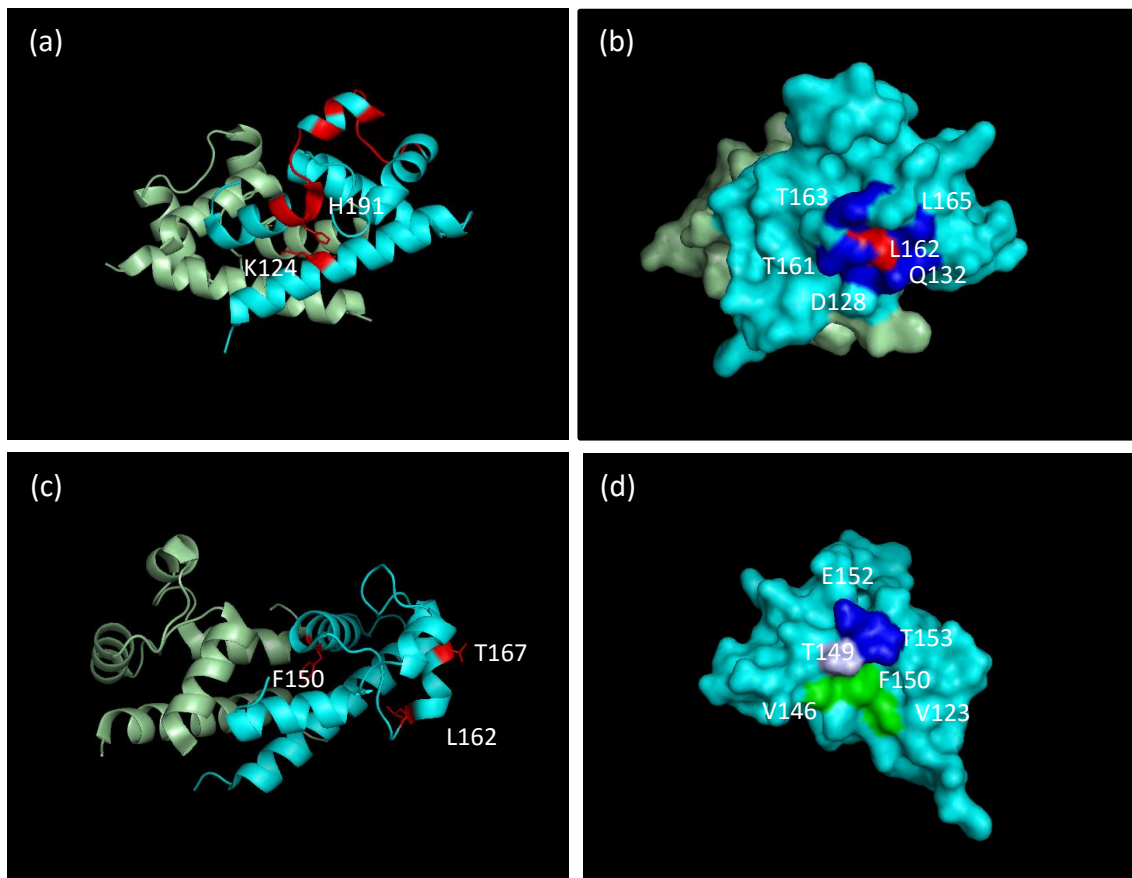
Figure 3.1: Ribbon diagrams and surface representations of the epitopes studied. K124 in the A helix and H191 in the E helix (a); T161, T163, L165, Q132 and D128 surrounding the L162 in the 3-10 helix (b); F150, T167 and L162 in the B, C and 3-10 helices (c); and T149, E152 and T153 alongside V146, F150 and V123 (d). V146, T149, F150 and V123 form a binding pocket. (Farquhar et al., in preparation).

The initial attachment steps of the viral lifecycle are essential and highly conserved, and therefore represent an attractive target for antiviral therapies. Indeed, host-generated antibodies to HCV glycoproteins appear to contribute to disease outcome (Chapel, Christie et al. 2001, Pestka, Zeisel et al. 2007). Some degree of prophylactic protection has been demonstrated in animal models using anti-HCV antibodies (Chapel, Christie et al. 2001, Pestka, Zeisel et al. 2007, Keck, Machida et al. 2008), however this success has not been replicated in human clinical trials. Whilst a number of anti-E2 antibody therapies have been tested, none have demonstrated a significant effect on viral load, and in one study escape mutations were seen in all patients (Gordon, Lynch et al. 2011, Vercauteren 2012). This failure may to some degree be attributed to the extreme plasticity in the HVR1 of the HCV glycoprotein E2, to which many of these antibodies are targeted. An alternative target for antibody therapy therefore is the host factors themselves, as they are completely conserved and cannot develop escape mutations. Inhibiting the virus-receptor interaction by blocking either the virus or host proteins may occur through direct blocking of binding sites or by antibody coating.

To date, a number of antibodies to CD81 have been described and the most widely used are JS-81 and 1.3.3.22, both of which bind a conformational epitope within the CD81-LEL and are capable of recognising CD81 on a variety of cell types (Bertaux and Dragic 2006, Meuleman, Hesselgesser et al. 2008). Both antibodies have been shown to inhibit HCVpp and HCVcc infection, (Bertaux and Dragic 2006, Meuleman, Hesselgesser et al. 2008, Farquhar, Hu et al. 2012) and with JS-81 neutralisation has been demonstrated across genotypes 1-6. The binding site of 1.3.3.22 overlaps with the L162 residue (Drummer, Wilson et al. 2002), providing a

mechanism for at least some aspects of its neutralizing activity. JS-81 has also been shown to act at additional stages of the viral lifecycle during the formation of receptor complexes and at post-internalisation steps (Bertaux and Dragic 2006, Schwarz, Grove et al. 2009, Farquhar, Hu et al. 2012). The use of these antibodies demonstrates their therapeutic potential, and this is supported by a study in 2008 in which prophylactic protection from genotype 1a and 4a infections in human liver uPA-SCID mice was observed using anti-CD81 antibodies (Meuleman, Hesselgesser et al. 2008).

It should be noted that antibodies can block infection via a number of mechanisms throughout the virus entry process (reviewed in (Klasse and Sattentau 2002, Marasco and Sui 2007). Alongside simply blocking interactions, antibodies may also induce the aggregation of the virus or promote the endocytosis of receptors, as has been reported for a number of CD81 mAbs (Farquhar, Hu et al. 2012). Furthermore, they may inhibit the fusion of the virus with the target cell by inhibiting the conformational changes necessary for fusion.

The well-characterised interaction between CD81 and HCV-E2 has made it a preferred target for intervention. However, CD81 is expressed almost ubiquitously, and therefore it is probable that widespread CD81 ligation with antibody would cause off-target effects *in vivo*. As the CD81 protein has an important role in the immune response, its engagement on immune cells has been investigated and shown to cause: the activation of T cells via Lck (Wack, Soldaini et al. 2001, Crotta, Ronconi et al. 2006); the activation and induction of B-cell proliferation (Cocquerel, Kuo et al. 2003, Rosa, Saletti et al. 2005, Coffey, Rajapaksa et al. 2009); the promotion of T and B cell collaboration (VanCompernolle, Levy et al. 2001); and the inhibition

of NK cell activation, proliferation and cytokine production (Crotta, Stilla et al. 2002, Tseng and Klimpel 2002, Maecker 2003). Within the cell antibody ligation of CD81 has been shown to activate the MAPK-ERK and Rho-family GTPase signalling pathways (Carloni, Mazzocca et al. 2004, Zhao, Wang et al. 2005, Brazzoli, Bianchi et al. 2008) in addition to promoting hepatoma spread in an actin-dependent manner (Brimacombe, Wilson et al. 2014) and stimulating clathrin-dependent internalisation of CD81 (Farquhar, Hu et al. 2012). A study in uPA-SCID mice showed that administration of antibodies to CD81 caused an elevation of transaminase levels and syncytia formation in the human portion of the liver (Pilot-Matias T. 2010). Given this list of potential side effects, antibodies which cannot distinguish between CD81 expressed in hepatic and non-hepatic backgrounds are likely to be of limited therapeutic use in preventing HCV infection.

Previous reports have shown that the conformations of CD151 and of CD63 are altered by epitope masking in the presence cell type-specific binding partners, and that these resulting changes in conformation alter antibody binding affinities (Rubinstein, Le Naour et al. 1996, Serru, Le Naour et al. 1999, Sincock, Fitter et al. 1999). Similarly, CD81 structure is altered by the interaction with E2 (Rajesh, Sridhar et al. 2012), and with other tetraspanins (Silvie, Charrin et al. 2006). Indeed, this latter study has demonstrated that murine CD81 in the presence of other tetraspanins can be specifically identified with the antibody MT81w (Silvie, Charrin et al. 2006).

As cell-specific interactions are formed by the protein, distinguishing CD81 in a hepatic background from CD81 in other cell types may be theoretically possible due to the formation of cell-type specific interactions. Perhaps the most relevant of these interactions is the

hepatocyte-specific interaction between CD81 and the cleavage product of EWI-2, EWI-2wint, which has been suggested to contribute to the liver tropism of HCV (Rocha-Perugini, Montpellier et al. 2008, Montpellier, Tews et al. 2011). CD81 has additionally been reported to form T cell-specific interactions with CD4 (Fournier et al., 2010) and CD8 (Todd et al., 1996), and B cell-specific interactions with CD63, very late antigen (VLA) integrins and human leukocyte antigen – DR (HLA-DR antigens) (Rubinstein, Le Naour et al. 1996).

Given these known interactions it is possible that a hepatocyte-specific conformation of human CD81 may exist. If this were identified, an antibody could be designed which preferentially bound hepatocyte CD81 with limited recognition of CD81 on other cell types, thus causing limited off-target effects.

The McKeating group has produced a panel of antibodies targeting human CD81 expressed in *Pichia Pastoris* (Jamshad, Rajesh et al. 2008) (Figure 3.1). These antibodies were identified by their reactivity with recombinant forms of full length (FL) and truncated CD81-LEL in an ELISA assay. These screening assays identified 17 LEL-specific monoclonal antibodies (mAbs) which were tested for reactivity with a panel of CD81 proteins with mutations in regions necessary for HCV-E2 binding and CD81 dimerisation (Farquhar et al., in preparation) (Higginbottom, Quinn et al. 2000, Drummer, Wilson et al. 2005) (Table 3.1, Figure 3.1). They were also shown to be able to inhibit HCV infection in a manner strongly correlated with their binding affinity to CD81.

This panel of mAbs was used to probe the availability of CD81-LEL epitopes on different cell types with the goal of identifying antibodies that preferentially recognise hepatocellular CD81. It should be noted that in the experiments described below members of the antibody panel

were used at identical concentrations across all cell lines studied. As a result, in the absence of proper optimisation the data presented here should be treated as a starting point for more thorough investigation. The caveats of the methodology used will be elaborated upon in the discussion.

Table 3.1 — mAb (5 µg/mL) reactivity with wild type (WT) and mutant MBP-CD81-LEL proteins.

Epitope Group	Antibody	WT	Dimer								Monomer					
			V123A	T149A	L162P	T167I	P176S	I182F	N184Y	F186S	K124T	V146E	F150S	C157S	T166I	C190R
		-	A helix	B helix	3-10 helix	C helix	CD loop	D helix	D helix	D helix	A helix	B helix	B helix	BC loop	C helix	E helix
I	2.s20													↓↓↓	↓↓↓	↓↓↓
	2.s24													↓↓↓	↓↓↓	↓↓↓
	2.s131													↓↓↓	↓↓↓	↓↓↓
	2.s63													↓↓↓	↓↓↓	↓↓↓
	2.s66													↓↓↓	↓↓↓	↓↓↓
	2.s48										↓			↓↓↓	↓↓↓	↓↓↓
	2.s139										↓			↓↓↓	↓↓↓	↓↓↓
II	1.s201				↓↓↓									↓↓↓	↓↓↓	↓↓↓
	1.s290				↓↓↓								↓	↓↓↓	↓↓↓	↓↓↓
III	1.s337				↓↓↓	↓↓↓							↓	↓↓↓	↓↓↓	↓↓↓
IV	1.s262		↓↓	↓↓	↓↓	↓↓↓						↓	↓↓↓	↓↓↓	↓↓↓	↓↓↓
V	1.s135		↓	↓↓	↓↓↓								↓↓↓	↓↓↓	↓↓↓	↓↓↓
	1.s73		↓↓	↓↓	↓	↓						↓↓	↓↓↓	↓↓↓	↓↓↓	↓↓↓
VI	1.s141		↓		↓								↓↓	↓↓↓	↓↓↓	↓↓↓
	2.s155		↓		↓								↓	↓↓↓	↓↓↓	↓↓↓
	2.s169												↓	↓↓↓	↓↓↓	↓↓↓

Table 3.1: mAb (5 µg/mL) reactivity with wild type (WT) and mutant MBP-CD81-LEL proteins where: ↓ denotes a 25 – 75% reduction in binding; ↓↓ - a 75 – 90% reduction and ↓↓↓ >90% reduction in binding. Farquhar et al., in preaparation.

3.2 RESULTS

3.2.1. Anti-CD81 mAbs show variable binding to Huh-7.5 hepatoma cells.

Previous work has examined the ability of the antibody panel to bind to recombinant MBP-CD81-FL and -LEL, and the antibodies demonstrate varying binding efficiencies to both proteins (Farquhar et al., in preparation, appendix table 1). To characterise the ability of the panel to bind to full length CD81 expressed in the background of a hepatic membrane, the antibodies were used at a saturating concentration and examined for their ability to bind Huh-7.5 hepatoma cells (optimisation work carried out by Michelle Farquhar). This cell line was chosen since it supports robust HCV replication and naturally expresses CD81. Representative FACS profiles are shown for each antibody (Figure 3.2 a-n). Whereas the majority of antibodies bound with high median fluorescent intensities (MFI), mAbs 2s24, 2s131, 1s73 and 2s141 (Figure 3.2f, e, n, and l respectively) exhibited somewhat lower binding capacities.
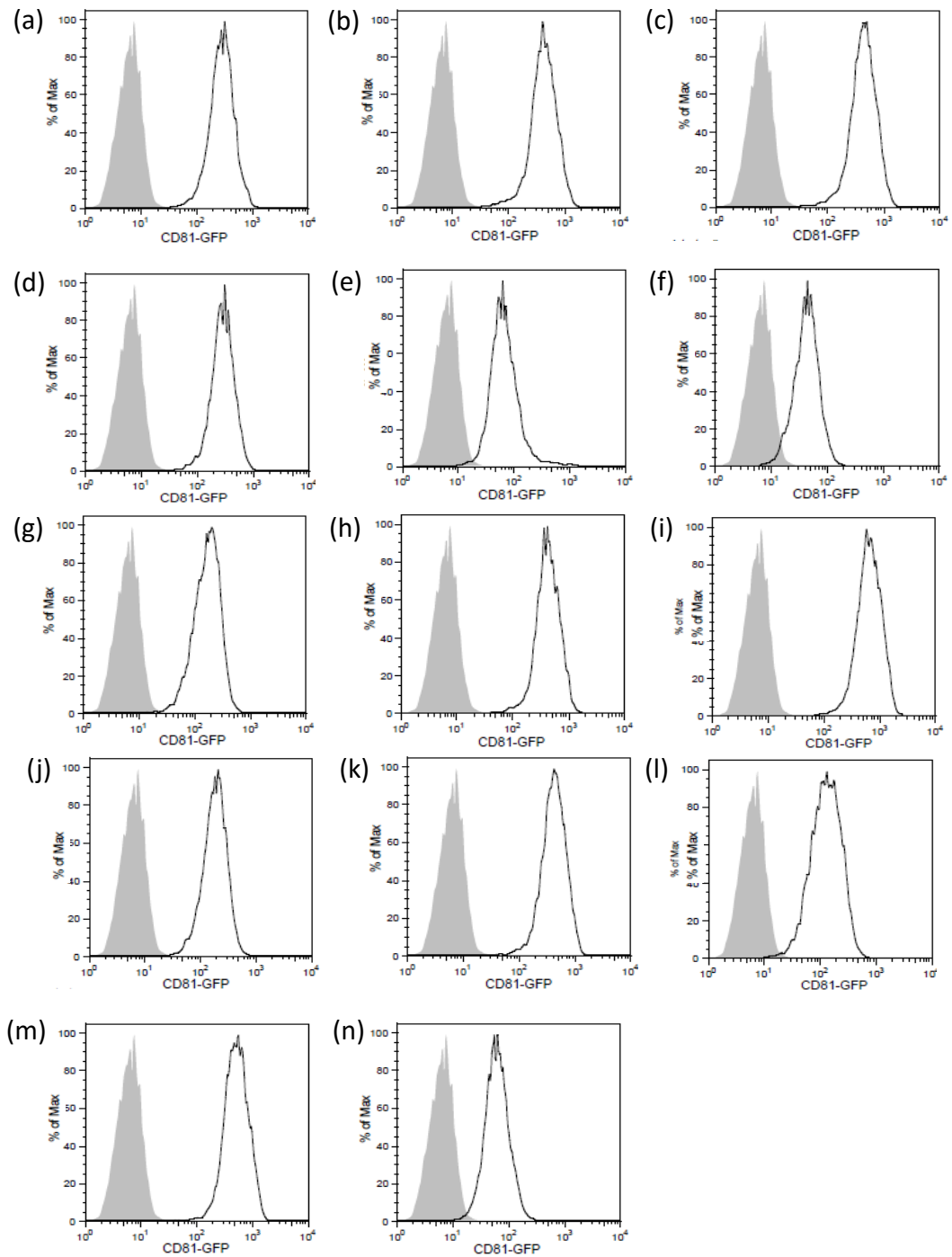
Figure 3.2: Representative FACS curves of anti- CD81 monoclonal antibody panel on Huh-7.5. A representative curve (black line) of three duplicate repeats is shown against isotype matched control (grey shaded). (a) 2s20, (b) 2s48, (c) 2s63, (d) 2s66, (e) 2s131, (f) 2s24, (g) 2s139, (h) 1s201, (i) 1s337, (j) 1s262, (k) 1s135, (l) 2s141, (m) 2s155, (n) 1s73. Antibodies were used at 1 μg/ml.

In order to establish whether some of these epitopes are less accessible on the Huh-7.5 cell surface in comparison to others, mAb binding was expressed relative to an irrelevant IgG control and defined as relative fold change (RFC) to normalise binding levels over multiple experiments. The antibodies were organised into groups of high, medium, or low binding intensity (Figure 3.3a). 2s24, 2s131, 1s73, 2s141 and 2s139 are placed in the lowest group, with an RFC range of 6.69 to 24.36; 1s262 and 2s66 were assigned to the medium group, with RFCs of 36 and 53.1 respectively; and 2s63, 1s135, 2s48, 2s20, 1s201, 1s169, 2s155 and 1s337 constituted the highest binding group with RFCs ranging from 67.53 to 93.72. This wide range of RFC values may demonstrate the varied availability of the epitopes studied in this cellular background if confirmed following proper optimisation of antibody usage.
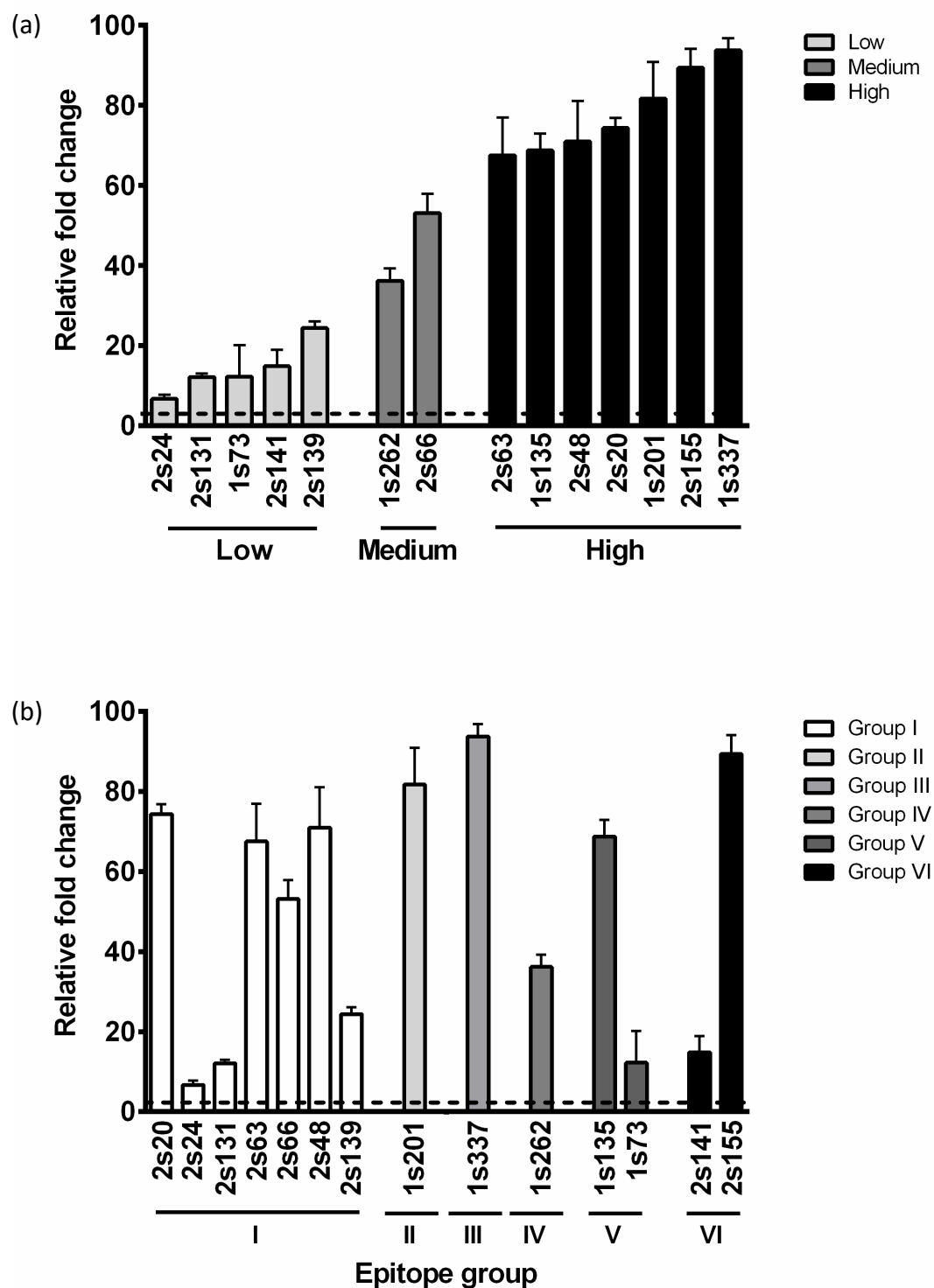
***Figure 3.3: Epitope recognition of anti- CD81 monoclonal antibody panel on Huh-7.5
hepatoma cells.*** *Fold change in MFI from IgG for each antibody on CD81 expressed on Huh-
7.5 cells (n=3) organised by binding level (a) and epitope group (b). Staining was carried out
live before fixing and analysis using flow cytometry. All data shown are representative of 3
repeats.*

In previous work Farquhar et al., classified the mAbs into 6 groups according to their binding to a panel of recombinant CD81 proteins containing mutations at specific LEL residues involved in E2 binding and dimerisation (Table 3.1). In order to establish whether the variation in epitope availability on Huh-7.5 cells could be linked to these epitope groupings, the RFC values for each antibody were compared between the groups (Figure 3.3b). This analysis revealed no apparent relationship between the parameters. RFC values in group I range from 6.6 -74.3 RFC. MAbs 2s20, 2s48 and 2s63 in group I have similar values, but the presence of the much lower 2s24 and 2s131 in group I, along with that of 1s135 in group V negates the low level of binding as being specific to group I. Groups V and VI are also variable, displaying values of 12.2 - 68.7 RFC and 14.8 - 89.4 RFC respectively. The antibodies in group II and III have similar binding levels, with 1s201 and 1s337 displaying values of 81.7 RFC and 93.7 RFC. The single antibody in group IV has an intermediate binding value of 36.2 RFC. These data demonstrate no direct relationship between the epitope grouping of an antibody and its ability to bind to Huh-7.5 cells. These epitope groups are based on binding in a membrane-free system, and one possible interpretation of the discrepancy observed with the data presented here is that the differences in epitope binding patterns are due to the presence of a membrane in a cell background.

3.2.3   Comparative binding of anti-CD81 on hepatocytes and immune cells

CD81 is expressed on T and B cells in addition to hepatocytes, and forms cell-type specific interactions in these cells. To begin to investigate whether CD81 epitope availability can be affected by the type of cell membrane in which it is expressed, the ability of the antibody panel to bind CD81 expressed on hepatocytes and immune cells was examined by live cell staining

and FACS analysis. In addition to PBMC-derived primary T and B cells, antibody binding to the T cell line Jurkat and the B cell line Raji was assessed. Four separate donor isolations were used for the primary immune cells, whilst two separate isolations were used for PHH. Representative FACS profiles are shown for antibodies from each Huh-7.5-defined binding group for all cell types (Figure 3.4). As before, the antibodies were used at an identical concentration across all cell types studied. Therefore, this work would need to be repeated following optimisation on each cell type before any valid conclusions could be derived.

Initially, binding capacity was measured for primary human hepatocytes (PHH) (Figure 3.4a-c), as these are most representative of the hepatocytes in the liver. Whilst the antibodies were capable of binding to this cell type, they did so to a much lower degree than observed with Huh-7.5 cells and displayed less variation in binding across the groups. For example, 2s141 (Figure 3.4a) in the low binding group has an intensity of 6.8 MFI whereas 1s290 in the high binding group has an intensity of 29.9 MFI (Figure 3.5c), for both mAbs irrelevant IgGs bound with an MFI of 3.4.
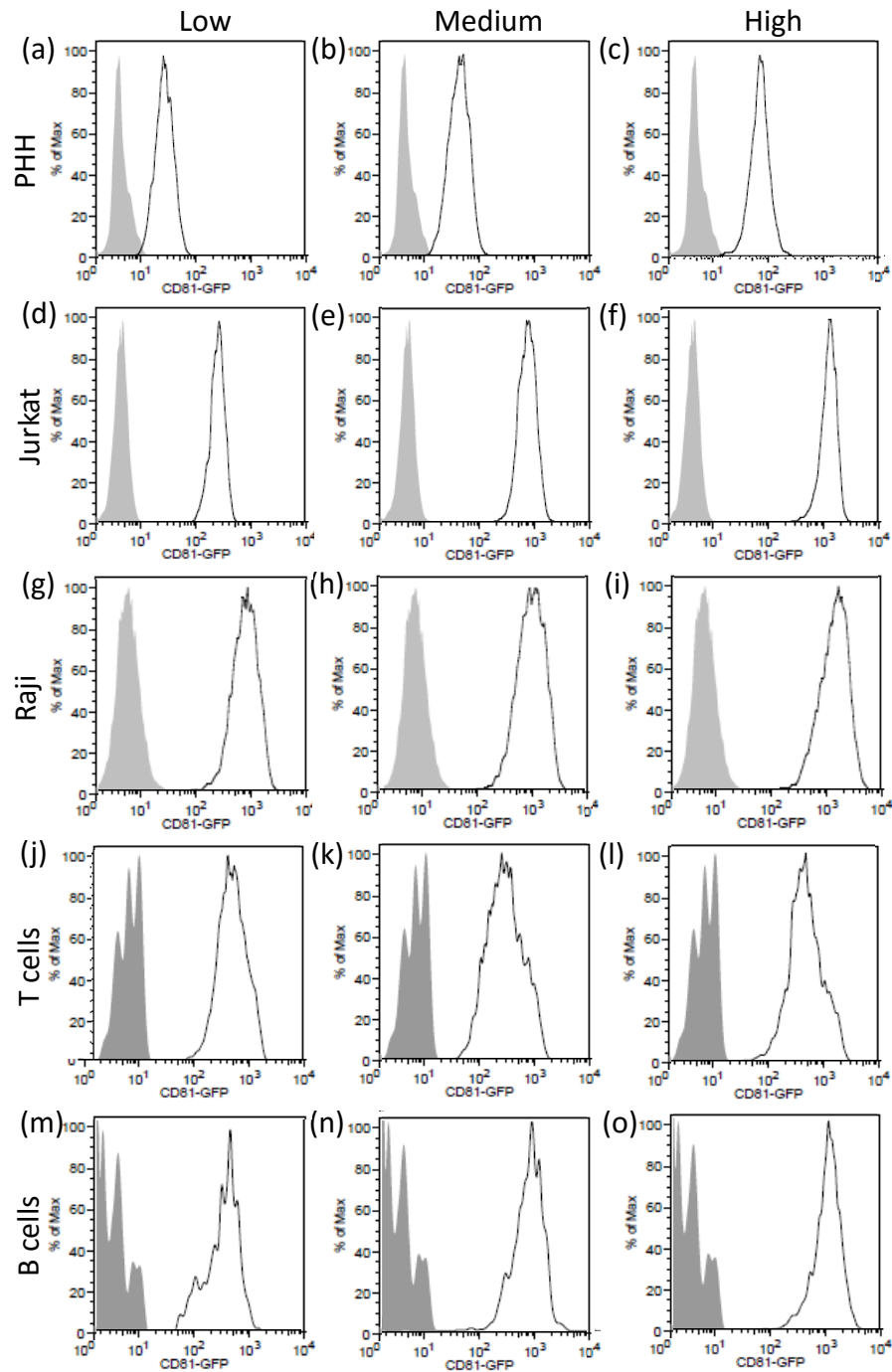
Figure 3.4: Representative FACS curves of anti-CD81 monoclonal antibody panel on primary and immune cell types. *A representative curve (black line) of three duplicate repeats is shown against isotype matched control (grey shaded) for one antibody from each of the Huh-7.5-defined binding groups. (a) 2s141, (b) 2s66, (c) 2s20, (d) 2s141, (e) 2s66, (f) 1s337, (g) 2s141, (h) 1s262, (i) 1s135, (j) 2s141, (k) 2s66, (l) 1s337, (m) 2s131, (n) 1s262 (o) 1s201.*

Using the current methodology, the relative binding of the antibody panel to the Jurkat cell line shows broad similarities to that observed with Huh-7.5, with the representative antibodies showing an increase in binding capacity between the low, medium and high groups. 2s141 in the low group binds with 180 MFI (Figure 3.4d), and 1s337 in the high binding group displays a value of 1056 MFI (Figure 3.4f), the irrelevant IgG bound with 3.2 MFI. The Raji cell line exhibits a similar range, from 329.5 MFI (2s141, Figure 3.4g) to 1467.5 MFI (1s135, Figure 3.4i). The binding of all antibodies to both immune cell lines was around ten times higher than Huh-7.5 cells, which may reflect their higher CD81 expression if confirmed following optimisation.

With primary T and B cells, the levels of binding are lower than are observed on the immune cell lines. On primary T cells, antibodies in all binding groups displayed very similar MFI values, with 2s141 (Figure 3.4j), 2s66 (Figure 3.4k) and 1s337 (Figure 3.4l) displaying values of 50.5 MFI, 61.3 MFI and 77.2 MFI respectively. In contrast, on primary B cells binding capacities were more varied between the high binding group and other groups. MAbs 2s131 (Figure 3.4m) and 1s262 (Figure 3.4n) in the low and medium binding groups bound with an MFI of 3.5 and 3.8 respectively, whereas 1s201 (Figure 3.4o) in the high binding group had an MFI of 6.7.

These data suggest considerable variation in antibody binding capacities across the cell lines tested. As a result, all members of the antibody panel were carried forward for continued screening across all cell types to attempt to identify epitopes which are particularly accessible in a hepatic background.

3.2.4 The expression of CD81 in a membrane background has considerable effects on availability of epitopes in the LEL

To investigate cell-type specific patterns of epitope availability, the binding capacities of the antibody panel were compared to their binding efficiencies to purified full length recombinant CD81 (MBP-CD81-FL). To do this, the binding capacity was plotted against the MBP-CD81-FL binding affinity and the 95% confidence interval (CI) of the data found. Any antibodies which fell outside of this interval could then be described as binding either to a higher or lower degree in the membrane than would be predicted by their binding to MBP-CD81-FL. As previously discussed, without the proper optimisation of antibody staining on all cell types tested, the conclusions taken from this data can remain only speculation. This is reviewed further in the discussion.

3.2.4.1 Hepatocyte-specific alterations in epitope availability

The comparison of MBP-CD81-FL binding efficiency with Huh-7.5 affinity showed a positive correlation between the two parameters, with those antibodies which displayed a higher binding efficiency to MBP-CD81-FL in general also displaying a high binding capacity to Huh-7.5 (Figure 3.5a). However, when the 95% CI of this association was plotted, there were a number of antibodies which fell outside of the boundaries. Notably mAbs 1s337, 2s20, 1s135 and 2s63 were above the CI, suggesting that the epitopes recognised by these antibodies are more accessible on Huh-7.5 than on the recombinant protein. By the same reasoning, the epitopes bound by the antibodies 2s141, 2s131 and 2s24 are relatively less accessible in the Huh-7.5 background. These data suggest that CD81 in a Huh-7.5 membrane has considerable differences in the availability of epitopes compared to the purified CD81 protein in isolation.

When this analysis was repeated for primary human hepatocytes, the data again show a positive correlation (Figure 3.5b). However, we found fewer antibodies falling outside of the CI than were observed in the Huh-7.5 background (Figure 3.5a). In this case, only 2s20 and 2s139 bind to a higher degree on PHH than on MBP-CD81-FL, whereas 2s24 and 2s131 binding capacities were higher on the MBP-CD81-FL protein. Therefore, in the PHH membrane CD81 shows further changes in the availability of the epitopes.

These data suggest a positive correlation between the binding of the antibodies to MBP-CD81-FL and to CD81 in hepatic backgrounds. However, there are individual differences in the availability of a number of epitopes between these backgrounds, which may reflect considerable changes in the conformation of the LEL region. The relatively higher number of antibodies deviating from the CI in Huh-7.5 cells compared to PHH suggests that CD81 in the membrane of the hepatic cell line presents its epitopes in a different way from CD81 in primary cells.
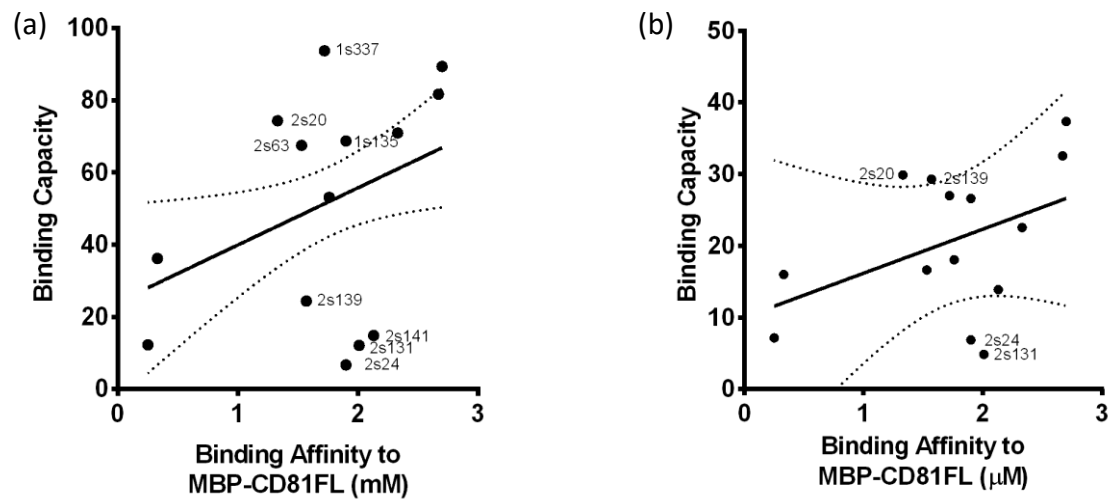
Figure 3.5: Comparison of antibody binding on recombinant CD81 to hepatic cells. *Fold change in MFI from IgG for each antibody on CD81 expressed on Huh-7.5 cells (binding capacity, n=3) (a) and PHH (binding capacity, n=2) (b) was plotted against the observed binding affinity to MBP-CD81-FL. Each black spot represents one antibody, and the full black line the regression line. Dotted curves above and below represent 95% confidence interval.*

3.2.4.2 T cell-specific alterations in epitope availability

As the availability of CD81 epitopes is affected not only by the presence of a membrane, but also in a cell-specific manner, we were interested to investigate the impact of an immune cell membrane on epitope availability.

The binding capacity of the antibodies to the Jurkat T cell line demonstrated a positive correlation with their binding efficiency to MBP-CD81-FL (Figure 3.6a). However, there were many outliers from the 95% CI. MAbs 1s201, 2s155, 2s139, 1s337, 2s20 and 1s135 were located above the CI, suggesting that the epitopes recognised by these antibodies are more exposed on Jurkat cells than on the recombinant protein. In contrast, 2s131, 2s141 and 2s24 were found below the CI, suggesting that these epitopes are more accessible in MBP-CD81-FL.

Repeating this analysis with primary T cells demonstrates that there are considerable differences between the binding of the antibody panel to these cells and to MBP-CD81-FL (Figure 3.6b). The epitopes recognised by the antibodies 2s63, 2s139 and 2s20 are more available on primary T cells, whilst those targeted by 2s66, 2s131 and 2s24 are more accessible on MBP-CD81-FL.

These data again suggest considerable differences between the availability of the mAb epitopes in the background of a cell membrane and in a recombinant, full length protein. However, there are many more differences between Jurkat cells and MBP-CD81-FL than between primary T cell CD81 and the recombinant protein.
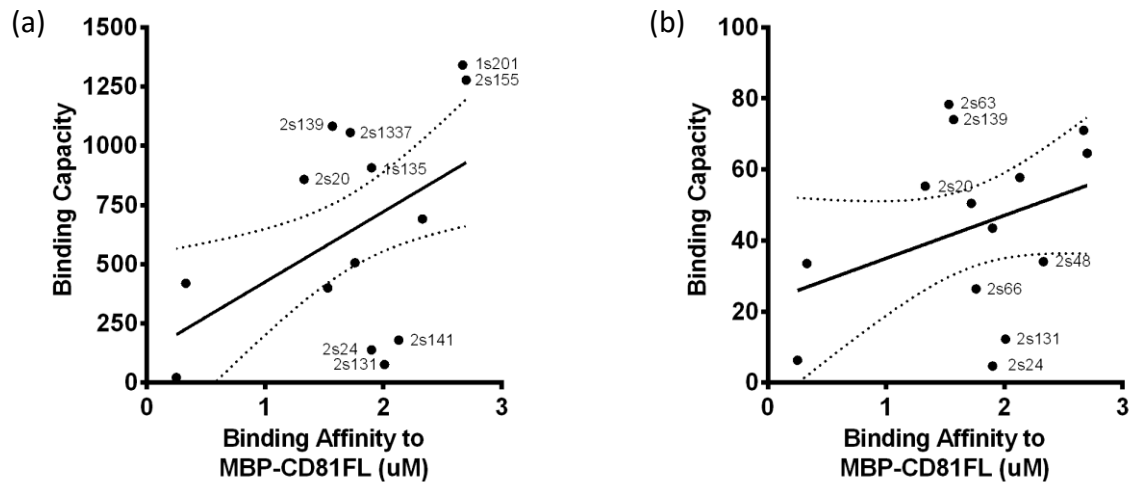
Figure 3.6: Comparison of antibody binding on recombinant CD81 to T cells. *Fold change in MFI from IgG for each antibody on CD81 expressed on Jurkats (binding capacity, n=3) (b) and primary T cells (binding capacity, n=4) (b) was plotted against the observed binding affinity to MBP-CD81-FL. Each black spot represents one antibody, and the full black line the regression line. Dotted curves above and below represent 95% confidence interval.*

3.2.4.3 B cell-specific alterations in epitope availability

CD81 is expressed not only on T cells, but also on B cells. In order to interrogate the effect of B cell membranes on the conformation of CD81, the binding capacity of the antibodies to Raji cells and primary B cells were compared to MBP-CD81-FL binding efficiency. As in all the other studies, we found a positive correlation between the observed binding affinities and binding efficiencies in both the Raji B cell line and primary B cells.

Again, there are a number of antibodies which display a considerable divergence from the overall trend. The epitopes recognised by 1s201, 1s135, 1s337, 2s139 and 2s20 are relatively more accessible on CD81 expressed in the Raji cell line than on MBP-CD81-FL (Figure 3.7a), whereas those recognised by 2s63, 2s141, 2s131 and 2s24 are more accessible in MBP-CD81-FL. These data show that there are epitopes in the LEL of CD81 whose availability is considerably altered in the Raji cell membrane.

Similarly, for primary B cells, the antibodies 2s155, 2s139 and 2s20 bind to a higher degree on primary B cells than MBP-CD81-FL, whereas 2s131, 2s141 and 2s24 bound preferentially to MBP-CD81-FL (Figure 3.7b).

These data suggest that there are considerable changes in the availability of the epitopes recognised by these antibodies when in the background of either a Raji B cell line or primary B cells. Interestingly, there are fewer differences between MBP-CD81-FL and the primary cells than between MBP-CD81-FL and the Raji B cell line. This trend has been seen in all cell types studied, with both PHH and primary T cells having fewer outliers from the 95% confidence interval than their corresponding cell lines.
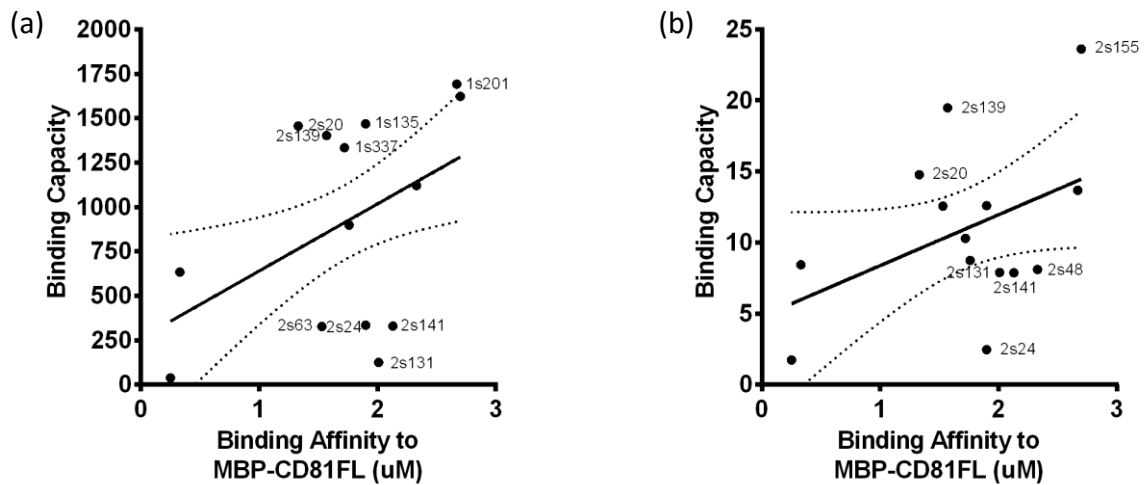
Figure 3.7: Comparison of antibody binding on recombinant CD81 to B cells. Fold change in MFI from IgG for each antibody on CD81 expressed on Rajis (binding capacity, n=3) (b) and primary B cells (binding capacity, n=4) (b) was plotted against the observed binding affinity to MBP-CD81-FL. Each black spot represents one antibody, and the full black line the regression line. Dotted curves above and below represent 95% confidence interval.

3.2.5 Cell-type specific alterations in epitope availability in comparison to the LEL in isolation

The binding efficiencies of the antibody panel to a recombinant protein containing just the CD81-LEL in isolation from the full length molecule, MBP-CD81-LEL, have also been determined. Given the considerable variation in epitope availability observed in the background of a cell membrane compared to MBP-CD81-FL, we were interested to understand whether such differences were conserved when the binding capacities were compared to the binding efficiencies of the panel to MBP-CD81-LEL. In this protein, the LEL is expressed in isolation without the other constituents of the CD81 molecule, the SEL, TM regions 3 and 4 and the carboxy terminus.

When compared to MBP-CD81-LEL, all cell types exhibited very similar patterns of outliers to those identified in the comparison with MBP-CD81-FL (Figure 3.8, Table 3.3). The greatest difference in binding patterns was observed with the hepatic cell types. Whilst the epitopes recognised by 1s337, 2s20 and 1135 were all more accessible on Huh-7.5 cells than on both MBP-CD81-LEL and MBP-CD81-FL, those recognised by 2s155 and 1s201 were additionally more accessible when compared to MBP-CD81-LEL (Figure 3.8a). In addition, whilst 2s139 2s141 and 2s131 were again bound more strongly to the recombinant protein, 2s24 did not fall outside of the confidence interval when compared to MBP-CD81-LEL binding efficiencies.

The comparisons of PHH and MBP-CD81-LEL were the most divergent from those observed with MBP-CD81-FL (Figure 3.8b). In this data set mAbs 2s20, 2s24 and 2s141 no longer fell outside of the 95% confidence interval, whereas 2s155 displayed higher RFC values on PHH than the LEL recombinant protein, and the epitopes recognised by 2s141 were more

accessible on the recombinant protein. These data suggest that availability of epitopes differs between CD81 in a PHH and MBP-CD81-LEL in a manner which is distinct from MBP-CD81-FL.

In contrast to hepatocytes, the outliers observed when comparing Jurkat cells to MBP-CD81-LEL are identical to those that were identified following comparison to MBP-CD81-FL, with only exception being mAb 2s63, that replaces 2s24 in falling below the CI (Figure 3.8c). This once again suggests that epitope availability in CD81 expressed in the background of a Jurkat cell differs greatly from CD81 LEL in isolation, but Jurkat cells differ from both CD81-MBP-FL and CD81-MBP-LEL in a very similar way.

When the binding efficiencies of the antibodies to MBP-CD81-LEL were compared to binding capacities on the remaining immune cells and cell lines they displayed almost identical outliers to those previously identified in the comparison to MBP-CD81-FL (Figure 3.6 and 3.7). Although in the case of primary T cells, mAbs 2s20 and 2s24 were no longer outliers from the CI (Figure 3.8d), and in Raji cells mAb 2s155 was an additional outlier above the CI with 2s24 no longer falling below the CI (Figure 3.8e). MAb 2s24 also no longer fell below the CI in primary B cells (Figure 3.8f).

If these findings were confirmed with properly optimised antibody concentrations, these data would confirm that the availability of CD81 –LEL epitopes differs in a membrane-specific manner from CD81 in a cell membrane, as with full length CD81.
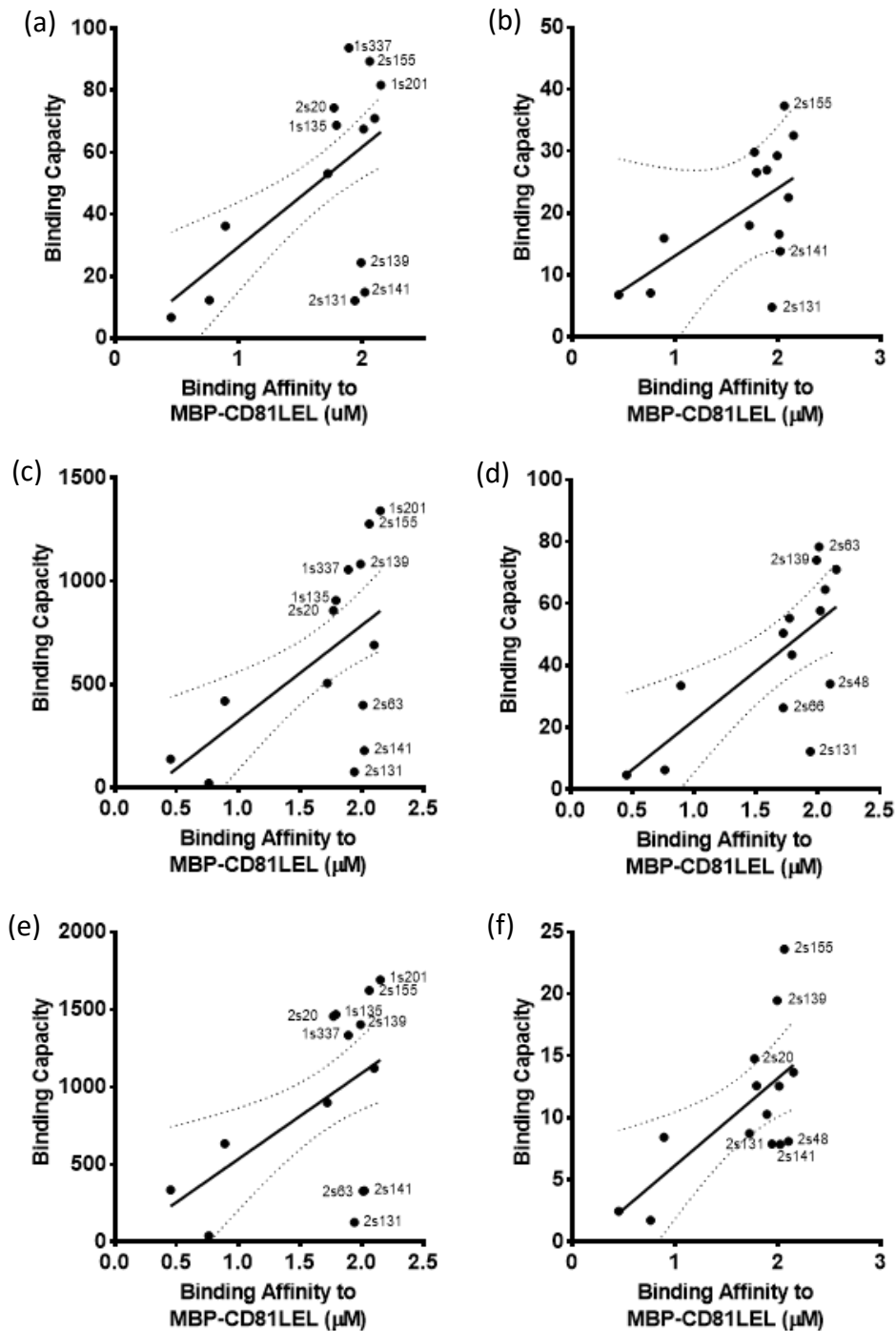
Figure 3.8: Comparison of antibody binding on MBP-CD81-LEL to CD81 in a membrane background. Fold change in MFI relative to an isotype matched IgG control for each antibody (binding capacity, n=3) for CD81 expressed on Huh-7.5 (a), PHH (b), on Jurkat (c) on CD3+ T cell (d), on Raji (e) and on CD19+ B cells (f) was plotted against the binding affinity to MBP-CD81-LEL. Each black circle represents one antibody. The solid line the regression best fit. Dotted curves above and below depict the 95% confidence interval.

3.2.6 Anti-CD81 antibodies show cell-type specific binding.

Having observed multiple differences between cell-expressed CD81 and recombinant CD81, we were interested to interrogate any differences or similarities in epitope availabilities between these cell types and hepatocellular CD81. To do this, the RFC for each antibody on each cell type was compared to its ability to bind CD81 expressed on Huh-7.5 (shown in figure 3.3a) (Figure 3.9).

The RFCs for antibody recognition of PHHs (Figure 3.9a) was much lower than that observed with Huh-7.5 (Figure 3.3), and was associated with a higher error, a characteristic which is likely a reflection of the smaller amounts of mAb bound and variability between the two donor isolations. However, the overall binding pattern of the antibodies to PHH largely reflected that for Huh-7.5, with the majority remaining in the previously defined low, medium and high binding categories. The only exception to this is 2s139, which was placed in the low group on the basis of Huh-7.5 binding but bound well to PHH. This implies a significant change in the epitopes recognised by 2s139 which causes it to be more strongly recognised on the primary cell type than on Huh-7.5. However, for all of the other antibodies the binding patterns are very similar, suggesting that the overall conformation of CD81 is very similar in PHH and Huh-7.5.

The pattern of antibody binding to the CD81 transduced cell line Jurkat-CD81 is also similar to that observed with Huh-7.5, with the majority of antibodies being placed in the same groups as the Huh-7.5 ranking (Figure 3.9b). However, there are a number of anomalies. Both 2s63 and 1s73 are placed higher in the Huh-7.5 ranking than their RFC values would suggest, implying that the epitopes recognised by these antibodies are less accessible on Jurkats than

on Huh-7.5. In contrast, the epitope recognised by 2s139 is better recognised on Jurkats than Huh-7.5.

The pattern of antibody binding observed on Jurkat-CD81 is repeated almost exactly for Raji-CD81, with very similar RFC values and trends (Figure 3.9d). 2s139 is recognised more strongly on Raji cells than on Huh-7.5 cells, whereas 1s73 and 2s63 are recognised to a lesser degree.

In contrast to the consistency observed between PHH and Huh-7.5 recognition, the relationship between the binding capacities of antibodies on the primary immune cells and on immune cell lines is not so consistent. As with PHH, the RFC values are much lower on the primary cells than the cell lines, with primary B cells having a particularly low level of binding.

The majority of antibodies which bind Huh-7.5 to a high level also bind very strongly to primary T cells (Figure 3.9c), with the exception of mAbs 1s135 and 2s48, both of which bind to a lower degree in this cell type (Figure 3.9d). Conversely, mAbs 2s63, 2s141 and 2s139 bind more strongly on primary T cells than on Huh-7.5.

The overall antibody binding levels in primary B cells are around a third of that seen in primary T cells, and are much lower and less varied than in the Raji cell line (Figure 3.9e). Whilst 2s24, 1s73 and 2s155 are all appropriately placed following the Huh-7.5 ranking, 2s139 a member of the low binding group for Huh-7.5, would fit more appropriately into the high binding group on Raji. These findings suggest that CD81 has either low expression or an inaccessible conformation on B primary B cells, but that there are some regions around the epitopes recognised by 2s139 and 2s155 which are particularly accessible.

In the absence of the proper optimisation of antibody binding on each cell type used, it is not possible to form any valid conclusions from the data presented here in terms of the availability

of the epitopes studied. The caveats of the methodology used are discussed below, but the results presented here provide a basis for further work examining the conformation of CD81 between relevant cell types.
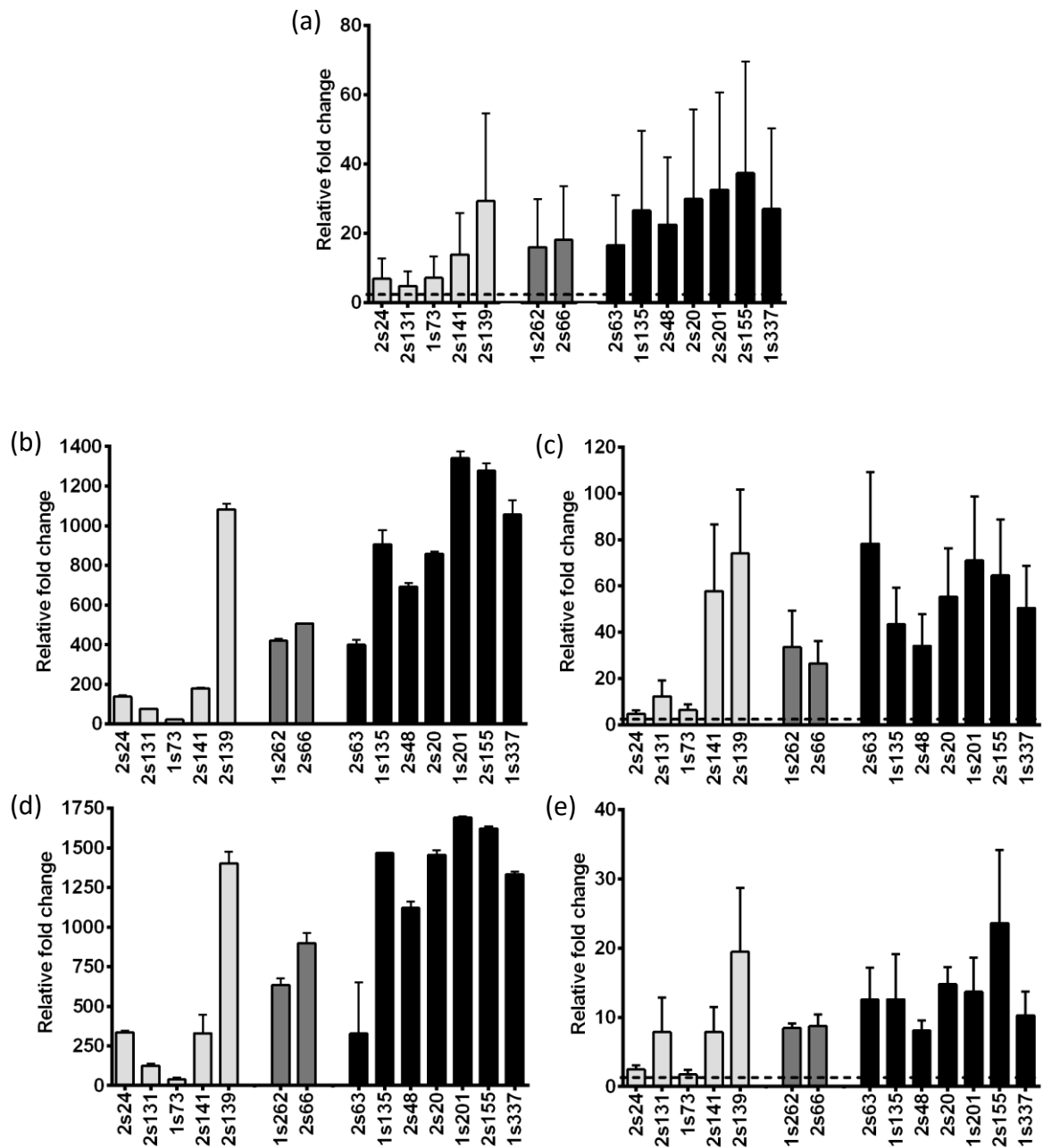
Figure 3.9: Epitope recognition of anti-CD81 monoclonal antibody panel on the surface of primary and immune cell types. *Fold change in MFI from IgG for each antibody on CD81 expressed on PHH (n=3) (a), Jurkat cells (n=3), (b) primary T cells (n=4), (c), Raji cells (n=3) (d) and primary B cells (n=4) (e). In all cases, staining was carried out live before fixing and analysis using flow cytometry.*

3.3 DISCUSSION

The data presented here attempt to utilise a characterised panel of CD81 mAbs to elucidate differences in CD81-LEL epitope availability between cell types.

Initial experiments looked at antibody binding patterns to the Huh-7.5 cell line in comparison to their binding to purified MBP-CD81-FL (Farquhar et al., in preparation, appendix). When the antibodies were incubated with Huh-7.5 cells, they displayed a wide range of binding capacities, However, this variation did not clearly map to the current epitope groupings of the mAbs (Farquhar et al., in preparation, table 3.1), as antibodies in groups I, V and VI exhibited no consistent pattern of binding capacities.

One possible explanation for the variation in binding levels observed on Huh-7.5 cells is that there are differences in CD81-LEL epitope availability in this background which can be detected by the antibody panel. If so, the discrepancy observed between the antibody binding patterns on the MBP-CD81-FL and Huh-7.5 may be related to the effect of the membrane on protein conformation, as the binding studies carried out by Farquhar et al., to determine epitope groupings used a membrane-free system. In this case, these antibodies would represent a useful resource for determining the exposure of CD81-LEL epitopes in a cell membrane.

However, to confirm this and to further explore these results, it would be necessary to carry out further optimisation and repeat the experiment. Of paramount importance would be to define the optimal concentration of the antibodies in an Huh-7.5 cell to enable a thorough and valid comparison of differences in binding between the two backgrounds studied. With the

current methodology it is not possible to rule out that the differences in binding levels seen are due to sub-optimal antibody concentrations.

In brief, a full optimisation of antibody usage necessitates carrying out an antibody titration in relevant staining conditions. This involves a serial dilution of the antibody and the subsequent identification of the lowest concentration at which the maximal fluorescence intensity is achieved. Determining the optimal antibody concentration is necessary as too high a concentration of antibody can lead to non-specific binding which masks the true amount of target antigen in the target cell, whilst too low a concentration leads to the insufficient labelling of cells. Only once optimum staining conditions have been determined can any significant changes in binding then be attributed to alterations to the antibody binding site.

To begin to understand how cell membrane background may influence the availability of CD81-LEL epitopes, live staining of the antibody panel was carried out on a variety of cell types in which CD81 is known to form cell type-specific interactions and which exhibit responses to CD81 engagement. This was achieved using flow cytometry with the antibodies being used at identical concentrations. As previously discussed, it would be necessary to optimise staining conditions on all cell types in order to form any valid conclusions regarding the differences in antibody presentation of the CD81 LEL between the cell types tested.

PHH, which are considered the 'gold standard' model for hepatocytes, were compared alongside the Huh-7.5 cell line. As a primary cell line which exhibits hepatic polarity and morphology (Lindenbach, Evans et al. 2005, Flint, von Hahn et al. 2006, Narbus, Israelow et al. 2011) the structure and constituents of the membrane of PHH are likely to be

considerably different to that of Huh-7.5. In a similar manner, primary immune cells and immune cell lines were tested, with primary T cell and B cells being compared alongside the cell lines Jurkat and Raji respectively. All antibodies exhibited positive binding to the cell types tested.

To attempt to model how CD81 expressed in a cell background differs from MBP-CD81-FL in a membrane-free system, the abilities of mAbs to bind to these cell types were compared to the previously reported binding affinities for the recombinant full length protein (Farquhar et al., in preparation. Appendix table 1). A summary of the outliers can be found in table 3.3.

When this analysis was applied to Huh-7.5 cells the antibodies 1s337, 1s135 and 2s141 which bind similar epitopes were found on both sides of the line of best fit, as were 2s20, 2s63, 2s131 and 2s24, which also bind identical epitopes. The residues recognised by 2s139, which showed an unusually low RFC on Huh-7.5 cells, are very similar to those of other group I antibodies, but it additionally recognises K124 in the A helix. However, this pattern is similar to that recognised by the antibody 2s48, which showed no unusual binding. With PHH, outliers from main the relationship trend demonstrated no obvious epitope specificity: the outliers 2s20, 2s24 and 2s131, which all belong to epitope group I, recognise an identical group of epitopes in the BC loop and C and E helices.

As previously observed with the hepatic cells, there is no striking epitope specificity between the antibodies which bind either above or below the line of association between antibody binding capacity to Jurkat cells and binding efficiency to MBP-CD81-FL. Antibodies with identical recognition patterns were found on both sides of the confidence interval, with the only exception being 2s139. This antibody fell above the CI and additionally recognises the

residue K124 in the A helix. The antibody 2s48 has an identical recognition pattern to 2s139, and does not fall outside of the CI. The trends observed with primary T cells were similar to those observed with PHH, as all outlying antibodies were in group I, and recognise identical epitopes C157, T166 and C190 in the BC loop, A, C and E helices.

When the binding affinities of the antibodies to the Raji cell line were compared to their binding efficiency to MBP-CD81-FL, there was again no apparent relationship between the epitopes recognised by the antibodies with unusual recognition profiles, and in these cells 2s139 binds above the line of best fit. The results seen with primary B cells were identical to those described for the Raji cell line, as the outliers recognise the same epitopes.

These analyses may suggest a significant variation between the availability of the epitopes between the full-length CD81 protein in isolation and various membranes. If so, the locations of the epitopes discussed above suggest that the changes occur predominantly in the BC loop and A, C and E helices. However, in the absence of proper optimisation the causes of this difference cannot be with any certainty attributed to the presentation of the target epitopes. Instead, it is possible that the differences in binding intensities seen are due to the use of sub-optimal concentrations of the antibodies on the cell types studied.

To investigate whether these binding patterns could be affected by the dimerisation and TM domains of the protein, the same analysis was carried out in comparison to a second purified protein, MBP-CD81-LEL which does not contain these regions.

In general, there are very few differences in the outliers identified by comparison to MBP-CD81-LEL instead of MBP-CD81-FL. This trend is particularly clear for the immune cell lines and primary immune cells, where only one antibody differed in our comparisons of MBP-

CD81-FL and MBP-CD81-LEL. In these cases, these antibodies have identical recognition patterns to those identified in the previous analysis (Table 3.3).

This recapitulation seen for immune cells was not as complete for PHH and MBP-CD81-LEL. For MBP-CD81-FL, 2s20 was an outlier above the line of best fit with 2s24 and 2s131 outliers below (Figure 6b), however for MBP-CD81-LEL, 2s155 was the only outlier above the line, whilst 2s131 and 2s141 fell below the line.

The epitopes recognised by 2s155 differ from those targeted by 2s20 by additionally recognising V123, L162 and F150 in the A, 3-10 and B helices. However, these residues are also recognised by 2s141, which falls below the line. Similarly, the outlier 2s131 binds identical epitopes to a number of other antibodies which did not exhibit exceptional binding.

Interestingly, the only epitope group which routinely binds inside the CI is epitope group IV, whose sole member is antibody 1s262. This antibody recognises residues V123, T149, L162, T167, V146, F150, C157, T166 and C190. The consistent binding of this antibody may reflect the wide range of residues recognised, whereby unavailability of a few residues may be compensated for by the presence of others.

These data may demonstrate that the availability of epitopes in the CD81 –LEL differ from one another and from recombinant CD81 proteins in a very similar manner to the variations seen with CD81-FL. However, these changes cannot be elucidated using this current methodology. Optimisation of antibody binding on all cell types studied here would be necessary in order to carry out a valid comparison of antibody binding between the cell types.

As these data may suggest considerable differences in epitope availability between cell types, we were interested to understand whether CD81 in different membrane backgrounds could be discriminated by the antibody panel. To examine this, the RFC of each antibody on each cell type was plotted and the antibodies organised into the low, medium, and high binding groups established using Huh-7.5 to identify outliers from the trend.

Comparison of antibody RFCs on Huh-7.5 and PHH revealed a strong similarity between binding levels on the two cell types, although the levels of CD81 expression are much lower and more varied on PHH, demonstrating what has been previously observed in human liver sections (Brimacombe et al., 2014), and it would be interesting to confirm this with western blot. The only anomaly is 2s139, which has a comparatively higher RFC on PHH than on Huh-7.5.

Both Raji and Jurkat cells display around a 15-fold higher level of CD81 expression than Huh-7.5 and there are number of differences in binding patterns: 2s63 and 1s73 have lower than expected RFC on the immune cell lines, whereas 2s139 exhibits a higher RFC. Aside from C157, T166 and C190, 2s63 and 1s73 do not display any similarities in residue binding patterns, and all antibodies recognise these epitopes. 2s139 binds to K124 in the A helix in addition to C157, T166 and C190. However, this binding pattern is similar to that of 2s48, which did not exhibit the same tendencies.

Examination of antibody binding on primary immune cells demonstrated that both 2s141 and 2s63 exhibit a higher RFC on T cells and 2s139 and 2s48 show very high binding to both primary T and B cells. 2s139 and 2s48 bind identical epitopes and they both bind C157, T166 and C190 in common with 2s63 and 2s141.

If these findings were confirmed following proper optimisation of antibody staining, it would be possible to hypothesise that some CD81-LEL epitopes are more available in certain backgrounds than others. However, due to the often vast differences in binding affinities between antibodies with identical recognition patterns it would not be possible to be more specific about what these may be. The data would therefore suggest a significant role for other epitopes or factors in determining their binding, and would be an interesting area for further characterisation of these antibodies.

One factor which may cause differences in epitope availability between cell types is the formation of distinct associations by CD81 which lead to changes in protein conformation or epitope masking. To confirm this, it would be interesting to look at the direct interactions formed by CD81 in these cell types using co-immunoprecipation and FRET. As the CD81-LEL sequence has been demonstrated to be well conserved (Houldsworth, Metzner et al. 2014) any changes are unlikely to be related to changes in protein sequence between the cell types.

The data presented here form a basis for further and more thorough investigation into the possibility that the conformation of CD81 is dependent on cell type, as has been shown for other tetraspanins (Sincock, Fitter et al. 1999; Geary, Cambareri et al. 2001). However, without proper optimisation of antibody staining protocols, it is not possible to rule out that any trends highlighted in this work are caused or influenced by inappropriate antibody dilutions and procedure. The importance of choosing an optimal antibody concentration has already been described, and for future reference, further caveats of the methodology used here are briefly discussed below.

This study used flow cytometry to measure antibody binding, a technique which gives an estimate of binding on a large number of cells at a point in time. However, the binding of antibodies to ligands is a dynamic process, and therefore using this method of assessing antibody binding may not be the most informative. Instead, a more appropriate method may be to look at the on/off rate of association with the ligand under flow, for example by using surface plasmon resonance (SPR). By looking at the rates of antibody association and disassociation of the antibodies with target cells under flow conditions, a more accurate understanding of the interaction between the antibodies and the cells used could be gained.

The data presented here used live cell staining in an attempt to preserve the conformation of CD81 proteins and avoid the protein cross-linking which can occur during fixed cell staining. Aside from the effects of cross-linking, fixation of cells can remove lipids from the membrane. As lipids are a vital membrane component and are could integral to membrane domains, their removal may significantly alter the interactions within or stoichiometry of areas of the membrane in which CD81 is anchored.

However, live cell staining also carries a specific set of caveats and it could be argued that it would be more accurate to carry out the staining at a lower temperature than at the 37˚C described here, or following fixation. Both approaches would prevent activation of cellular signalling pathways during the live staining process which may affect the interactions formed by CD81, and therefore its presentation. However, it has been shown that the stability of the antibody-paratope interaction varies with the temperature at which they are incubated (Hughes-Jones 1975). Therefore, in order to examine the usefulness of these antibodies *in*

vivo, staining at 37˚C may be most useful. However, a combination of both staining techniques would likely be most informative.

Similarly, it is possible that using bivalent antibodies such as those described here would cause the clustering of CD81 molecules on the surface of the cell during live cell staining. This could have a number of effects. Firstly, the ligation of CD81 using antibodies has been shown to have multiple effects (VanCompernolle, Levy et al. 2001, Tseng and Klimpel 2002, Crotta, Ronconi et al. 2006, Brazzoli, Bianchi et al. 2008, Coffey, Rajapaksa et al. 2009, Lin, Rossi et al. 2011), and secondly and most importantly for this study, the clustering of CD81 molecules may cause the protein to form unusual or physiologically unlikely interactions. This could result in changes in the CD81-LEL conformation or steric interference, both of which would affect the ability of antibodies to bind to their target epitopes. This aspect of the antibody action would also be a significant concern were these antibodies to be used therapeutically.

To conclude, using the methods and antibodies described in this chapter it is not possible to elucidate any differences in CD81 conformation between cell types due to the wide range of distinct factors which can affect antibody binding. To remedy this, it would be necessary to carry out antibody titrations to determine the correct amount of antibody to use and to give serious consideration to the use of live or fixed cell staining. In addition to then repeating these experiments, it would be useful to additionally look at antibody binding under flow to determine antibody binding efficiencies to these cell types.

Cell line	Direction of deviance from CI	Comparison to FL (epitope group)	Comparison to LEL (epitope group)	Epitopes recognised
Huh-7.5	Above	1s337 (III)	1s337 (III)	L162, T167, F150, C157, T166, C190
		2s20 (I)	2s20 (I)	C157, T166, C190
		1s135 (V)	1s135 (V)	V123, L162, F150, C157, T166, C190
		2s63 (I)		C157, T166, C190
			2s155 (VI)	V123, L162, F150, C157, T166, C190
			1s201 (II)	L162, C157, T166, C190
	Below	2s139 (I)	2s139 (I)	K124, C157, T166, C190
		2s141 (VI)	2s141(VI)	V123, L162, F150, C157, T166, C190
		2s131 (I)	2s131 (I)	C157, T166, C190
		2s24 (I)		C157, T166, C190
PHH	Above	2s20 (I)		C157, T166, C190
			2s155 (VI)	V123, L162, F150, C157, C190
	Below	2s24 (I)		C157, T166, C190
		2s131 (I)	2s131 (I)	C157, T166, C190
			2s141 (VI)	V123, L162, F150, C157, T166, C190
Jurkat	Above	1s201 (II)	1s201 (II)	L162, C157, T166, C190
		2s155 (VI)	2s155 (VI)	V123, L162, F150, C157, T166, C190
		2s139 (I)	2s139 (I)	K124, C157, T166, C190
		1s337 (III)	1s337 (III)	L162, T167, F150, C157, T166, C190
		2s20 (I)	2s20 (I)	C157, T166, C190
		1s135 (V)	1s135 (V)	V123, L162, F150, C157, T166, C190
	Below	2s131(I)	2s131 (I)	C157, T166, C190
		2s141 (VI)	2s141 (VI)	V123, L162, F150, C157, T166, C190
		2s24 (I)		C157, T166, C190
			2s63 (I)	C157, T166, C190
T cells	Above	2s63 (I)	2s63 (I)	C157, T166, C190
		2s139 (I)	2s139 (I)	K124, C157, T166, C190
		2s20 (I)		C157, T166, C190
	Below	2s48 (I)	2s48 (I)	C157, T166, C190
		2s66 (I)	2s66 (I)	C157, T166, C190
		2s131 (I)	2s131 (I)	C157, T166, C190
		2s24 (I)		C157, T166, C190
Raji	Above	1s201 (II)	1s201 (II)	L162, C157, T166, C190
		1s135 (V)	1s135 (V)	V123, L162, F150, C157, T166, C190
		1s337 (III)	1s337 (III)	L162, T167, F150, C157, T166, C190
		2s139 (I)	2s139 (I)	K124, C157, T166, C190
		2s20 (I)	2s20 (I)	C157, T166, C190
			2s155 (VI)	V123, L162, F150, C157, T166, C190
	Below	2s63 (I)	2s63 (I)	C157, T166, C190
		2s141 (VI)	2s141 (VI)	V123, L162, F150, C157, T166, C190
		2s131 (I)	2s131 (I)	C157, T166, C190
		2s24 (I)		C157, T166, C190
B cells	Above	2s155 (VI)	2s155 (VI)	V123, L162, F150, C157, T166, C190
		2s139 (I)	2s139 (I)	K124, C157, T166, C190
		2s20 (I)	2s20 (I)	C157, T166, C190
	Below	2s131 (I)	2s131 (I)	C157, T166, C190
		2s141 (VI)	2s141 (VI)	V123, L162, F150, C157, T166, C190
		2s48 (I)	2s48 (I)	C157, T166, C190
		2s24 (I)		C157, T166, C190

Table 3.3: Trends in epitope binding of antibodies which lie outside of the CI. *Target epitopes epitope groupings of antibodies which lie above or below the confidence interval of the association of binding capacity and binding affinities to MBP-CD81-FL and MBP-CD81 – LEL.*

4 EFFECT OF HEPATIC POLARITY ON CD81 DIFFUSION

4.1 INTRODUCTION

Cells which exhibit simple epithelial polarity are found at barrier sites throughout the body, for example in the gut and airways. In such cells, the apical surface is located above the tight junctions and facing a lumen or outer surface. The remaining membrane is basolateral surface and is in contact with other cells or the basal lamina (Figure 4.1a). Hepatic polarity is distinct from this simple polarity in a number of ways (Figure 4.1b). Hepatocytes are multipolar and may have several apical and basolateral membranes that are separated by tight junctions. The apical membranes of adjacent hepatic cells form the walls of a lumen, the bile canaliculus (BC) which forms a continuous branched network into which bile is secreted and transported through the liver. The development of this complex polarity is essential for the correct functionality of the hepatocyte, and requires the formation of specific membrane domains, cytoskeletal and ER networks to allow for the polar trafficking of proteins, drugs and biliary salts (reviewed in (Decaens, Durand et al. 2008).

The *in vitro* cell culture model which most accurately recapitulates *in vivo* hepatic polarity is the HepG2 hepatoma cell line, which can polarise over time in culture and forms pseudo BC-like structures (van, Zegers et al. 1997, van and Hoekstra 2000, Mee, Grove et al. 2008, Ohgaki, Matsushita et al. 2010). Furthermore, the HCV receptors show comparable patterns of localization in polarised HepG2s with that seen in healthy liver tissue (Mee, Farquhar et al. 2010). Specifically, both CD81 and SR-BI are located at apical and basolateral membranes, claudin-1 predominantly at the TJ with low intensity staining at the basolateral surface, and occludin exclusively at the TJ. Studies using this cell line have shown that polarisation

(a) Polarised epithelial cell   (b) Polarised hepatocyte

apical (lumen)   basal (sinusoid)

TJ
AJ

Apical
Bile Canalicula (BC)

basal (tissue)   basal (sinusoid)
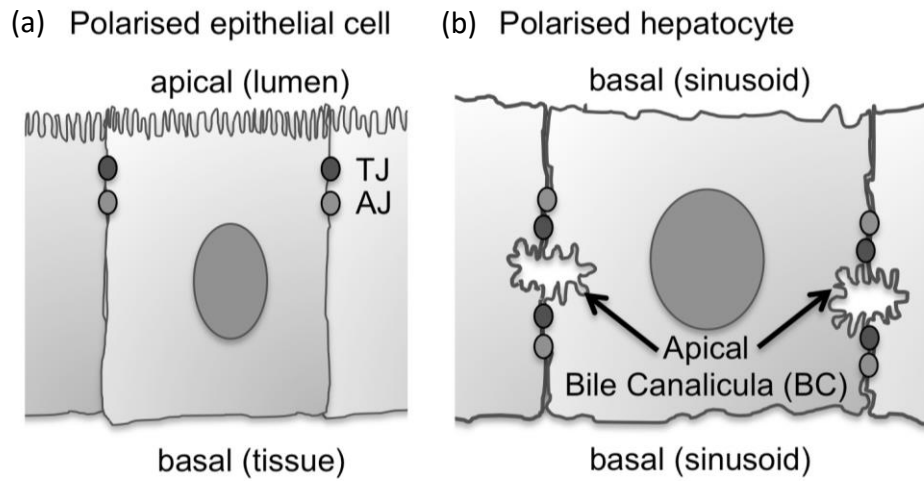
Figure 4.1: A comparison of epithelial and hepatic polarity. *In polarised epithelial cells a single apical and basal membrane appose each other and are separated by tight junctions (TJ) and adherens junctions (AJ), with the apical surface facing the lumen and the basal surface facing the tissue (a). Polarised hepatocytes have several apical membranes which form the walls of the bile canaliculus, and these are separated by TJs and AJs from the basal membranes which face the sinusoids (b).*

restricts HCV entry (Mee, Harris et al. 2009, Mee, Farquhar et al. 2010), highlighting the importance of studying receptor trafficking in a polarised cell type.

CD81 diffusion has been relatively well studied, and a number of factors affecting this have been elucidated. Using single particle tracking, it has been shown that CD81 confinement in polarised HepG2s overlaps with TEMs, (Harris, Clerte et al. 2013, Potel, Rassam et al. 2013), demonstrating that in this cell type the immobile fraction of the protein is correlated with CD81 localisation to these areas.

Recent work has found that the TEM-specific interactions between CD81 and interacting proteins play a central role in HCV infection (Zona, Lupberger et al. 2013). Furthermore, CD81 and its partner proteins can interact with the actin cytoskeleton (Sala-Valdes, Ursa et al. 2006, Coffey, Rajapaksa et al. 2009, Treanor, Depoil et al. 2011, Mattila, Feest et al. 2013) and this association has been shown to confine CD81 diffusion (Harris, Clerte et al. 2013) as reported for other membrane proteins such as CD9 (Kusumi, Sako et al. 1993, Sako, Nagafuchi et al. 1998, Treanor, Depoil et al. 2011). Additionally, recent work has shown that the formation of associations between CD81 and partner proteins claudin-1 and EWI-2wint affects lateral protein diffusion speed (Harris, Davis et al. 2010, Potel, Rassam et al. 2013), consistent with previous data demonstrating that the diffusion coefficient of a protein is dependent on molecular weight (Saffman and Delbruck 1975, Gambin, Lopez-Esparza et al. 2006).

FRAP is a powerful live imaging technique used to study the diffusion dynamics of fluorescent tagged proteins within the cell membrane. Briefly, one or more regions are

selected on the surface of a cell expressing a fluorescently tagged protein (Figure 4.2a) and

are bleached using an appropriate laser until the fluorescence intensity is reduced to around

40% (Figure 4.2b). Bleaching to this level prevents phototoxicity of the cell. The fluorescence

intensity of the region is monitored as photobleached proteins move out of the bleached

regions and are replaced by non-bleached proteins (Figure 4.2c).
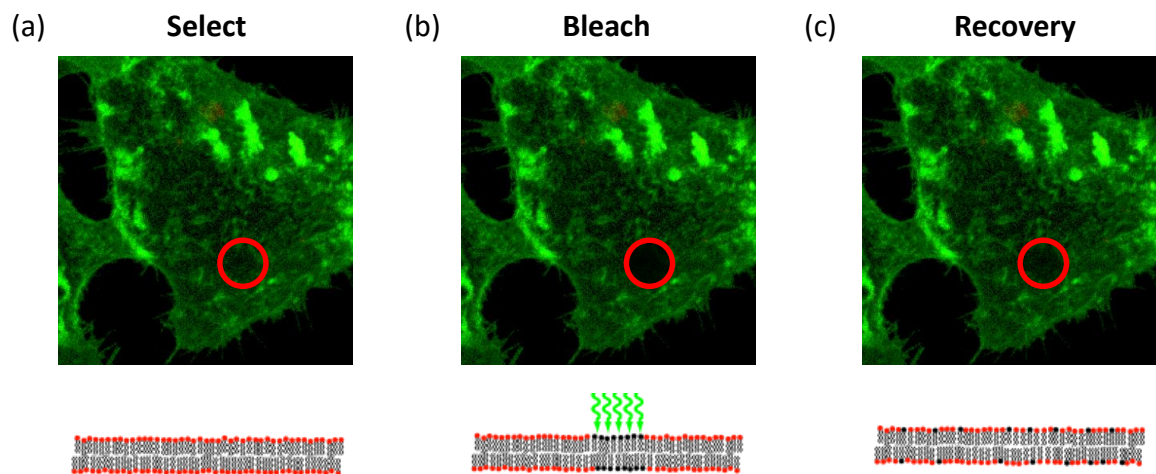
Figure 4.2: FRAP methodology: *To carry out FRAP, an area of the membrane is selected (a) and bleached (b), and the fluorescence intensity of the selected region monitored over time whilst recovery is taking place (c).*
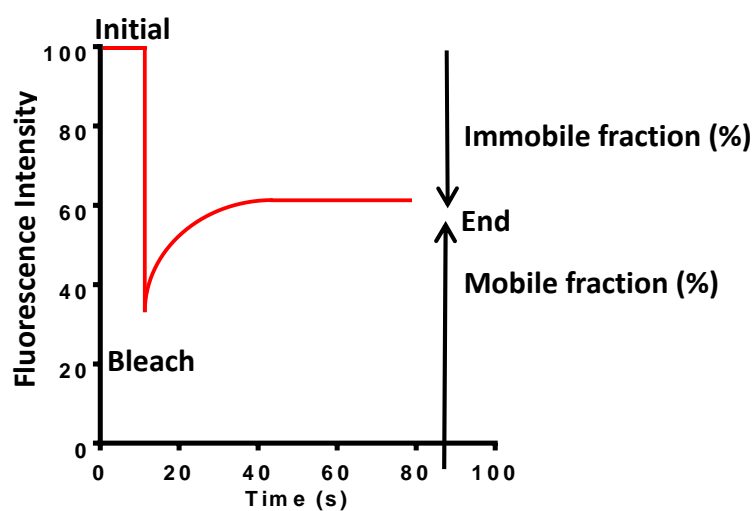
Figure 4.3: Interpreting the FRAP curve. Following bleaching, the fluorescence intensity recovers over time (red line) and can be used to interpret the mobile and immobile fraction of the protein under study along with the $T_{1/2}$.

The fluorescence intensity of the region can be plotted over time (Figure 4.3). A typical graph involves an 'initial' pre-bleach recording of the fluorescence intensity of the region, and this is normalised to become the 100% fluorescence intensity. The region is then bleached and the fluorescence intensity recorded until it stabilizes. The mobile fraction can then be found by subtracting the initial fluorescence intensity from the end point value (Figure 4.3).

Analysis of the recovery curve is essential to correctly interpreting the diffusion patterns of the protein under study. A single exponential curve (equation 1) shows that the protein is diffusing by one mode only, whereas a double exponential curve suggests multiple modes of diffusion. Additionally, from the equation of the curve the rate of protein diffusion (diffusion coefficient, equation 3) and the time taken for half the fluorescence intensity to recover (T½, equation 2) can be calculated by solving the appropriate single or double exponential formula for *K*.

$$Y = Y_{max}(1 - e^{Kx})$$

Equation 1: Simple exponential

$$T_{1/2} = \frac{0.69}{k}$$

Equation 2

$$\frac{0.224r^2}{T_{1/2}}$$

Equation 3: Diffusion Coefficient

The T½ value is essential for determining the mode of protein diffusion. Proteins can diffuse into a bleached region by one or both of two methods: lateral diffusion or exchange. In

lateral diffusion, proteins diffuse into the bleached region from within the plane of the

membrane, and in this case the T½ of a small and large bleached region are not equal (Figure

4.4a). In contrast, exchange diffusion occurs by proteins trafficking to the membrane from

within the cell, in which case the T½ of small and large regions are the same (Figure 4.4b).

(a)
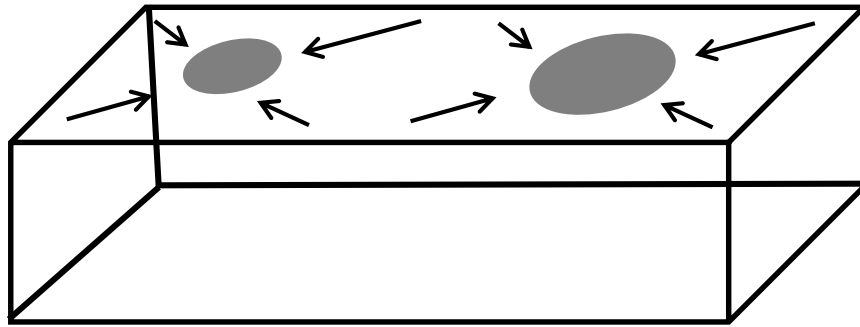
Lateral
$T_{1/2}$ small≠$T_{1/2}$ large

(b)
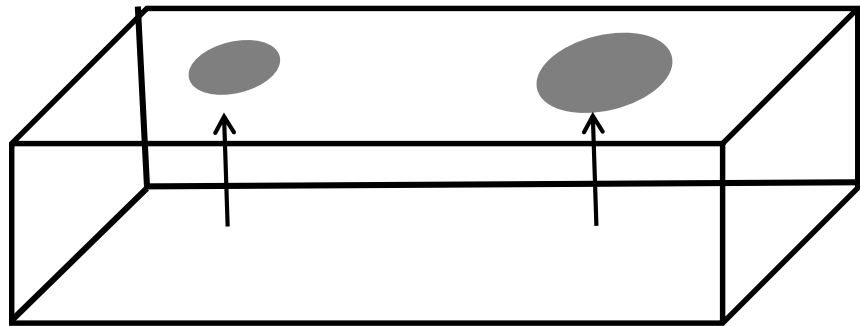
Exchange
$T_{1/2}$ small≠$T_{1/2}$ large

Figure 4.4: Modes of protein diffusion. Lateral diffusion occurs from only within the plane of the membrane, where the $T_{1/2}$ differs between small and large bleach spots (grey circles) (a). In exchange, the protein diffuses from intracellular compartments and the $T_{1/2}$ is the same for small and large bleached regions (b).

As with many diseases, HCV exists in an inflamed setting with activated immune cells and the associated release of cytokines (Zampino, Marrone et al. 2013). Inflammation has been implicated in the initiation or development of a number of diseases associated with barrier dysfunction, including irritable bowel disorder (IBD) and infection by other viruses such as West Nile Virus (WNV). In IBD, which encompasses ulcerative colitis and Crohn's disease, the release of TNF-α causes a redistribution of tight and adherens junction proteins to the basolateral surface of intestinal epithelial cells, and also causes the shedding of these cells via p53 and caspase-3 mediated apoptosis (Marchiando, Shen et al. 2011, Goretsky, Dirisina et al. 2012). The loss of barrier function is compounded by an increase in myosin light chain kinase (MLCK) leading to a contraction of the perijunctional actin and myosin ring (Cunningham and Turner 2012). In the case of WNV infection, the detection of the dsRNA WNV intermediate by peripheral lymphoid cells leads to the release of TNF-α. This activates the canonical NF-κB signalling pathway in polarised cells, followed by MLCK activation leading to a reorganisation of the perijunctional F – actin and TJ proteins (Shen L 2006, Lim, Koraka et al. 2011). As a result, the target blood brain barrier cells are depolarised and the virus is able to cross the barrier without infecting the barrier cells (Wang, Town et al. 2004). The inflammatory environment present during chronic HCV infection includes interleukin (IL)-1β, IL-6 and tumour necrosis factor α (TNFα) (Liaskou, Wilson et al. 2012). These cytokines promote entry of HCV into polarised hepatoma cells, and TNF-α is the central cytokine involved in this process (Fletcher, Sutaria et al. 2014) and has been shown to reduce tight junction integrity (Mashukova, Wald et al. 2011).

It is well established that hepatocyte polarity limits HCV entry, with polarised cells supporting lower levels of entry and infection, and that this occurs concomitant with slower receptor diffusion (Mee, Grove et al. 2008, Mee, Harris et al. 2009, Mee, Farquhar et al. 2010, Harris, Clerte et al. 2013). Therefore, in order to establish whether receptor diffusion defines HCV entry rate, the effect of polarisation and the processes that regulate it in the liver on CD81 diffusion were studied in a relevant, polarised model.

4.2 RESULTS

4.2.1 Validation of FRAP methodology

Inherent in studying the diffusion of proteins over a large area of membrane is a variance in the data, and thus it is necessary to define the sample size required to accurately represent the population. To find the optimal sample size for measuring CD81 diffusion in HepG2 cells we employed MonteCarlo bootstrap analysis. Bootstrapping is a method of estimating the precision of statistics, in this case the mean CD81 diffusion coefficient or mobile fraction, of a sample by repeatedly selecting with replacement from a set of data points. Sample sizes from 4 to 60 cells were analysed to measure mean CD81 diffusion coefficient and mobile fraction (Figure 4.5 a,b), and the means of each analysis compared to that of the total sample size (60 cells). 10 spots were bleached per cell as this is the highest number possible to bleach in one experiment without compromising the speed of data collection. This analysis showed 10 cells to be sufficient to model the mean of 60 cells for both diffusion coefficient and mobile fraction (Figure 4.5a, b).

Once the necessary number of cells had been established, the same technique was applied to define the total number of bleach spots needed in a triplicate sample size of 10 cells. Analysis showed that a minimum of 55 bleached regions across triplicate experiments studying 10 cells each was necessary to accurately represent the population in terms of both diffusion coefficient and mobile fraction (Figure 4.5 c, d).
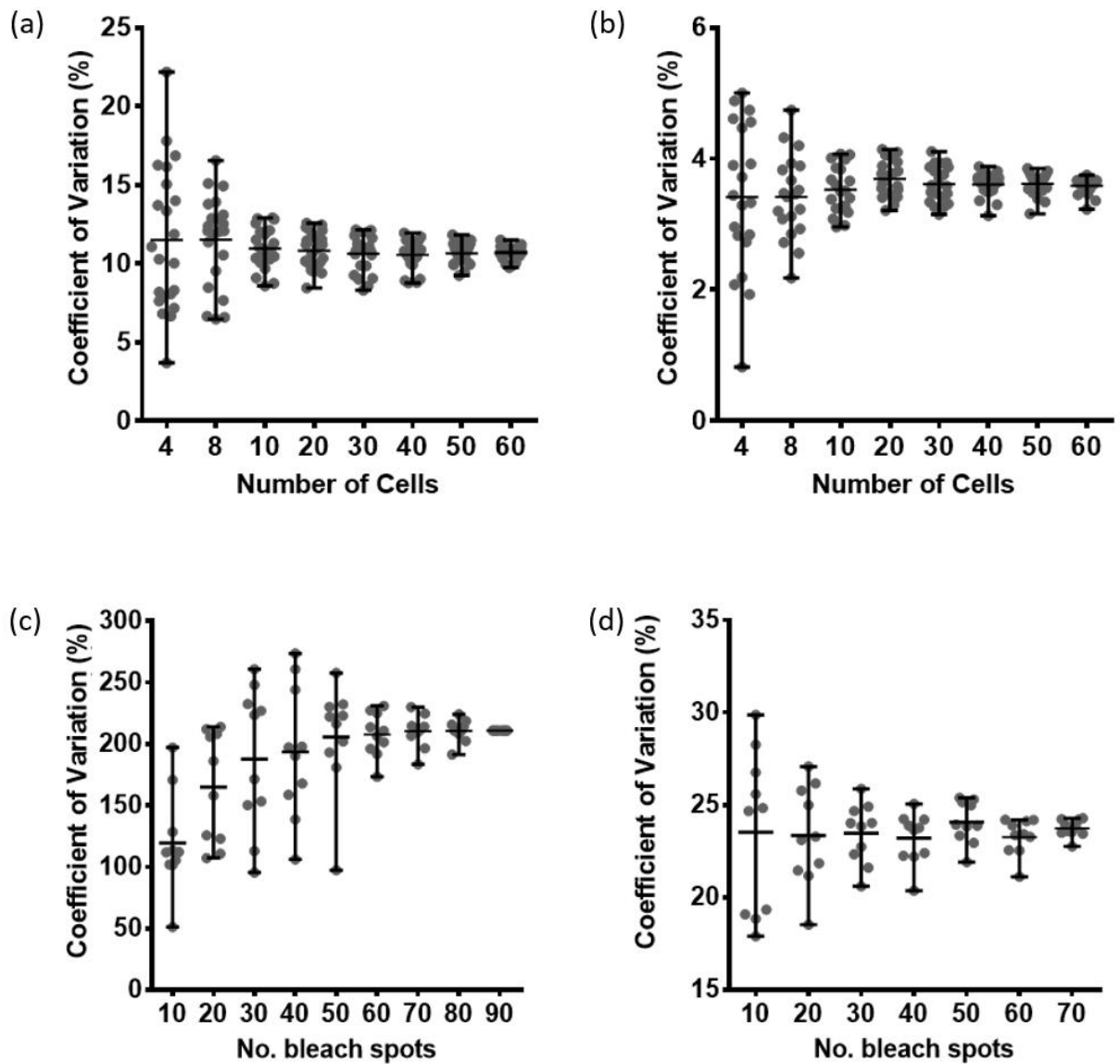
Figure 4.5: Coefficient of variation analysis of fluorescently tagged proteins in polarised HepG2.*HepG2 cells expressing AcGFP.CD81 were allowed to polarise for 5 days. 10 bleached spots per cell were subjected to FRAP analysis to determine the diffusion coefficient and mobile fraction of CD81. MonteCarlo bootstrap analysis was carried out on the specified number of variables to determine the number of cells (a and b) and bleached spots (c and d) necessary to accurately represent the population in terms of both diffusion coefficient (a and c) and mobile fraction (b and d). Cells were imaged using a 100x Plan Achromat 1.4 NA oil immersion objective on a Zeiss LSM 780 confocal microscope with a GaAsP spectral detector, and GraphPad prism used to carry out analysis.*

The recovery of fluorescence intensity relies on fluorescent proteins moving into bleached regions via lateral or exchange diffusion (Figure 4.4), and it is important to determine which is occurring to ensure that results are properly interpreted. The first step is to identify the shape of the FRAP recovery curve. A single exponential recovery curve represents a single mode of diffusion, whereas a double exponential represents multiple modes of diffusion. The protocol used for FRAP analysis includes a requirement of the software to establish whether the data best fits a single or double exponential curve for every bleached region. In all cases the best fit was a single exponential and a representative curve is shown (Figure 4.6a). To establish which mode of diffusion a protein is undergoing, the T½ is plotted against the area of the corresponding bleached region. In HepG2 cells the T½ increases with the area of the bleached region (Figure 4.6b), and thus CD81 is diffusing laterally within the plane of the membrane with minimal contribution from exchange diffusion. Therefore, all interpretations relating to changes in protein diffusion will explore factors affecting this mode of diffusion only.
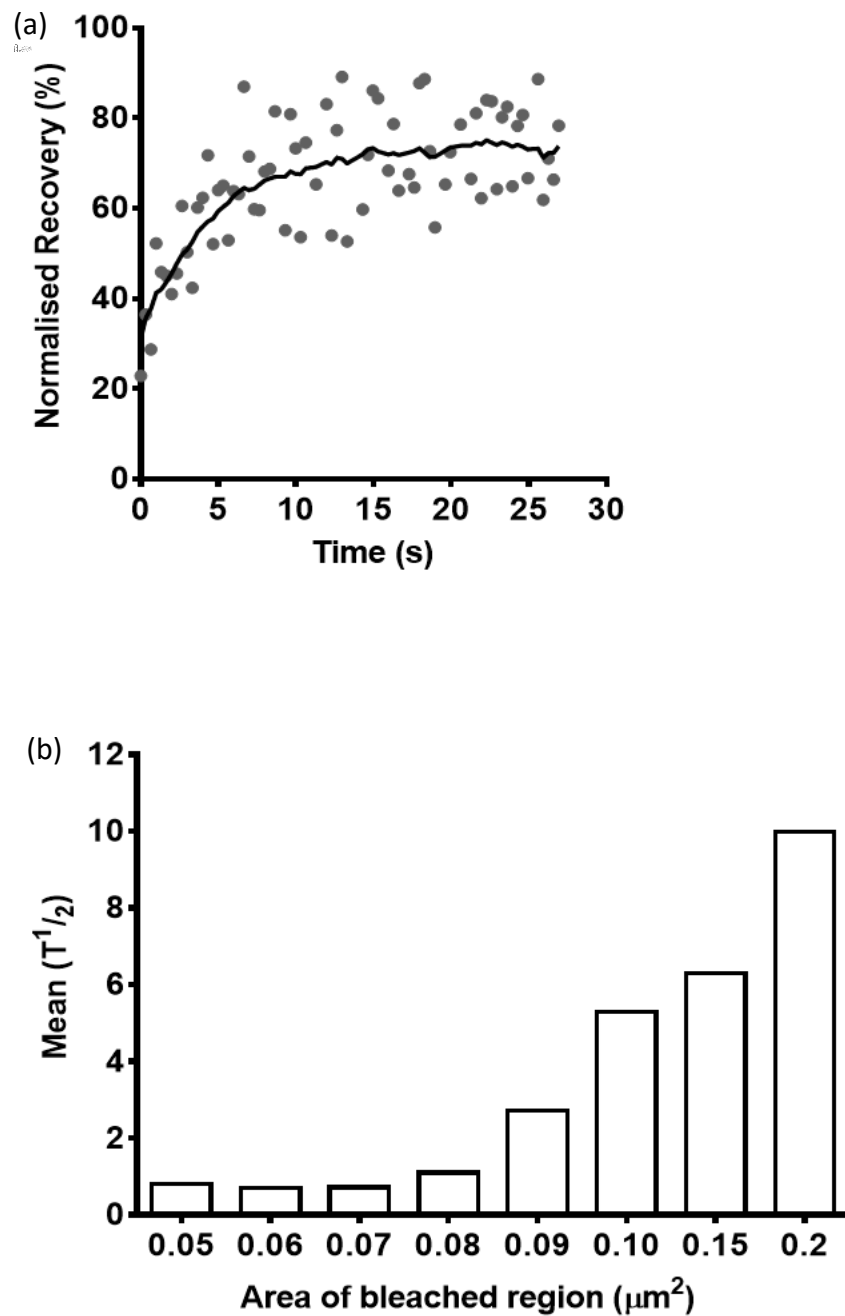
Figure 4.6: Determination of protein diffusion mode. *HepG2 cells expressing Ac-GFP.CD81 were used to carry out FRAP. Representative AcGFP-CD81recovery curve displaying line of best fit (a). Plotting the T½ against area of the corresponding bleached region was used to assess the mode of protein diffusion (b).*

4.2.2   CD81 diffusion is defined by cellular location

Data collected during my Masters project showed that the diffusion coefficient and mobile fraction of HCV receptors SR-B1, claudin-1 and occludin varied depending upon their location within the membrane. Diffusion was studied specifically at the basolateral plasma membrane (PM) in contact with the growth substrate, filopodia in contact with the growth media and cell-cell contacts. These regions were chosen because they represent areas of the membrane with important roles in the infection and transmission of HCV. The basolateral membrane and filopodia regions represent the hepatocellular membrane in contact with Space of Disse, the first likely point of contact with HCV. Additionally, cell-cell contacts represent the junctions between hepatocytes that have been hypothesized to support HCV transmission (Timpe, Stamataki et al. 2008, Brimacombe, Grove et al. 2011).

In all cases, filopodia were defined as motile protrusions on the plasma membrane of a few microns in length that adhered to the glass surface and attached to the cell at one end only. As they are visible by confocal microscopy they are distinct from microvilli, but are smaller in length then nanotubes, which can extend to over 100 µm (Davis and Sowinski 2008, Sowinski, Jolly et al. 2008). Additionally, nanotubes form a connection between two cells, further differentiating them from filopodia.

In order to establish whether CD81 diffusion is affected by membrane structure, the diffusion coefficient and mobile fraction of CD81 at the basolateral plasma membrane (PM), filopodia and cell junctions in polarized HepG2 cells was studied. The diffusion coefficients of CD81 at these locations all differed significantly from each other, with CD81 diffusing at a rate of 0.058 μm^2/s at the plasma membrane, 0.009 μm^2/s at the filopodia, and 0.003 μm^2/s

at areas of cell-cell contact (Figure 4.7a, Table 4.1). Similarly, the mobile fraction varied between locations, but was similar between regions in the PM and filopodia (56% and 58% respectively) whilst it was more confined at cell-cell junctions (33%) (Figure 4.7b, Table 4.1). Therefore, CD81 diffuses more slowly at structures such as the filopodia and cell-cell contacts than at the basolateral plasma membrane, with an increased confinement at cell contacts.

To date there has been no evidence for filopodia playing a role in HCV entry. Therefore, given the significant differences in diffusion parameters between the structures examined, it was decided to only study plasma membrane-located CD81 as it best represents the basolateral membrane of cells which HCV will first encounter on entering the liver.

Cellular location	Diffusion Coefficient (µm²/s)	IQ range (µm²/s)	Mobile Fraction (%)	IQ range (pp)	Sample size
PM	0.058	0.113	56	40	55
Filopodia	0.009	0.044	59	41	55
Cell contact	0.003	0.032	33	34	55

Table 4.1: Quantification of figure 4.7. The diffusion coefficient and mobile fraction with interquartile (IQ) range and sample size are shown for each cellular location. The IQ range of the mobile fraction is given in percentage points (PP).
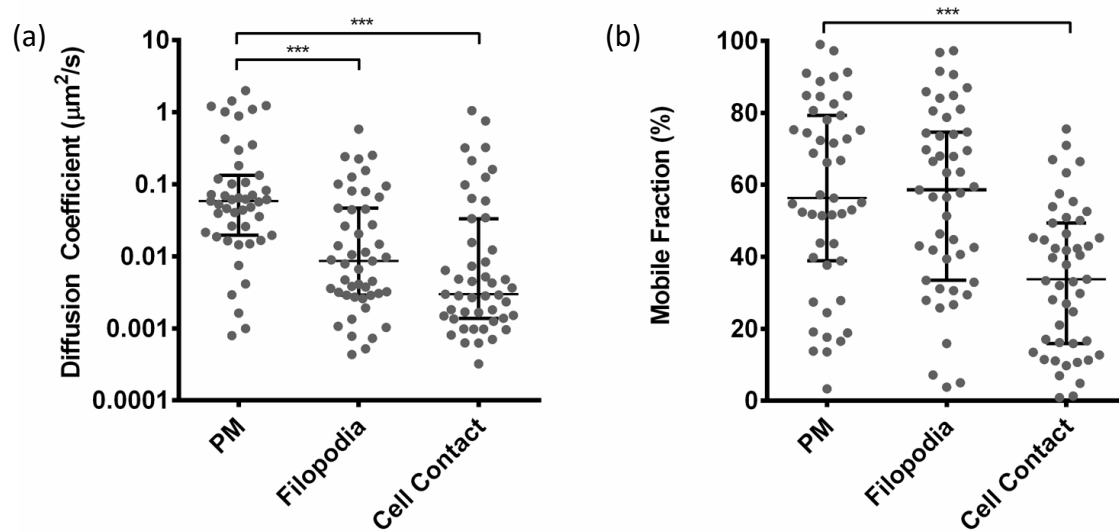
Figure 4.7: Effect of cellular location on CD81 diffusion. *HepG2 cells expressing AcGFP-CD81 were allowed to polarise for 5 days and the diffusion coefficient (a) and mobile fraction (b) found at the specific cellular structures stated. Cells were imaged using a 100x Plan Achromat 1.4 NA oil immersion objective on a Zeiss LSM 780 confocal microscope with a GaAsP spectral detector, and groups were compared by Mann-Whitney U test (GraphPad Prism 6.0). Each spot represents one bleached region. *P<0.05, **P<0.001, ***P<0.0001.*

4.2.3 Effect of polarisation on CD81 diffusion

Development of hepatic polarity is a key characteristic of hepatocytes *in vivo* and we were keen to understand the extent to which this can be replicated *in vitro*. Cell polarity can be quantified by estimating the number of BCs per hundred nuclei expressing the apical marker MRP2 (polarity index). HepG2 cells were plated for 1, 3, or 5 days (Figure 4.8a) and their polarity index measured. Tight junction integrity is independent of cellular polarity (Mee, Harris et al. 2009) and can be measured by following BC retention of the fluorescent dye 5-chloromethylfluorescein diacetate (CMFDA). Briefly, CMFDA is added to live HepG2 cells for 15 minutes to allow trafficking to the apical membrane. At this point the function of the TJs is calculated by enumerating the percentage of BC structures visible by phase microscopy that retain CMFDA. HepG2 polarity increased from 12% on day 1 to 33% on day 3 and 53% by day 5 (Figure 4.8a). This was supported by the CMFDA assay showing that 42% of BC-expressing cells retained CMFDA on day 1, increasing to 78% by day 3 and 81% by day 5 (Figure 4.8b).

It has previously been shown that hepatoma polarity decreases the permissivity of cells to HCV infection (Mee, Grove et al. 2008, Mee, Harris et al. 2009), and to confirm this HepG2 cells at 1 and 5 days post plating were challenged with HCVpp and incubated for 72 hrs. Quantification of the infection showed that while cells that had been plated for one day showed infection levels of $5x10^5$, cells which had been plated for 5 days prior to infection showed a much lower infection level of $1.1x10^5$ (Figure 4.8c). These data show that 5 days of polarisation are necessary for the majority of cells within a sample to polarise and form

integral tight junctions. Additionally, these data confirm hepatic polarity reduces the

susceptibility of HepG2 cells to HCV infection.
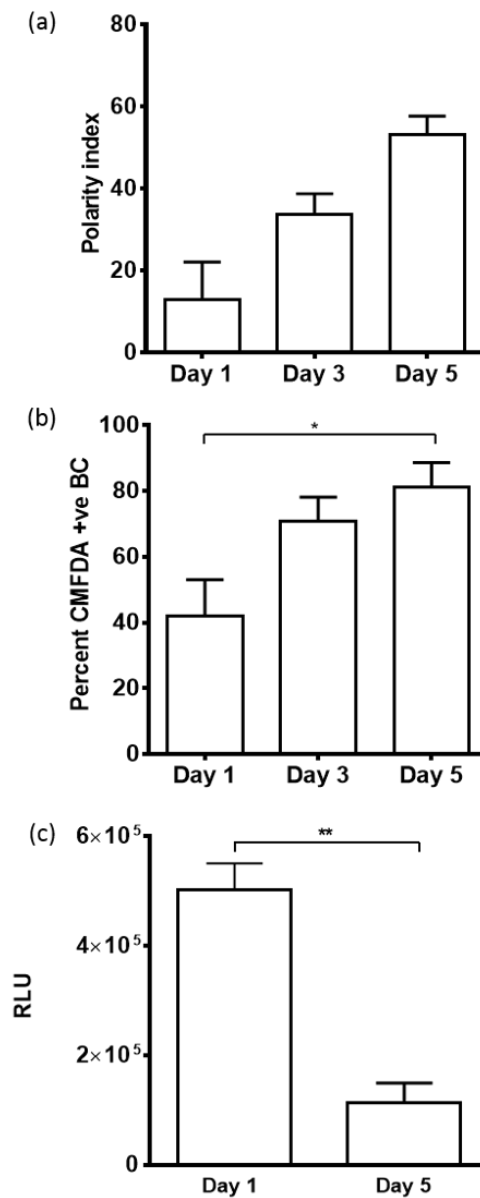
Figure 4.8: Effect of polarisation on tight junctions and HCVpp infection. *HepG2.CD81 cells were plated and allowed to polarise for 1, 3, and 5 days. HepG2 polarity was assessed by measuring the percentage of bile canaliculi staining for MRP2 (a). Tight junction integrity was assessed by quantifying the number of bile canaliculi per 100 cells which retain CMFDA (b). HepG2.CD81 cells at either 1 or 5 days post plating were challenged with HCVpp strain H77 and infection read at 72 hrs (c). Groups were compared by T-test (GraphPad Prism 6.0)*P<0.05, **P<0.001.*

Previous work using live imaging has demonstrated that an increased protein diffusion or mobility is linked to a higher level of HCV entry (Harris, Davis et al. 2010, Fletcher, Sutaria et al. 2014). Therefore, the diffusion coefficients (Figure 4.9 a, c) and mobile fractions (Figure 4.9 b, d) of AcGFP-CD81 and AcGFP-claudin-1 on polarised (5 days post plating) and non-polarised (1 day post plating) HepG2 cells were studied. In the case of CD81, there was no change in mobile fraction with polarisation, with 68% of CD81 mobile in polarised cells compared to 67% in non-polarised cells (Figure 4. 9b, Table 4.2). In contrast, the mobile fraction of claudin-1 decreased from 68% to 61% following polarisation. The diffusion coefficient of both proteins was higher in non-polarised cells compared to polarised cells. AcGFP-CD81 diffusion coefficient was 0.057 μm^2/s in polarised cells compared to 0.094 μm^2/s in non-polarised cells (Figure 4.9a), and in those expressing AcGFP-claudin-1 the diffusion speed increased from 0.075 μm^2/s in polarised cells to 0.117 μm^2/s in non-polarised cells (Figure 4.9c, Table 4.2). Therefore, the diffusion speeds of both CD81 and claudin-1 are lower in polarised cells than in non-polarised cells.

Protein	Polarity	Diffusion Coefficient (µm²/s)	IQ range (µm²/s)	Mobile Fraction (%)	IQ range (pp)	Sample size
CD81	Pol	0.057	0.075	68	23	73
	Non-Pol	0.094	0.109	68	14	73
CLDN-1	Pol	0.075	0.201	61	26	73
	Non-Pol	0.117	0.271	68	22	73

Table 4.2: Quantification of figure 4.8. *The diffusion coefficient and mobile fraction with interquartile (IQ) range and sample size are shown for each cell type. The IQ range of the mobile fraction is given in percentage points (PP).*
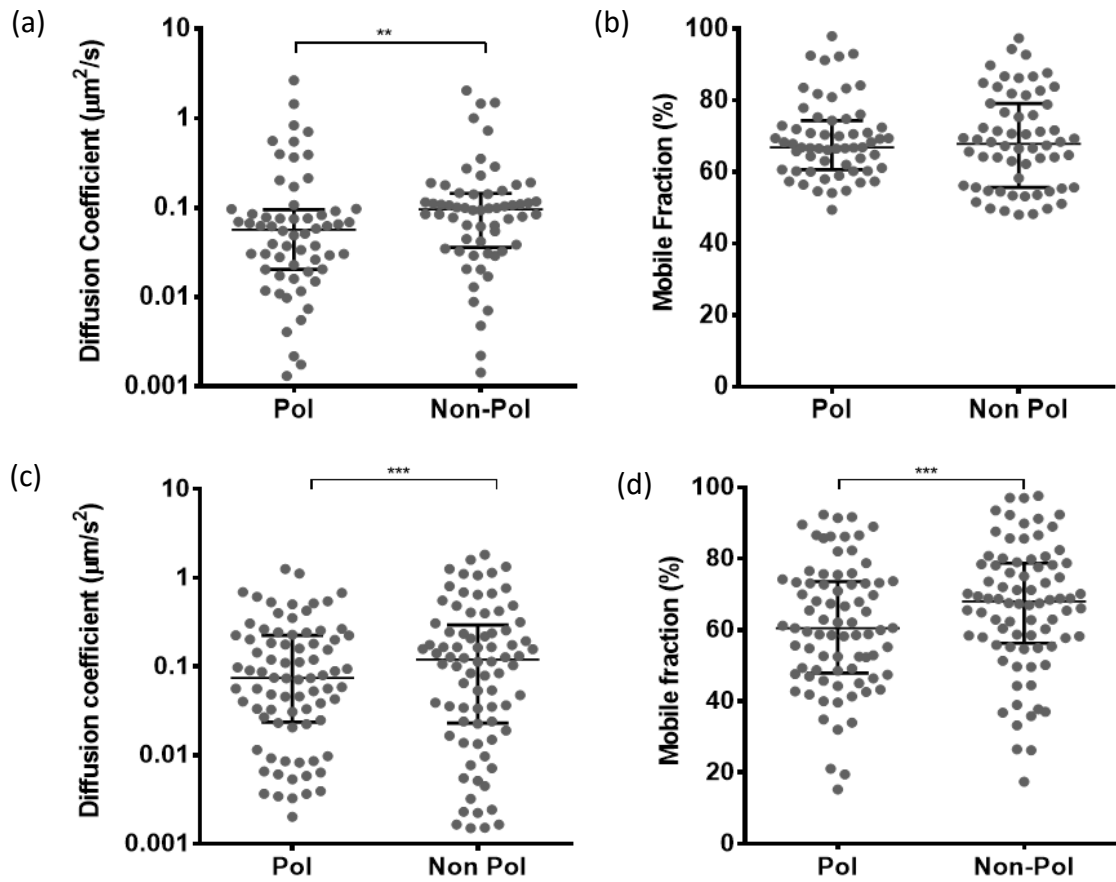
Figure 4.9: Effect of hepatoma polarity on protein diffusion. *HepG2 cells expressing either AcGFP-CD81 (a and b) or ACGP-claudin-1 (c and d) were allowed to polarise for either 5 days (Pol, polarised) or 1 day (Non-Pol, non-polarised) and the diffusion coefficient (a and c) and mobile fraction (b and d) found for each. Cells were imaged using a 100x Plan Achromat 1.4 NA oil immersion objective on a Zeiss LSM 780 confocal microscope with a GaAsP spectral detector, groups were compared by Mann-Whitney U test (GraphPad Prism 6.0). Each spot represents one bleached region. *P<0.05, **P<0.001, ***P<0.0001.*

4.2.4 CD81 diffusion is affected by TNF-α

During chronic HCV infection the liver becomes inflamed, with an infiltration of immune cells associated with a release of inflammatory cytokines (Zampino, Marrone et al. 2013) including TNF-α (Fletcher, Sutaria et al. 2014). Work from the McKeating group has shown that TNFα causes the relocation of occludin from apical junctions to the basolateral membrane and increased permissivity to support HCV entry (Figure 4.10a, carried out by Nicola Fletcher). To ascertain whether the increased HCV entry could be linked to a loss of polarity, the effect of TNFα treatment on hepatic polarity was investigated. Following treatment of polarised HepG2.AcGFP-CD81 cells with TNF- α, the polarity index decreased from 50% to 19% (Figure 4.10b). In addition, TNFα reduced the percentage of CMFDA positive bile canaliculi to around half the pre-treated number from 79% to 41% (Figure 4.10c). As it has previously been shown that HepG2 polarisation reduces CD81 diffusion (Figure 4.9), we studied the effect of TNFα on CD81 diffusion. Polarized HepG2.AcGFP-CD81 were treated with TNFα for one hour and CD81 diffusion monitored by FRAP. An increase in the diffusion coefficient of CD81 was observed from 0.135 μm^2/s in the untreated sample to 0.198 μm^2/s following TNFα treatment (Figure 4.11a, table 4.3), and the mobile fraction increased from 81% to 85% following treatment (Figure 4.11b, table 4.3). These results show that TNFα depolarizes HepG2 cells and increases CD81 diffusion. In addition, TNF-α has the additive effect of increasing CD81 mobile fraction, suggestive of a relocation of the protein from areas of confinement.
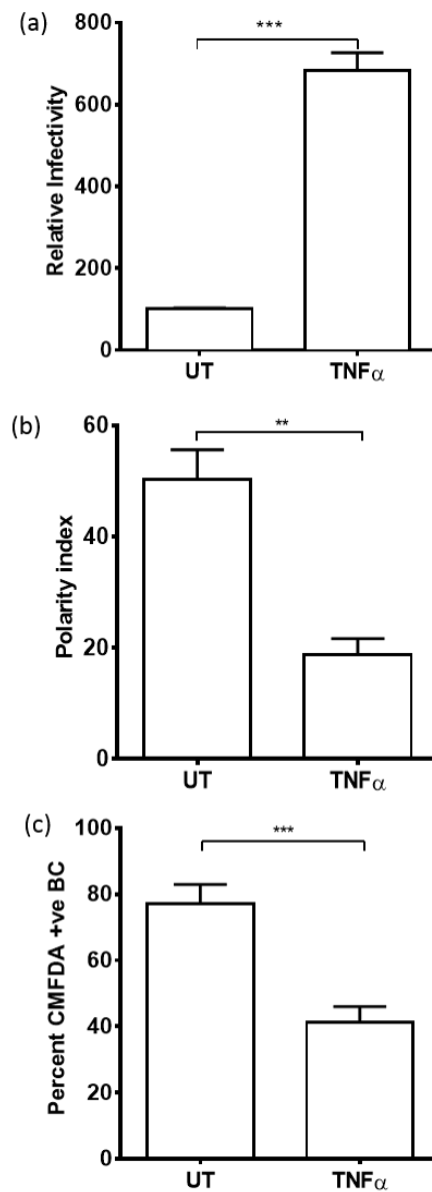
Figure 4.10: Effect of cytokine treatment on tight junction function and HCVpp infection.
HepG2.CD81 cells were plated and allowed to polarise for 5 days. HepG2.CD81 cells were left untreated or pre-treated with 10 ng/mL TNF- α for 1 hour before challenge with H77-HCVpp and the infection read at 72 hrs (a). Polarity was assessed by staining for MRP2 in HepG2 cells treated with TNF-α (10ng/mL) for 1 hour. Tight junction functionality was assessed by quantifying the frequency of bile canaliculi retaining CMFDA (4=, 6=-diamidino-2-phenylindole) (c). Groups were compared by Mann-Whitney U test (GraphPad Prism 6.0)*P<0.05, **P<0.001, ***P<0.0001.
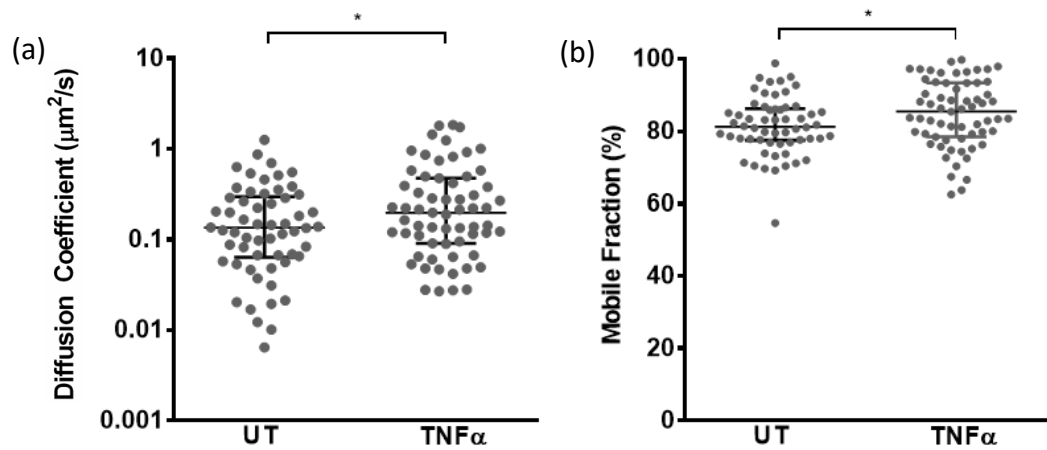
Figure 4.11: Effect of TNFa cytokine on protein diffusion. *HepG2 cells expressing AcGFP-CD81 were allowed to polarise for 5 days and treated with TNF-α (100ng/mL) or a control for 1hr before imaging and the diffusion coefficient (a) and mobile fraction (b) found. Cells were imaged using a 100x Plan Achromat 1.4 NA oil immersion objective on a Zeiss LSM 780 confocal microscope with a GaAsP spectral detector, and groups were compared by Mann-Whitney U test (GraphPad Prism 6.0). Each spot represents one bleached region. *P<0.05.*

Treatment	Diffusion Coefficient (µm²/s)	IQ range (µm²/s)	Mobile Fraction (%)	IQ range (pp)	Sample size
Untreated	0.135	0.233	81	9	58
TNFα	0.198	0.385	85	15	58

Table 4.3: Quantification of figure 4.9. *The diffusion coefficient and mobile fraction with interquartile (IQ) range and sample size are shown for each treatment type. The IQ range of the mobile fraction is given in percentage points (PP).*

4.2.5 Effect of actin organisation on CD81 diffusion

The actin cytoskeleton is a key determinant of hepatocyte polarity (Tsukada and Phillips 1993) and links to CD81 via ERM proteins (Sala-Valdes, Ursa et al. 2006). To determine whether CD81 lateral diffusion is regulated mediated by its linkage to the actin cytoskeleton, an inhibitor of actin polymerisation (cytochalasin D, Cyt D) and an inhibitor of actin assembly (latrunculin B, Lat B) were added to polarised HepG2 cells expressing AcGFP-CD81. Phalloidin staining of the actin cytoskeleton shows the effect of these agents on the cells (Figure 4.12). In the untreated cells, a BC – like structure is evident with strong cortical actin filaments, and CD81 localisation at the basolateral and apical cell membrane as previously described (Mee, Grove et al. 2008). Additionally, actin-dense filopodia are seen at the membrane. Following addition of cytochalasin D (Cyt D), the bile canaliculus is misshapen and appears to lack a strong actin structure. Furthermore, there appears to be some membrane deformation and fewer filopodia, although CD81 localisation is not noticeably different from untreated cells. In contrast, following addition of latrunculin B there is no obvious ordered actin structure at all, with the actin forming an intracellular 'cloud'. There is no evidence of a bile canaliculus or filopodia, and CD81 shows relocation to a more diffuse staining pattern.
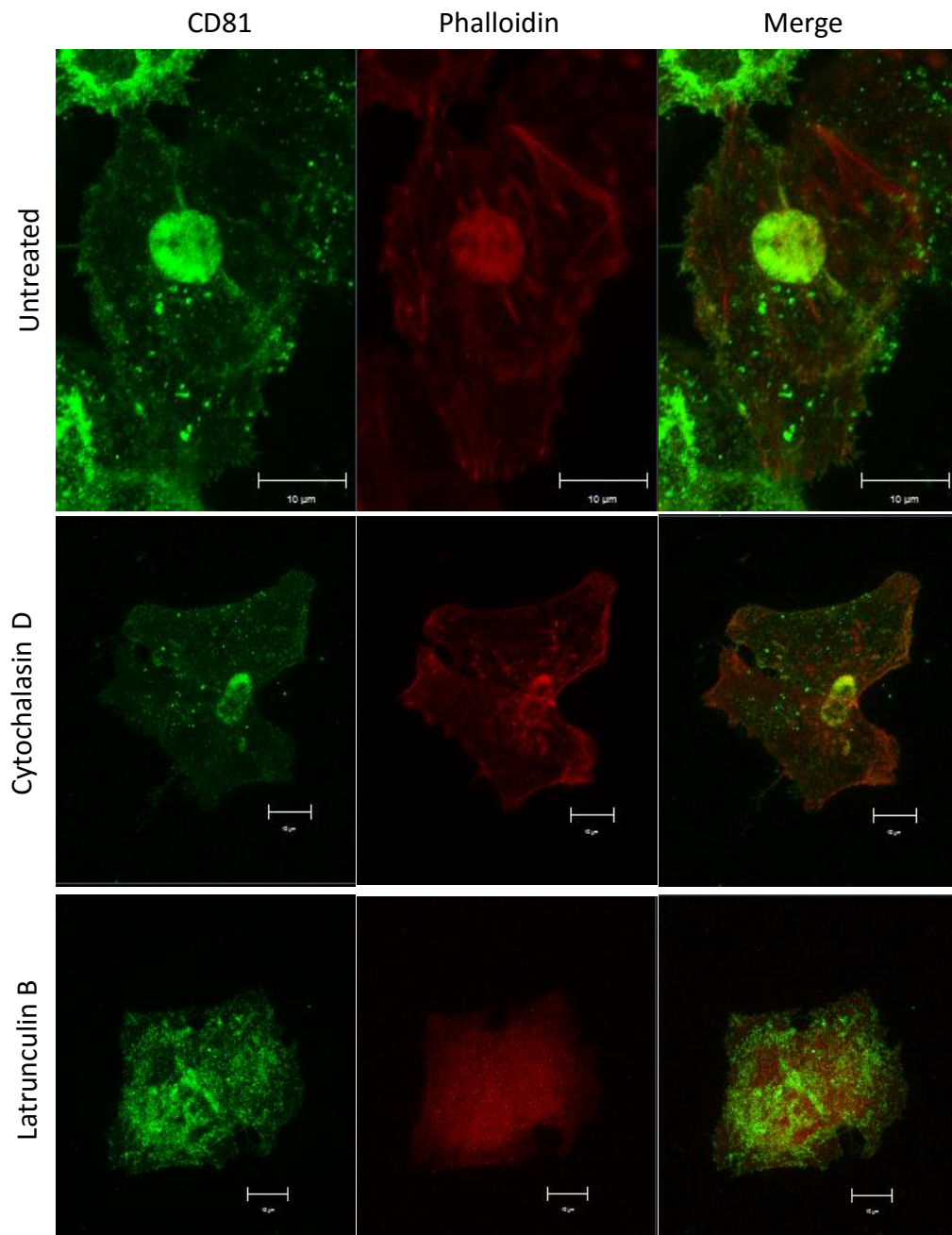
Figure 4.12: The level of actin organisation affects CD81 distribution. *Confocal images of polarised (day 5) HepG2. AcGFP-CD81 cells treated with cytochalasin D (2.5µM) and latrunculin B (1 µM) for 1 hr and stained with 633-phalloidin (red). 16 bit images were taken with optimal pixel resolution using a 100x Plan Achromat 1.4 NA oil immersion objective on a Zeiss 780 confocal microscope. Representative maximum projections were constructed from Z sections.*

The observed changes in tight junction morphology are supported by polarity and tight

junction assays. Both compounds reduced the polarity index, with cytochalasin D having only

a subtle effect and latrunculin B reducing the polarity index from 50% to 25% (Figure 4.13a).

In contrast, cytochalasin D reduced the tight junction integrity from 82% to 62% but

latrunculin B had the largest effect, reducing the integrity to 35% (Figure 4.13b). Having

observed the effect of cytoskeletal disruption on HepG2 polarity and CD81 location, we

investigated the dependency of CD81 diffusion on actin cytoskeleton integrity.
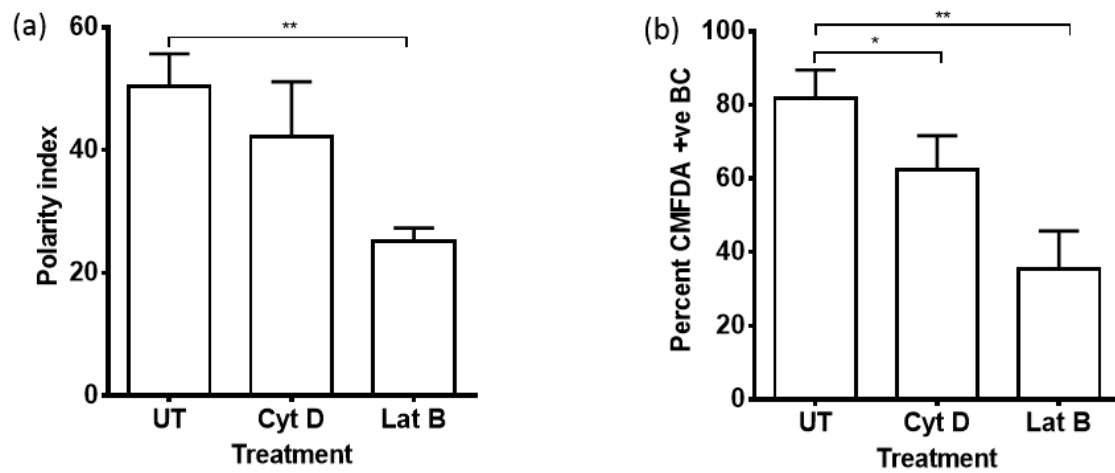
Figure 4.13: Effect of actin inhibitors on tight junction function. *HepG2 polarity was assessed by staining for MRP2 in cells which were untreated or treated with cytochalasin D (Cyt D, 2.5 µM) or latrunculin B (Lat B, 1 µM) for 1 hour (a). Tight junction functionality was assessed by quantifying the frequency of bile canaliculi per 100 able to retain CMFDA (b). Groups were compared by T-test (GraphPad Prism 6.0)*P<0.05, **P<0.001, ***P<0.0001.*

Polarised HepG2 cells expressing AcGFP-CD81 were treated with cytochalasin D or latrunculin B for 1 hour and the cells imaged over a 1 hour period. CD81 diffusion was reduced from 0.072 $\mu m^2/s$ to 0.038 $\mu m^2/s$ in cells treated with cytochalasin D and Latrunculin B (Figure 4.14a, table 4.4). In addition, both treatments increased the fraction of mobile CD81 from 57% in untreated cells to 58% and 61% in those treated with cytochalasin D and latrunculin B respectively (Figure 4.14b, table 4.4). These data highlight the importance of the linkage of CD81 to actin cytoskeleton in defining CD81 diffusion.

Treatment	Diffusion Coefficient ($\mu m^2/s$)	IQ range ($\mu m^2/s$)	Mobile Fraction (%)	IQ range (pp)	Sample size
Untreated	0.072	0.160	57	31	80
Cytochalasin D	0.038	0.177	58	24	80
Latrunculin B	0.040	0.138	61	11	80

Table 4.4: Quantification of figure 4.14. The diffusion coefficient and mobile fraction with interquartile (IQ) range and sample size are shown for each treatment. The IQ range of the mobile fraction is given in percentage points (PP).
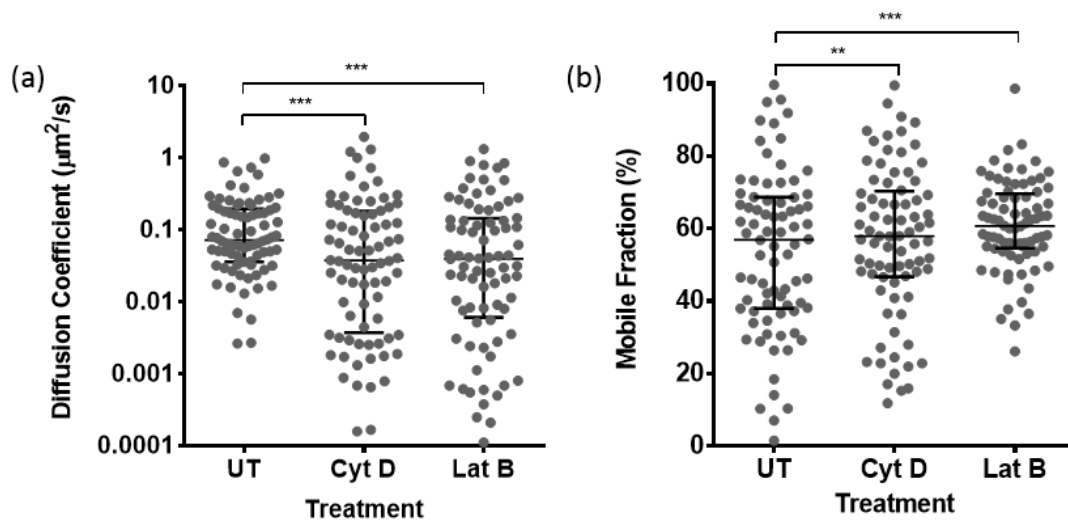
Figure 4.14: Effect of actin inhibitors on CD81 diffusion. *HepG2 cells expressing AcGFP-CD81 were allowed to polarise for 5 days before FRAP was carried out and the diffusion coefficient (a) and mobile fraction (b) found. Cells were untreated or treated with cytochalasin D (Cyt D, 2.5 µM) or latrunculin B (Lat B, 1 µM) for 1 hour before imaging. Cells were imaged using a 100x Plan Achromat 1.4 NA oil immersion objective on a Zeiss LSM 780 confocal microscope with a GaAsP spectral detector, and groups were compared by Mann-Whitney U test (GraphPad Prism 6.0). Each spot represents one bleached region. *P<0.05, **P<0.001, ***P<0.0001.*

4.3 DISCUSSION

The lateral organisation of membrane components into specific domains is essential for the correct functioning of many cellular processes. That the membrane of eukaryotic cells is best viewed as a 'mosaic' of microdomains of varying size, composition and dynamics is now well established (Singer and Nicolson 1972, Maxfield 2002), but the content of these domains and the behaviour of the proteins within them is still to be explored. To understand the behaviour of CD81 in the membrane of HepG2 cells, FRAP was used to establish its diffusion under a number of conditions.

Initially the variation in CD81 diffusion across the cell surface was investigated, and the regions of the cell identified for study represent areas we believe to play a role in HCV entry. The two areas of the membrane likely to undergo initial contact with HCV are the basolateral membrane of polarised hepatocytes and associated filopodia. *In vitro*, these regions are analogous to the basolateral membrane in contact with the growth substrate and the filopodia in contact with the media. Additionally, HCV has been shown to transmit between cells (Timpe, Stamataki et al. 2008, Brimacombe, Grove et al. 2011) and so membranes involved in cell-cell contacts were included.

The diffusion coefficient of CD81 is lower at the filopodia than at the PM, but exhibits a slightly higher mobile fraction. Examination of the filopodial cytoskeleton using electron microscopy has shown it to be composed of tightly packed actin filaments, with a dense protein complex at the tip and a high expression of ERM (Lewis and Bridgman 1992), an adaptor protein which links CD81 and actin (Sala-Valdes, Ursa et al. 2006, Coffey, Rajapaksa et al. 2009). The link between CD81 and actin has been reported to be necessary for

147

Brownian diffusion of CD81 at the basolateral membrane but to have a minimal effect on the diffusion coefficient (Harris, Clerte et al. 2013). Actin activity is enhanced at the cell periphery (Chierico, Joseph et al. 2014), and the observation that a number of viruses use filopodia to 'surf' onto a target cell in an actin-dependent manner (Lehmann, Sherer et al. 2005, Sherer, Lehmann et al. 2007, Schelhaas, Ewers et al. 2008, Oh, Akhtar et al. 2010) suggests that surface protein movement in these membrane structures is ordered and directional. Furthermore, filopodia have a high proportion of lipid domains (Goswami, Gowrishankar et al. 2008, Gowrishankar, Ghosh et al. 2012, Chierico, Joseph et al. 2014), in addition to being dependent on the presence of cholesterol microdomains for formation (Roux, Cuvelier et al. 2005). The high proportion of lipid and cholesterol in these membrane structures is likely to reduce membrane fluidity. These factors along with a high degree of actin linkage may provide a mechanism for the lower diffusion coefficient but increased mobile fraction.

In the model used here, we distinguished between parts of the basolateral membrane in contact with other cells ('cell contact') and those in contact with the growth substrate (plasma membrane, 'PM'). Many proteins are expressed on both the sinusoidal and lateral faces of the basolateral membrane of hepatocytes (reviewed in (Treyer and Musch 2013), but the interactions formed by CD81 in these two regions are likely to be different. For example, interactions at the basal membrane may involve integrins, whereas those at cell contacts will be affected by the presence of adherens and tight junctions (Kojima, Yamamoto et al. 2003, Nelson 2003, Theard, Steiner et al. 2007). Junction structures are highly ordered and in polarised epithelial cells are tethered to the actin cytoskeleton, an association which may reduce CD81 mobility compared to the PM (Harris, Clerte et al. 2013). As a junctional

protein, claudin-1 is expressed in these structures. The extracellular loops of claudin-1 can form interactions both within and between cells (Krause, Winkler et al. 2008, Piontek, Winkler et al. 2008), likely reducing the movement of the protein. As the presence of claudin-1 has been shown to reduce CD81 diffusion (Harris, Davis et al. 2010), its high expression and relative confinement may partially account for the reduced diffusion coefficient observed at cell contact locations.

In all locations the variation in diffusion coefficient and mobile fraction are similar, suggesting that similar factors affect CD81 diffusion both within and between membrane structures. Notably however, median CD81 diffusion coefficient at the cell contacts are skewed towards the lower values, suggesting that there is a subset of CD81 at the cell contact that is diffusing at a higher rate. As the diffusion rates of this set of proteins are similar to those observed at the PM, they may represent an overlap in bleached regions between the cell contact and PM. Another possible explanation may be found in the behaviour of actin at cell junctions, where two distinct pools of actin have been observed – dynamic and stable populations (Yamada, Pokutta et al. 2005, Kovacs, Verma et al. 2011, Mangold, Wu et al. 2011). If CD81 is linked to actin in these regions, these different pools of actin may be dictating CD81 diffusion.

These data highlight the novel observation that there is a large variation in CD81 diffusion parameters between cell membrane structures, thus supporting the fluid mosaic model and highlighting the need to study and compare defined regions of the cell in experimental studies. As there have been no reported instances of HCV contacting filopodia, the basolateral membrane in contact with the growth substrate was chosen for further study to

model the initial interactions between HCV and hepatocytes. This is consistent with other studies employing live imaging to study protein dynamics (Harris, Clerte et al. 2013).

Hepatic polarity is complex, and involves the formation of distinct basolateral and apical membranes and integral tight junctions, developments which can be measurably quantified (Mee, Grove et al. 2008, Mee, Harris et al. 2009). Data presented here show that following five days in culture 53% of HepG2.AcGFP-CD81 cells share a bile canaliculus, and 81% of these have functional tight junctions, consistent with published data (Theard, Steiner et al. 2007). Additionally, it confirms published work showing that hepatocyte polarisation limits the permissivity of cells to HCV infection (Mee, Grove et al. 2008, Mee, Harris et al. 2009).

The specialisation of membrane regions is central to the correct functioning of the polarised hepatocyte, and inherent in this is the arrangement of membrane lipids and proteins into microdomains, and apical and basal membranes in polarised cells. Between these domains there are likely to be differences in lipid composition and this will affect their fluidity (Espenel, Margeat et al. 2008, Danglot, Chaineau et al. 2010).

CD81 diffusion coefficient is lower in polarised cells compared to non-polarised cells, however the mobile fraction is comparable. This is consistent with published single particle tracking data showing that in polarised cells CD81 undergoes slower diffusion with more mixed trajectories (Harris, Clerte et al. 2013, Potel, Rassam et al. 2013). A proportion of these areas of confinement overlap with TEMs (Harris, Clerte et al. 2013, Potel, Rassam et al. 2013), as previously reported for CD9 (Espenel, Margeat et al. 2008).

In a polarised HepG2 cell lipid diffusion is less than half that observed in a non-polarised cell, (Harris, Clerte et al. 2013) and therefore the reduced diffusion of both CD81 and claudin-1 is

likely to be affected by this to some degree. It is unlikely to be related to an increase in the formation of the coreceptor complex as the FRET values between CD81 and claudin-1 have been reported to be very similar between polarised and non-polarised cells (Mee, Harris et al. 2009). The observed reduction in the fraction of mobile claudin-1 is likely to be due to an increase in confinement to membrane domains with limited diffusion potential, possibly due to an increase in association with other proteins. In polarised HepG2 cells the phosphorylated CD81 adaptor protein ERM relocalises from the basolateral membrane to the apical membrane as with polarised airway cells, with a decreased incidence of CD81-ERM associations at the basal membrane (Berryman, Franck et al. 1993, Berbari, O'Connor et al. 2009, Harris, Clerte et al. 2013). ERM links CD81 to the actin cytoskeleton, and actin polymerisation is necessary for the Brownian diffusion of CD81(Harris, Clerte et al. 2013). Thus, a reduction in CD81-ERM linkage may contribute to the observed lower diffusion coefficient (Harris, Clerte et al. 2013).

The data presented here show that polarity is a central determinant of CD81 diffusion, and demonstrate a role for polarisation-dependent CD81 lateral diffusion in regulating HCV infection as previously reported (Harris, Clerte et al. 2013). However *in vivo*, hepatocytes do not exhibit a 'non-polarised' phenotype. Instead, they may become depolarised in response to inflammatory cytokines (Khakoo, Soni et al. 1997), and this often occurs in chronic hepatitis (Guidotti and Chisari 2006).

Recent data has shown that TNF-α is the central cytokine involved in the inflammation-driven depolarisation of hepatocytes (Fletcher, Sutaria et al. 2014), and therefore the effect of TNF-α on CD81 diffusion was examined. TNF-α reduces tight junctional integrity via NFκB-

dependent activation of MLCK and MLC phosphorylation, and affects occludin localisation (Ye, Ma et al. 2006, Fletcher, Sutaria et al. 2014). However, TNF-α has no reported effect on the establishment of cellular polarity (Ye, Ma et al. 2006, Mee, Harris et al. 2009, Petecchia, Sabatini et al. 2012), an aspect distinct from tight junctional integrity, although administration of TNF-α and VEGF have been shown to increase permissivity to HCV infection (Mee, Harris et al. 2009, Mee, Farquhar et al. 2010, Fletcher, Sutaria et al. 2014). Data presented here supports a decrease in tight junction integrity and increase in infection levels but also shows a decrease in polarity following addition of TNFα. This discrepancy with published data is likely due to differences in the treatment times used, as data from our lab (not shown) has highlighted the transitional activation of the TNF-α signalling pathway in hepatocytes, with a treatment time longer than 4 hours losing any effect on polarity. The experiments presented here used a treatment time of only an hour whereas others used a much longer treatment time of 24 or 48 hours (Mee, Farquhar et al. 2010, Petecchia, Sabatini et al. 2012).

The TNF-α-dependent depolarisation of HepG2.AcGFP-CD81 cells modulates CD81 diffusion alongside permissivity to HCV infection, and this supports recent data demonstrating that lateral diffusion of CD81 is a key determinant of HCV entry (Harris, Clerte et al. 2013),. Whilst the increase in diffusion coefficient represents a reversal of the impact of polarisation, the concomitant increase in mobile fraction suggests that there are additional processes affecting CD81 diffusion in depolarised cells. Given the short treatment time, this is likely to be related to the widespread structural changes occurring during depolarisation, which will affect not only membrane architecture relating to specialised regions but also the significant changes occurring in the cytoskeleton (reviewed in (Delorme-Axford and Coyne 2011).

Whilst this unstable environment would not model the long term inflammatory environment observed in HCV infection, it may well be representative of a liver during allograft transplant. As the focus of this study is to examine the interaction of HCV with CD81 in a normal liver, the basolateral membrane of a polarised cell was chosen for further study.

To this point, the diffusion of CD81 has varied in a manner which implicates large scale cellular organisation in determining its diffusion. There have been numerous reports illustrating the limiting effects of F-actin on the diffusion of membrane proteins (Kusumi, Sako et al. 1993, Sako, Nagafuchi et al. 1998, Treanor, Depoil et al. 2011), and the reorganisation of the actin cytoskeleton is central to the establishment of polarity. As CD81 links to the cytoskeleton via its C-terminal association with phosphorylated ezrin in a Syk-dependent manner (Sala-Valdes, Ursa et al. 2006, Coffey, Rajapaksa et al. 2009), we were interested to examine the importance of the actin cytoskeleton in modulating CD81 diffusion.

Phalloidin staining showed that addition of cytochalasin D has little effect on the localisation of CD81, but causes a deformation of bile canaliculi and the membrane, with a loss of filopodia. The deformation of the tight junction was supported by CMFDA data showing a loss of integrity, but there was no significant change in polarity index. In contrast, latrunculin B causes a loss of cytoskeletal organisation, with no visible bile canaliculus or membrane structures. CMFDA and MRP2 assays supported a significant loss of polarity and TJ integrity. CD81 localisation in these cells was completely cytoplasmic, supporting previous data that the actin cytoskeleton defines CD81 localisation (Brazzoli, Bianchi et al. 2008). That the integrity of the actin cytoskeleton is key to maintaining tight junctional integrity and polarity

has been previously observed (Harris, Clerte et al. 2013), and is in part due to the interaction between tight junction proteins such as occludin and the ZO family of proteins (Fanning, Jameson et al. 1998, Wittchen, Haskins et al. 1999, Wittchen, Haskins et al. 2000, Fanning, Ma et al. 2002).

CD81 diffusion was significantly reduced by the addition of both cytochalasin D and latrunculin B, with latrunculin B having the largest effect. As the structure of the cytoskeleton is less disrupted with cytochalasin D, this suggests that the diffusion of CD81 is dependent on the integrity of the actin cytoskeleton, in support of published data using SPT (Harris, Clerte et al. 2013). The use of both drugs increased the fraction of mobile CD81, with latrunculin B again having a greater effect. This implies that whilst the cytoskeleton is necessary for CD81 diffusion, it is also responsible for confining it. This again supports more recent data using latrunculin B showing that its addition decreased the number of confined trajectories observed and increased the amount of mixed and Brownian paths (Harris, Clerte et al. 2013). The dependence of these results on the actin cytoskeleton has since been demonstrated by Harris and colleagues who examined the effect of these drugs following deletion of the CD81 C-terminal domain, through which CD81 is linked to the cytoskeleton. The resulting data showed that these effects were ablated when the CD81 molecule could no longer connect to actin (Harris, Clerte et al. 2013). The observation that the actin cytoskeleton limits diffusion is not specific to CD81, with a number of other membrane proteins exhibiting limited mobility as a result of their linkage (Kusumi, Sako et al. 1993, Sako, Nagafuchi et al. 1998, Treanor, Depoil et al. 2011). For example, L1CAM diffusion is confined by linkage to the actin cytoskeleton through ankyrin, but promoted through linkage via ERM (Sakurai, Gil et al. 2008, Brachet, Leterrier et al. 2010).

154

The data presented here offers an insight into the organisation of the hepatic membrane and show that CD81 diffusion is dictated not only by the level of hepatic polarity, but also by its location within the cell. We additionally show that the integrity of the actin cytoskeleton plays a key role in maintaining and confining CD81 Brownian diffusion. Furthermore, the values described here are similar to those previously observed for CD81 using FRAP and also fit within a similar order of magnitude to that described for other tetraspanins (Table 4.5). Therefore, these data support the current model in which a more mobile and faster diffusing CD81 has a higher capability of supporting infection. We hypothesise that this may allow it to form transient interactions with partner proteins such as claudin-1 and EGFR more frequently, and enhance their ability to move to sites of clathrin-mediated endocytosis.

Protein	Diffusion Coefficient ($\mu m^2/s$)	Mobile Fraction (%)	Reference
CD9	0.23 ± 0.15	77	(Espenel, Margeat et al. 2008)
CD45	0.45	-	(Douglass and Vale 2005)
CD46	0.13 ± 0.08	87	(Espenel, Margeat et al. 2008)
CD50	0.19, 0.46 ± 0.05	-	(Suzuki, Fujiwara et al. 2007, Wieser, Moertelmaier et al. 2007)
CD55	0.24 ± 0.37	82	(Espenel, Margeat et al. 2008)
CD81 (FRAP defined)	0.07 ± 0.13	66 ± 10	(Harris, Clerte et al. 2013)
CD81 (SPT defined)	0.11 ± 0.11	70 ± 7	(Harris, Clerte et al. 2013)

Table 4.5: Diffusion parameters for CD81 and other tetraspanins

5 THE EFFECT OF CORECEPTOR COMPLEX FORMATION ON THE RESPONSE TO EGF-INDUCED EGFR STIMULATION

5.1 INTRODUCTION

Epidermal growth factor receptor (EGFR) has been shown to play a role in the uptake of numerous viruses including human cytomegalovirus and influenza A virus (Chan, Nogalski et al. 2009, Eierhoff, Hrincius et al. 2010, Karlas, Machuy et al. 2010), and recent publications demonstrate its role in increasing the rate of HCV entry (Lupberger, Zeisel et al. 2011, Diao, Pantua et al. 2012, Zona, Tawar et al. 2014).

A functional RNAi kinase screen has demonstrated that inhibiting EGFR signalling limits HCVcc infection and the entry of diverse HCVpp genotypes (Lupberger, Zeisel et al. 2011). Further investigation using Förster resonance energy transfer (FRET), demonstrated that following EGF stimulation an increased frequency of CD81-claudin-1 complexes was observed in Huh-7.5.1 cells (Zona, Lupberger et al. 2013). Following stimulation with EGFR, it was shown that activated HRas moves to the plasma membrane where it associates with CD81. Detergent extraction and proteomic analysis of polarised HepG2 cells expressing CD81 demonstrated that CD81-HRas interactions occur in regions which contain claudin-1, tetraspanins, and tetraspanin-associated proteins such as integrins. Thus these regions were classified as TEMs (Jensen, Kuhn et al. 2009, Lupberger, Zeisel et al. 2011, Zona, Lupberger et al. 2013).

Therefore, in the current model HRas provides a possible physical link between the EGFR signalling pathway and the formation of the CD81-claudin-1 complex (Figure 5.1).

EGF has been reported to stimulate EGFR signalling in a number of hepatic cell types (Lupberger, Zeisel et al. 2011, Diao, Pantua et al. 2012) and Diao and colleagues have shown that recombinant forms of HCV-E2 and anti-CD81 ligation of CD81 can stimulate EGFR phosphorylation in Huh-7.5. They suggest that HCV particles can activate EGFR signalling, thus stimulating entry (Diao, Pantua et al. 2012).

EGFR is a receptor tyrosine kinase (RTK) and a member of the ErbB family of signalling receptors. RTKs are transmembrane proteins with an extracellular ligand binding domain and an intracellular tyrosine kinase domain. Ligand binding promotes EGFR homo- or hetero-dimerisation and autophosphorylation of tyrosine residues in the intracytoplasmic kinase domain (Schlessinger 2002). Following this, downstream signalling is mediated by proteins that interact with these phosphorylated tyrosines through their Src homology 2 (SH2) domains, such as the Src homology domain containing transforming protein 1 (Shc1) and growth factor receptor bound protein 2 (Grb2) (Kolch 2005). Signalling pathways activated downstream of EGFR phosphorylation include mitogen-activated protein kinase (MAPK), phosphoinositide 3-kinase (PI3K)/Akt and c-Jun N-terminal kinases (JNK) (Oda, Matsuoka et al. 2005) (Figure 5.2).

There are 8 ligands that have been shown to bind the ErbB receptor family (Henriksen, Grandal et al. 2013) (Harris, Chung et al. 2003, Wilson, Mill et al. 2012) but the best studied are EGF and transforming growth factor α (TGFα). The affinity of EGF for EGFR on hepatocytes is 20-fold higher than that of TGFα (Thoresen, Guren et al. 1998), and EGF stimulation in hepatocytes activates the Ras/MAPK signalling pathway with minimal evidence for JNK or PI3K/Akt activation (Zona, Lupberger et al. 2013).
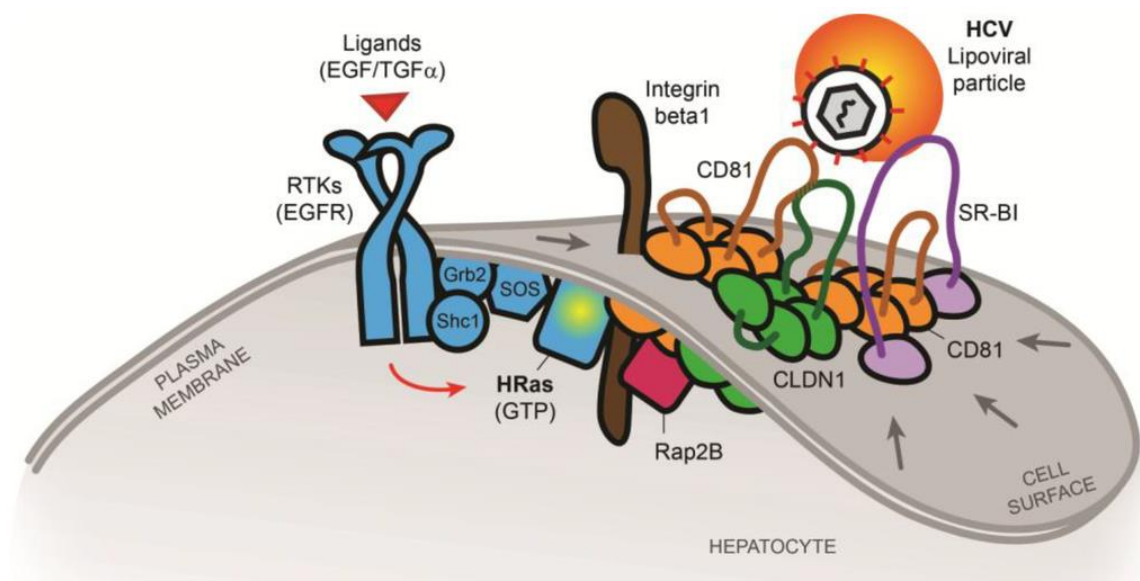
Figure 5.1: Proposed model of effect of EGF stimulation on HCV entry. (Zona, Tawar et al. 2014)
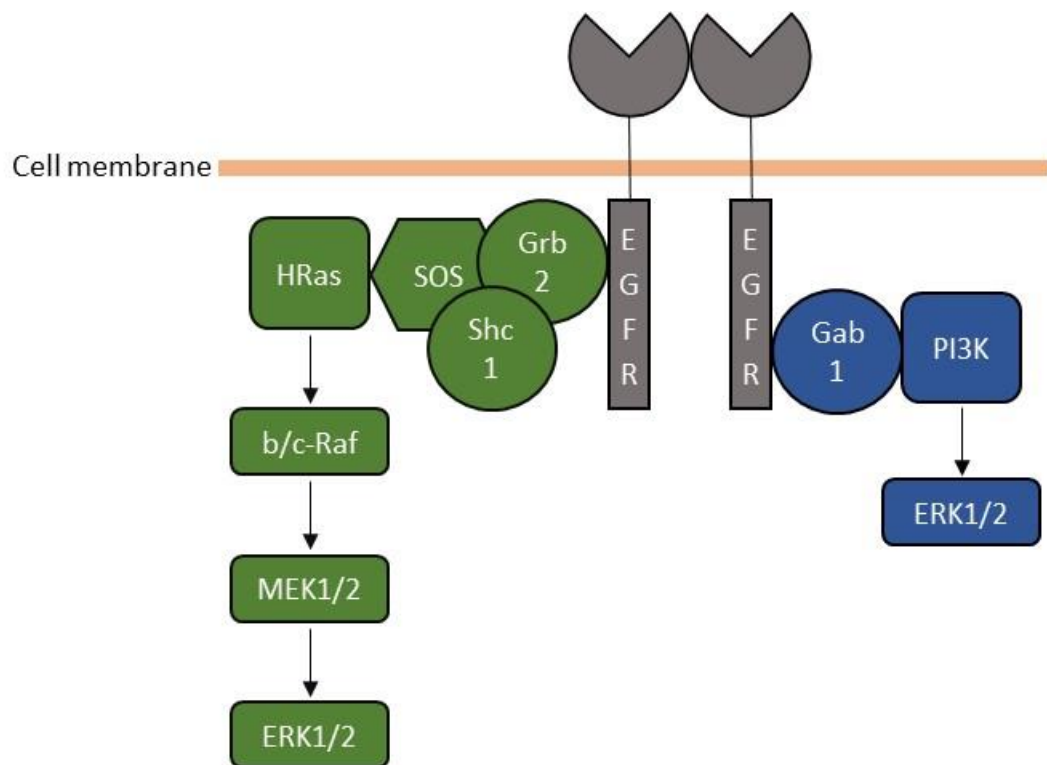
Figure 5.2: Signalling pathways downstream of EGF stimulation of hepatocytes. Also shown are the targets of inhibitors of early stages of the pathway for which results have been demonstrated. Adapted from (Zona, Tawar et al. 2014)

EGFR signalling is reported to play a role in a number of cellular processes, including cell proliferation, survival, migration and adhesion (Schneider and Wolf 2009) and as such is frequently upregulated in various cancers. Endocytosis of ErbB family receptors has long been accepted as an essential mechanism to control their signalling and the binding of different ligands results in distinct methods of internalisation and diverse downstream effects (Wilson, Mill et al. 2012, Henriksen, Grandal et al. 2013). For example, the binding of EGF to EGFR promotes clathrin-dependent internalisation of the receptor followed by its degradation. This occurs as a result of c-Cbl recruitment by Grb2, leading to the subsequent ubiquitination and lysosomal degradation of EGFR (Ravid, Heidinger et al. 2004, Roepstorff, Grandal et al. 2009). This is in contrast to the outcome of TGF-α-induced signalling, in which the receptor is recycled to the membrane due to the rapid intracellular dissociation of TGF-α from the receptor. This may be due to the low pH of the endosome (Alwan, van Zoelen et al. 2003, Roepstorff, Grandal et al. 2009), and leads to the de-ubiquitination of the receptor and its recycling to the membrane (Roepstorff, Grandal et al. 2009).

Zona and colleagues (Zona, Lupberger et al. 2013) demonstrated an increased interaction between CD81 and claudin-1 following EGF stimulation which was to some extent dependent on HRas, but the underlying mechanism for this is not understood. The formation of the EGF-induced CD81-HRas complex may be dependent upon an association between CD81 and claudin-1, or may precede the formation of this coreceptor complex.

To investigate whether EGF regulates CD81 diffusion in a polarised cell type and whether this is dependent on CD81 association with claudin-1, a panel of CD81 mutants previously shown

to have varying associations with claudin-1 were employed (Davis, Harris et al. 2012) (Figure

5.6).

5.2 RESULTS

5.2.1 Effects of EGF and anti-CD81 mAbs on EGFR phosphorylation.

A number of papers have demonstrated that addition of EGF to hepatic cell lines boosts levels of HCV infection. This has been shown in derivatives of the Huh-7 cell line, PHH and in polarised HepG2 cells expressing CD81 (Lupberger, Zeisel et al. 2011, Diao, Pantua et al. 2012, Zona, Lupberger et al. 2013). Prior to confirming that HepG2 cells expressing AcGFP-CD81 respond in the same way, we initially tested the timeframe of EGFR phosphorylation in these cells.

Given the recent report demonstrating that addition of α-CD81 antibodies can promote EGFR phosphorylation (Diao, Pantua et al. 2012), we were interested to screen our panel of α-CD81 mAbs alongside EGF for their phosphorylation potential. Polarised HepG2 cells were incubated with EGF or anti-CD81 mAbs and at defined times the cells were lysed and probed for EGFR phosphorylation by Western Blot. Grb2 binds to EGFR at the pY1068 residue following EGF stimulation (Batzer, Rotin et al. 1994, Tan, Wang et al. 2007), and therefore this residue was selected for study. The timeframe was chosen for its relevance to FRAP experiments (Figure 5.3).

EGF or members of the anti-CD81 antibody panel presented in chapter 3were added at concentrations of 1 µg/ml and 30 µg/ml respectively following a serum starvation period of 30 minutes, sufficient to prevent any phosphorylation of EGFR (Figure 5.3a). 2s155 is shown as a representative antibody. EGF promoted EGFR phosphorylation at all time points tested. In contrast, anti-CD81 mAbs had no detectable effect (Figure 5.3a). Normalising the pY1068 band intensity to the respective β-actin band showed EGFR phosphorylation at Y1068 from

15 minutes to 60 minutes (Figure 5.3b), and therefore this time period was chosen for later experiments. CD81 mAbs were from this point discounted as a method to stimulate EGFR in polarised HepG2.AcGFP-CD81 cells.

(a)

(b)
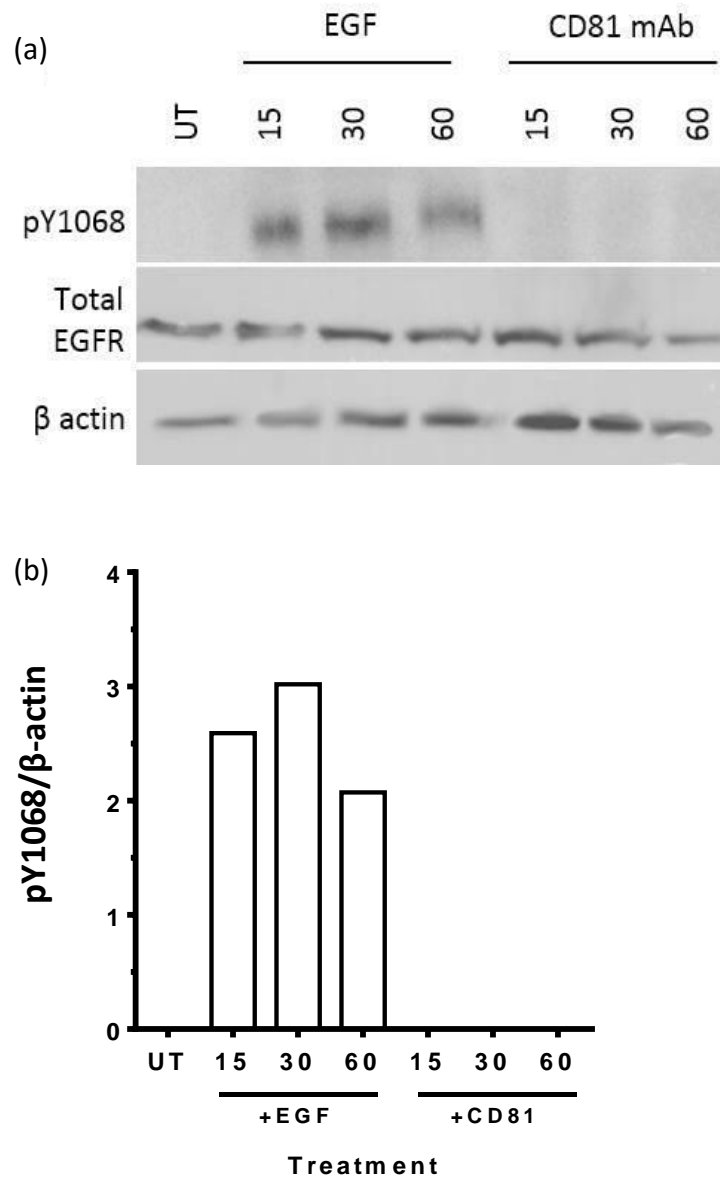
Figure 5.3: Addition of EGF but not CD81 mAbs leads to phosphorylation of EGFR.
Following a serum starvation of 30 minutes, EGF was added at 1 μg/ml and the CD81 mAbs 2s155 at 30 μg/ml for the stated timepoints. EGFR phosphorylation at Y1068 was examined by Western Blot in relation to β actin (a) and quantified (b).

5.2.2 Effect of EGF stimulation on HCV entry into hepatic cell lines

To ascertain whether cells expressing AcGFP-CD81 were capable of supporting infection in an EGF manner dependent, 5 day polarised HepG2.AcGFP-CD81 cells were serum starved for 30 minutes before a 30 minute EGF treatment and the addition of H77 pseudoparticles. Huh-7.5 and wild type HepG2 cells were tested for comparison (Figure 5.4). The results showed that, whilst addition of EGF prior to infection had no effect on CD81-negative HepG2 cells, the level of infection was increased from 5.4×10^4 RLU to 11×10^4 RLU in polarised cells expressing HepG2.AcGFP-CD81 and from 1.9×10^6 RLU to 3.4×10^6 in Huh-7.5 cells (Figure 5.4). These data indicate that AcGFP-CD81 is capable of acting as a receptor for HCV and that pre-treatment of cells expressing this protein leads to a boost in infection similar to that seen with Huh-7.5. We were interested to understand the protein diffusion events underlying this effect.
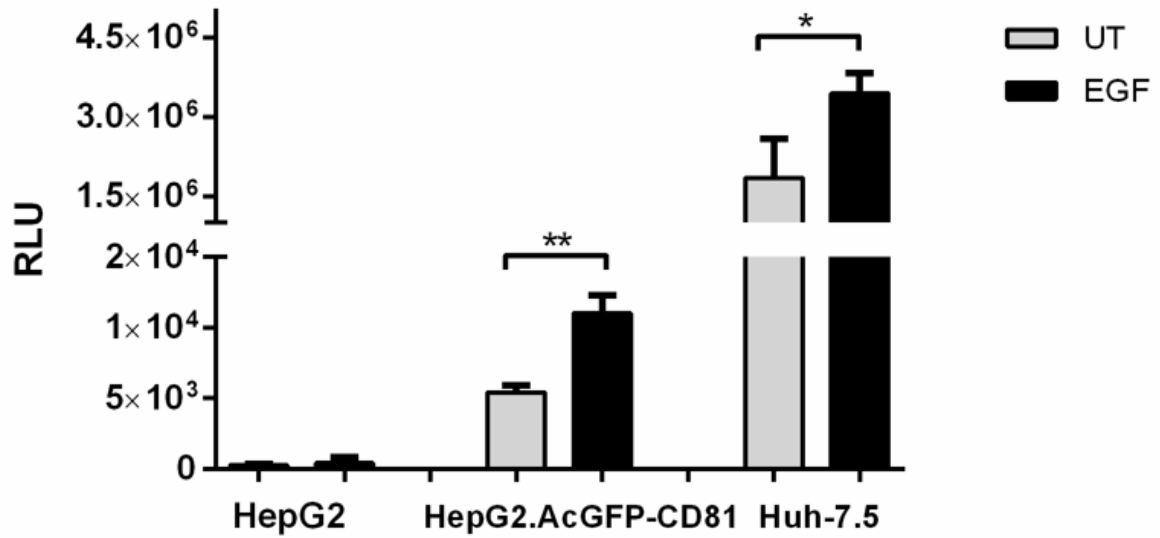
Figure 5.4 EGF stimulation increases the HCV infection levels in polarised and non-polarised hepatic cell lines. *HepG2.AcGFP-CD81 cells were allowed to polarise for 5 days prior to infection, whereas Huh-7.5 cells were plated the day before. Cells were serum starved for 30 minutes prior to the addition of 1 μg/ml for 30 minutes prior to infection. H77-HCVpp was then added and incubated for 72 hours at 37˚C before lysis and quantification. Groups were compared by Mann-Whitney U test (GraphPad Prism 6.0) *P<0.05, **P<0.001, ***P<0.0001.*

5.2.3 Effect of EGF on CD81 and claudin-1 diffusion

Initial experiments were performed to verify recent work presented by Zona (Zona, Lupberger et al. 2013), who demonstrated that inhibition of EGFR signalling increases CD81 diffusion and decreases the association with claudin-1 in the Huh-7.5.1 cell type (Zona, Lupberger et al. 2013). However, no data on the effect of EGFR signalling on CD81 diffusion has been reported for polarised cell lines, nor has the effect of EGFR signalling on the diffusion of the coreceptor claudin-1 been assessed. The effect of EGFR signalling on CD81 and on claudin-1 diffusion was examined in polarised HepG2 cells using the reversible RTK inhibitor Erlotinib. Erlotinib is an EGFR-specific RTK inhibitor which binds reversibly to the ATP binding site of the receptor and prevents tyrosine phosphorylation (Raymond, Faivre et al. 2000) (Figure 5.5).

Cells expressing either AcGFP-CD81 or AcGFP-claudin-1 were allowed to polarise for 5 days prior to imaging. Cells were serum starved for 30 minutes prior to imaging (untreated sample, UT) or prior to the addition of 10μM Erlotinib for 1 hour prior to imaging. In all cases, cells were imaged within the following 30 minutes.

Inhibition of EGFR signalling with Erlotinib significantly decreased the diffusion coefficient of CD81, from 0.070 μm^2/s to 0.028 μm^2/s, (Figure 5.5a, table 5.2). At the same time, the mobile fraction of CD81 increased from 83% to 87% following addition of Erlotinib (Figure 5.5b, table 5.2).
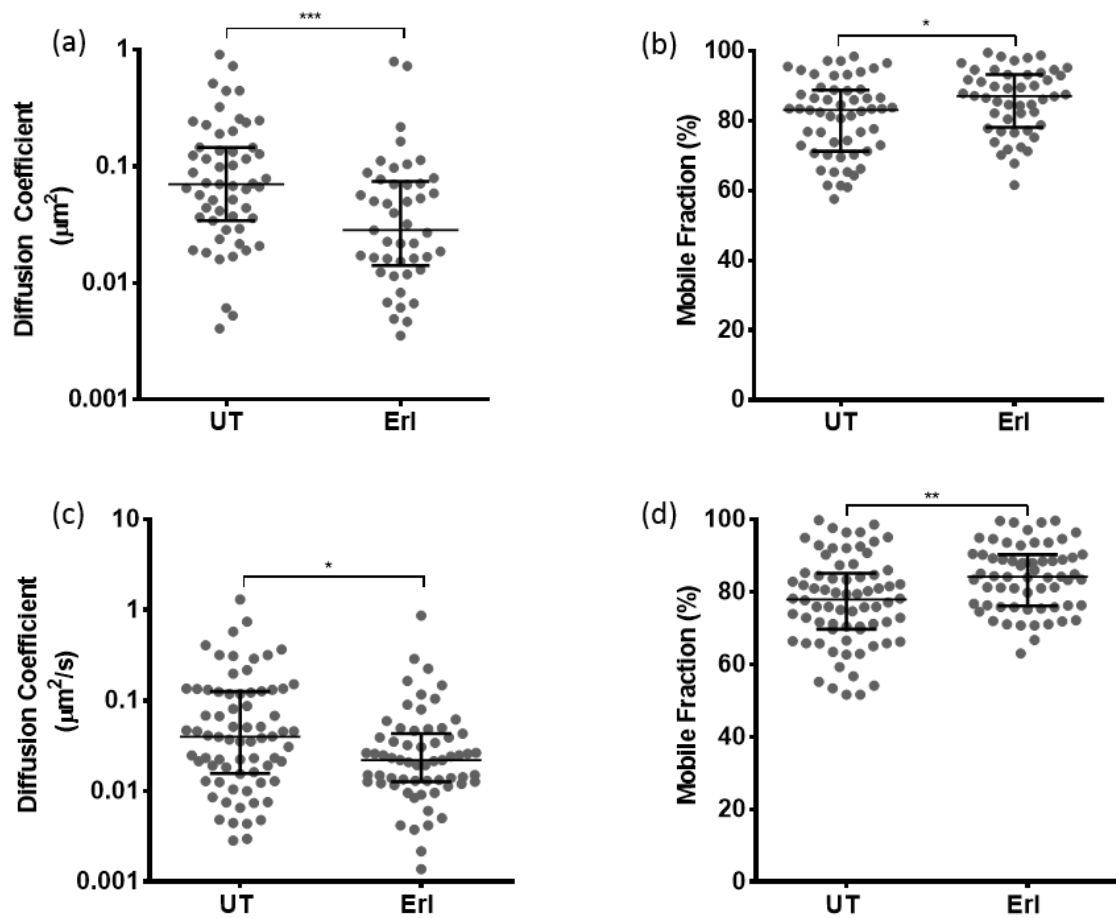
Figure 5.5: Effect of EGFR signalling stimulation on CD81 and claudin-1 diffusion. *Following a serum starvation of 30 minutes, cells were imaged with no stimulation (UT), following a 30 minute stimulation with at 1 µg/ml EGF (EGF) , or following an EGF stimulation with a 60 minute erlotinib pre-treatment (10 µM) (Erl then EGF). This was carried out in HepG2.AcgFP-CD81 (a,b) or HepG2.CD81.AcGFP-claudin-1 (c,d) following a 5 day polarisation period. Cells were imaged using a 100x Plan Achromat 1.4 NA oil immersion objective on a Zeiss LSM 780 confocal microscope with a GaAsP spectral detector, and groups were compared by Mann-Whitney U test (GraphPad Prism 6.0). *P<0.05, **P<0.001, ***P<0.0001.*

As EGFR signalling has been reported to influence claudin-1 interactions, we studied the effect of inhibition of EGFR signalling on claudin-1 diffusion in polarised HepG2 cells. Inhibition of EGFR signalling led to a reduction in diffusion coefficient, from 0.040 μm^2/s to 0.022 μm^2/s relative to the untreated sample (Figure 5.5c, table 5.2), whereas the mobile fraction was increased from 78% to 84% (Figure 5.5d, table 5.2).

These data show that in a polarised cell line, inhibition of EGFR signalling affects both CD81 and claudin-1 diffusion coefficients and mobile fractions similarly, and results in both proteins exhibiting a higher mobility but a lower rate of diffusion.

No study has yet examined the changes in protein diffusion which accompany EGF stimulation. We therefore examined this effect and whether any changes were modulated via the CD81-claudin-1 complex or through the proteins are individually. We studied a series of CD81 mutants that have previously been characterised to no longer interact with claudin-1 (Davis, Harris et al. 2012). CD81 was chosen for study as it has been shown to interact directly with HRas in polarised HepG2 cells (Zona, Lupberger et al. 2013).

HepG2.AcG FP-CD81	Diffusion Coefficient ($\mu m^2/s$)	IQ Range ($\mu m^2/s$)	Mobile Fraction (%)	IQ Range (pp)	Number of cells
UT	0.070	0.111	83.09	17.56	55
Erlotinib	0.028	0.063	87.07	15.15	55

Table 5.1 – Quantification of figure 5.5 a, b

HepG2.CD81.AcGFP-CLDN-1	Diffusion Coefficient ($\mu m^2/s$)	IQ Range ($\mu m^2/s$)	Mobile Fraction (%)	IQ Range (pp)	Number of cells
UT	0.040	0.110	77.93	15.46	55
Erlotinib	0.022	0.031	84.19	14.13	55

Table 5.2 – Quantification of figure 5.5 c, d

5.2.4 Effect of CD81-LEL mutations on CD81 and EGFR localisation

The key residues in the CD81-LEL which are involved in the claudin-1 interaction have been previously identified (Figure 5.6). These are K148A, T149A, E152A and T153A. We had available engineered CD81 proteins expressing these mutants, in addition to the double mutants K148A/T149A and E152A/T153A, the former of which has a similar receptor activity to WT CD81 (Davis, Harris et al. 2012) (Table 5.4). HepG2 cells expressing the mutant proteins show varying abilities to support HCVpp infection (Davis, Harris et al. 2012) (Table 5.4) and we assessed whether they had any effect on the localisation of either CD81 or EGFR. Cells were transduced to express fluorescent forms of these proteins and allowed to polarise for 5 days before costaining with antibodies specific for EGFR (Figure 5.7) to investigate how these proteins are localised.
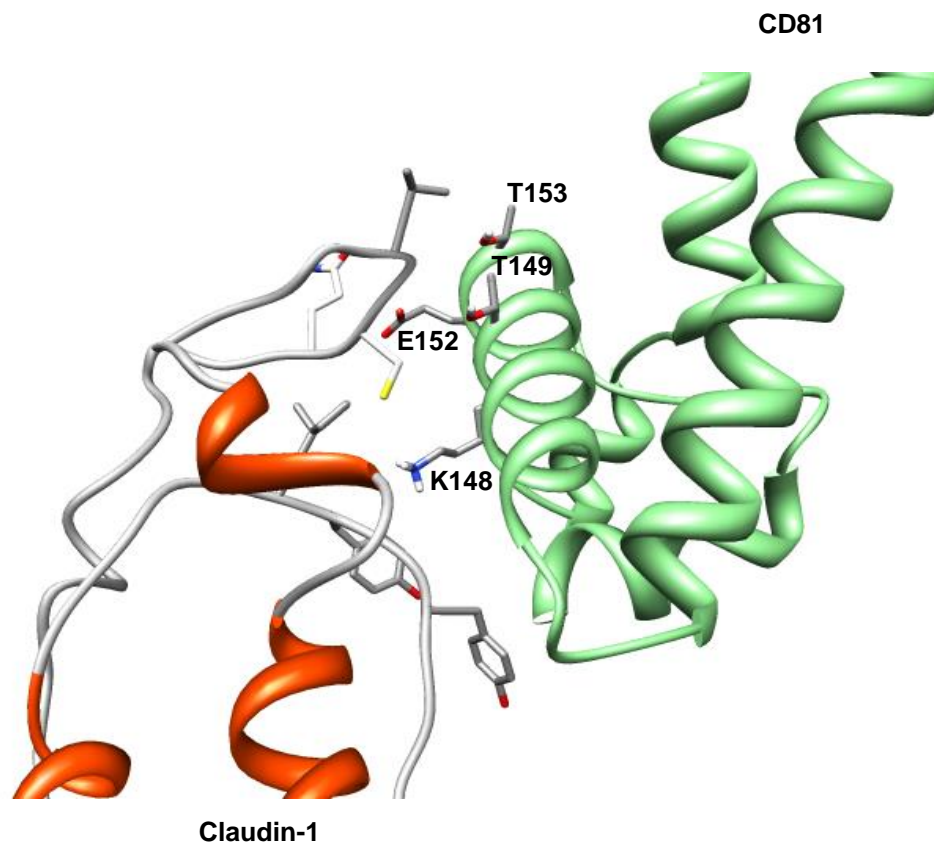
Figure 5.6: Structural modelling of CD81-Claudin-1 association. Ribbon model of the predicted structure of the LEL domain of native claudin-1 (alpha helices in red, beta turn in white) with CD81 in green, key interacting residues are labelled (Davis et al., 2012).

AcGFP-CD81 displayed a classic 'chicken-wire'-like pattern, consistent with cell membrane localisation as previously described (Mee, Harris et al. 2009), with EGFR also predominantly expressed in the same regions. The staining patterns of CD81 and EGFR in cells expressing mutant CD81 proteins were in all cases similar to those seen in the WT cells (Figure 5.7).

As the proteins localised normally in polarised HepG2 cells, we examined the response of cells expressing these proteins to EGF stimulation. As a preliminary step prior to examining the effect of the CD81-claudin-1 complex on EGF-induced CD81 diffusion, the basal levels of diffusion of these mutant proteins were examined by FRAP in the absence of any EGFR signalling.
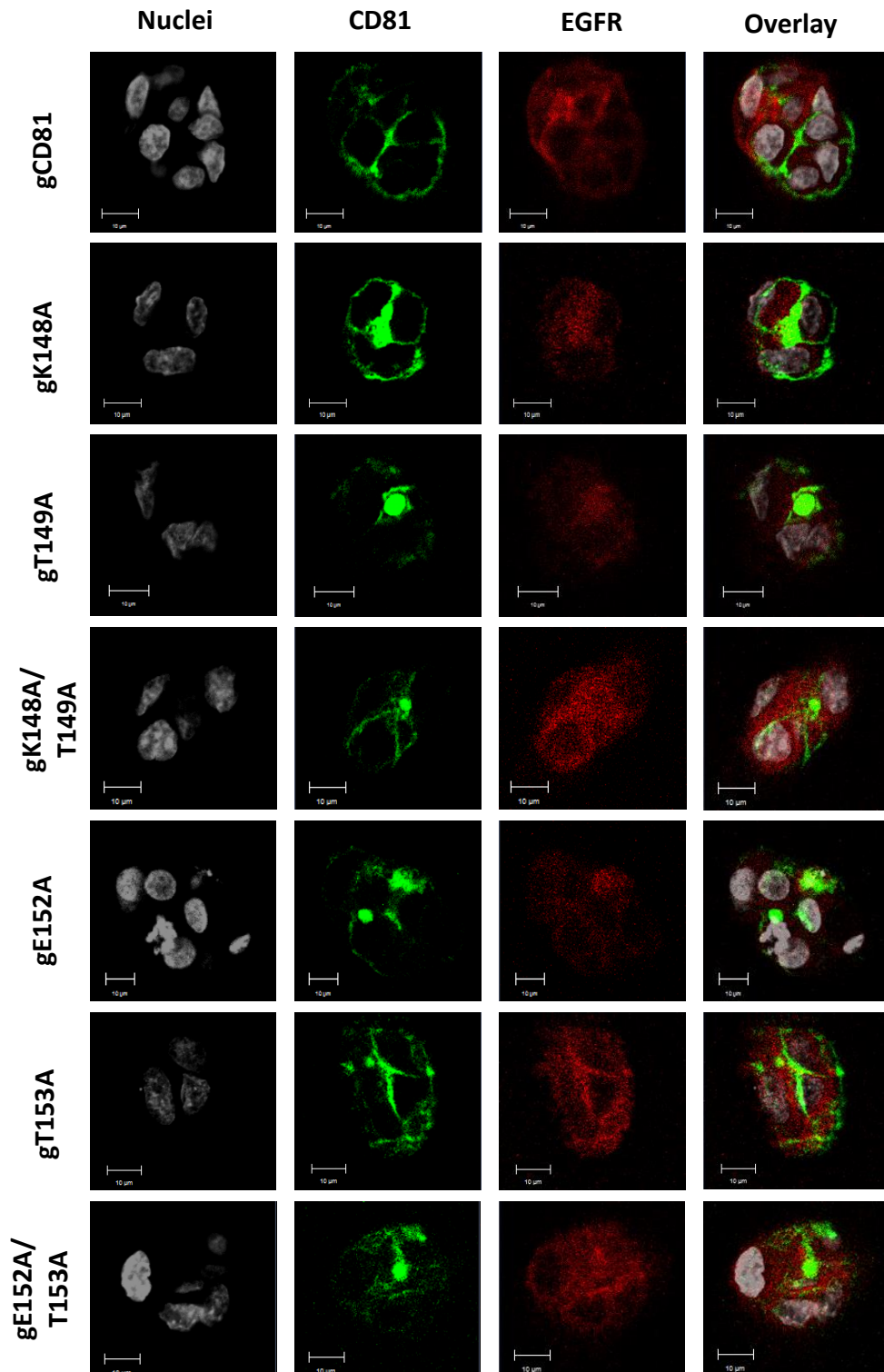
Figure 5.7: Effect of CD81 mutant proteins on CD81 and EGFR expression. *Cells expressing the mutant forms of CD81 were allowed to polarise for 5 days before fixing and costaining with EGFR-633. Cells were imaged using a 100x Plan Achromat 1.4 NA oil immersion objective on a Zeiss LSM 780 confocal microscope with a GaAsP spectral detector.*

5.2.5 Mutations in the CD81-LEL affect protein diffusion

The AcGFP-CD81 protein was shown to diffuse at 0.070 μm^2/s, and the K148A and T149A variants displayed similar diffusion coefficients of 0.077 μm^2/s and 0.062 μm^2/s respectively. The double mutant K148A/T149A diffused at a higher rate of 0.088 μm^2/s. In contrast, the other three mutant forms of CD81 diffused at much lower rates, with E152A, T153A and E152A/T153A diffusing at 0.039 μm^2/s, 0.026 μm^2/s and 0.046 μm^2/s respectively (Figure 5.8, table 5.3). Conversely, the mobile fractions show no significant alterations, with a variation of only 6%, between 85% and 79% respectively (data not shown).

These results show that the mutations which ablate the interaction between CD81 and claudin-1 have diverse effects on the rate of diffusion, but have little effect on the mobility of CD81. There appear to be two groups of CD81 mutants – K148A, T149A and K148A/T149A which diffuse at a similar rate to WT CD81, and E152A, T153A and E152A/T153A – which diffuse at around half that rate (Figure 5.8 table 5.3).

These data suggest that claudin-1 association can alter CD81 diffusion. However, this is not seen with every mutant, suggesting that there may be more than one contact site between CD81 and claudin-1, including the residues E152A and T153A, or that there may be additional, as yet unidentified, binding partners. The observed reduction in diffusion coefficient suggests an indirect mechanism contributing to the reduction in association with claudin-1.
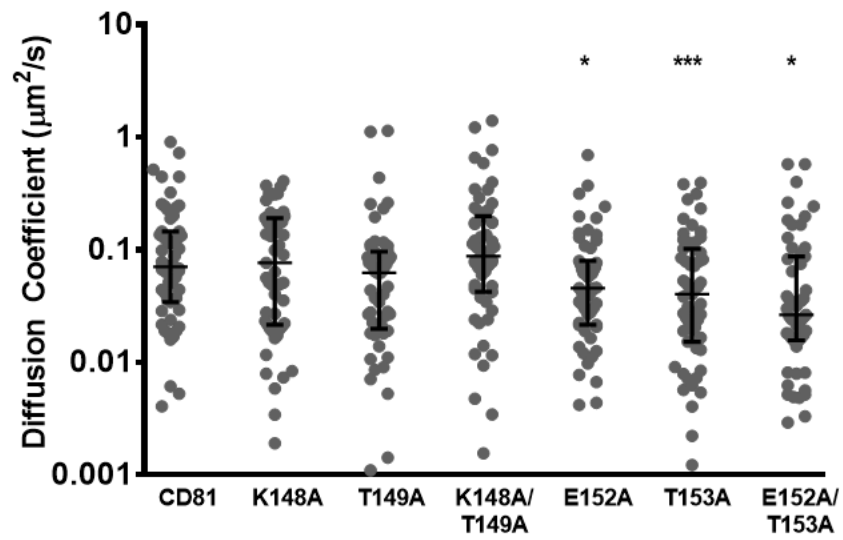
Figure 5.8: Effect of CD81 EC2 mutations on protein diffusion. *Cells expressing mutant forms of CD81 were allowed to polarise for 5 days. Cells were imaged using a 100x Plan Achromat 1.4 NA oil immersion objective on a Zeiss LSM 780 confocal microscope with a GaAsP spectral detector, and groups were compared by Mann-Whitney U test (GraphPad Prism 6.0). *P<0.05, **P<0.001, ***P<0.0001.*

	Diffusion Coefficient ($\mu m^2/s$)	IQ Range ($\mu m^2/s$)	Mobile Fraction (%)	IQ Range (pp)	Number of cells
gCD81	0.070	0.113	83	17.56	55
gK148A	0.077	0.167	81	13.17	55
gT149A	0.062	0.083	79	22.2	55
gK148A/T149A	0.088	0.162	85	12.67	55
gE152A	0.039	0.088	82	19.05	55
gT153A	0.026	0.066	79	22.20	55
gE152A/T153A	0.046	0.061	81	19.62	55

Table 5.3: Effect of EGFR signalling stimulation and stimulation on protein diffusion. Quantification of figure 5.8.

5.2.6   CD81-LEL mutations have varying effects on EGFR phosphorylation

The diffusion speeds recorded for E152A, T153A and E152/T153A are similar to those observed for CD81 in the absence of any EGFR signalling. To determine whether these lower diffusion coefficients are related to an altered sensitivity to EGFR signalling, the effect of EGF stimulation on EGFR phosphorylation was examined in cells containing the mutant proteins.

Polarised HepG2 cells expressing WT AcGFP-CD81 and mutant forms of CD81 were treated with EGF and the level of total EGFR and EGFR-pY1068 measured. Monitoring the cell's response to this treatment showed that all mutants responded to EGFR phosphorylation to some degree (Figure 5.9a), however analysis demonstrated that the levels of pY1068 differed significantly between the cell lines (Figure 5.9b). Cells expressing AcGFP-CD81, E152A or T153A exhibited similar high levels of EGFR phosphorylation. The levels of

phosphorylation observed following stimulation of cells expressing K148A, T149A or

K148A/T149A were significantly lower. In cells expressing E152A/T153A, the levels of

pEGFR, although depressed, were not significantly lower than seen in WT AcGFP-CD81 (after

correction of the statistical tests for multiple comparisons). These data lead us to conclude

that mutations in the LEL which modulate the association of CD81 and claudin-1 alter EGFR

phosphorylation in response to EGF stimulation.
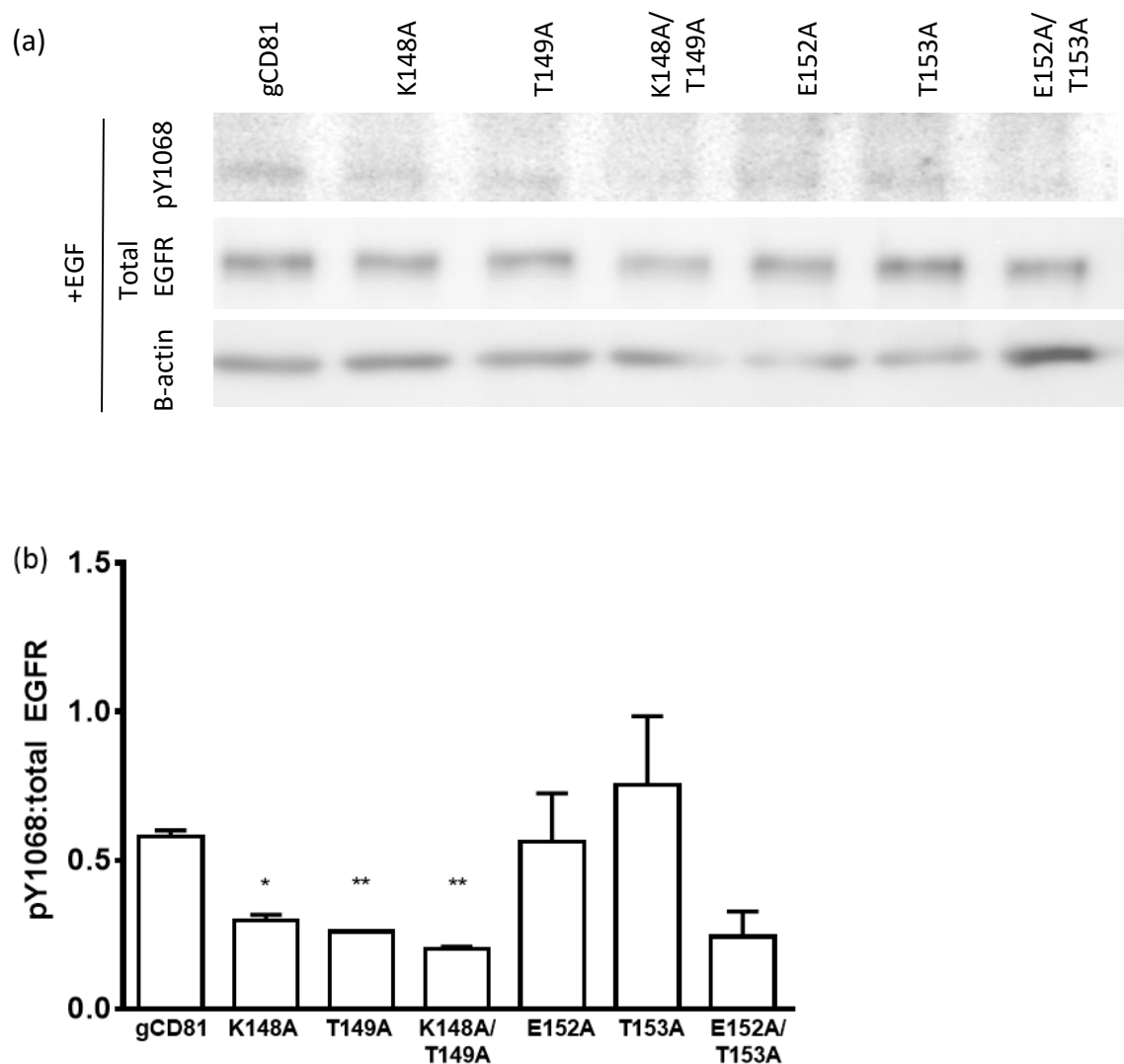
Figure 5.9: Effect of CD81 mutant proteins on cellular response to EGF stimulation.
Cells expressing the mutant forms of CD81 were allowed to polarise for 5 days. Following a 30 minute serum starvation period, cells were treated with 1 µg/ml EGF for 60 minutes. Cells were lysed and stained for total EGFR, EGFR-pY1068 and β-actin (a). Levels of pY1068 were compared to total EGFR (b). Groups were compared by Mann-Whitney U test (GraphPad Prism 6.0). *P<0.05, **P<0.001, ***P<0.0001.

Since EGF priming of EGFR phosphorylation predominantly leads to degradation of the receptor (Ravid, Heidinger et al. 2004, Roepstorff, Grandal et al. 2009), levels of total EGFR were compared in HepG2 cells expressing mutant CD81 proteins before and after EGF stimulation to examine the effect of the altered EGF signalling on downstream events. In cells expressing K148A and E152/T153A, total EGFR is reduced to around a third of pre-exposure levels following EGF addition (Figure 5.10). This reduction is slightly less in T149A and K148A/T149A and suggests that in these cells, mutations in the LEL of CD81 which affect the interaction with claudin-1 have little effect on the levels of EGFR in comparison to AcGFP- CD81. In contrast, in cells expressing E152A and T153A there was a smaller reduction in total EGFR observed following EGF addition (Figure 5.10), with E152A showing a reduction of about half, and T153A around a quarter. Therefore, total EGFR levels are considerably influenced by mutations governing the interaction between CD81 and claudin-1, and this may be as a result of altered trafficking. When these findings are compared with published data (table 1), there appeared to be no direct correlation between the levels of EGFR-pY1068 and CD81:claudin-1 association, which suggests that the mutations studied are having affects outside of those directly related to the interaction between CD81 and claudin-1, and that these relate to EGFR signalling.
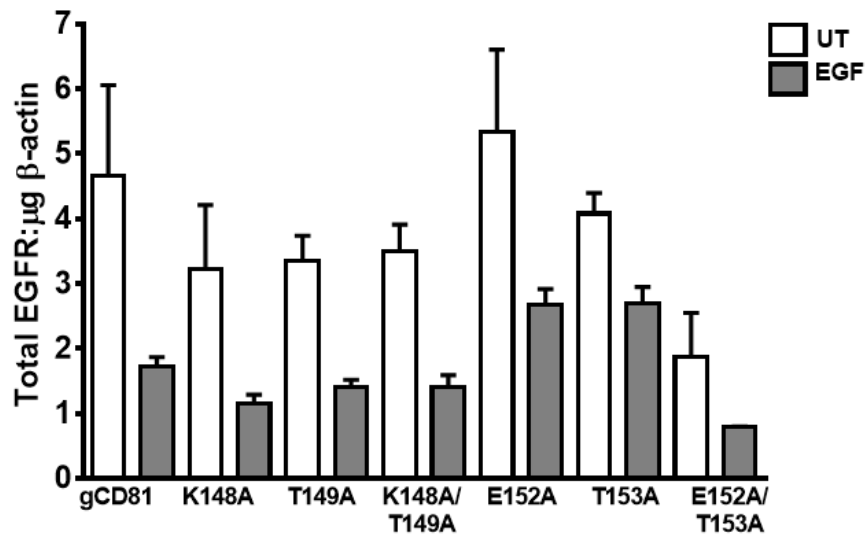
Figure 5.10: Effect of CD81 mutant proteins on cellular response to EGF stimulation.
Cells expressing the mutant forms of CD81 were allowed to polarise for 5 days. Following a 30 minute serum starvation, cells were either left untreated or treated with 1 µg/ml for 60 minutes. Cells were then lysed and lysates were stained for total EGFR, EGFR-pY1068 and β-actin. Levels of total EGFR were compared between UT and EGF treated samples.

5.2.7 CD81 proteins bearing mutations in the LEL display varying reactions to EGF stimulation

Having demonstrated that polarised HepG2.AcGFP-CD81 cells show an increase in infection levels following administration of EGF (Figure 5.4), we examined this further by studying the response of receptor diffusion to EGFR signalling and its dependence on the CD81-claudin-1 complex. As pY1068 was visible from 15 minutes to 60 minutes post-EGF stimulation (Figure 5.3), the period between 30 minutes and 60 minutes was chosen as the optimal time to observe EGF stimulation of EGFR phosphorylation in imaging experiments.

WT AcGFP-CD81 and a number of the mutant proteins did not show any change in diffusion coefficient following the stimulation of EGFR. However, following EGF addition the K148A/T149A mutant became less mobile and diffused more slowly, with mobile fractions and diffusion coefficients of 85% and 70% and 0.088 μm^2/s and 0.061 μm^2/s respectively (Figure 11 a, b. Table 5.4). K148A also showed a significant reduction in diffusion, from 0.077 μm^2/s to 0.046 μm^2/s, following EGF addition but showed no change in mobility (Figure 11 a, b. Table 5.4). In contrast, the T153A protein mobile fraction increased from 79% to 85% after the addition of EGF and the diffusion coefficient increased from 0.026 μm^2/s to 0.080 μm^2/s (Figure 11 a, b. Table 5.4).

These data suggest that mutations in the CD81-LEL have additional effects beyond their role in defining the association between CD81 and claudin-1. This may be as a result of altered quaternary interactions formed by CD81 and claudin-1 which are dependent on the prior interaction between the two.
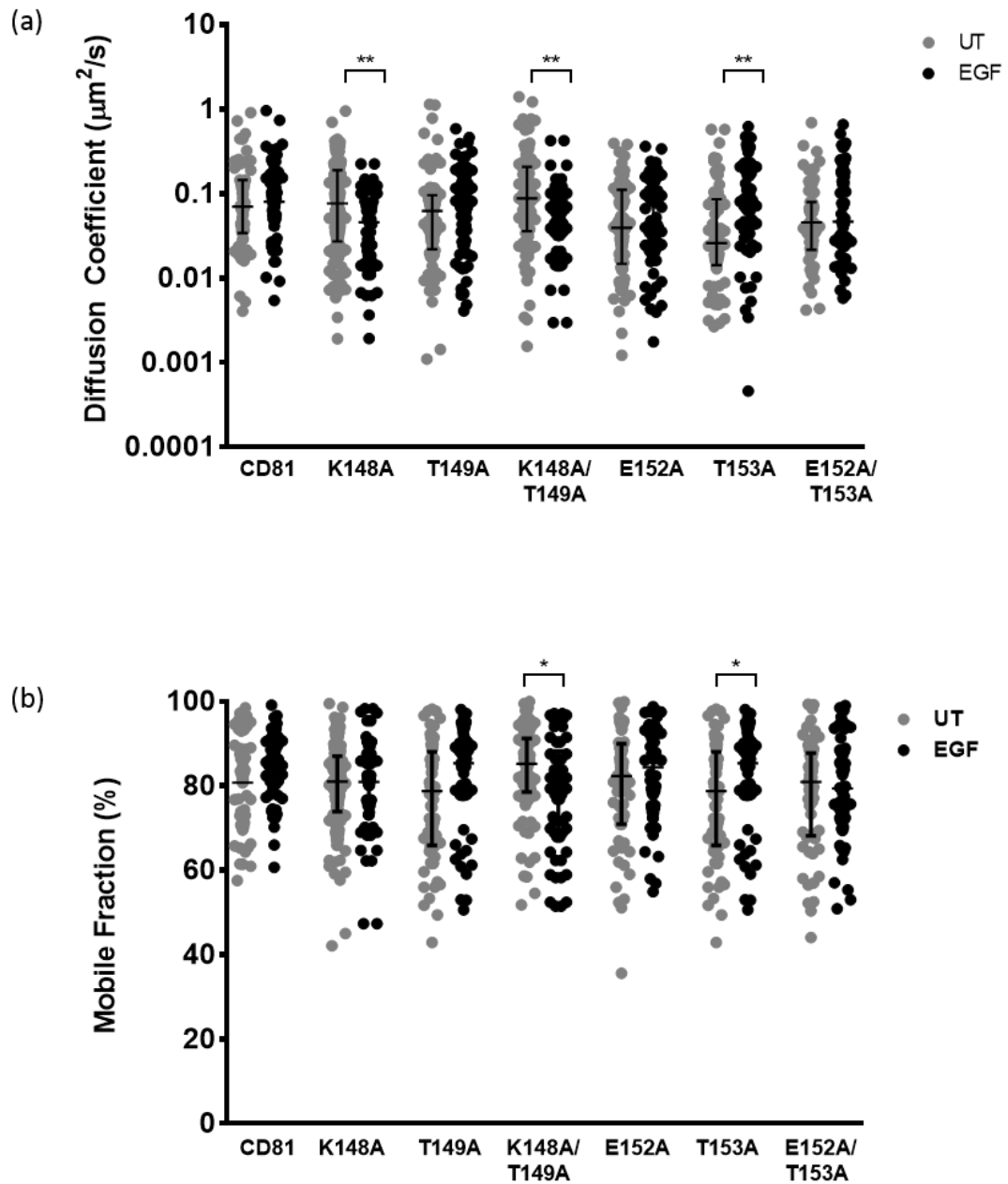
Figure 5.11: Effect of EGFR signalling on CD81 protein diffusion. *Cells expressing mutant forms of CD81 were allowed to polarise for 5 days. Following a 30 minute period of serum starvation, cells were either left untreated (UT) or treated with 1 µg/ml EGF for 30 minutes (EGF). Diffusion coefficient (a) and mobile fraction (b) are shown. Cells were imaged using a 100x Plan Achromat 1.4 NA oil immersion objective on a Zeiss LSM 780 confocal microscope with a GaAsP spectral detector, and groups were compared by Mann-Whitney U test (GraphPad Prism 6.0). *P<0.05, **P<0.001, ***P<0.0001.*

FRET with claudin-1 (significance of change from WT CD81)	Receptor activity	Cell line	Diffusion Coefficient (μm^2/s)		Mobile Fraction (%)		Number of cells	
			UT	EGF	UT	EGF	UT	EGF
35%	+++	HepG2.gCD81	0.070	0.079	83	85	55	55
25%	+++	HepG2.gK148A/T149A	**0.088**	**0.061 ****	**85**	**70 ***	55	55
23%	++	HepG2.gK148A	**0.077**	**0.046 ****	81	81	55	55
12%*	-	HepG2.T149A	0.062	0.080	79	85	55	55
10%*	-	HepG2.T153A	**0.026**	**0.080 ****	**79**	**85 ***	55	55
8%*	-	HepG2.gE152A	0.039	0.041	82	84	55	55
8%*	-	HepG2.gE152A/T153A	0.046	0.047	81	79	55	55

Table 5.4: Summary table of receptor activity and FRET with CLDN-1 for each mutant and WT CD81. Significant changes in FRET between CD81 mutants and CLDN-1 are shown alongside their associated receptor activities, both of which are previously published by Dr. Christopher Davis (Davis, Harris et al. 2012). Cell lines which exhibit significant changes in diffusion following stimulation are highlighted in light grey, and the values which exhibit the significant change are in bold font. Groups were compared by Mann-Whitney U test (GraphPad Prism 6.0). * Represents those mutants with a diffusion coefficient which differs from WT CD81 with a $P \leq 0.05$, ** $P \leq 0.001$, *** $P \leq 0.0001$

5.3 DISCUSSION

A recent publication has shown that EGF-induced EGFR stimulation and signalling increases HCV entry into non-polarized Huh-7.5.1 cells (Zona, Lupberger et al. 2013). Based on inhibition and siRNA data in this cell line, the authors hypothesized that stimulation with EGF reduced CD81 lateral diffusion, inducing an interaction with claudin-1 to form the coreceptor complex (Lupberger, Zeisel et al. 2011, Zona, Lupberger et al. 2013).

In brief, the current model for this process is as follows: EGFR phosphorylation at pY1068 allows Grb2 to bind, and the subsequent downstream signalling leads to the activation of HRas and its relocation to the cell membrane. Here, HRas binds CD81 and modulates an increase in the association with claudin-1. However, the underlying mechanism for this increase in CD81-claudin-1 association has not yet been studied. It remains unclear whether HRas binds to the CD81 homodimer or to CD81 as part of the heteromeric coreceptor complex, as both CD81 and claudin-1 have been demonstrated to be present in membrane domains in polarised HepG2 cells which have not been stimulated with EGF (Zona, Lupberger et al. 2013). In order to further our understanding of this process, we examined the dependence of the effects of EGF stimulation on the CD81-claudin-1 coreceptor complex.

Initial experiments determined the correct timeframe of EGF stimulation for imaging and infection experiments. Phosphorylation of EGFR in hepatocytes has been shown to occur for up to 60 minutes following stimulation with EGF or TGFα (Lupberger, Zeisel et al. 2011) or with HCV-E2 and CD81-specific mAbs (Diao, Pantua et al. 2012). Whilst we confirmed that EGF is capable of stimulating EGFR for up to 60 minutes in polarised HepG2.AcGFP-CD81 cells, this effect was not replicated with CD81 mAbs even when used at very high concentrations. No

stimulation of EGFR phosphorylation was observed following the addition of the panel of antibodies described in Chapter 3, therefore a possible explanation for this difference is the cell types used - the published work used the non-polarised Huh-7.5 cell type (Diao, Pantua et al. 2012), whereas this study used polarised HepG2 cells. Although JS-81 was not tested, this discrepancy is unlikely to be related to the antibodies used as JS-81, 2s155 and other members of the antibody panel all recognise the L162 residue (Farquhar et al., in preparation, appendix table 2) (Diao, Pantua et al. 2012). It may be interesting to examine the ability of our antibody panel to stimulate signalling pathways in this cell type, as previous work has shown that some pathways which are known to be stimulated downstream of EGF stimulation are not active following EGF administration in either Huh-7.5.1 or PHH cells (Zona, Lupberger et al. 2013), suggesting that cell type may have an impact on signal transmission following receptor stimulation.

After showing that our cells responded to EGF stimulation, we examined their response to this stimulus during infection. The data presented here confirm that polarised HepG2 cells expressing AcGFP-CD81 are capable of supporting infection with HCV (Harris, Farquhar et al. 2008) and also that there is a boost in infection of these cells following EGF stimulation of a similar magnitude to that seen in Huh-7.5 cells. These results are novel and support a number of published studies in other hepatic cell lines which show an increase in infection following EGF stimulation (Lupberger, Zeisel et al. 2011, Diao, Pantua et al. 2012, Zona, Lupberger et al. 2013). As numerous studies speculate that there is a relationship between CD81 diffusion and HCV infection (Harris, Clerte et al. 2013, Potel, Rassam et al. 2013, Zona, Lupberger et al. 2013, Fletcher, Sutaria et al. 2014), we examined the effect of EGFR signalling on the diffusion of both CD81 and claudin-1.

Inhibition of the EGFR pathway with Erlotinib led to a decrease in the diffusion coefficients of both CD81 and claudin-1 alongside an increase the mobile fraction of both proteins. This increase in the mobile fraction of CD81 and claudin-1 following Erlotinib treatment is consistent with previous work in which the authors have hypothesised that signalling through EGFR leads to a recruitment of CD81 and claudin-1 to TEM domains (Zona, Lupberger et al. 2013). A possible mechanism for the observed lower diffusion is that, following EGF stimulation, the mobile CD81 and claudin-1 proteins form new interactions or diffuse as part of a larger complex. This suggestion is supported by the observation that the diffusion coefficient of protein or complex is dependent upon its molecular weight (Saffman and Delbruck 1975, Gambin, Lopez-Esparza et al. 2006), and CD81 has been demonstrated to diffuse at a slower speed when it is part of a larger complex with EWI-2wint (Potel, Rassam et al. 2013).

To assess whether EGFR signalling mediates its effect on infection and diffusion through the CD81-claudin-1 complex or on either protein independently, a panel of previously described CD81 proteins bearing mutations in the CD81-LEL which affect coreceptor complex formation were studied (Table 5.1) (Davis, Harris et al. 2012). The localisation of both CD81 and EGFR were examined in these cells using fluorescence microscopy.

The mutant CD81 proteins were not differentially localised in comparison to WT AcGFP-CD81, in agreement with previously published data (Davis, Harris et al. 2012), and EGFR was similarly localised in all of the cells expressing the mutant forms of CD81. However, there was no evidence of CD81-EGFR colocalisation. These data suggest that any differences in CD81 diffusion are unlikely to be related to abnormal localisation or an interaction with EGFR.

Examining the basal diffusion parameters of the mutant proteins demonstrated that, whilst they did not differ significantly from the WT AcGFP-CD81 protein in terms of their mobility, there was a subset of the mutant proteins which did display a significantly lower diffusion coefficient from the WT protein. Whilst the diffusion coefficients of K148A, T149A and K148A/T149A were similar to that observed for AcGFP-CD81, this value was much lower for E152A, T153A and E152A/T153A. These proteins also exhibited the lowest reported FRET with claudin-1, with E152A, T153A and E152A/T153A exhibiting values of 8%, 10% and 8% respectively (Davis, Harris et al. 2012). It is therefore likely that these specific mutant proteins form distinct interactions in the absence of claudin-1 from those formed by K148A, T149A and K148A/T149A. In the case of these proteins therefore, diffusion speed and receptor activity are related, and their low diffusion speed may contribute to the poor FRET with claudin-1 by reducing the number of interactions that form over a given time period.

As E152A, T153A and E152A/T153A all show a similar diffusion coefficient to WT CD81 when treated with Erlotinib, we were interested to examine whether their altered interactions with CD81 may reflect an altered response to EGF stimulation.

The effects of the CD81-claudin-1 complex on EGFR signalling, levels of phosphorylation and total EGFR were examined in cells expressing mutant forms of CD81. The level of Y1068 phosphorylation varied widely between polarised cells expressing these mutant CD81 proteins. Both E152A and T153A exhibited a high level of EGFR phosphorylation which was not significantly different to that observed in AcGFP-CD81. However these two mutants display very low levels of CD81-claudin-1 FRET – 10% and 8% respectively in comparison to 35% for AcGFP-CD81. In contrast, the mutations which exhibited higher levels of FRET with

claudin-1 (Davis, Harris et al. 2012) - K148A and K148A/T149A - displayed significantly reduced levels of EGFR phosphorylation. However, the level of EGFR phosphorylation was very similar in cells expressing E152A/T153A or K148A. These results show that, whilst EGFR phosphorylation is influenced by the interaction between CD81 and claudin-1, it is not a direct product of the interaction itself.

The effect of the coreceptor complex on pEGFR levels may be mediated by interactions formed by either CD81 or claudin-1 which impact on the recruitment or action of downstream EGFR signalling proteins. A possible candidate protein for this is ITGβ1. It has been demonstrated that ITGβ1, a protein which interacts with both CD81 and HRas, is involved in HCV entry (Zona, Lupberger et al. 2013), and it is known that ITGβ1 controls EGFR phosphorylation (Morello, Cabodi et al. 2011). That CD81 could be forming altered interactions with ITGβ1 following EGF stimulation is supported by preliminary data (not shown) demonstrating an altered interaction between CD81 and α-integrins following EGF stimulation. If this is the case, a possible candidate for the observed altered interaction is the α3 integrin, which ITGβ1 has been shown to bind.

The mutant CD81 proteins also influenced the level of total EGFR in EGF-stimulated cells. In untreated samples the level of EGFR was not significantly different between the majority of mutant proteins, however the level of total EGFR in the untreated E152A/T153A sample was considerably lower than that in AcGFP-CD81 or the other mutant cell lines. Following EGF stimulation AcGFP-CD81 and all of the mutants, with the exception of E152A and T153A, showed a reduction in total EGFR levels to around a third. In contrast, E152A and T153A

showed a reduction of a half and quarter respectively, showing that these proteins do indeed have an altered response to EGFR signalling.

As the mutant proteins are all capable of responding to EGF stimulation to some degree, we used these proteins to probe the dependence of the EGF response on the interaction between CD81 and claudin-1. As numerous studies have demonstrated that addition of EGF to polarised HepG2 cells stimulates HCV entry (Lupberger, Zeisel et al. 2011, Diao, Pantua et al. 2012), we studied EGF stimulation of the EGFR signalling pathway. The effect of the mutant CD81 proteins on viral infection of polarised HepG2 cells was investigated, but the levels of infection observed were too low to draw significant conclusions. This is consistent with many previous reports showing that HepG2 cells support low levels of infection (Lindenbach, Evans et al. 2005, Flint, von Hahn et al. 2006, Narbus, Israelow et al. 2011).

Stimulation of WT AcGFP-CD81 with EGF had no effect on the diffusion coefficient or mobile fraction of CD81. This is unexpected given the effect of Erlotinib, but is consistent with a published observation that adding EGF to Huh-7.5.1 had no effect on the interaction between CD81 and claudin-1 (Zona, Lupberger et al. 2013). However, as stimulation with EGF increases the level of HCV entry, it is clear that in this case the diffusion speed of proteins is not mediating the increase in HCV entry levels. Instead, stimulation with EGF may induce a rearrangement of membrane domains in a manner which promotes HCV entry in cells expressing WT AcGFP-CD81. The data presented here suggest that this rearrangement may involve proteins activated by and involved in downstream EGFR signalling.

In contrast to the WT protein, a number of the mutant CD81 proteins did demonstrate changes in diffusion following EGF stimulation. The diffusion coefficient of the K148A mutant

was decreased following EGF stimulation, whilst K148A/T149A displayed a decrease both in diffusion coefficient and mobile fraction. Conversely, T153A showed an increase in diffusion coefficient and mobile fraction. Therefore, these CD81 variants form EGF-dependent interactions in their mobile fractions which differ from those formed by WT AcGFP-CD81. Furthermore T153A and K148A/T153A are differentially localised following stimulation. If these changes are caused by HRas, as has been suggested in the Huh-7.5.1 cell line (Zona, Lupberger et al. 2013), then these data show that HRas is capable of binding CD81 when it is not interacting with claudin-1.

The CD81 residues K148, K148/T149 and T153 appear to be central to EGF-dependent diffusion, as mutation of these residues causes the protein to behave significantly differently to the WT protein. Interestingly, the pattern of diffusion of K148A/T149A and T153A following appear to be opposites of one another. Therefore, it is likely that CD81 forms distinct interactions through these residues as a result of EGF stimulation, and that these interactions have directly contrasting effects on diffusion despite the relatively close proximity of K148A/T149A and E152A in the CD81 molecule. Our model that the two protein variants form different interactions is supported by the variation in diffusion and the level of total and phosphorylated EGFR between the two.

The effect of the T153A mutation partially recapitulates the effect of Tipifarnib, whereas K148A/T149A mimics the effect of Erlotinib. Therefore, T153A may be responsible for forming the interaction with HRas. In contrast, the diffusion of K148A/T149A following EGF administration recapitulates the effect of Erlotinib on WT AcGFP-CD81, suggesting an interaction with another EGFR-related protein.

There are a number of possible interpretations of the diffusion and the EGFR signalling data:

- The CD81 mutant proteins which have the highest receptor activity and which FRET with claudin-1 respond in a similar manner to EGF stimulation (K148A and K148A/T149A) and exhibit a decrease in diffusion coefficient following EGF stimulation. This implies that some level of interaction between CD81 and claudin-1 may be necessary for the observed decrease in CD81 diffusion coefficient and mobile fraction in response to EGF signalling. These residues may be involved in recruitment of the coreceptor complex to a larger complex with other proteins following EGF stimulation. The dominant residue is K148, which causes a decrease in diffusion rates following EGF stimulation. However, the further mutation of residue 149 for T to A causes an additive effect, demonstrating that both residues are involved in this process.

- The mutant T153A exhibits a considerably different pattern of diffusion following EGF stimulation from the other proteins – an increase in both diffusion coefficient and mobile fraction following EGF stimulation. Cells expressing this protein show defective EGFR trafficking, and the unusual pattern of diffusion in response to EGF may reflect this, possibly as a result of a higher amount of EGFR being retained at the membrane. The mutation at T153A is similar to the pattern of diffusion observed following Tipifarnib treatment (Zona, Lupberger et al. 2013), suggesting that this residue may be involved in the association of CD81 with HRas and this may provide a mechanism for the poor receptor activity of this protein (Davis, Harris et al. 2012).

In conclusion, the data presented here highlight the complex relationship between the CD81-claudin-1 complex and EGFR signalling. We identified three residues or groups of residues which appear to play an important role in the diffusion response of CD81 to EGF stimulation and suggest that T153 may be key the residue involved in the interaction with HRas.

These data expand the simplistic observation that CD81 diffusion defines HCV entry (Harris, Clerte et al. 2013) as we show that, whilst the diffusion speeds of the mutant proteins in their basal state mirrors their receptor activity, the boost in infection normally seen following EGF stimulation is not correlated with WT AcGFP-CD81 diffusion speed and the mobile fraction. Instead, the boost observed in HCV entry may be due to a reorganisation of putative TEM domains to promote entry. Studying EGF signal transduction suggests that this reorganisation may involve proteins or complexes which affect EGFR phosphorylation and trafficking, as EGFR signalling appears to be affected by the interactions formed by CD81. A possible candidate for mediating these effects is the α3 integrin and ITGβ1.

6 GENERAL DISCUSSION AND CONCLUDING REMARKS

6.1 A COMPARATIVE ANALYSIS OF CD81 PRESENTATION BETWEEN CELL TYPES

CD81 is expressed ubiquitously on all cell types with the exception of platelets and neutrophils and is an essential receptor in HCV entry. Residues in the CD81-LEL interact with HCV-E2, and several studies have demonstrated that inhibiting this association both *in vivo* and *in vitro* reduces infection (Chapel, Christie et al. 2001, Bertaux and Dragic 2006, Pestka, Zeisel et al. 2007, Keck, Machida et al. 2008, Meuleman, Hesselgesser et al. 2008, Farquhar, Hu et al. 2012). Antibody disruption of the CD81-HCV-E2 interaction therefore provides a promising target for therapeutic intervention. However, antibody ligation of CD81 can induce a variety of biological effects including activation of T, B and NK cells alongside stimulation of various signalling pathways.

Tetraspanin conformation has been shown to be altered by partner proteins in a manner which can be detected with antibody probes (Rubinstein, Le Naour et al. 1996, Serru, Le Naour et al. 1999, Sincock, Fitter et al. 1999). CD81 forms cell-type specific interactions on hepatocytes and T and B cells (Rubinstein, Le Naour et al. 1996, Todd, Lipps et al. 1996, Rocha-Perugini, Montpellier et al. 2008, Fournier, Peyrou et al. 2010, Montpellier, Tews et al. 2011) and using a panel of anti-CD81 mAbs I sought to identify hepatocyte-specific epitopes in the CD81-LEL that could be of therapeutic value.

Due to the lack of proper optimisation of antibody staining in the experiments presented here, initial steps for continuation of this work would require this to be carried out. Optimisation would require the titration of antibodies on all cell types used to determine the

optimal staining concentration, followed by a consideration of appropriate staining conditions and fixation. If, as a result, the repetition of these experiments identify differences in antibody binding, it would be interesting to carry out a number of further experiments.

It would be ideal to confirm initial flow cytometry binding data to binding affinity data captured by surface plasmon resonance (SPR). Instead of looking at antibody binding at a single point in time as with flow cytometry, SPR data allows the researcher to understand the association and dissociation rates and affinity of an antibody for the antigen. This would provide information as to the number and strength of interactions formed between the antibody and antigen, and experiments could be extended to look at epitope mapping.

Ideally, SPR would be carried out *in situ* on the cell surface. In a recent paper, van Spriel et al., reported using an ultrasound pulse to generate flat 'membrane sheets' in which the spatial localisation of membrane proteins is not affected and the cytoskeleton is at least partially intact (Zuidscherwoude, Gottfert et al. 2015). By using these sheets, it may be theoretically possible to look at the binding of these antibodies to CD81 in a more relevant background than following detergent extraction. However, this would involve a number of practical issues involving the size the membrane, adhesion to the chip, and the level of signal generated from a mixed population of proteins.

It would also be informative to confirm the dependence of the binding of antibodies of interest on the conformation of the protein by examining their binding by western blot under reducing and non-reducing conditions. If these results were to show a dependence on conformation, I could then look at this in more detail by looking at the effect of mutating the

essential CD81 cysteine residues to determine their impact on the presentation of these epitopes.

Using immunoprecipitation it would be possible to use these antibodies to carry out pull-downs to examine any differences in binding partners such as integrins and other tetraspanin-associated proteins between different cell types or between antibodies with different binding patterns. In a similar manner, further wok for this project could include examining the propensity of these antibodies to stimulate common or published signalling pathways as this may help in establishing interacting partners and therapeutic use.

6.2 EFFECT OF HEPATIC POLARITY ON CD81 DIFFUSION

In recent years our understanding of protein dynamics has increased, and the relationship between receptor diffusion and viral entry has become a topic of research interest. In terms of CD81, studies have demonstrated that situations in which CD81 diffusion is limited coincides with a restriction of HCV entry (Harris, Clerte et al. 2013, Potel, Rassam et al. 2013, Fletcher, Sutaria et al. 2014).

I used the HepG2 cell line to examine the importance of polarity and cell membrane organisation on CD81 diffusion properties. In addition to providing further support to the observation that CD81 diffusion speed is reduced upon polarisation, I found that TNF-α depolarised cells and reversed the effects on diffusion coefficient and infection that are caused by polarisation. The mobile fraction of CD81 also increased following TNF-α treatment, providing an additional mechanism for the increased level of infection observed

in inflammatory environments (Fletcher, Sutaria et al. 2014). This observation may be pertinent to our understanding of how re-infection occurs during allograft transplant.

Both the data I present and previous publications (Harris, Clerte et al. 2013) highlight the importance of studying physiologically relevant models when assessing receptor diffusion and related effects. I extended previous work by showing that cell membrane structures dictate protein diffusion parameters in a manner which is likely to be actin-dependent. Studying relevant membrane features has led to breakthroughs in our understanding of MLV infection mechanisms (Sherer, Lehmann et al. 2007), and given data presented here I would encourage that this is considered in the design of future studies looking at the diffusion of either viruses or proteins.

I also provide evidence to demonstrate that the diffusion of the CD81 coreceptor protein, claudin-1, may play a role in defining HCV entry, as the diffusion parameters of this protein are also mediated by polarisation. Notably, there is a large variation seen across the diffusion parameters of both CD81 and claudin-1. This variation suggests that both proteins may be forming multiple interactions, and provides an explanation for the lack of an obvious pattern in binding of the CD81 antibodies tested in chapter 3.

Therefore, I present a model in which the diffusion parameters and receptor activity of CD81 is regulated by the polarised status of the cell, cellular structures, and the local environment including the proteins with which it forms interactions. I speculate that this is related to the actin linkage of the protein.

There are a number of possible future directions for this work. In order to confirm the mechanism of CD81 and claudin-1 restriction, it would be necessary to establish the

localisation of both proteins to TEM or lipid domains, and this could be established by detergent extraction or colocalisation of the proteins with known members of TEMs such as other tetraspanins and integrins, or using high resolution imaging of these regions. It would also be interesting to look at the ERM association of these proteins, as this has previously been shown to affect CD81 diffusion (Harris, Clerte et al. 2013).

In order to further investigate the effect of cellular structures on CD81 diffusion, it would be useful to examine the actin dynamics in these regions along with cholesterol or lipid staining in these areas. This is an area in which SPT would be very useful, as it may be possible to see direction flow of receptors on filopodia as has been observed with MLV virions (Sherer, Lehmann et al. 2007).

6.3 THE EFFECT OF CORECEPTOR COMPLEX FORMATION ON THE RESPONSE TO EGF-INDUCED EGFR STIMULATION

Recent work has demonstrated that EGF increases the level of HCV infection and that this is related to an increase in the formation of CD81-claudin-1 coreceptor complexes (Lupberger, Zeisel et al. 2011, Diao, Pantua et al. 2012, Zona, Lupberger et al. 2013). Although supported by FRAP data in a non-polarised cell type, I examined this effect further to address CD81 diffusion and its dependence on coreceptor complexes. To do this, I used a panel of previously characterised CD81 mutants where claudin-1 interactions were disrupted.

I present novel data showing that the interaction between CD81 and claudin-1 influences the level and transmission of EGFR signalling, although this is not directly related to the interaction between the two proteins. Additionally, in contrast to previous instances where an increase in infection occurs concomitantly with an increase in CD81 diffusion speed, there

is no effect on CD81 diffusion following EGFR stimulation despite the increase in infection observed. As CD81 is increasingly confined in polarised cells (Harris, Farquhar et al. 2008, Harris, Clerte et al. 2013), I suggest a model in which stimulation of the EGFR signalling pathway induces a reorganisation of TEM or domains of restricted diffusion in a manner which promotes virus entry rather than a recruitment of new proteins to these regions. Preliminary data looking at the associations formed by CD81 following EGF stimulation suggests that this rearrangement may involve the integrin ITGB1 and specifically the α3 integrin. ITGB1 has previously been shown to affect EGFR signal transduction, strengthening this hypothesis (Morello, Cabodi et al. 2011) and providing a possible mechanism for the effect observed on EGFR signalling. I further hypothesise that three residues or groups of residues in the CD81-claudin-1 interacting region are key to this reorganisation and to dictating CD81 diffusion following EGF stimulation – K148, K148/T149 and T153. However, their involvement in this process is complex and requires more investigation.

Further work is needed to substantiate these models. In order to ascertain whether ITGB1 regulates the interaction between CD81 and claudin-1 and stimulation of the EGFR pathway, it would be necessary to repeat immunoprecipitation experiments with a probe specific to ITGB1. It would also be interesting to examine the recruitment of c-Cbl and the phosphorylation status of other members of the EGFR signalling pathway in stimulated cells. It would be necessary to do this with and without mutant CD81 proteins to examine where and if the pathway is affected by the formation of the CD81-claudin-1 complex.

In this thesis I have studied the presentation and behaviour of CD81 on hepatocytes. I have shown that functionally important epitopes in the LEL of CD81 differ between hepatocytes

and T and B cells, and postulate that this may contribute to the hepatic specificity of the virus. Additionally, I have shown significant changes in the conformation and level of expression of CD81 between primary cells and immortalised cell lines, demonstrating a possible side-effect of transformation. This may have significant impacts on the use of such cells for testing administration of antibodies for blocking virus-receptor interactions.

Using live imaging studies I have shown that receptor diffusion is dependent not only on the state of polarity of the cell, but also on the presence of specific membrane structures and inflammatory mediators. With live imaging studies using both SPT and FRAP becoming a rapidly growing area of research, these data demonstrate a number of crucial factors which must be taken into account when designing and interpreting such data.

Additionally, I have demonstrated that claudin-1 diffusion is affected in situations in which HCV entry is enhanced, suggesting that the diffusion of claudin-1 may be influencing the entry of HCV to same extent as CD81. Indeed, the diffusion speed of claudin-1 but not CD81 is increased following EGF stimulation. However, I demonstrate that CD81 diffusion rates do not always define entry.

Finally, I demonstrate a complex relationship between stimulation of the EGFR signalling pathway and the formation of the coreceptor complex, and hypothesise that the presence of the receptor complex may be necessary for the formation of larger, EGF-induced complexes which promote the rate of HCV entry in a manner distinct from the rate of receptor diffusion. I suggest that the K148, K148/T149 and T153 residues in the CD81-LEL play a central role in this reorganisation.

7 APPENDICES

Clone ID	Reactivity with[1]	
	CD81$_{FL}$	CD81$_{LEL}$
1s73	0.25	0.76
1s135	1.90	1.79
1s201	2.67	2.15
1s262	0.33	0.89
1s337	1.72	1.89
2s20	1.33	1.77
2s24	1.90	0.45
2s48	2.33	2.10
2s63	1.53	2.01
2s66	1.76	1.72
2s131	2.01	1.94
2s139	1.57	1.99
2s141	2.13	2.02
2s155	2.70	2.06

Appendix table 1: Assessing antibody interaction with CD81 by EIA. *mAb (1 µg/mL) EIA reactivity for CD81-FL and CD81-LEL where the data is expressed at optical density at 450nm.*

Group	mAb	Dimeric							Monomeric				
		WT	T149A	L162P	T167I	I182F	N184Y	F186S	V123A	K124T	V146E	F150S	C157S[1]
		-	B helix	3-10 helix	C helix	D helix	D helix	D helix	A helix	A helix	B helix	B Helix	BC loop
I	2s20												↓↓↓
	2s24												↓↓↓
	2s48									↓			↓↓↓
	2s63												↓↓↓
	2s66												↓↓↓
	2s131												↓↓↓
	2s139									↓			↓↓↓
II	1s201			↓↓↓									↓↓↓
	JS81[3]			↓↓↓									↓↓↓
III	1s337			↓↓↓	↓↓↓							↓	↓↓↓
IV	1s262		↓↓	↓↓↓	↓↓↓				↓↓		↓↓	↓↓↓	↓↓↓
V	1s135			↓↓↓					↓			↓↓↓	↓↓↓
	2s141			↓					↓			↓↓	↓↓↓
	2s155			↓					↓			↓↓	↓↓↓
VI	1s73		↓↓		↓				↓↓		↓↓	↓↓↓	↓↓↓

Appendix table 2: mAb (5 μg/mL) reactivity with wild type (WT) and mutant MBP-CD81-LEL proteins *where: ↓ denotes a 25 – 75% reduction in binding; ↓↓ - a 75 – 90% reduction and ↓↓↓ >90% reduction in binding. Farquhar et al., in preaparation.*

[1] mAb (5 μg/mL) reactivity for overlapping LEL peptides, reactivity was only observed with peptide 1144 representing amino acids 173-192

[3] JS81 was obtained from BD Biosciences

REFERENCES

Akazawa, D., T. Date, K. Morikawa, A. Murayama, M. Miyamoto, M. Kaga, H. Barth, T. F. Baumert, J. Dubuisson and T. Wakita (2007). "CD81 expression is important for the permissiveness of Huh7 cell clones for heterogeneous hepatitis C virus infection." J Virol **81**(10): 5036-5045.

Allander, T., X. Forns, S. U. Emerson, R. H. Purcell and J. Bukh (2000). "Hepatitis C virus envelope protein E2 binds to CD81 of tamarins." Virology **277**(2): 358-367.

Alter, H. J., P. V. Holland, A. G. Morrow, R. H. Purcell, S. M. Feinstone and Y. Moritsugu (1975). "Clinical and serological analysis of transfusion-associated hepatitis." Lancet **2**(7940): 838-841.

Alter, H. J., P. V. Holland and R. H. Purcell (1975). "The emerging pattern of post-transfusion hepatitis." Am J Med Sci **270**(2): 329-334.

Alter, H. J., P. V. Holland, R. H. Purcell, J. J. Lander, S. M. Feinstone, A. G. Morrow and P. J. Schmidt (1972). "Posttransfusion hepatitis after exclusion of commercial and hepatitis-B antigen-positive donors." Ann Intern Med **77**(5): 691-699.

Alter, M. J. (1997). "Epidemiology of hepatitis C." Hepatology **26**(3 Suppl 1): 62S-65S.

Alwan, H. A., E. J. van Zoelen and J. E. van Leeuwen (2003). "Ligand-induced lysosomal epidermal growth factor receptor (EGFR) degradation is preceded by proteasome-dependent EGFR de-ubiquitination." J Biol Chem **278**(37): 35781-35790.

Andre, P., F. Komurian-Pradel, S. Deforges, M. Perret, J. L. Berland, M. Sodoyer, S. Pol, C. Brechot, G. Paranhos-Baccala and V. Lotteau (2002). "Characterization of low- and very-low-density hepatitis C virus RNA-containing particles." J Virol **76**(14): 6919-6928.

Ashfaq, U. A., T. Javed, S. Rehman, Z. Nawaz and S. Riazuddin (2011). "An overview of HCV molecular biology, replication and immune responses." Virol J **8**: 161.

Asselah, T., E. Estrabaud, I. Bieche, M. Lapalus, S. De Muynck, M. Vidaud, D. Saadoun, V. Soumelis and P. Marcellin (2010). "Hepatitis C: viral and host factors associated with non-response to pegylated interferon plus ribavirin." Liver Int **30**(9): 1259-1269.

ATCC "HB-8065, Hep G2." American Type Culture Collection.

Bacallao, R., C. Antony, C. Dotti, E. Karsenti, E. H. Stelzer and K. Simons (1989). "The subcellular organization of Madin-Darby canine kidney cells during the formation of a polarized epithelium." J Cell Biol **109**(6 Pt 1): 2817-2832.

Balogun, M. A., M. E. Ramsay, L. M. Hesketh, N. Andrews, K. P. Osborne, N. J. Gay and P. Morgan-Capner (2002). "The prevalence of hepatitis C in England and Wales." J Infect **45**(4): 219-226.

Bankwitz, D., E. Steinmann, J. Bitzegeio, S. Ciesek, M. Friesland, E. Herrmann, M. B. Zeisel, T. F. Baumert, Z. Y. Keck, S. K. Foung, E. I. Pecheur and T. Pietschmann (2010). "Hepatitis C virus hypervariable region 1 modulates receptor interactions, conceals the CD81 binding site, and protects conserved neutralizing epitopes." J Virol **84**(11): 5751-5763.

Barreiro, O., M. Zamai, M. Yanez-Mo, E. Tejera, P. Lopez-Romero, P. N. Monk, E. Gratton, V. R. Caiolfa and F. Sanchez-Madrid (2008). "Endothelial adhesion receptors are recruited to adherent leukocytes by inclusion in preformed tetraspanin nanoplatforms." J Cell Biol **183**(3): 527-542.

Bartenschlager, R. and V. Lohmann (2001). "Novel cell culture systems for the hepatitis C virus." Antiviral Res **52**(1): 1-17.

Barth, H., E. K. Schnober, F. Zhang, R. J. Linhardt, E. Depla, B. Boson, F. L. Cosset, A. H. Patel, H. E. Blum and T. F. Baumert (2006). "Viral and cellular determinants of the hepatitis C virus envelope-heparan sulfate interaction." J Virol **80**(21): 10579-10590.

Bartosch, B., J. Dubuisson and F. L. Cosset (2003). "Infectious hepatitis C virus pseudo-particles containing functional E1-E2 envelope protein complexes." J Exp Med **197**(5): 633-642.

Bartosch, B., G. Verney, M. Dreux, P. Donot, Y. Morice, F. Penin, J. M. Pawlotsky, D. Lavillette and F. L. Cosset (2005). "An interplay between hypervariable region 1 of the hepatitis C virus E2 glycoprotein,

the scavenger receptor BI, and high-density lipoprotein promotes both enhancement of infection and protection against neutralizing antibodies." J Virol **79**(13): 8217-8229.

Bartosch, B., A. Vitelli, C. Granier, C. Goujon, J. Dubuisson, S. Pascale, E. Scarselli, R. Cortese, A. Nicosia and F. L. Cosset (2003). "Cell entry of hepatitis C virus requires a set of co-receptors that include the CD81 tetraspanin and the SR-B1 scavenger receptor." J Biol Chem **278**(43): 41624-41630.

Bassendine, M. F., D. A. Sheridan, D. J. Felmlee, S. H. Bridge, G. L. Toms and R. D. Neely (2011). "HCV and the hepatic lipid pathway as a potential treatment target." J Hepatol **55**(6): 1428-1440.

Batzer, A. G., D. Rotin, J. M. Urena, E. Y. Skolnik and J. Schlessinger (1994). "Hierarchy of binding sites for Grb2 and Shc on the epidermal growth factor receptor." Mol Cell Biol **14**(8): 5192-5201.

Baumann, O. and B. Walz (2001). "Endoplasmic reticulum of animal cells and its organization into structural and functional domains." Int Rev Cytol **205**: 149-214.

Bayer, M. E., B. S. Blumberg and B. Werner (1968). "Particles associated with Australia antigen in the sera of patients with leukaemia, Down's Syndrome and hepatitis." Nature **218**(5146): 1057-1059.

Behrens, S. E., L. Tomei and R. De Francesco (1996). "Identification and properties of the RNA-dependent RNA polymerase of hepatitis C virus." EMBO J **15**(1): 12-22.

Berbari, N. F., A. K. O'Connor, C. J. Haycraft and B. K. Yoder (2009). "The primary cilium as a complex signaling center." Curr Biol **19**(13): R526-535.

Berditchevski, F., E. Odintsova, S. Sawada and E. Gilbert (2002). "Expression of the palmitoylation-deficient CD151 weakens the association of alpha 3 beta 1 integrin with the tetraspanin-enriched microdomains and affects integrin-dependent signaling." J Biol Chem **277**(40): 36991-37000.

Bergelson, J. M., J. F. Modlin, W. Wieland-Alter, J. A. Cunningham, R. L. Crowell and R. W. Finberg (1997). "Clinical coxsackievirus B isolates differ from laboratory strains in their interaction with two cell surface receptors." J Infect Dis **175**(3): 697-700.

Berkova, Z., S. E. Crawford, S. E. Blutt, A. P. Morris and M. K. Estes (2007). "Expression of rotavirus NSP4 alters the actin network organization through the actin remodeling protein cofilin." J Virol **81**(7): 3545-3553.

Berman, K. and P. Y. Kwo (2009). "Boceprevir, an NS3 protease inhibitor of HCV." Clin Liver Dis **13**(3): 429-439.

Berryman, M., Z. Franck and A. Bretscher (1993). "Ezrin is concentrated in the apical microvilli of a wide variety of epithelial cells whereas moesin is found primarily in endothelial cells." Journal of Cell Science **105 (Pt 4)**: 1025-1043.

Bertaux, C. and T. Dragic (2006). "Different domains of CD81 mediate distinct stages of hepatitis C virus pseudoparticle entry." J Virol **80**(10): 4940-4948.

Berthiaume, F., P. V. Moghe, M. Toner and M. L. Yarmush (1996). "Effect of extracellular matrix topology on cell structure, function, and physiological responsiveness: hepatocytes cultured in a sandwich configuration." FASEB J **10**(13): 1471-1484.

Bhatnagar, S., K. Shinagawa, F. J. Castellino and J. S. Schorey (2007). "Exosomes released from macrophages infected with intracellular pathogens stimulate a proinflammatory response in vitro and in vivo." Blood **110**(9): 3234-3244.

Blanchard, E., S. Belouzard, L. Goueslain, T. Wakita, J. Dubuisson, C. Wychowski and Y. Rouille (2006). "Hepatitis C virus entry depends on clathrin-mediated endocytosis." J Virol **80**(14): 6964-6972.

Blumberg, B. S., H. J. Alter and S. Visnich (1965). "A "New" Antigen in Leukemia Sera." JAMA **191**: 541-546.

Boon, C. J., A. I. den Hollander, C. B. Hoyng, F. P. Cremers, B. J. Klevering and J. E. Keunen (2008). "The spectrum of retinal dystrophies caused by mutations in the peripherin/RDS gene." Prog Retin Eye Res **27**(2): 213-235.

Boucheix, C. and E. Rubinstein (2001). "Tetraspanins." Cell Mol Life Sci **58**(9): 1189-1205.

Boulant, S., R. Montserret, R. G. Hope, M. Ratinier, P. Targett-Adams, J. P. Lavergne, F. Penin and J. McLauchlan (2006). "Structural determinants that target the hepatitis C virus core protein to lipid droplets." J Biol Chem **281**(31): 22236-22247.

Bowen, D. G. and C. M. Walker (2005). "Adaptive immune responses in acute and chronic hepatitis C virus infection." Nature **436**(7053): 946-952.

Brachet, A., C. Leterrier, M. Irondelle, M. P. Fache, V. Racine, J. B. Sibarita, D. Choquet and B. Dargent (2010). "Ankyrin G restricts ion channel diffusion at the axonal initial segment before the establishment of the diffusion barrier." Journal of Cell Biology **191**(2): 383-395.

Branch, A. D., D. D. Stump, J. A. Gutierrez, F. Eng and J. L. Walewski (2005). "The hepatitis C virus alternate reading frame (ARF) and its family of novel products: the alternate reading frame protein/F-protein, the double-frameshift protein, and others." Semin Liver Dis **25**(1): 105-117.

Brazzoli, M., A. Bianchi, S. Filippini, A. Weiner, Q. Zhu, M. Pizza and S. Crotta (2008). "CD81 is a central regulator of cellular events required for hepatitis C virus infection of human hepatocytes." Journal of Virology **82**(17): 8316-8329.

Brimacombe, C. L., J. Grove, L. W. Meredith, K. Hu, A. J. Syder, M. V. Flores, J. M. Timpe, S. E. Krieger, T. F. Baumert, T. L. Tellinghuisen, F. Wong-Staal, P. Balfe and J. A. McKeating (2011). "Neutralizing antibody-resistant hepatitis C virus cell-to-cell transmission." J Virol **85**(1): 596-605.

Brimacombe, C. L., G. K. Wilson, S. G. Hubscher, J. A. McKeating and M. J. Farquhar (2014). "A role for CD81 and hepatitis C virus in hepatoma mobility." Viruses **6**(3): 1454-1472.

Bukh, J. (2004). "A critical role for the chimpanzee model in the study of hepatitis C." Hepatology **39**(6): 1469-1475.

Bukh, J. (2012). "Animal models for the study of hepatitis C virus infection and related liver disease." Gastroenterology **142**(6): 1279-1287 e1273.

Bukh, J., P. Meuleman, R. Tellier, R. E. Engle, S. M. Feinstone, G. Eder, W. C. Satterfield, S. Govindarajan, K. Krawczynski, R. H. Miller, G. Leroux-Roels and R. H. Purcell (2010). "Challenge pools of hepatitis C virus genotypes 1-6 prototype strains: replication fitness and pathogenicity in chimpanzees and human liver-chimeric mouse models." J Infect Dis **201**(9): 1381-1389.

Bukong, T. N., F. Momen-Heravi, K. Kodys, S. Bala and G. Szabo (2014). "Exosomes from hepatitis C infected patients transmit HCV infection and contain replication competent viral RNA in complex with Ago2-miR122-HSP90." PLoS Pathog **10**(10): e1004424.

Burckhardt, C. J. and U. F. Greber (2009). "Virus movements on the plasma membrane support infection and transmission between cells." PLoS Pathog **5**(11): e1000621.

Burckhardt, C. J., M. Suomalainen, P. Schoenenberger, K. Boucke, S. Hemmi and U. F. Greber (2011). "Drifting motions of the adenovirus receptor CAR and immobile integrins initiate virus uncoating and membrane lytic protein exposure." Cell Host Microbe **10**(2): 105-117.

Busch, M. P. (2001). "Insights into the epidemiology, natural history and pathogenesis of hepatitis C virus infection from studies of infected donors and blood product recipients." Transfus Clin Biol **8**(3): 200-206.

Callens, N., Y. Ciczora, B. Bartosch, N. Vu-Dac, F. L. Cosset, J. M. Pawlotsky, F. Penin and J. Dubuisson (2005). "Basic residues in hypervariable region 1 of hepatitis C virus envelope glycoprotein e2 contribute to virus entry." J Virol **79**(24): 15331-15341.

Carloni, V., A. Mazzocca and K. S. Ravichandran (2004). "Tetraspanin CD81 is linked to ERK/MAPKinase signaling by Shc in liver tumor cells." Oncogene **23**(8): 1566-1574.

Catanese, M. T., K. Uryu, M. Kopp, T. J. Edwards, L. Andrus, W. J. Rice, M. Silvestry, R. J. Kuhn and C. M. Rice (2013). "Ultrastructural analysis of hepatitis C virus particles." Proc Natl Acad Sci U S A **110**(23): 9505-9510.

Cereijido, M., J. Valdes, L. Shoshani and R. G. Contreras (1998). "Role of tight junctions in establishing and maintaining cell polarity." Annu Rev Physiol **60**: 161-177.

Chan, G., M. T. Nogalski and A. D. Yurochko (2009). "Activation of EGFR on monocytes is required for human cytomegalovirus entry and mediates cellular motility." Proc Natl Acad Sci U S A **106**(52): 22369-22374.

Chang, K. S., J. Jiang, Z. Cai and G. Luo (2007). "Human apolipoprotein e is required for infectivity and production of hepatitis C virus in cell culture." J Virol **81**(24): 13783-13793.

Chang, M., O. Williams, J. Mittler, A. Quintanilla, R. L. Carithers, Jr., J. Perkins, L. Corey and D. R. Gretch (2003). "Dynamics of hepatitis C virus replication in human liver." Am J Pathol **163**(2): 433-444.

Chapel, H. M., J. M. Christie, V. Peach and R. W. Chapman (2001). "Five-year follow-up of patients with primary antibody deficiencies following an outbreak of acute hepatitis C." Clin Immunol **99**(3): 320-324.

Charrin, S., F. le Naour, O. Silvie, P. E. Milhiet, C. Boucheix and E. Rubinstein (2009). "Lateral organization of membrane proteins: tetraspanins spin their web." Biochem J **420**(2): 133-154.

Charrin, S., S. Manie, M. Billard, L. Ashman, D. Gerlier, C. Boucheix and E. Rubinstein (2003). "Multiple levels of interactions within the tetraspanin web." Biochem Biophys Res Commun **304**(1): 107-112.

Charrin, S., S. Manie, M. Oualid, M. Billard, C. Boucheix and E. Rubinstein (2002). "Differential stability of tetraspanin/tetraspanin interactions: role of palmitoylation." FEBS Lett **516**(1-3): 139-144.

Charrin, S., S. Manie, C. Thiele, M. Billard, D. Gerlier, C. Boucheix and E. Rubinstein (2003). "A physical and functional link between cholesterol and tetraspanins." Eur J Immunol **33**(9): 2479-2489.

Charrin, S., S. Yalaoui, B. Bartosch, L. Cocquerel, J. F. Franetich, C. Boucheix, D. Mazier, E. Rubinstein and O. Silvie (2009). "The Ig domain protein CD9P-1 down-regulates CD81 ability to support Plasmodium yoelii infection." J Biol Chem **284**(46): 31572-31578.

Chen, S. L. and T. R. Morgan (2006). "The natural history of hepatitis C virus (HCV) infection." Int J Med Sci **3**(2): 47-52.

Chierico, L., A. S. Joseph, A. L. Lewis and G. Battaglia (2014). "Live cell imaging of membrane / cytoskeleton interactions and membrane topology." Sci Rep **4**: 6056.

Choo, H. Y., H. K. Kaya and J. B. Kim (1989). "Agamermis unka (Mermithidae) Parasitism of Nilaparvata lugens in Rice Fields in Korea." J Nematol **21**(2): 254-259.

Choo, Q. L., G. Kuo, A. J. Weiner, L. R. Overby, D. W. Bradley and M. Houghton (1989). "Isolation of a cDNA clone derived from a blood-borne non-A, non-B viral hepatitis genome." Science **244**(4902): 359-362.

Choo, Q. L., A. J. Weiner, L. R. Overby, G. Kuo, M. Houghton and D. W. Bradley (1990). "Hepatitis C virus: the major causative agent of viral non-A, non-B hepatitis." Br Med Bull **46**(2): 423-441.

Cocquerel, L., C. C. Kuo, J. Dubuisson and S. Levy (2003). "CD81-dependent binding of hepatitis C virus E1E2 heterodimers." J Virol **77**(19): 10677-10683.

Cocquerel, L., C. Wychowski, F. Minner, F. Penin and J. Dubuisson (2000). "Charged residues in the transmembrane domains of hepatitis C virus glycoproteins play a major role in the processing, subcellular localization, and assembly of these envelope proteins." J Virol **74**(8): 3623-3633.

Coffey, G. P., R. Rajapaksa, R. Liu, O. Sharpe, C. C. Kuo, S. W. Krauss, Y. Sagi, R. E. Davis, L. M. Staudt, J. P. Sharman, W. H. Robinson and S. Levy (2009). "Engagement of CD81 induces ezrin tyrosine phosphorylation and its cellular redistribution with filamentous actin." Journal of Cell Science **122**(Pt 17): 3137-3144.

Cohen, D., P. J. Brennwald, E. Rodriguez-Boulan and A. Musch (2004). "Mammalian PAR-1 determines epithelial lumen polarity by organizing the microtubule cytoskeleton." J Cell Biol **164**(5): 717-727.

Coller, K. E., K. L. Berger, N. S. Heaton, J. D. Cooper, R. Yoon and G. Randall (2009). "RNA interference and single particle tracking analysis of hepatitis C virus endocytosis." PLoS Pathog **5**(12): e1000702.

Cormier, E. G., F. Tsamis, F. Kajumo, R. J. Durso, J. P. Gardner and T. Dragic (2004). "CD81 is an entry coreceptor for hepatitis C virus." Proc Natl Acad Sci U S A **101**(19): 7270-7274.

Coyne, C. B. and J. M. Bergelson (2006). "Virus-induced Abl and Fyn kinase signals permit coxsackievirus entry through epithelial tight junctions." Cell **124**(1): 119-131.

Crotta, S., V. Ronconi, C. Ulivieri, C. T. Baldari, N. M. Valiante, S. Abrignani and A. Wack (2006). "Cytoskeleton rearrangement induced by tetraspanin engagement modulates the activation of T and NK cells." Eur J Immunol **36**(4): 919-929.

Crotta, S., A. Stilla, A. Wack, A. D'Andrea, S. Nuti, U. D'Oro, M. Mosca, F. Fillipon, R. M. Brunetto, F. Bonino, S. Abrignani and N. M. Valiante (2002). "Inhibition of natural killer cells through engagement of CD81 by the major hepatitis C virus envelope protein." J Exp Med **195**(1): 35-41.

Cruz-Rivera, M., J. C. Carpio-Pedroza, A. Escobar-Gutierrez, D. Lozano, A. Vergara-Castaneda, P. Rivera-Osorio, A. Martinez-Guarneros, C. A. Chacon, S. Fonseca-Coronado and G. Vaughan (2013). "Rapid hepatitis C virus divergence among chronically infected individuals." J Clin Microbiol **51**(2): 629-632.

Cukierman, L., L. Meertens, C. Bertaux, F. Kajumo and T. Dragic (2009). "Residues in a highly conserved claudin-1 motif are required for hepatitis C virus entry and mediate the formation of cell-cell contacts." J Virol **83**(11): 5477-5484.

Cunningham, K. E. and J. R. Turner (2012). "Myosin light chain kinase: pulling the strings of epithelial tight junction function." Ann N Y Acad Sci **1258**: 34-42.

Dane, D. S., C. H. Cameron and M. Briggs (1970). "Virus-like particles in serum of patients with Australia-antigen-associated hepatitis." Lancet **1**(7649): 695-698.

Danglot, L., M. Chaineau, M. Dahan, M. C. Gendron, N. Boggetto, F. Perez and T. Galli (2010). "Role of TI-VAMP and CD82 in EGFR cell-surface dynamics and signaling." Journal of Cell Science **123**(Pt 5): 723-735.

Davis, C., H. J. Harris, K. Hu, H. E. Drummer, J. A. McKeating, J. G. Mullins and P. Balfe (2012). "In silico directed mutagenesis identifies the CD81/claudin-1 hepatitis C virus receptor interface." Cell Microbiol **14**(12): 1892-1903.

Davis, D. M. and S. Sowinski (2008). "Membrane nanotubes: dynamic long-distance connections between animal cells." Nat Rev Mol Cell Biol **9**(6): 431-436.

Davis, G. L., J. B. Wong, J. G. McHutchison, M. P. Manns, J. Harvey and J. Albrecht (2003). "Early virologic response to treatment with peginterferon alfa-2b plus ribavirin in patients with chronic hepatitis C." Hepatology **38**(3): 645-652.

de Oliveria Andrade, L. J., A. D'Oliveira, R. C. Melo, E. C. De Souza, C. A. Costa Silva and R. Parana (2009). "Association between hepatitis C and hepatocellular carcinoma." J Glob Infect Dis **1**(1): 33-37.

Decaens, C., M. Durand, B. Grosse and D. Cassio (2008). "Which in vitro models could be best used to study hepatocyte polarity?" Biol Cell **100**(7): 387-398.

Delandre, C., T. R. Penabaz, A. L. Passarelli, S. K. Chapes and R. J. Clem (2009). "Mutation of juxtamembrane cysteines in the tetraspanin CD81 affects palmitoylation and alters interaction with other proteins at the cell surface." Exp Cell Res **315**(11): 1953-1963.

Delorme-Axford, E. and C. B. Coyne (2011). "The actin cytoskeleton as a barrier to virus infection of polarized epithelial cells." Viruses **3**(12): 2462-2477.

Deneka, M., A. Pelchen-Matthews, R. Byland, E. Ruiz-Mateos and M. Marsh (2007). "In macrophages, HIV-1 assembles into an intracellular plasma membrane domain containing the tetraspanins CD81, CD9, and CD53." J Cell Biol **177**(2): 329-341.

Di Bisceglie, A. M. and J. H. Hoofnagle (2002). "Optimal therapy of hepatitis C." Hepatology **36**(5 Suppl 1): S121-127.

Diao, J., H. Pantua, H. Ngu, L. Komuves, L. Diehl, G. Schaefer and S. B. Kapadia (2012). "Hepatitis C virus induces epidermal growth factor receptor activation via CD81 binding for viral internalization and entry." J Virol **86**(20): 10935-10949.

Dorner, M., J. A. Horwitz, J. B. Robbins, W. T. Barry, Q. Feng, K. Mu, C. T. Jones, J. W. Schoggins, M. T. Catanese, D. R. Burton, M. Law, C. M. Rice and A. Ploss (2011). "A genetically humanized mouse model for hepatitis C virus infection." Nature **474**(7350): 208-211.

Douam, F., V. L. Dao Thi, G. Maurin, J. Fresquet, D. Mompelat, M. B. Zeisel, T. F. Baumert, F. L. Cosset and D. Lavillette (2014). "Critical interaction between E1 and E2 glycoproteins determines binding and fusion properties of hepatitis C virus during cell entry." Hepatology **59**(3): 776-788.

Douglass, A. D. and R. D. Vale (2005). "Single-molecule microscopy reveals plasma membrane microdomains created by protein-protein networks that exclude or trap signaling molecules in T cells." Cell **121**(6): 937-950.

Dreux, M. and F. L. Cosset (2009). "Detection of neutralizing antibodies with HCV pseudoparticles (HCVpp)." Methods Mol Biol **510**: 427-438.

Dreux, M., U. Garaigorta, B. Boyd, E. Decembre, J. Chung, C. Whitten-Bauer, S. Wieland and F. V. Chisari (2012). "Short-range exosomal transfer of viral RNA from infected cells to plasmacytoid dendritic cells triggers innate immunity." Cell Host Microbe **12**(4): 558-570.

Drexler, J. F., V. M. Corman, M. A. Muller, A. N. Lukashev, A. Gmyl, B. Coutard, A. Adam, D. Ritz, L. M. Leijten, D. van Riel, R. Kallies, S. M. Klose, F. Gloza-Rausch, T. Binger, A. Annan, Y. Adu-Sarkodie, S. Oppong, M. Bourgarel, D. Rupp, B. Hoffmann, M. Schlegel, B. M. Kummerer, D. H. Kruger, J. Schmidt-Chanasit, A. A. Setien, V. M. Cottontail, T. Hemachudha, S. Wacharapluesadee, K. Osterrieder, R. Bartenschlager, S. Matthee, M. Beer, T. Kuiken, C. Reusken, E. M. Leroy, R. G. Ulrich and C. Drosten (2013). "Evidence for novel hepaciviruses in rodents." PLoS Pathog **9**(6): e1003438.

Drummer, H. E., K. A. Wilson and P. Poumbourios (2002). "Identification of the hepatitis C virus E2 glycoprotein binding site on the large extracellular loop of CD81." J Virol **76**(21): 11143-11147.

Drummer, H. E., K. A. Wilson and P. Poumbourios (2005). "Determinants of CD81 dimerization and interaction with hepatitis C virus glycoprotein E2." Biochem Biophys Res Commun **328**(1): 251-257.

Egger, D., B. Wolk, R. Gosert, L. Bianchi, H. E. Blum, D. Moradpour and K. Bienz (2002). "Expression of hepatitis C virus proteins induces distinct membrane alterations including a candidate viral replication complex." J Virol **76**(12): 5974-5984.

Eierhoff, T., E. R. Hrincius, U. Rescher, S. Ludwig and C. Ehrhardt (2010). "The epidermal growth factor receptor (EGFR) promotes uptake of influenza A viruses (IAV) into host cells." PLoS Pathog **6**(9): e1001099.

Elazar, M., P. Liu, C. M. Rice and J. S. Glenn (2004). "An N-terminal amphipathic helix in hepatitis C virus (HCV) NS4B mediates membrane association, correct localization of replication complex proteins, and HCV RNA replication." J Virol **78**(20): 11393-11400.

Ellerman, D. A., C. Ha, P. Primakoff, D. G. Myles and G. S. Dveksler (2003). "Direct binding of the ligand PSG17 to CD9 requires a CD9 site essential for sperm-egg fusion." Mol Biol Cell **14**(12): 5098-5103.

Espenel, C., E. Margeat, P. Dosset, C. Arduise, C. Le Grimellec, C. A. Royer, C. Boucheix, E. Rubinstein and P. E. Milhiet (2008). "Single-molecule analysis of CD9 dynamics and partitioning reveals multiple modes of interaction in the tetraspanin web." Journal of Cell Biology **182**(4): 765-776.

Evans, M. J., T. von Hahn, D. M. Tscherne, A. J. Syder, M. Panis, B. Wolk, T. Hatziioannou, J. A. McKeating, P. D. Bieniasz and C. M. Rice (2007). "Claudin-1 is a hepatitis C virus co-receptor required for a late step in entry." Nature **446**(7137): 801-805.

Fafi-Kremer, S., I. Fofana, E. Soulier, P. Carolla, P. Meuleman, G. Leroux-Roels, A. H. Patel, F. L. Cosset, P. Pessaux, M. Doffoel, P. Wolf, F. Stoll-Keller and T. F. Baumert (2010). "Viral entry and escape from antibody-mediated neutralization influence hepatitis C virus reinfection in liver transplantation." J Exp Med **207**(9): 2019-2031.

Fanning, A. S., B. J. Jameson, L. A. Jesaitis and J. M. Anderson (1998). "The tight junction protein ZO-1 establishes a link between the transmembrane protein occludin and the actin cytoskeleton." J Biol Chem **273**(45): 29745-29753.

Fanning, A. S., T. Y. Ma and J. M. Anderson (2002). "Isolation and functional characterization of the actin binding region in the tight junction protein ZO-1." FASEB J **16**(13): 1835-1837.

Farci, P., A. Shimoda, A. Coiana, G. Diaz, G. Peddis, J. C. Melpolder, A. Strazzera, D. Y. Chien, S. J. Munoz, A. Balestrieri, R. H. Purcell and H. J. Alter (2000). "The outcome of acute hepatitis C predicted by the evolution of the viral quasispecies." Science **288**(5464): 339-344.

Farquhar, M. J., H. J. Harris, M. Diskar, S. Jones, C. J. Mee, S. U. Nielsen, C. L. Brimacombe, S. Molina, G. L. Toms, P. Maurel, J. Howl, F. W. Herberg, S. C. van Ijzendoorn, P. Balfe and J. A. McKeating (2008). "Protein kinase A-dependent step(s) in hepatitis C virus entry and infectivity." J Virol **82**(17): 8797-8811.

Farquhar, M. J., K. Hu, H. J. Harris, C. Davis, C. L. Brimacombe, S. J. Fletcher, T. F. Baumert, J. Z. Rappoport, P. Balfe and J. A. McKeating (2012). "Hepatitis C virus induces CD81 and claudin-1 endocytosis." J Virol **86**(8): 4305-4316.

Feinstone, S. M., A. Z. Kapikian and R. H. Purceli (1973). "Hepatitis A: detection by immune electron microscopy of a viruslike antigen associated with acute illness." Science **182**(4116): 1026-1028.

Feinstone, S. M., A. Z. Kapikian, R. H. Purcell, H. J. Alter and P. V. Holland (1975). "Transfusion-associated hepatitis not due to viral hepatitis type A or B." N Engl J Med **292**(15): 767-770.

Feldmann, G. (1989). "The cytoskeleton of the hepatocyte. Structure and functions." J Hepatol **8**(3): 380-386.

Feneant, L., S. Levy and L. Cocquerel (2014). "CD81 and hepatitis C virus (HCV) infection." Viruses **6**(2): 535-572.

Fidge, N. H. (1999). "High density lipoprotein receptors, binding proteins, and ligands." J Lipid Res **40**(2): 187-201.

Fletcher, N. F., R. Sutaria, J. Jo, A. Barnes, M. Blahova, L. W. Meredith, F. L. Cosset, S. M. Curbishley, D. H. Adams, A. Bertoletti and J. A. McKeating (2014). "Activated macrophages promote hepatitis C virus entry in a tumor necrosis factor-dependent manner." Hepatology **59**(4): 1320-1330.

Flint, M., C. Maidens, L. D. Loomis-Price, C. Shotton, J. Dubuisson, P. Monk, A. Higginbottom, S. Levy and J. A. McKeating (1999). "Characterization of hepatitis C virus E2 glycoprotein interaction with a putative cellular receptor, CD81." J Virol **73**(8): 6235-6244.

Flint, M., T. von Hahn, J. Zhang, M. Farquhar, C. T. Jones, P. Balfe, C. M. Rice and J. A. McKeating (2006). "Diverse CD81 proteins support hepatitis C virus infection." J Virol **80**(22): 11331-11342.

Fournier, M., M. Peyrou, L. Bourgoin, C. Maeder, I. Tchou and M. Foti (2010). "CD4 dimerization requires two cysteines in the cytoplasmic domain of the molecule and occurs in microdomains distinct from lipid rafts." Mol Immunol **47**(16): 2594-2603.

Fried, M. W., M. L. Shiffman, K. R. Reddy, C. Smith, G. Marinos, F. L. Goncales, Jr., D. Haussinger, M. Diago, G. Carosi, D. Dhumeaux, A. Craxi, A. Lin, J. Hoffman and J. Yu (2002). "Peginterferon alfa-2a plus ribavirin for chronic hepatitis C virus infection." N Engl J Med **347**(13): 975-982.

Furuse, M., K. Fujita, T. Hiiragi, K. Fujimoto and S. Tsukita (1998). "Claudin-1 and -2: novel integral membrane proteins localizing at tight junctions with no sequence similarity to occludin." J Cell Biol **141**(7): 1539-1550.

Furuse, M., M. Hata, K. Furuse, Y. Yoshida, A. Haratake, Y. Sugitani, T. Noda, A. Kubo and S. Tsukita (2002). "Claudin-based tight junctions are crucial for the mammalian epidermal barrier: a lesson from claudin-1-deficient mice." J Cell Biol **156**(6): 1099-1111.

Gambin, Y., R. Lopez-Esparza, M. Reffay, E. Sierecki, N. S. Gov, M. Genest, R. S. Hodges and W. Urbach (2006). "Lateral mobility of proteins in liquid membranes revisited." Proc Natl Acad Sci U S A **103**(7): 2098-2102.

Gao, M., R. E. Nettles, M. Belema, L. B. Snyder, V. N. Nguyen, R. A. Fridell, M. H. Serrano-Wu, D. R. Langley, J. H. Sun, D. R. O'Boyle, 2nd, J. A. Lemm, C. Wang, J. O. Knipe, C. Chien, R. J. Colonno, D. M. Grasela, N. A. Meanwell and L. G. Hamann (2010). "Chemical genetics strategy identifies an HCV NS5A inhibitor with a potent clinical effect." Nature **465**(7294): 96-100.

Gardet, A., M. Breton, P. Fontanges, G. Trugnan and S. Chwetzoff (2006). "Rotavirus spike protein VP4 binds to and remodels actin bundles of the epithelial brush border into actin bodies." J Virol **80**(8): 3947-3956.

Gastaminza, P., K. A. Dryden, B. Boyd, M. R. Wood, M. Law, M. Yeager and F. V. Chisari (2010). "Ultrastructural and biophysical characterization of hepatitis C virus particles produced in cell culture." J Virol **84**(21): 10999-11009.

Gondeau, C., L. Pichard-Garcia and P. Maurel (2009). "Cellular models for the screening and development of anti-hepatitis C virus agents." Pharmacol Ther **124**(1): 1-22.

Gordon, L. G., B. M. Lynch, V. L. Beesley, N. Graves, C. McGrath, P. O'Rourke and P. M. Webb (2011). "The Working After Cancer Study (WACS): a population-based study of middle-aged workers diagnosed with colorectal cancer and their return to work experiences." BMC Public Health **11**: 604.

Goretsky, T., R. Dirisina, P. Sinh, N. Mittal, E. Managlia, D. B. Williams, D. Posca, H. Ryu, R. B. Katzman and T. A. Barrett (2012). "p53 mediates TNF-induced epithelial cell apoptosis in IBD." Am J Pathol **181**(4): 1306-1315.

Goswami, D., K. Gowrishankar, S. Bilgrami, S. Ghosh, R. Raghupathy, R. Chadda, R. Vishwakarma, M. Rao and S. Mayor (2008). "Nanoclusters of GPI-anchored proteins are formed by cortical actin-driven activity." Cell **135**(6): 1085-1097.

Gottwein, J. M., T. K. Scheel, B. Callendret, Y. P. Li, H. B. Eccleston, R. E. Engle, S. Govindarajan, W. Satterfield, R. H. Purcell, C. M. Walker and J. Bukh (2010). "Novel infectious cDNA clones of hepatitis C virus genotype 3a (strain S52) and 4a (strain ED43): genetic analyses and in vivo pathogenesis studies." J Virol **84**(10): 5277-5293.

Gottwein, J. M., T. K. Scheel, A. M. Hoegh, J. B. Lademann, J. Eugen-Olsen, G. Lisby and J. Bukh (2007). "Robust hepatitis C genotype 3a cell culture releasing adapted intergenotypic 3a/2a (S52/JFH1) viruses." Gastroenterology **133**(5): 1614-1626.

Gottwein, J. M., T. K. Scheel, T. B. Jensen, J. B. Lademann, J. C. Prentoe, M. L. Knudsen, A. M. Hoegh and J. Bukh (2009). "Development and characterization of hepatitis C virus genotype 1-7 cell culture systems: role of CD81 and scavenger receptor class B type I and effect of antiviral drugs." Hepatology **49**(2): 364-377.

Gower, E., C. Estes, S. Blach, K. Razavi-Shearer and H. Razavi (2014). "Global epidemiology and genotype distribution of the hepatitis C virus infection." J Hepatol **61**(1 Suppl): S45-57.

Gower, E., C. Estes, S. Blach, K. Razavi-Shearer and H. Razavi (2014). "Global epidemiology and genotype distribution of the hepatitis C virus infection." J Hepatol.

Gowrishankar, K., S. Ghosh, S. Saha, R. C, S. Mayor and M. Rao (2012). "Active remodeling of cortical actin regulates spatiotemporal organization of cell surface molecules." Cell **149**(6): 1353-1367.

Grebely, J., K. Page, R. Sacks-Davis, M. S. van der Loeff, T. M. Rice, J. Bruneau, M. D. Morris, B. Hajarizadeh, J. Amin, A. L. Cox, A. Y. Kim, B. H. McGovern, J. Schinkel, J. George, N. H. Shoukry, G. M. Lauer, L. Maher, A. R. Lloyd, M. Hellard, G. J. Dore and M. Prins (2014). "The effects of female sex, viral genotype, and IL28B genotype on spontaneous clearance of acute hepatitis C virus infection." Hepatology **59**(1): 109-120.

Grove, J., T. Huby, Z. Stamataki, T. Vanwolleghem, P. Meuleman, M. Farquhar, A. Schwarz, M. Moreau, J. S. Owen, G. Leroux-Roels, P. Balfe and J. A. McKeating (2007). "Scavenger receptor BI and BII expression levels modulate hepatitis C virus infectivity." J Virol **81**(7): 3162-3169.

Grove, J., S. Nielsen, J. Zhong, M. F. Bassendine, H. E. Drummer, P. Balfe and J. A. McKeating (2008). "Identification of a residue in hepatitis C virus E2 glycoprotein that determines scavenger receptor BI and CD81 receptor dependency and sensitivity to neutralizing antibodies." J Virol **82**(24): 12020-12029.

Guess, C. M. and V. Quaranta (2009). "Defining the role of laminin-332 in carcinoma." Matrix Biol **28**(8): 445-455.

Guidotti, L. G. and F. V. Chisari (2006). "Immunobiology and pathogenesis of viral hepatitis." Annu Rev Pathol **1**: 23-61.

Ha, C. T., R. Waterhouse, J. Warren, W. Zimmermann and G. S. Dveksler (2008). "N-glycosylation is required for binding of murine pregnancy-specific glycoproteins 17 and 19 to the receptor CD9." Am J Reprod Immunol **59**(3): 251-258.

Ha, C. T., R. Waterhouse, J. Wessells, J. A. Wu and G. S. Dveksler (2005). "Binding of pregnancy-specific glycoprotein 17 to CD9 on macrophages induces secretion of IL-10, IL-6, PGE2, and TGF-beta1." J Leukoc Biol **77**(6): 948-957.

Haid, S., C. Grethe, M. T. Dill, M. Heim, L. Kaderali and T. Pietschmann (2013). "Isolate-dependent use of Claudins for cell entry by hepatitis C virus." Hepatology.

Harris, H. J., C. Clerte, M. J. Farquhar, M. Goodall, K. Hu, P. Rassam, P. Dosset, G. K. Wilson, P. Balfe, S. C. Ijzendoorn, P. E. Milhiet and J. A. McKeating (2013). "Hepatoma polarization limits CD81 and hepatitis C virus dynamics." Cell Microbiol **15**(3): 430-445.

Harris, H. J., C. Davis, J. G. Mullins, K. Hu, M. Goodall, M. J. Farquhar, C. J. Mee, K. McCaffrey, S. Young, H. Drummer, P. Balfe and J. A. McKeating (2010). "Claudin association with CD81 defines hepatitis C virus entry." J Biol Chem **285**(27): 21092-21102.

Harris, H. J., M. J. Farquhar, C. J. Mee, C. Davis, G. M. Reynolds, A. Jennings, K. Hu, F. Yuan, H. Deng, S. G. Hubscher, J. H. Han, P. Balfe and J. A. McKeating (2008). "CD81 and claudin 1 coreceptor association: role in hepatitis C virus entry." J Virol **82**(10): 5007-5020.

Harris, R. C., E. Chung and R. J. Coffey (2003). "EGF receptor ligands." Exp Cell Res **284**(1): 2-13.

Havens, P. W., Ward, R., Drill, V. A., Paul, J. R. (1944). "Experimental Production of Hepatitis by Feeding Icterogenic Materials." Exp Biol Med (Maywood) **57**: 206-208.

He, J., E. Sun, M. V. Bujny, D. Kim, M. W. Davidson and X. Zhuang (2013). "Dual function of CD81 in influenza virus uncoating and budding." PLoS Pathog **9**(10): e1003701.

Hemler, M. E. (2003). "Tetraspanin proteins mediate cellular penetration, invasion, and fusion events and define a novel type of membrane microdomain." Annu Rev Cell Dev Biol **19**: 397-422.

Hemler, M. E. (2005). "Tetraspanin functions and associated microdomains." Nat Rev Mol Cell Biol **6**(10): 801-811.

Henriksen, L., M. V. Grandal, S. L. Knudsen, B. van Deurs and L. M. Grovdal (2013). "Internalization mechanisms of the epidermal growth factor receptor after activation with different ligands." PLoS One **8**(3): e58148.

Herker, E., C. Harris, C. Hernandez, A. Carpentier, K. Kaehlcke, A. R. Rosenberg, R. V. Farese, Jr. and M. Ott (2010). "Efficient hepatitis C virus particle formation requires diacylglycerol acyltransferase-1." Nat Med **16**(11): 1295-1298.

Herrema, H., D. Czajkowska, D. Theard, J. M. van der Wouden, D. Kalicharan, B. Zolghadr, D. Hoekstra and S. C. van Ijzendoorn (2006). "Rho kinase, myosin-II, and p42/44 MAPK control extracellular matrix-mediated apical bile canalicular lumen morphogenesis in HepG2 cells." Mol Biol Cell **17**(7): 3291-3303.

Higginbottom, A., E. R. Quinn, C. C. Kuo, M. Flint, L. H. Wilson, E. Bianchi, A. Nicosia, P. N. Monk, J. A. McKeating and S. Levy (2000). "Identification of amino acid residues in CD81 critical for interaction with hepatitis C virus envelope glycoprotein E2." J Virol **74**(8): 3642-3649.

Hishiki, T., Y. Shimizu, R. Tobita, K. Sugiyama, K. Ogawa, K. Funami, Y. Ohsaki, T. Fujimoto, H. Takaku, T. Wakita, T. F. Baumert, Y. Miyanari and K. Shimotohno (2010). "Infectivity of hepatitis C virus is influenced by association with apolipoprotein E isoforms." J Virol **84**(22): 12048-12057.

Honegger, J. R., S. Kim, A. A. Price, J. A. Kohout, K. L. McKnight, M. R. Prasad, S. M. Lemon, A. Grakoui and C. M. Walker (2013). "Loss of immune escape mutations during persistent HCV infection in pregnancy enhances replication of vertically transmitted viruses." Nat Med **19**(11): 1529-1533.

Houghton, M. (2009). "The long and winding road leading to the identification of the hepatitis C virus." J Hepatol **51**(5): 939-948.

Houldsworth, A., M. M. Metzner, A. Demaine, A. Hodgkinson, E. Kaminski and M. Cramp (2014). "CD81 sequence and susceptibility to hepatitis C infection." J Med Virol **86**(1): 162-168.

Hsu, M., J. Zhang, M. Flint, C. Logvinoff, C. Cheng-Mayer, C. M. Rice and J. A. McKeating (2003). "Hepatitis C virus glycoproteins mediate pH-dependent cell entry of pseudotyped retroviral particles." Proc Natl Acad Sci U S A **100**(12): 7271-7276.

Huang, S., H. Tian, Z. Chen, T. Yu and A. Xu (2010). "The evolution of vertebrate tetraspanins: gene loss, retention, and massive positive selection after whole genome duplications." BMC Evol Biol **10**: 306.

Huang, S., S. Yuan, M. Dong, J. Su, C. Yu, Y. Shen, X. Xie, Y. Yu, X. Yu, S. Chen, S. Zhang, P. Pontarotti and A. Xu (2005). "The phylogenetic analysis of tetraspanins projects the evolution of cell-cell interactions from unicellular to multicellular organisms." Genomics **86**(6): 674-684.

Hughes-Jones, N. C. (1975). "Red-cell antigens, antibodies and their interaction." Clin Haematol **4**(1): 29-43.

Itzhaki, R. F., W. L. Irving and M. A. Wozniak (2003). "Apolipoprotein E and hepatitis C virus." Hepatology **38**(4): 1060.

Jacobson, I. M., J. G. McHutchison, G. Dusheiko, A. M. Di Bisceglie, K. R. Reddy, N. H. Bzowej, P. Marcellin, A. J. Muir, P. Ferenci, R. Flisiak, J. George, M. Rizzetto, D. Shouval, R. Sola, R. A. Terg, E. M. Yoshida, N. Adda, L. Bengtsson, A. J. Sankoh, T. L. Kieffer, S. George, R. S. Kauffman and S. Zeuzem (2011). "Telaprevir for previously untreated chronic hepatitis C virus infection." N Engl J Med **364**(25): 2405-2416.

Jamshad, M., S. Rajesh, Z. Stamataki, J. A. McKeating, T. Dafforn, M. Overduin and R. M. Bill (2008). "Structural characterization of recombinant human CD81 produced in Pichia pastoris." Protein Expr Purif **57**(2): 206-216.

Jensen, L. J., M. Kuhn, M. Stark, S. Chaffron, C. Creevey, J. Muller, T. Doerks, P. Julien, A. Roth, M. Simonovic, P. Bork and C. von Mering (2009). "STRING 8--a global view on proteins and their functional interactions in 630 organisms." Nucleic Acids Res **37**(Database issue): D412-416.

Jolly, C., K. Kashefi, M. Hollinshead and Q. J. Sattentau (2004). "HIV-1 cell to cell transfer across an Env-induced, actin-dependent synapse." J Exp Med **199**(2): 283-293.

Jolly, C., I. Mitar and Q. J. Sattentau (2007). "Requirement for an intact T-cell actin and tubulin cytoskeleton for efficient assembly and spread of human immunodeficiency virus type 1." J Virol **81**(11): 5547-5560.

Jopling, C. L., M. Yi, A. M. Lancaster, S. M. Lemon and P. Sarnow (2005). "Modulation of hepatitis C virus RNA abundance by a liver-specific MicroRNA." Science **309**(5740): 1577-1581.

Kapadia, S. B., H. Barth, T. Baumert, J. A. McKeating and F. V. Chisari (2007). "Initiation of hepatitis C virus infection is dependent on cholesterol and cooperativity between CD81 and scavenger receptor B type I." J Virol **81**(1): 374-383.

Kapoor, A., P. Simmonds, G. Gerold, N. Qaisar, K. Jain, J. A. Henriquez, C. Firth, D. L. Hirschberg, C. M. Rice, S. Shields and W. I. Lipkin (2011). "Characterization of a canine homolog of hepatitis C virus." Proc Natl Acad Sci U S A **108**(28): 11608-11613.

Kapoor, A., P. Simmonds, T. K. Scheel, B. Hjelle, J. M. Cullen, P. D. Burbelo, L. V. Chauhan, R. Duraisamy, M. Sanchez Leon, K. Jain, K. J. Vandegrift, C. H. Calisher, C. M. Rice and W. I. Lipkin (2013). "Identification of rodent homologs of hepatitis C virus and pegiviruses." MBio **4**(2): e00216-00213.

Karamatic Crew, V., N. Burton, A. Kagan, C. A. Green, C. Levene, F. Flinter, R. L. Brady, G. Daniels and D. J. Anstee (2004). "CD151, the first member of the tetraspanin (TM4) superfamily detected on erythrocytes, is essential for the correct assembly of human basement membranes in kidney and skin." Blood **104**(8): 2217-2223.

Karlas, A., N. Machuy, Y. Shin, K. P. Pleissner, A. Artarini, D. Heuer, D. Becker, H. Khalil, L. A. Ogilvie, S. Hess, A. P. Maurer, E. Muller, T. Wolff, T. Rudel and T. F. Meyer (2010). "Genome-wide RNAi screen identifies human host factors crucial for influenza virus replication." Nature **463**(7282): 818-822.

Keck, Z. Y., K. Machida, M. M. Lai, J. K. Ball, A. H. Patel and S. K. Foung (2008). "Therapeutic control of hepatitis C virus: the role of neutralizing monoclonal antibodies." Curr Top Microbiol Immunol **317**: 1-38.

Khakoo, S. I., P. N. Soni, K. Savage, D. Brown, A. P. Dhillon, L. W. Poulter and G. M. Dusheiko (1997). "Lymphocyte and macrophage phenotypes in chronic hepatitis C infection. Correlation with disease activity." Am J Pathol **150**(3): 963-970.

Khan, A. G., J. Whidby, M. T. Miller, H. Scarborough, A. V. Zatorski, A. Cygan, A. A. Price, S. A. Yost, C. D. Bohannon, J. Jacob, A. Grakoui and J. Marcotrigiano (2014). "Structure of the core ectodomain of the hepatitis C virus envelope glycoprotein 2." Nature **509**(7500): 381-384.

Kim, Y. and P. Rajagopalan (2010). "3D hepatic cultures simultaneously maintain primary hepatocyte and liver sinusoidal endothelial cell phenotypes." PLoS One **5**(11): e15456.

Kitadokoro, K., D. Bordo, G. Galli, R. Petracca, F. Falugi, S. Abrignani, G. Grandi and M. Bolognesi (2001). "CD81 extracellular domain 3D structure: insight into the tetraspanin superfamily structural motifs." EMBO J **20**(1-2): 12-18.

Kitadokoro, K., G. Galli, R. Petracca, F. Falugi, G. Grandi and M. Bolognesi (2001). "Crystallization and preliminary crystallographic studies on the large extracellular domain of human CD81, a tetraspanin receptor for hepatitis C virus." Acta Crystallogr D Biol Crystallogr **57**(Pt 1): 156-158.

Klasse, P. J. and Q. J. Sattentau (2002). "Occupancy and mechanism in antibody-mediated neutralization of animal viruses." J Gen Virol **83**(Pt 9): 2091-2108.

Kojima, T., T. Yamamoto, M. Murata, H. Chiba, Y. Kokai and N. Sawada (2003). "Regulation of the blood-biliary barrier: interaction between gap and tight junctions in hepatocytes." Med Electron Microsc **36**(3): 157-164.

Kolch, W. (2005). "Coordinating ERK/MAPK signalling through scaffolds and inhibitors." Nat Rev Mol Cell Biol **6**(11): 827-837.

Kolykhalov, A. A., E. V. Agapov, K. J. Blight, K. Mihalik, S. M. Feinstone and C. M. Rice (1997). "Transmission of hepatitis C by intrahepatic inoculation with transcribed RNA." Science **277**(5325): 570-574.

Kong, L., E. Giang, T. Nieusma, R. U. Kadam, K. E. Cogburn, Y. Hua, X. Dai, R. L. Stanfield, D. R. Burton, A. B. Ward, I. A. Wilson and M. Law (2013). "Hepatitis C virus E2 envelope glycoprotein core structure." Science **342**(6162): 1090-1094.

Konig, R., S. Stertz, Y. Zhou, A. Inoue, H. H. Hoffmann, S. Bhattacharyya, J. G. Alamares, D. M. Tscherne, M. B. Ortigoza, Y. Liang, Q. Gao, S. E. Andrews, S. Bandyopadhyay, P. De Jesus, B. P. Tu, L. Pache, C. Shih, A. Orth, G. Bonamy, L. Miraglia, T. Ideker, A. Garcia-Sastre, J. A. Young, P. Palese, M. L. Shaw and S. K. Chanda (2010). "Human host factors required for influenza virus replication." Nature **463**(7282): 813-817.

Koutsoudakis, G., E. Herrmann, S. Kallis, R. Bartenschlager and T. Pietschmann (2007). "The level of CD81 cell surface expression is a key determinant for productive entry of hepatitis C virus into host cells." J Virol **81**(2): 588-598.

Koutsoudakis, G., A. Kaul, E. Steinmann, S. Kallis, V. Lohmann, T. Pietschmann and R. Bartenschlager (2006). "Characterization of the early steps of hepatitis C virus infection by using luciferase reporter viruses." J Virol **80**(11): 5308-5320.

Kovacs, E. M., S. Verma, R. G. Ali, A. Ratheesh, N. A. Hamilton, A. Akhmanova and A. S. Yap (2011). "N-WASP regulates the epithelial junctional actin cytoskeleton through a non-canonical post-nucleation pathway." Nat Cell Biol **13**(8): 934-943.

Kovalenko, O. V., X. Yang, T. V. Kolesnikova and M. E. Hemler (2004). "Evidence for specific tetraspanin homodimers: inhibition of palmitoylation makes cysteine residues available for cross-linking." Biochem J **377**(Pt 2): 407-417.

Krause, G., L. Winkler, S. L. Mueller, R. F. Haseloff, J. Piontek and I. E. Blasig (2008). "Structure and function of claudins." Biochim Biophys Acta **1778**(3): 631-645.

Krementsov, D. N., P. Rassam, E. Margeat, N. H. Roy, J. Schneider-Schaulies, P. E. Milhiet and M. Thali (2010). "HIV-1 assembly differentially alters dynamics and partitioning of tetraspanins and raft components." Traffic **11**(11): 1401-1414.

Krementsov, D. N., J. Weng, M. Lambele, N. H. Roy and M. Thali (2009). "Tetraspanins regulate cell-to-cell transmission of HIV-1." Retrovirology **6**: 64.

Krey, T., J. d'Alayer, C. M. Kikuti, A. Saulnier, L. Damier-Piolle, I. Petitpas, D. X. Johansson, R. G. Tawar, B. Baron, B. Robert, P. England, M. A. Persson, A. Martin and F. A. Rey (2010). "The disulfide bonds in glycoprotein E2 of hepatitis C virus reveal the tertiary organization of the molecule." PLoS Pathog **6**(2): e1000762.

Krieger, N., V. Lohmann and R. Bartenschlager (2001). "Enhancement of hepatitis C virus RNA replication by cell culture-adaptive mutations." J Virol **75**(10): 4614-4624.

Krieger, S. E., M. B. Zeisel, C. Davis, C. Thumann, H. J. Harris, E. K. Schnober, C. Mee, E. Soulier, C. Royer, M. Lambotin, F. Grunert, V. L. Dao Thi, M. Dreux, F. L. Cosset, J. A. McKeating, C. Schuster and T. F. Baumert (2010). "Inhibition of hepatitis C virus infection by anti-claudin-1 antibodies is mediated by neutralization of E2-CD81-claudin-1 associations." Hepatology **51**(4): 1144-1157.

Krugman, S. (1976). "Viral hepatitis: overview and historical perspectives." Yale J Biol Med **49**(3): 199-203.

Kubitz, R., G. Sutfels, T. Kuhlkamp, R. Kolling and D. Haussinger (2004). "Trafficking of the bile salt export pump from the Golgi to the canalicular membrane is regulated by the p38 MAP kinase." Gastroenterology **126**(2): 541-553.

Kuntzen, T., J. Timm, A. Berical, N. Lennon, A. M. Berlin, S. K. Young, B. Lee, D. Heckerman, J. Carlson, L. L. Reyor, M. Kleyman, C. M. McMahon, C. Birch, J. Schulze Zur Wiesch, T. Ledlie, M. Koehrsen, C. Kodira, A. D. Roberts, G. M. Lauer, H. R. Rosen, F. Bihl, A. Cerny, U. Spengler, Z. Liu, A. Y. Kim, Y. Xing, A. Schneidewind, M. A. Madey, J. F. Fleckenstein, V. M. Park, J. E. Galagan, C. Nusbaum, B. D. Walker, G. V. Lake-Bakaar, E. S. Daar, I. M. Jacobson, E. D. Gomperts, B. R. Edlin, S. M. Donfield, R. T. Chung, A. H. Talal, T. Marion, B. W. Birren, M. R. Henn and T. M. Allen (2008). "Naturally occurring dominant resistance mutations to hepatitis C virus protease and polymerase inhibitors in treatment-naive patients." Hepatology **48**(6): 1769-1778.

Kuo, G., Q. L. Choo, H. J. Alter, G. L. Gitnick, A. G. Redeker, R. H. Purcell, T. Miyamura, J. L. Dienstag, M. J. Alter, C. E. Stevens and et al. (1989). "An assay for circulating antibodies to a major etiologic virus of human non-A, non-B hepatitis." Science **244**(4902): 362-364.

Kusumi, A., Y. Sako and M. Yamamoto (1993). "Confined lateral diffusion of membrane receptors as studied by single particle tracking (nanovid microscopy). Effects of calcium-induced differentiation in cultured epithelial cells." Biophys J **65**(5): 2021-2040.

Lagging, L. M., K. Meyer, R. J. Owens and R. Ray (1998). "Functional role of hepatitis C virus chimeric glycoproteins in the infectivity of pseudotyped virus." J Virol **72**(5): 3539-3546.

Lango Allen, H., K. Estrada, G. Lettre, S. I. Berndt, M. N. Weedon, F. Rivadeneira, C. J. Willer, A. U. Jackson, S. Vedantam, S. Raychaudhuri, T. Ferreira, A. R. Wood, R. J. Weyant, A. V. Segre, E. K. Speliotes, E. Wheeler, N. Soranzo, J. H. Park, J. Yang, D. Gudbjartsson, N. L. Heard-Costa, J. C. Randall, L. Qi, A. Vernon Smith, R. Magi, T. Pastinen, L. Liang, I. M. Heid, J. Luan, G. Thorleifsson, T. W. Winkler, M. E. Goddard, K. Sin Lo, C. Palmer, T. Workalemahu, Y. S. Aulchenko, A. Johansson, M. C. Zillikens, M. F. Feitosa, T. Esko, T. Johnson, S. Ketkar, P. Kraft, M. Mangino, I. Prokopenko, D. Absher, E. Albrecht, F. Ernst, N. L. Glazer, C. Hayward, J. J. Hottenga, K. B. Jacobs, J. W. Knowles, Z. Kutalik, K. L. Monda, O. Polasek, M. Preuss, N. W. Rayner, N. R. Robertson, V. Steinthorsdottir, J. P. Tyrer, B. F. Voight, F. Wiklund, J. Xu, J. H. Zhao, D. R. Nyholt, N. Pellikka, M. Perola, J. R. Perry, I. Surakka, M. L. Tammesoo, E. L. Altmaier, N. Amin, T. Aspelund, T. Bhangale, G. Boucher, D. I. Chasman, C. Chen, L. Coin, M. N. Cooper, A. L. Dixon, Q. Gibson, E. Grundberg, K. Hao, M. Juhani Junttila, L. M. Kaplan, J. Kettunen, I. R. Konig, T. Kwan, R. W. Lawrence, D. F. Levinson, M. Lorentzon, B. McKnight, A. P. Morris, M. Muller, J. Suh Ngwa, S. Purcell, S. Rafelt, R. M. Salem, E. Salvi, S. Sanna, J. Shi, U. Sovio, J.

R. Thompson, M. C. Turchin, L. Vandenput, D. J. Verlaan, V. Vitart, C. C. White, A. Ziegler, P. Almgren, A. J. Balmforth, H. Campbell, L. Citterio, A. De Grandi, A. Dominiczak, J. Duan, P. Elliott, R. Elosua, J. G. Eriksson, N. B. Freimer, E. J. Geus, N. Glorioso, S. Haiqing, A. L. Hartikainen, A. S. Havulinna, A. A. Hicks, J. Hui, W. Igl, T. Illig, A. Jula, E. Kajantie, T. O. Kilpelainen, M. Koiranen, I. Kolcic, S. Koskinen, P. Kovacs, J. Laitinen, J. Liu, M. L. Lokki, A. Marusic, A. Maschio, T. Meitinger, A. Mulas, G. Pare, A. N. Parker, J. F. Peden, A. Petersmann, I. Pichler, K. H. Pietilainen, A. Pouta, M. Ridderstrale, J. I. Rotter, J. G. Sambrook, A. R. Sanders, C. O. Schmidt, J. Sinisalo, J. H. Smit, H. M. Stringham, G. Bragi Walters, E. Widen, S. H. Wild, G. Willemsen, L. Zagato, L. Zgaga, P. Zitting, H. Alavere, M. Farrall, W. L. McArdle, M. Nelis, M. J. Peters, S. Ripatti, J. B. van Meurs, K. K. Aben, K. G. Ardlie, J. S. Beckmann, J. P. Beilby, R. N. Bergman, S. Bergmann, F. S. Collins, D. Cusi, M. den Heijer, G. Eiriksdottir, P. V. Gejman, A. S. Hall, A. Hamsten, H. V. Huikuri, C. Iribarren, M. Kahonen, J. Kaprio, S. Kathiresan, L. Kiemeney, T. Kocher, L. J. Launer, T. Lehtimaki, O. Melander, T. H. Mosley, Jr., A. W. Musk, M. S. Nieminen, C. J. O'Donnell, C. Ohlsson, B. Oostra, L. J. Palmer, O. Raitakari, P. M. Ridker, J. D. Rioux, A. Rissanen, C. Rivolta, H. Schunkert, A. R. Shuldiner, D. S. Siscovick, M. Stumvoll, A. Tonjes, J. Tuomilehto, G. J. van Ommen, J. Viikari, A. C. Heath, N. G. Martin, G. W. Montgomery, M. A. Province, M. Kayser, A. M. Arnold, L. D. Atwood, E. Boerwinkle, S. J. Chanock, P. Deloukas, C. Gieger, H. Gronberg, P. Hall, A. T. Hattersley, C. Hengstenberg, W. Hoffman, G. M. Lathrop, V. Salomaa, S. Schreiber, M. Uda, D. Waterworth, A. F. Wright, T. L. Assimes, I. Barroso, A. Hofman, K. L. Mohlke, D. I. Boomsma, M. J. Caulfield, L. A. Cupples, J. Erdmann, C. S. Fox, V. Gudnason, U. Gyllensten, T. B. Harris, R. B. Hayes, M. R. Jarvelin, V. Mooser, P. B. Munroe, W. H. Ouwehand, B. W. Penninx, P. P. Pramstaller, T. Quertermous, I. Rudan, N. J. Samani, T. D. Spector, H. Volzke, H. Watkins, J. F. Wilson, L. C. Groop, T. Haritunians, F. B. Hu, R. C. Kaplan, A. Metspalu, K. E. North, D. Schlessinger, N. J. Wareham, D. J. Hunter, J. R. O'Connell, D. P. Strachan, H. E. Wichmann, I. B. Borecki, C. M. van Duijn, E. E. Schadt, U. Thorsteinsdottir, L. Peltonen, A. G. Uitterlinden, P. M. Visscher, N. Chatterjee, R. J. Loos, M. Boehnke, M. I. McCarthy, E. Ingelsson, C. M. Lindgren, G. R. Abecasis, K. Stefansson, T. M. Frayling and J. N. Hirschhorn (2010). "Hundreds of variants clustered in genomic loci and biological pathways affect human height." Nature **467**(7317): 832-838.

Lavillette, D., E. I. Pecheur, P. Donot, J. Fresquet, J. Molle, R. Corbau, M. Dreux, F. Penin and F. L. Cosset (2007). "Characterization of fusion determinants points to the involvement of three discrete regions of both E1 and E2 glycoproteins in the membrane fusion process of hepatitis C virus." J Virol **81**(16): 8752-8765.

Lavillette, D., A. W. Tarr, C. Voisset, P. Donot, B. Bartosch, C. Bain, A. H. Patel, J. Dubuisson, J. K. Ball and F. L. Cosset (2005). "Characterization of host-range and cell entry properties of the major genotypes and subtypes of hepatitis C virus." Hepatology **41**(2): 265-274.

Lawitz, E., J. P. Lalezari, T. Hassanein, K. V. Kowdley, F. F. Poordad, A. M. Sheikh, N. H. Afdhal, D. E. Bernstein, E. Dejesus, B. Freilich, D. R. Nelson, D. T. Dieterich, I. M. Jacobson, D. Jensen, G. A. Abrams, J. M. Darling, M. Rodriguez-Torres, K. R. Reddy, M. S. Sulkowski, N. H. Bzowej, R. H. Hyland, H. Mo, M. Lin, M. Mader, R. Hindes, E. Albanis, W. T. Symonds, M. M. Berrey and A. Muir (2013). "Sofosbuvir in combination with peginterferon alfa-2a and ribavirin for non-cirrhotic, treatment-naive patients with genotypes 1, 2, and 3 hepatitis C infection: a randomised, double-blind, phase 2 trial." Lancet Infect Dis **13**(5): 401-408.

Lehmann, M. J., N. M. Sherer, C. B. Marks, M. Pypaert and W. Mothes (2005). "Actin- and myosin-driven movement of viruses along filopodia precedes their entry into cells." Journal of Cell Biology **170**(2): 317-325.

Lemm, J. A., D. O'Boyle, 2nd, M. Liu, P. T. Nower, R. Colonno, M. S. Deshpande, L. B. Snyder, S. W. Martin, D. R. St Laurent, M. H. Serrano-Wu, J. L. Romine, N. A. Meanwell and M. Gao (2010). "Identification of hepatitis C virus NS5A inhibitors." J Virol **84**(1): 482-491.

Lewis, A. K. and P. C. Bridgman (1992). "Nerve growth cone lamellipodia contain two populations of actin filaments that differ in organization and polarity." Journal of Cell Biology **119**(5): 1219-1243.

Li, K., E. Foy, J. C. Ferreon, M. Nakamura, A. C. Ferreon, M. Ikeda, S. C. Ray, M. Gale, Jr. and S. M. Lemon (2005). "Immune evasion by hepatitis C virus NS3/4A protease-mediated cleavage of the Toll-like receptor 3 adaptor protein TRIF." Proc Natl Acad Sci U S A **102**(8): 2992-2997.

Liaskou, E., D. V. Wilson and Y. H. Oo (2012). "Innate immune cells in liver inflammation." Mediators Inflamm **2012**: 949157.

Lim, S. M., P. Koraka, A. D. Osterhaus and B. E. Martina (2011). "West Nile virus: immunity and pathogenesis." Viruses **3**(6): 811-828.

Lin, C., A. D. Kwong and R. B. Perni (2006). "Discovery and development of VX-950, a novel, covalent, and reversible inhibitor of hepatitis C virus NS3.4A serine protease." Infect Disord Drug Targets **6**(1): 3-16.

Lin, K. K., L. Rossi, N. C. Boles, B. E. Hall, T. C. George and M. A. Goodell (2011). "CD81 is essential for the re-entry of hematopoietic stem cells to quiescence following stress-induced proliferation via deactivation of the Akt pathway." PLoS Biol **9**(9): e1001148.

Lindenbach, B. D., M. J. Evans, A. J. Syder, B. Wolk, T. L. Tellinghuisen, C. C. Liu, T. Maruyama, R. O. Hynes, D. R. Burton, J. A. McKeating and C. M. Rice (2005). "Complete replication of hepatitis C virus in cell culture." Science **309**(5734): 623-626.

Lindenbach, B. D., P. Meuleman, A. Ploss, T. Vanwolleghem, A. J. Syder, J. A. McKeating, R. E. Lanford, S. M. Feinstone, M. E. Major, G. Leroux-Roels and C. M. Rice (2006). "Cell culture-grown hepatitis C virus is infectious in vivo and can be recultured in vitro." Proc Natl Acad Sci U S A **103**(10): 3805-3809.

Liu, S., W. Yang, L. Shen, J. R. Turner, C. B. Coyne and T. Wang (2009). "Tight junction proteins claudin-1 and occludin control hepatitis C virus entry and are downregulated during infection to prevent superinfection." J Virol **83**(4): 2011-2014.

Lohmann, V., F. Korner, J. Koch, U. Herian, L. Theilmann and R. Bartenschlager (1999). "Replication of subgenomic hepatitis C virus RNAs in a hepatoma cell line." Science **285**(5424): 110-113.

London, W. T., A. I. Sutnick and B. S. Blumberg (1969). "Australia antigen and acute viral hepatitis." Ann Intern Med **70**(1): 55-59.

Lupberger, J., M. B. Zeisel, F. Xiao, C. Thumann, I. Fofana, L. Zona, C. Davis, C. J. Mee, M. Turek, S. Gorke, C. Royer, B. Fischer, M. N. Zahid, D. Lavillette, J. Fresquet, F. L. Cosset, S. M. Rothenberg, T. Pietschmann, A. H. Patel, P. Pessaux, M. Doffoel, W. Raffelsberger, O. Poch, J. A. McKeating, L. Brino and T. F. Baumert (2011). "EGFR and EphA2 are host factors for hepatitis C virus entry and possible targets for antiviral therapy." Nat Med **17**(5): 589-595.

Lutschg, V., K. Boucke, S. Hemmi and U. F. Greber (2011). "Chemotactic antiviral cytokines promote infectious apical entry of human adenovirus into polarized epithelial cells." Nat Commun **2**: 391.

MacCallum, F. O. (1972). "1971 International Symposium on Viral Hepatitis. Historical perspectives." Can Med Assoc J **106**: Suppl:423-426.

MacCallum, F. O., Bradley, W.H. (1944). "Transmission of infective hepatitis to human volunteers: effect on rheumatoid arthritis." The Lancet **244**(6311).

Maecker, H. T. (2003). "Human CD81 directly enhances Th1 and Th2 cell activation, but preferentially induces proliferation of Th2 cells upon long-term stimulation." BMC Immunol **4**: 1.

Maecker, H. T., S. C. Todd and S. Levy (1997). "The tetraspanin superfamily: molecular facilitators." FASEB J **11**(6): 428-442.

Mangold, S., S. K. Wu, S. J. Norwood, B. M. Collins, N. A. Hamilton, P. Thorn and A. S. Yap (2011). "Hepatocyte growth factor acutely perturbs actin filament anchorage at the epithelial zonula adherens." Curr Biol **21**(6): 503-507.

Manns, M. P. and M. Cornberg (2013). "Sofosbuvir: the final nail in the coffin for hepatitis C?" Lancet Infect Dis **13**(5): 378-379.

Manns, M. P., J. G. McHutchison, S. C. Gordon, V. K. Rustgi, M. Shiffman, R. Reindollar, Z. D. Goodman, K. Koury, M. Ling and J. K. Albrecht (2001). "Peginterferon alfa-2b plus ribavirin compared

with interferon alfa-2b plus ribavirin for initial treatment of chronic hepatitis C: a randomised trial." Lancet **358**(9286): 958-965.

Marasco, W. A. and J. Sui (2007). "The growth and potential of human antiviral monoclonal antibody therapeutics." Nat Biotechnol **25**(12): 1421-1434.

Marchiando, A. M., L. Shen, W. V. Graham, K. L. Edelblum, C. A. Duckworth, Y. Guan, M. H. Montrose, J. R. Turner and A. J. Watson (2011). "The epithelial barrier is maintained by in vivo tight junction expansion during pathologic intestinal epithelial shedding." Gastroenterology **140**(4): 1208-1218 e1201-1202.

Marsh, M. and A. Helenius (2006). "Virus entry: open sesame." Cell **124**(4): 729-740.

Martin, D. N. and S. L. Uprichard (2013). "Identification of transferrin receptor 1 as a hepatitis C virus entry factor." Proc Natl Acad Sci U S A **110**(26): 10777-10782.

Masciopinto, F., S. Campagnoli, S. Abrignani, Y. Uematsu and P. Pileri (2001). "The small extracellular loop of CD81 is necessary for optimal surface expression of the large loop, a putative HCV receptor." Virus Res **80**(1-2): 1-10.

Masciopinto, F., G. Freer, V. L. Burgio, S. Levy, L. Galli-Stampino, M. Bendinelli, M. Houghton, S. Abrignani and Y. Uematsu (2002). "Expression of human CD81 in transgenic mice does not confer susceptibility to hepatitis C virus infection." Virology **304**(2): 187-196.

Masciopinto, F., C. Giovani, S. Campagnoli, L. Galli-Stampino, P. Colombatto, M. Brunetto, T. S. Yen, M. Houghton, P. Pileri and S. Abrignani (2004). "Association of hepatitis C virus envelope proteins with exosomes." Eur J Immunol **34**(10): 2834-2842.

Mashukova, A., F. A. Wald and P. J. Salas (2011). "Tumor necrosis factor alpha and inflammation disrupt the polarity complex in intestinal epithelial cells by a posttranslational mechanism." Mol Cell Biol **31**(4): 756-765.

Mattila, P. K., C. Feest, D. Depoil, B. Treanor, B. Montaner, K. L. Otipoby, R. Carter, L. B. Justement, A. Bruckbauer and F. D. Batista (2013). "The actin and tetraspanin networks organize receptor nanoclusters to regulate B cell receptor-mediated signaling." Immunity **38**(3): 461-474.

Maxfield, F. R. (2002). "Plasma membrane microdomains." Current Opinion in Cell Biology **14**(4): 483-487.

Mazzeo, C., F. Azzaroli, S. Giovanelli, A. Dormi, D. Festi, A. Colecchia, A. Miracolo, P. Natale, G. Nigro, A. Alberti, E. Roda and G. Mazzella (2003). "Ten year incidence of HCV infection in northern Italy and frequency of spontaneous viral clearance." Gut **52**(7): 1030-1034.

McCaffrey, K., H. Gouklani, I. Boo, P. Poumbourios and H. E. Drummer (2011). "The variable regions of hepatitis C virus glycoprotein E2 have an essential structural role in glycoprotein assembly and virion infectivity." J Gen Virol **92**(Pt 1): 112-121.

McHutchison, J. G., E. J. Lawitz, M. L. Shiffman, A. J. Muir, G. W. Galler, J. McCone, L. M. Nyberg, W. M. Lee, R. H. Ghalib, E. R. Schiff, J. S. Galati, B. R. Bacon, M. N. Davis, P. Mukhopadhyay, K. Koury, S. Noviello, L. D. Pedicone, C. A. Brass, J. K. Albrecht and M. S. Sulkowski (2009). "Peginterferon alfa-2b or alfa-2a with ribavirin for treatment of hepatitis C infection." N Engl J Med **361**(6): 580-593.

McLauchlan, J., M. K. Lemberg, G. Hope and B. Martoglio (2002). "Intramembrane proteolysis promotes trafficking of hepatitis C virus core protein to lipid droplets." EMBO J **21**(15): 3980-3988.

Mee, C. J., M. J. Farquhar, H. J. Harris, K. Hu, W. Ramma, A. Ahmed, P. Maurel, R. Bicknell, P. Balfe and J. A. McKeating (2010). "Hepatitis C virus infection reduces hepatocellular polarity in a vascular endothelial growth factor-dependent manner." Gastroenterology **138**(3): 1134-1142.

Mee, C. J., J. Grove, H. J. Harris, K. Hu, P. Balfe and J. A. McKeating (2008). "Effect of cell polarization on hepatitis C virus entry." J Virol **82**(1): 461-470.

Mee, C. J., H. J. Harris, M. J. Farquhar, G. Wilson, G. Reynolds, C. Davis, I. S. C. van, P. Balfe and J. A. McKeating (2009). "Polarization restricts hepatitis C virus entry into HepG2 hepatoma cells." J Virol **83**(12): 6211-6221.

Meertens, L., C. Bertaux, L. Cukierman, E. Cormier, D. Lavillette, F. L. Cosset and T. Dragic (2008). "The tight junction proteins claudin-1, -6, and -9 are entry cofactors for hepatitis C virus." J Virol **82**(7): 3555-3560.

Meertens, L., C. Bertaux and T. Dragic (2006). "Hepatitis C virus entry requires a critical postinternalization step and delivery to early endosomes via clathrin-coated vesicles." J Virol **80**(23): 11571-11578.

Meola, A., A. Sbardellati, B. Bruni Ercole, M. Cerretani, M. Pezzanera, A. Ceccacci, A. Vitelli, S. Levy, A. Nicosia, C. Traboni, J. McKeating and E. Scarselli (2000). "Binding of hepatitis C virus E2 glycoprotein to CD81 does not correlate with species permissiveness to infection." J Virol **74**(13): 5933-5938.

Meredith, L. W., H. J. Harris, G. K. Wilson, N. F. Fletcher, P. Balfe and J. A. McKeating (2013). "Early infection events highlight the limited transmissibility of hepatitis C virus in vitro." J Hepatol **58**(6): 1074-1080.

Meredith, L. W., G. K. Wilson, N. F. Fletcher and J. A. McKeating (2012). "Hepatitis C virus entry: beyond receptors." Rev Med Virol **22**(3): 182-193.

Merz, A., G. Long, M. S. Hiet, B. Brugger, P. Chlanda, P. Andre, F. Wieland, J. Krijnse-Locker and R. Bartenschlager (2011). "Biochemical and morphological properties of hepatitis C virus particles and determination of their lipidome." J Biol Chem **286**(4): 3018-3032.

Meuleman, P., J. Hesselgesser, M. Paulson, T. Vanwolleghem, I. Desombere, H. Reiser and G. Leroux-Roels (2008). "Anti-CD81 antibodies can prevent a hepatitis C virus infection in vivo." Hepatology **48**(6): 1761-1768.

Meunier, J. C., R. E. Engle, K. Faulk, M. Zhao, B. Bartosch, H. Alter, S. U. Emerson, F. L. Cosset, R. H. Purcell and J. Bukh (2005). "Evidence for cross-genotype neutralization of hepatitis C virus pseudo-particles and enhancement of infectivity by apolipoprotein C1." Proc Natl Acad Sci U S A **102**(12): 4560-4565.

Meylan, E., J. Curran, K. Hofmann, D. Moradpour, M. Binder, R. Bartenschlager and J. Tschopp (2005). "Cardif is an adaptor protein in the RIG-I antiviral pathway and is targeted by hepatitis C virus." Nature **437**(7062): 1167-1172.

Michalak, J. P., C. Wychowski, A. Choukhi, J. C. Meunier, S. Ung, C. M. Rice and J. Dubuisson (1997). "Characterization of truncated forms of hepatitis C virus glycoproteins." J Gen Virol **78 (Pt 9)**: 2299-2306.

Mitry, R. R. (2009). "Isolation of human hepatocytes." Methods Mol Biol **481**: 17-23.

Miyado, K., G. Yamada, S. Yamada, H. Hasuwa, Y. Nakamura, F. Ryu, K. Suzuki, K. Kosai, K. Inoue, A. Ogura, M. Okabe and E. Mekada (2000). "Requirement of CD9 on the egg plasma membrane for fertilization." Science **287**(5451): 321-324.

Molina, S., V. Castet, L. Pichard-Garcia, C. Wychowski, E. Meurs, J. M. Pascussi, C. Sureau, J. M. Fabre, A. Sacunha, D. Larrey, J. Dubuisson, J. Coste, J. McKeating, P. Maurel and C. Fournier-Wirth (2008). "Serum-derived hepatitis C virus infection of primary human hepatocytes is tetraspanin CD81 dependent." J Virol **82**(1): 569-574.

Monk, P. N. and L. J. Partridge (2012). "Tetraspanins: gateways for infection." Infect Disord Drug Targets **12**(1): 4-17.

Montpellier, C., B. A. Tews, J. Poitrimole, V. Rocha-Perugini, V. D'Arienzo, J. Potel, X. A. Zhang, E. Rubinstein, J. Dubuisson and L. Cocquerel (2011). "Interacting regions of CD81 and two of its partners, EWI-2 and EWI-2wint, and their effect on hepatitis C virus infection." J Biol Chem **286**(16): 13954-13965.

Moradpour, D., F. Penin and C. M. Rice (2007). "Replication of hepatitis C virus." Nat Rev Microbiol **5**(6): 453-463.

Morello, V., S. Cabodi, S. Sigismund, M. P. Camacho-Leal, D. Repetto, M. Volante, M. Papotti, E. Turco and P. Defilippi (2011). "beta1 integrin controls EGFR signaling and tumorigenic properties of lung cancer cells." Oncogene **30**(39): 4087-4096.

Musat, A. I., C. A. Sattler, G. L. Sattler and H. C. Pitot (1993). "Reestablishment of cell polarity of rat hepatocytes in primary culture." Hepatology **18**(1): 198-205.

Nakajima, H., L. Cocquerel, N. Kiyokawa, J. Fujimoto and S. Levy (2005). "Kinetics of HCV envelope proteins' interaction with CD81 large extracellular loop." Biochem Biophys Res Commun **328**(4): 1091-1100.

Narbus, C. M., B. Israelow, M. Sourisseau, M. L. Michta, S. E. Hopcraft, G. M. Zeiner and M. J. Evans (2011). "HepG2 cells expressing microRNA miR-122 support the entire hepatitis C virus life cycle." J Virol **85**(22): 12087-12092.

Neddermann, P., M. Quintavalle, C. Di Pietro, A. Clementi, M. Cerretani, S. Altamura, L. Bartholomew and R. De Francesco (2004). "Reduction of hepatitis C virus NS5A hyperphosphorylation by selective inhibition of cellular kinases activates viral RNA replication in cell culture." J Virol **78**(23): 13306-13314.

Neefe, J. R., J. Stokes, J. G. Reinhold and F. D. Lukens (1944). "Hepatitis Due to the Injection of Homologous Blood Products in Human Volunteers." J Clin Invest **23**(5): 836-855.

Nelson, W. J. (2003). "Adaptation of core mechanisms to generate cell polarity." Nature **422**(6933): 766-774.

Novikoff, P. M., M. Cammer, L. Tao, H. Oda, R. J. Stockert, A. W. Wolkoff and P. Satir (1996). "Three-dimensional organization of rat hepatocyte cytoskeleton: relation to the asialoglycoprotein endocytosis pathway." J Cell Sci **109 (Pt 1)**: 21-32.

Oda, K., Y. Matsuoka, A. Funahashi and H. Kitano (2005). "A comprehensive pathway map of epidermal growth factor receptor signaling." Mol Syst Biol **1**: 2005 0010.

Odintsova, E., T. D. Butters, E. Monti, H. Sprong, G. van Meer and F. Berditchevski (2006). "Gangliosides play an important role in the organization of CD82-enriched microdomains." Biochem J **400**(2): 315-325.

Oh, M. J., J. Akhtar, P. Desai and D. Shukla (2010). "A role for heparan sulfate in viral surfing." Biochem Biophys Res Commun **391**(1): 176-181.

Ohgaki, R., M. Matsushita, H. Kanazawa, S. Ogihara, D. Hoekstra and S. C. van Ijzendoorn (2010). "The Na+/H+ exchanger NHE6 in the endosomal recycling system is involved in the development of apical bile canalicular surface domains in HepG2 cells." Mol Biol Cell **21**(7): 1293-1304.

Olaby, R. A., H. M. Azzazy, R. Harris, B. Chromy, J. Vielmetter and R. Balhorn (2013). "Identification of ligands that target the HCV-E2 binding site on CD81." J Comput Aided Mol Des **27**(4): 337-346.

Ooi, Y. S., K. M. Stiles, C. Y. Liu, G. M. Taylor and M. Kielian (2013). "Genome-wide RNAi screen identifies novel host proteins required for alphavirus entry." PLoS Pathog **9**(12): e1003835.

Oren, R., S. Takahashi, C. Doss, R. Levy and S. Levy (1990). "TAPA-1, the target of an antiproliferative antibody, defines a new family of transmembrane proteins." Mol Cell Biol **10**(8): 4007-4015.

Palanisamy, N., A. Danielsson, C. Kokkula, H. Yin, K. Bondeson, L. Wesslen, A. S. Duberg and J. Lennerstrand (2013). "Implications of baseline polymorphisms for potential resistance to NS3 protease inhibitors in Hepatitis C virus genotypes 1a, 2b and 3a." Antiviral Res **99**(1): 12-17.

Park, J. H., S. Park, J. S. Yang, O. S. Kwon, S. Kim and S. K. Jang (2013). "Discovery of cellular proteins required for the early steps of HCV infection using integrative genomics." PLoS One **8**(4): e60333.

Perrault, M. and E. I. Pecheur (2009). "The hepatitis C virus and its hepatic environment: a toxic but finely tuned partnership." Biochem J **423**(3): 303-314.

Pestka, J. M., M. B. Zeisel, E. Blaser, P. Schurmann, B. Bartosch, F. L. Cosset, A. H. Patel, H. Meisel, J. Baumert, S. Viazov, K. Rispeter, H. E. Blum, M. Roggendorf and T. F. Baumert (2007). "Rapid induction of virus-neutralizing antibodies and viral clearance in a single-source outbreak of hepatitis C." Proc Natl Acad Sci U S A **104**(14): 6025-6030.

Petecchia, L., F. Sabatini, C. Usai, E. Caci, L. Varesio and G. A. Rossi (2012). "Cytokines induce tight junction disassembly in airway cells via an EGFR-dependent MAPK/ERK1/2-pathway." Lab Invest **92**(8): 1140-1148.

Petracca, R., F. Falugi, G. Galli, N. Norais, D. Rosa, S. Campagnoli, V. Burgio, E. Di Stasio, B. Giardina, M. Houghton, S. Abrignani and G. Grandi (2000). "Structure-function analysis of hepatitis C virus envelope-CD81 binding." J Virol **74**(10): 4824-4830.

Pietschmann, T., V. Lohmann, A. Kaul, N. Krieger, G. Rinck, G. Rutter, D. Strand and R. Bartenschlager (2002). "Persistent and transient replication of full-length hepatitis C virus genomes in cell culture." J Virol **76**(8): 4008-4021.

Pileri, P., Y. Uematsu, S. Campagnoli, G. Galli, F. Falugi, R. Petracca, A. J. Weiner, M. Houghton, D. Rosa, G. Grandi and S. Abrignani (1998). "Binding of hepatitis C virus to CD81." Science **282**(5390): 938-941.

Pilot-Matias T., L. S., Ng T., Barbon J., Fung E., Pithawalla R., Barlow E., Kutskova Y., Hsieh C.-M., DiGiammarino E., et al. (2010). "Evaluation of a panel of anti-CD81 antibodies using human liver-uPA/SCID mice." Proceedings of the 17th International Meeting on Hepatitis C Virus and Related Viruses; Yokohama, Japan.

Piontek, J., L. Winkler, H. Wolburg, S. L. Muller, N. Zuleger, C. Piehl, B. Wiesner, G. Krause and I. E. Blasig (2008). "Formation of tight junction: determinants of homophilic interaction between classic claudins." FASEB J **22**(1): 146-158.

Ploss, A., M. J. Evans, V. A. Gaysinskaya, M. Panis, H. You, Y. P. de Jong and C. M. Rice (2009). "Human occludin is a hepatitis C virus entry factor required for infection of mouse cells." Nature **457**(7231): 882-886.

Poordad, F., J. McCone, Jr., B. R. Bacon, S. Bruno, M. P. Manns, M. S. Sulkowski, I. M. Jacobson, K. R. Reddy, Z. D. Goodman, N. Boparai, M. J. DiNubile, V. Sniukiene, C. A. Brass, J. K. Albrecht and J. P. Bronowicki (2011). "Boceprevir for untreated chronic HCV genotype 1 infection." N Engl J Med **364**(13): 1195-1206.

Popescu, C. I. and J. Dubuisson (2010). "Role of lipid metabolism in hepatitis C virus assembly and entry." Biol Cell **102**(1): 63-74.

Potel, J., P. Rassam, C. Montpellier, L. Kaestner, E. Werkmeister, B. A. Tews, C. Couturier, C. I. Popescu, T. F. Baumert, E. Rubinstein, J. Dubuisson, P. E. Milhiet and L. Cocquerel (2013). "EWI-2wint promotes CD81 clustering that abrogates Hepatitis C Virus entry." Cell Microbiol **15**(7): 1234-1252.

Preiss, S., A. Thompson, X. Chen, S. Rodgers, V. Markovska, P. Desmond, K. Visvanathan, K. Li, S. Locarnini and P. Revill (2008). "Characterization of the innate immune signalling pathways in hepatocyte cell lines." J Viral Hepat **15**(12): 888-900.

Prentoe, J., S. B. Serre, S. Ramirez, A. Nicosia, J. M. Gottwein and J. Bukh (2014). "Hypervariable region 1 deletion and required adaptive envelope mutations confer decreased dependency on scavenger receptor class B type I and low-density lipoprotein receptor for hepatitis C virus." J Virol **88**(3): 1725-1739.

Prince, A. M. (1968). "An antigen detected in the blood during the incubation period of serum hepatitis." Proc Natl Acad Sci U S A **60**(3): 814-821.

Quan, P. L., C. Firth, J. M. Conte, S. H. Williams, C. M. Zambrana-Torrelio, S. J. Anthony, J. A. Ellison, A. T. Gilbert, I. V. Kuzmin, M. Niezgoda, M. O. Osinubi, S. Recuenco, W. Markotter, R. F. Breiman, L. Kalemba, J. Malekani, K. A. Lindblade, M. K. Rostal, R. Ojeda-Flores, G. Suzan, L. B. Davis, D. M. Blau, A. B. Ogunkoya, D. A. Alvarez Castillo, D. Moran, S. Ngam, D. Akaibe, B. Agwanda, T. Briese, J. H. Epstein, P. Daszak, C. E. Rupprecht, E. C. Holmes and W. I. Lipkin (2013). "Bats are a major natural reservoir for hepaciviruses and pegiviruses." Proc Natl Acad Sci U S A **110**(20): 8194-8199.

Rajesh, S., P. Sridhar, B. A. Tews, L. Feneant, L. Cocquerel, D. G. Ward, F. Berditchevski and M. Overduin (2012). "Structural basis of ligand interactions of the large extracellular domain of tetraspanin CD81." J Virol **86**(18): 9606-9616.

Ralston, R., I. Jacobson and M. Scull (2011). "The conundrum of relapse in STAT-C therapy: does HCV play the Red Queen or Rip Van Winkle?" Semin Liver Dis **31**(4): 410-419.

Ramakrishnaiah, V., C. Thumann, I. Fofana, F. Habersetzer, Q. Pan, P. E. de Ruiter, R. Willemsen, J. A. Demmers, V. Stalin Raj, G. Jenster, J. Kwekkeboom, H. W. Tilanus, B. L. Haagmans, T. F. Baumert and L. J. van der Laan (2013). "Exosome-mediated transmission of hepatitis C virus between human hepatoma Huh7.5 cells." Proc Natl Acad Sci U S A **110**(32): 13109-13113.

Ravid, T., J. M. Heidinger, P. Gee, E. M. Khan and T. Goldkorn (2004). "c-Cbl-mediated ubiquitinylation is required for epidermal growth factor receptor exit from the early endosomes." J Biol Chem **279**(35): 37153-37162.

Ray, K. (2012). "Hepatitis: NPC1L1 identified as a novel HCV entry factor." Nat Rev Gastroenterol Hepatol **9**(3): 124.

Raymond, E., S. Faivre and J. P. Armand (2000). "Epidermal growth factor receptor tyrosine kinase as a target for anticancer therapy." Drugs **60 Suppl 1**: 15-23; discussion 41-12.

Regeard, M., C. Lepere, M. Trotard, P. Gripon and J. Le Seyec (2007). "Recent contributions of in vitro models to our understanding of hepatitis C virus life cycle." FEBS J **274**(18): 4705-4718.

Rehermann, B. (2009). "Hepatitis C virus versus innate and adaptive immune responses: a tale of coevolution and coexistence." J Clin Invest **119**(7): 1745-1754.

Resti, M., P. Jara, L. Hierro, C. Azzari, R. Giacchino, G. Zuin, L. Zancan, S. Pedditzi and F. Bortolotti (2003). "Clinical features and progression of perinatally acquired hepatitis C virus infection." J Med Virol **70**(3): 373-377.

Reuben, A. (2002). "The thin red line." Hepatology **36**(3): 770-773.

Reynolds, G. M., H. J. Harris, A. Jennings, K. Hu, J. Grove, P. F. Lalor, D. H. Adams, P. Balfe, S. G. Hubscher and J. A. McKeating (2008). "Hepatitis C virus receptor expression in normal and diseased liver tissue." Hepatology **47**(2): 418-427.

Rocha-Perugini, V., M. Lavie, D. Delgrange, J. Canton, A. Pillez, J. Potel, C. Lecoeur, E. Rubinstein, J. Dubuisson, C. Wychowski and L. Cocquerel (2009). "The association of CD81 with tetraspanin-enriched microdomains is not essential for Hepatitis C virus entry." BMC Microbiol **9**: 111.

Rocha-Perugini, V., C. Montpellier, D. Delgrange, C. Wychowski, F. Helle, A. Pillez, H. Drobecq, F. Le Naour, S. Charrin, S. Levy, E. Rubinstein, J. Dubuisson and L. Cocquerel (2008). "The CD81 partner EWI-2wint inhibits hepatitis C virus entry." PLoS One **3**(4): e1866.

Roepstorff, K., M. V. Grandal, L. Henriksen, S. L. Knudsen, M. Lerdrup, L. Grovdal, B. M. Willumsen and B. van Deurs (2009). "Differential effects of EGFR ligands on endocytic sorting of the receptor." Traffic **10**(8): 1115-1127.

Romero-Brey, I., A. Merz, A. Chiramel, J. Y. Lee, P. Chlanda, U. Haselman, R. Santarella-Mellwig, A. Habermann, S. Hoppe, S. Kallis, P. Walther, C. Antony, J. Krijnse-Locker and R. Bartenschlager (2012). "Three-dimensional architecture and biogenesis of membrane structures associated with hepatitis C virus replication." PLoS Pathog **8**(12): e1003056.

Rosa, D., G. Saletti, E. De Gregorio, F. Zorat, C. Comar, U. D'Oro, S. Nuti, M. Houghton, V. Barnaba, G. Pozzato and S. Abrignani (2005). "Activation of naive B lymphocytes via CD81, a pathogenetic mechanism for hepatitis C virus-associated B lymphocyte disorders." Proc Natl Acad Sci U S A **102**(51): 18544-18549.

Roux, A., D. Cuvelier, P. Nassoy, J. Prost, P. Bassereau and B. Goud (2005). "Role of curvature and phase transition in lipid sorting and fission of membrane tubules." EMBO J **24**(8): 1537-1545.

Rubinstein, E., F. Le Naour, C. Lagaudriere-Gesbert, M. Billard, H. Conjeaud and C. Boucheix (1996). "CD9, CD63, CD81, and CD82 are components of a surface tetraspan network connected to HLA-DR and VLA integrins." Eur J Immunol **26**(11): 2657-2665.

Rustgi, V. K. (2007). "The epidemiology of hepatitis C infection in the United States." J Gastroenterol **42**(7): 513-521.

Saffman, P. G. and M. Delbruck (1975). "Brownian motion in biological membranes." Proc Natl Acad Sci U S A **72**(8): 3111-3113.

Sainz, B., Jr., N. Barretto, D. N. Martin, N. Hiraga, M. Imamura, S. Hussain, K. A. Marsh, X. Yu, K. Chayama, W. A. Alrefai and S. L. Uprichard (2012). "Identification of the Niemann-Pick C1-like 1 cholesterol absorption receptor as a new hepatitis C virus entry factor." <u>Nat Med</u> **18**(2): 281-285.

Sakai, A., S. Takikawa, R. Thimme, J. C. Meunier, H. C. Spangenberg, S. Govindarajan, P. Farci, S. U. Emerson, F. V. Chisari, R. H. Purcell and J. Bukh (2007). "In vivo study of the HC-TN strain of hepatitis C virus recovered from a patient with fulminant hepatitis: RNA transcripts of a molecular clone (pHC-TN) are infectious in chimpanzees but not in Huh7.5 cells." <u>J Virol</u> **81**(13): 7208-7219.

Sako, Y., A. Nagafuchi, S. Tsukita, M. Takeichi and A. Kusumi (1998). "Cytoplasmic regulation of the movement of E-cadherin on the free cell surface as studied by optical tweezers and single particle tracking: corralling and tethering by the membrane skeleton." <u>Journal of Cell Biology</u> **140**(5): 1227-1240.

Sakurai, T., O. D. Gil, J. D. Whittard, M. Gazdoiu, T. Joseph, J. Wu, A. Waksman, D. L. Benson, S. R. Salton and D. P. Felsenfeld (2008). "Interactions between the L1 cell adhesion molecule and ezrin support traction-force generation and can be regulated by tyrosine phosphorylation." <u>J Neurosci Res</u> **86**(12): 2602-2614.

Sala-Valdes, M., A. Ursa, S. Charrin, E. Rubinstein, M. E. Hemler, F. Sanchez-Madrid and M. Yanez-Mo (2006). "EWI-2 and EWI-F link the tetraspanin web to the actin cytoskeleton through their direct association with ezrin-radixin-moesin proteins." <u>J Biol Chem</u> **281**(28): 19665-19675.

Scarselli, E., H. Ansuini, R. Cerino, R. M. Roccasecca, S. Acali, G. Filocamo, C. Traboni, A. Nicosia, R. Cortese and A. Vitelli (2002). "The human scavenger receptor class B type I is a novel candidate receptor for the hepatitis C virus." <u>EMBO J</u> **21**(19): 5017-5025.

Scheel, T. K., J. M. Gottwein, T. B. Jensen, J. C. Prentoe, A. M. Hoegh, H. J. Alter, J. Eugen-Olsen and J. Bukh (2008). "Development of JFH1-based cell culture systems for hepatitis C virus genotype 4a and evidence for cross-genotype neutralization." <u>Proc Natl Acad Sci U S A</u> **105**(3): 997-1002.

Scheffer, K. D., A. Gawlitza, G. A. Spoden, X. A. Zhang, C. Lambert, F. Berditchevski and L. Florin (2013). "Tetraspanin CD151 mediates papillomavirus type 16 endocytosis." <u>J Virol</u> **87**(6): 3435-3446.

Schelhaas, M., H. Ewers, M. L. Rajamaki, P. M. Day, J. T. Schiller and A. Helenius (2008). "Human papillomavirus type 16 entry: retrograde cell surface transport along actin-rich protrusions." <u>PLoS Pathog</u> **4**(9): e1000148.

Schlessinger, J. (2002). "Ligand-induced, receptor-mediated dimerization and activation of EGF receptor." <u>Cell</u> **110**(6): 669-672.

Schneider, M. R. and E. Wolf (2009). "The epidermal growth factor receptor ligands at a glance." <u>J Cell Physiol</u> **218**(3): 460-466.

Schwarz, A. K., J. Grove, K. Hu, C. J. Mee, P. Balfe and J. A. McKeating (2009). "Hepatoma cell density promotes claudin-1 and scavenger receptor BI expression and hepatitis C virus internalization." <u>J Virol</u> **83**(23): 12407-12414.

Seeff, L. B. (2002). "Natural history of chronic hepatitis C." <u>Hepatology</u> **36**(5 Suppl 1): S35-46.

Seeff, L. B. (2009). "The history of the "natural history" of hepatitis C (1968-2009)." <u>Liver Int</u> **29 Suppl 1**: 89-99.

Selden, C., M. Khalil and H. J. Hodgson (1999). "What keeps hepatocytes on the straight and narrow? Maintaining differentiated function in the liver." <u>Gut</u> **44**(4): 443-446.

Serru, V., F. Le Naour, M. Billard, D. O. Azorsa, F. Lanza, C. Boucheix and E. Rubinstein (1999). "Selective tetraspan-integrin complexes (CD81/alpha4beta1, CD151/alpha3beta1, CD151/alpha6beta1) under conditions disrupting tetraspan interactions." <u>Biochem J</u> **340 (Pt 1)**: 103-111.

Shen L, B. E., Witkowski ED *et al.,* (2006). "Myosin light chain phosphorylation regulates barrier function by remodeling tight junction structure." <u>*J. Cell. Sci.*</u> **119**(Pt 10): 2095-2106.

Shepard, C. W., L. Finelli and M. J. Alter (2005). "Global epidemiology of hepatitis C virus infection." <u>Lancet Infect Dis</u> **5**(9): 558-567.

Sherer, N. M., M. J. Lehmann, L. F. Jimenez-Soto, C. Horensavitz, M. Pypaert and W. Mothes (2007). "Retroviruses can establish filopodial bridges for efficient cell-to-cell transmission." Nat Cell Biol **9**(3): 310-315.

Shieh, J. T. and J. M. Bergelson (2002). "Interaction with decay-accelerating factor facilitates coxsackievirus B infection of polarized epithelial cells." J Virol **76**(18): 9474-9480.

Shin, K., V. C. Fogg and B. Margolis (2006). "Tight junctions and cell polarity." Annu Rev Cell Dev Biol **22**: 207-235.

Silverman, J. M. and N. E. Reiner (2011). "Exosomes and other microvesicles in infection biology: organelles with unanticipated phenotypes." Cell Microbiol **13**(1): 1-9.

Silvie, O., S. Charrin, M. Billard, J. F. Franetich, K. L. Clark, G. J. van Gemert, R. W. Sauerwein, F. Dautry, C. Boucheix, D. Mazier and E. Rubinstein (2006). "Cholesterol contributes to the organization of tetraspanin-enriched microdomains and to CD81-dependent infection by malaria sporozoites." Journal of Cell Science **119**(Pt 10): 1992-2002.

Silvie, O., C. Greco, J. F. Franetich, A. Dubart-Kupperschmitt, L. Hannoun, G. J. van Gemert, R. W. Sauerwein, S. Levy, C. Boucheix, E. Rubinstein and D. Mazier (2006). "Expression of human CD81 differently affects host cell susceptibility to malaria sporozoites depending on the Plasmodium species." Cell Microbiol **8**(7): 1134-1146.

Silvie, O., E. Rubinstein, J. F. Franetich, M. Prenant, E. Belnoue, L. Renia, L. Hannoun, W. Eling, S. Levy, C. Boucheix and D. Mazier (2003). "Hepatocyte CD81 is required for Plasmodium falciparum and Plasmodium yoelii sporozoite infectivity." Nat Med **9**(1): 93-96.

Simmonds, P. (2004). "Genetic diversity and evolution of hepatitis C virus--15 years on." J Gen Virol **85**(Pt 11): 3173-3188.

Simmonds, P., E. C. Holmes, T. A. Cha, S. W. Chan, F. McOmish, B. Irvine, E. Beall, P. L. Yap, J. Kolberg and M. S. Urdea (1993). "Classification of hepatitis C virus into six major genotypes and a series of subtypes by phylogenetic analysis of the NS-5 region." J Gen Virol **74 (Pt 11)**: 2391-2399.

Simmonds, P., F. McOmish, P. L. Yap, S. W. Chan, C. K. Lin, G. Dusheiko, A. A. Saeed and E. C. Holmes (1993). "Sequence variability in the 5' non-coding region of hepatitis C virus: identification of a new virus type and restrictions on sequence diversity." J Gen Virol **74 (Pt 4)**: 661-668.

Sincock, P. M., S. Fitter, R. G. Parton, M. C. Berndt, J. R. Gamble and L. K. Ashman (1999). "PETA-3/CD151, a member of the transmembrane 4 superfamily, is localised to the plasma membrane and endocytic system of endothelial cells, associates with multiple integrins and modulates cell function." Journal of Cell Science **112 (Pt 6)**: 833-844.

Singer, S. J. and G. L. Nicolson (1972). "The fluid mosaic model of the structure of cell membranes." Science **175**(4023): 720-731.

Sormunen, R., S. Eskelinen and V. P. Lehto (1993). "Bile canaliculus formation in cultured HEPG2 cells." Lab Invest **68**(6): 652-662.

Sowinski, S., C. Jolly, O. Berninghausen, M. A. Purbhoo, A. Chauveau, K. Kohler, S. Oddos, P. Eissmann, F. M. Brodsky, C. Hopkins, B. Onfelt, Q. Sattentau and D. M. Davis (2008). "Membrane nanotubes physically connect T cells over long distances presenting a novel route for HIV-1 transmission." Nat Cell Biol **10**(2): 211-219.

Spoden, G., K. Freitag, M. Husmann, K. Boller, M. Sapp, C. Lambert and L. Florin (2008). "Clathrin- and caveolin-independent entry of human papillomavirus type 16--involvement of tetraspanin-enriched microdomains (TEMs)." PLoS One **3**(10): e3313.

Stamatovic, S. M., R. F. Keep, M. M. Wang, I. Jankovic and A. V. Andjelkovic (2009). "Caveolae-mediated internalization of occludin and claudin-5 during CCL2-induced tight junction remodeling in brain endothelial cells." J Biol Chem **284**(28): 19053-19066.

Stipp, C. S. (2010). "Laminin-binding integrins and their tetraspanin partners as potential antimetastatic targets." Expert Rev Mol Med **12**: e3.

Sulkowski, G. N., J. Warren, C. T. Ha and G. S. Dveksler (2011). "Characterization of receptors for murine pregnancy specific glycoproteins 17 and 23." Placenta **32**(8): 603-610.

Susser, S., J. Vermehren, N. Forestier, M. W. Welker, N. Grigorian, C. Fuller, D. Perner, S. Zeuzem and C. Sarrazin (2011). "Analysis of long-term persistence of resistance mutations within the hepatitis C virus NS3 protease after treatment with telaprevir or boceprevir." J Clin Virol **52**(4): 321-327.

Suzuki, K. G., T. K. Fujiwara, F. Sanematsu, R. Iino, M. Edidin and A. Kusumi (2007). "GPI-anchored receptor clusters transiently recruit Lyn and G alpha for temporary cluster immobilization and Lyn activation: single-molecule tracking study 1." Journal of Cell Biology **177**(4): 717-730.

Syder, A. J., H. Lee, M. B. Zeisel, J. Grove, E. Soulier, J. Macdonald, S. Chow, J. Chang, T. F. Baumert, J. A. McKeating, J. McKelvy and F. Wong-Staal (2011). "Small molecule scavenger receptor BI antagonists are potent HCV entry inhibitors." J Hepatol **54**(1): 48-55.

Tabor, E., R. J. Gerety, J. A. Drucker, L. B. Seeff, J. H. Hoofnagle, D. R. Jackson, M. April, L. F. Barker and G. Pineda-Tamondong (1978). "Transmission of non-A, non-B hepatitis from man to chimpanzee." Lancet **1**(8062): 463-466.

Tafazoli, F., C. Q. Zeng, M. K. Estes, K. E. Magnusson and L. Svensson (2001). "NSP4 enterotoxin of rotavirus induces paracellular leakage in polarized epithelial cells." J Virol **75**(3): 1540-1546.

Takeda, Y., A. R. Kazarov, C. E. Butterfield, B. D. Hopkins, L. E. Benjamin, A. Kaipainen and M. E. Hemler (2007). "Deletion of tetraspanin Cd151 results in decreased pathologic angiogenesis in vivo and in vitro." Blood **109**(4): 1524-1532.

Tan, P. K., J. Wang, P. L. Littler, K. K. Wong, T. A. Sweetnam, W. Keefe, N. R. Nash, E. C. Reding, F. Piu, M. R. Brann and H. H. Schiffer (2007). "Monitoring interactions between receptor tyrosine kinases and their downstream effector proteins in living cells using bioluminescence resonance energy transfer." Mol Pharmacol **72**(6): 1440-1446.

Tham, T. N., E. Gouin, E. Rubinstein, C. Boucheix, P. Cossart and J. Pizarro-Cerda (2010). "Tetraspanin CD81 is required for Listeria monocytogenes invasion." Infect Immun **78**(1): 204-209.

Theard, D., M. Steiner, D. Kalicharan, D. Hoekstra and S. C. van Ijzendoorn (2007). "Cell polarity development and protein trafficking in hepatocytes lacking E-cadherin/beta-catenin-based adherens junctions." Mol Biol Cell **18**(6): 2313-2321.

Thoresen, G. H., T. K. Guren, D. Sandnes, M. Peak, L. Agius and T. Christoffersen (1998). "Response to transforming growth factor alpha (TGFalpha) and epidermal growth factor (EGF) in hepatocytes: lower EGF receptor affinity of TGFalpha is associated with more sustained activation of p42/p44 mitogen-activated protein kinase and greater efficacy in stimulation of DNA synthesis." J Cell Physiol **175**(1): 10-18.

Thorley, J. A., J. A. McKeating and J. Z. Rappoport (2010). "Mechanisms of viral entry: sneaking in the front door." Protoplasma **244**(1-4): 15-24.

Timpe, J. M., Z. Stamataki, A. Jennings, K. Hu, M. J. Farquhar, H. J. Harris, A. Schwarz, I. Desombere, G. L. Roels, P. Balfe and J. A. McKeating (2008). "Hepatitis C virus cell-cell transmission in hepatoma cells in the presence of neutralizing antibodies." Hepatology **47**(1): 17-24.

Todd, S. C., S. G. Lipps, L. Crisa, D. R. Salomon and C. D. Tsoukas (1996). "CD81 expressed on human thymocytes mediates integrin activation and interleukin 2-dependent proliferation." J Exp Med **184**(5): 2055-2060.

Torriani, F. J., M. Rodriguez-Torres, J. K. Rockstroh, E. Lissen, J. Gonzalez-Garcia, A. Lazzarin, G. Carosi, J. Sasadeusz, C. Katlama, J. Montaner, H. Sette, Jr., S. Passe, J. De Pamphilis, F. Duff, U. M. Schrenk and D. T. Dieterich (2004). "Peginterferon Alfa-2a plus ribavirin for chronic hepatitis C virus infection in HIV-infected patients." N Engl J Med **351**(5): 438-450.

Trauner, M. and J. L. Boyer (2003). "Bile salt transporters: molecular characterization, function, and regulation." Physiol Rev **83**(2): 633-671.

Treanor, B., D. Depoil, A. Bruckbauer and F. D. Batista (2011). "Dynamic cortical actin remodeling by ERM proteins controls BCR microcluster organization and integrity." J Exp Med **208**(5): 1055-1068.

Treyer, A. and A. Musch (2013). "Hepatocyte polarity." Compr Physiol **3**(1): 243-287.

Tribouillard-Tanvier, D., V. Beringue, N. Desban, F. Gug, S. Bach, C. Voisset, H. Galons, H. Laude, D. Vilette and M. Blondel (2008). "Antihypertensive drug guanabenz is active in vivo against both yeast and mammalian prions." PLoS One **3**(4): e1981.

Tscherne, D. M., C. T. Jones, M. J. Evans, B. D. Lindenbach, J. A. McKeating and C. M. Rice (2006). "Time- and temperature-dependent activation of hepatitis C virus for low-pH-triggered entry." J Virol **80**(4): 1734-1741.

Tseng, C. T. and G. R. Klimpel (2002). "Binding of the hepatitis C virus envelope protein E2 to CD81 inhibits natural killer cell functions." J Exp Med **195**(1): 43-49.

Tsukada, N. and M. J. Phillips (1993). "Bile canalicular contraction is coincident with reorganization of pericanalicular filaments and co-localization of actin and myosin-II." J Histochem Cytochem **41**(3): 353-363.

van, I. S. C. and D. Hoekstra (2000). "Polarized sphingolipid transport from the subapical compartment changes during cell polarity development." Mol Biol Cell **11**(3): 1093-1101.

van, I. S. C., M. M. Zegers, J. W. Kok and D. Hoekstra (1997). "Segregation of glucosylceramide and sphingomyelin occurs in the apical to basolateral transcytotic route in HepG2 cells." Journal of Cell Biology **137**(2): 347-357.

VanCompernolle, S. E., S. Levy and S. C. Todd (2001). "Anti-CD81 activates LFA-1 on T cells and promotes T cell-B cell collaboration." Eur J Immunol **31**(3): 823-831.

Vercauteren, K. L.-R., G; Meuleman, P (2012). "Blocking HCV entry as potential antiviral therapy." Future Virol. **7**(6).

Voisset, C., N. Callens, E. Blanchard, A. Op De Beeck, J. Dubuisson and N. Vu-Dac (2005). "High density lipoproteins facilitate hepatitis C virus entry through the scavenger receptor class B type I." J Biol Chem **280**(9): 7793-7799.

Voisset, C. and J. Dubuisson (2004). "Functional hepatitis C virus envelope glycoproteins." Biol Cell **96**(6): 413-420.

Voisset, C., A. Op de Beeck, P. Horellou, M. Dreux, T. Gustot, G. Duverlie, F. L. Cosset, N. Vu-Dac and J. Dubuisson (2006). "High-density lipoproteins reduce the neutralizing effect of hepatitis C virus (HCV)-infected patient antibodies by promoting HCV entry." J Gen Virol **87**(Pt 9): 2577-2581.

von Hahn, T., B. D. Lindenbach, A. Boullier, O. Quehenberger, M. Paulson, C. M. Rice and J. A. McKeating (2006). "Oxidized low-density lipoprotein inhibits hepatitis C virus cell entry in human hepatoma cells." Hepatology **43**(5): 932-942.

von Hahn, T. and C. M. Rice (2008). "Hepatitis C virus entry." J Biol Chem **283**(7): 3689-3693.

von Hahn, T., J. C. Yoon, H. Alter, C. M. Rice, B. Rehermann, P. Balfe and J. A. McKeating (2007). "Hepatitis C virus continuously escapes from neutralizing antibody and T-cell responses during chronic infection in vivo." Gastroenterology **132**(2): 667-678.

Wack, A., E. Soldaini, C. Tseng, S. Nuti, G. Klimpel and S. Abrignani (2001). "Binding of the hepatitis C virus envelope protein E2 to CD81 provides a co-stimulatory signal for human T cells." Eur J Immunol **31**(1): 166-175.

Wakita, T., T. Pietschmann, T. Kato, T. Date, M. Miyamoto, Z. Zhao, K. Murthy, A. Habermann, H. G. Krausslich, M. Mizokami, R. Bartenschlager and T. J. Liang (2005). "Production of infectious hepatitis C virus in tissue culture from a cloned viral genome." Nat Med **11**(7): 791-796.

Wang, L. and J. L. Boyer (2004). "The maintenance and generation of membrane polarity in hepatocytes." Hepatology **39**(4): 892-899.

Wang, T., T. Town, L. Alexopoulou, J. F. Anderson, E. Fikrig and R. A. Flavell (2004). "Toll-like receptor 3 mediates West Nile virus entry into the brain causing lethal encephalitis." Nat Med **10**(12): 1366-1373.

Waterhouse, R., C. Ha and G. S. Dveksler (2002). "Murine CD9 is the receptor for pregnancy-specific glycoprotein 17." J Exp Med **195**(2): 277-282.

Westbrook, R. H. and G. Dusheiko (2014). "Natural history of hepatitis C." J Hepatol **61**(1S): S58-S68.

Wieland, S., Z. Makowska, B. Campana, D. Calabrese, M. T. Dill, J. Chung, F. V. Chisari and M. H. Heim (2014). "Simultaneous detection of hepatitis C virus and interferon stimulated gene expression in infected human liver." Hepatology **59**(6): 2121-2130.

Wieser, S., M. Moertelmaier, E. Fuertbauer, H. Stockinger and G. J. Schutz (2007). "(Un)confined diffusion of CD59 in the plasma membrane determined by high-resolution single molecule microscopy." Biophys J **92**(10): 3719-3728.

Wilson, G. K., D. A. Tennant and J. A. McKeating (2014). "Hypoxia inducible factors in liver disease and hepatocellular carcinoma: current understanding and future directions." J Hepatol **61**(6): 1397-1406.

Wilson, K. J., C. Mill, S. Lambert, J. Buchman, T. R. Wilson, V. Hernandez-Gordillo, R. M. Gallo, L. M. Ades, J. Settleman and D. J. Riese, 2nd (2012). "EGFR ligands exhibit functional differences in models of paracrine and autocrine signaling." Growth Factors **30**(2): 107-116.

Wittchen, E. S., J. Haskins and B. R. Stevenson (1999). "Protein interactions at the tight junction. Actin has multiple binding partners, and ZO-1 forms independent complexes with ZO-2 and ZO-3." J Biol Chem **274**(49): 35179-35185.

Wittchen, E. S., J. Haskins and B. R. Stevenson (2000). "Exogenous expression of the amino-terminal half of the tight junction protein ZO-3 perturbs junctional complex assembly." J Cell Biol **151**(4): 825-836.

Yalaoui, S., S. Zougbede, S. Charrin, O. Silvie, C. Arduise, K. Farhati, C. Boucheix, D. Mazier, E. Rubinstein and P. Froissard (2008). "Hepatocyte permissiveness to Plasmodium infection is conveyed by a short and structurally conserved region of the CD81 large extracellular domain." PLoS Pathog **4**(2): e1000010.

Yamada, S., S. Pokutta, F. Drees, W. I. Weis and W. J. Nelson (2005). "Deconstructing the cadherin-catenin-actin complex." Cell **123**(5): 889-901.

Yanagi, M., R. H. Purcell, S. U. Emerson and J. Bukh (1997). "Transcripts from a single full-length cDNA clone of hepatitis C virus are infectious when directly transfected into the liver of a chimpanzee." Proc Natl Acad Sci U S A **94**(16): 8738-8743.

Yanagi, M., R. H. Purcell, S. U. Emerson and J. Bukh (1999). "Hepatitis C virus: an infectious molecular clone of a second major genotype (2a) and lack of viability of intertypic 1a and 2a chimeras." Virology **262**(1): 250-263.

Yanez-Mo, M., O. Barreiro, M. Gordon-Alonso, M. Sala-Valdes and F. Sanchez-Madrid (2009). "Tetraspanin-enriched microdomains: a functional unit in cell plasma membranes." Trends Cell Biol **19**(9): 434-446.

Yang, H., X. Xiao, S. Li, G. Mai and Q. Zhang (2011). "Novel TSPAN12 mutations in patients with familial exudative vitreoretinopathy and their associated phenotypes." Mol Vis **17**: 1128-1135.

Yang, X., C. Claas, S. K. Kraeft, L. B. Chen, Z. Wang, J. A. Kreidberg and M. E. Hemler (2002). "Palmitoylation of tetraspanin proteins: modulation of CD151 lateral interactions, subcellular distribution, and integrin-dependent cell morphology." Mol Biol Cell **13**(3): 767-781.

Yauch, R. L., F. Berditchevski, M. B. Harler, J. Reichner and M. E. Hemler (1998). "Highly stoichiometric, stable, and specific association of integrin alpha3beta1 with CD151 provides a major link to phosphatidylinositol 4-kinase, and may regulate cell migration." Mol Biol Cell **9**(10): 2751-2765.

Yauch, R. L. and M. E. Hemler (2000). "Specific interactions among transmembrane 4 superfamily (TM4SF) proteins and phosphoinositide 4-kinase." Biochem J **351 Pt 3**: 629-637.

Ye, D., I. Ma and T. Y. Ma (2006). "Molecular mechanism of tumor necrosis factor-alpha modulation of intestinal epithelial tight junction barrier." Am J Physiol Gastrointest Liver Physiol **290**(3): G496-504.

Younossi, Z. and L. Henry (2014). "The impact of the new antiviral regimens on patient reported outcomes and health economics of patients with chronic hepatitis C." Dig Liver Dis **46S5**: S186-S196.

Zampino, R., A. Marrone, L. Restivo, B. Guerrera, A. Sellitto, L. Rinaldi, C. Romano and L. E. Adinolfi (2013). "Chronic HCV infection and inflammation: Clinical impact on hepatic and extra-hepatic manifestations." World J Hepatol **5**(10): 528-540.

Zegers, M. M. and D. Hoekstra (1997). "Sphingolipid transport to the apical plasma membrane domain in human hepatoma cells is controlled by PKC and PKA activity: a correlation with cell polarity in HepG2 cells." Journal of Cell Biology **138**(2): 307-321.

Zeisel, M. B., I. Fofana, S. Fafi-Kremer and T. F. Baumert (2011). "Hepatitis C virus entry into hepatocytes: molecular mechanisms and targets for antiviral therapies." J Hepatol **54**(3): 566-576.

Zeisel, M. B., G. Koutsoudakis, E. K. Schnober, A. Haberstroh, H. E. Blum, F. L. Cosset, T. Wakita, D. Jaeck, M. Doffoel, C. Royer, E. Soulier, E. Schvoerer, C. Schuster, F. Stoll-Keller, R. Bartenschlager, T. Pietschmann, H. Barth and T. F. Baumert (2007). "Scavenger receptor class B type I is a key host factor for hepatitis C virus infection required for an entry step closely linked to CD81." Hepatology **46**(6): 1722-1731.

Zhang, J., G. Randall, A. Higginbottom, P. Monk, C. M. Rice and J. A. McKeating (2004). "CD81 is required for hepatitis C virus glycoprotein-mediated viral infection." J Virol **78**(3): 1448-1455.

Zhao, L. J., L. Wang, H. Ren, J. Cao, L. Li, J. S. Ke and Z. T. Qi (2005). "Hepatitis C virus E2 protein promotes human hepatoma cell proliferation through the MAPK/ERK signaling pathway via cellular receptors." Exp Cell Res **305**(1): 23-32.

Zheng, A., F. Yuan, Y. Li, F. Zhu, P. Hou, J. Li, X. Song, M. Ding and H. Deng (2007). "Claudin-6 and claudin-9 function as additional coreceptors for hepatitis C virus." J Virol **81**(22): 12465-12471.

Zhong, J., P. Gastaminza, G. Cheng, S. Kapadia, T. Kato, D. R. Burton, S. F. Wieland, S. L. Uprichard, T. Wakita and F. V. Chisari (2005). "Robust hepatitis C virus infection in vitro." Proc Natl Acad Sci U S A **102**(26): 9294-9299.

Zona, L., J. Lupberger, N. Sidahmed-Adrar, C. Thumann, H. J. Harris, A. Barnes, J. Florentin, R. G. Tawar, F. Xiao, M. Turek, S. C. Durand, F. H. Duong, M. H. Heim, F. L. Cosset, I. Hirsch, D. Samuel, L. Brino, M. B. Zeisel, F. Le Naour, J. A. McKeating and T. F. Baumert (2013). "HRas Signal Transduction Promotes Hepatitis C Virus Cell Entry by Triggering Assembly of the Host Tetraspanin Receptor Complex." Cell Host Microbe **13**(3): 302-313.

Zona, L., R. G. Tawar, M. B. Zeisel, F. Xiao, C. Schuster, J. Lupberger and T. F. Baumert (2014). "CD81-receptor associations--impact for hepatitis C virus entry and antiviral therapies." Viruses **6**(2): 875-892.

Zuidscherwoude, M., F. Gottfert, V. M. Dunlock, C. G. Figdor, G. van den Bogaart and A. B. Spriel (2015). "The tetraspanin web revisited by super-resolution microscopy." Sci Rep **5**: 12201.